Independent Review of Tsagaan Chuluut Gold Project, Mongolia

Report prepared for

SG Gold Mining LLC

Report prepared by

SRK Consulting MGL LLC

SMN079

July 2020

Independent Review of Tsagaan Chuluut Gold Project, Mongolia

SG Gold Mining LLC

Room 603, MSN Building, Mahatma Gandhi Street
15th Khoroo, Khan Uul District, 17010 Ulaanbaatar, Mongolia

SRK Consulting MGL LLC

Ambassador Office 4-403, Sukhbaatar District 1, Peace Avenue 15A/5
Ulaanbaatar 210848, Mongolia

e-mail: mongolia@srk.com
website: www.srk.com

Tel: +976 7014 0046
Fax: +976 7014 0046

SRK Project Number SMN079

July 2020

Compiled by

Petr Osvald
Principal Consultant

Email: posvald@srk.mn

Peer reviewed by

Chris Woodfull
Corporate Consultant

Authors:

Ganzorig Tuvshinbayar; Bayasgalan Erdenechuluun; Sarantungalag Garamjav; Peter Stuart Smith; Danny Kentwell; Ben Jupp

Executive Summary

SG Gold Mining LLC (SG, the Client or the Company) has requested SRK to undertake an Independent Technical Review (ITR) on the geology and Mineral Resource of Tsagaan Chuluut Gold Project (the Project) located in the Dornod Province of Mongolia. SRK was advised that its report will be used for the Company's internal assessment of the Project. The objective of the ITR is to provide unbiased assessment of the Project's exploration potential, current Mineral Resource and work required to increase the Mineral Resource and bring the Project into next stage of project development. As part of the scope of work, SRK was requested to include recommendations for future work that will enable SG, potential equity investors and possible future shareholders to assess the Project.

Outline of work program

SRK has undertaken the scope of work as follows:

- A site visit was undertaken by Ganzorig Tuvshinbayar (Senior Geologist) from 1 to 3 May 2020.
- The exploration drilling database, geophysical and geochemical data, the geological model and Mineral Resource estimate/s provided by the Client, were reviewed, incorporating SRK's in-house knowledge of the region and site inspection findings
- The ground geophysical survey data were interpreted.
- The exploration philosophy and priorities for the Project, including any proposed exploration programs, were reviewed to determine their suitability in terms of upgrading the Mineral Resources.
- An independent opinion and comments (or feedback) regarding the Project's additional exploration potential and assessment of the current Mineral Resources and their reasonable prospects of eventual economic extraction were provided.
- Where appropriate, recommendations on further exploration and project development, were provided.
- An ITR was prepared under the guidelines of the JORC Code.

Project general description

The Project is in the Eastern Province, northeast Mongolia and 600 km east of the capital, Ulaanbaatar. The Project is situated approximately 30 km from the nearest village Bayandun Soum and approximately 180 km from the Eastern Province capital, Choibalsan. The Project is also situated 40 km south of the border with Russia and 200 km east of Manzhouli, a prefecture city of Inner Mongolia, China. The distance by road between Ulaanbaatar and the Project area is about 740 km and includes 540 km of asphalted road and 200 km of gravel road.

The Project is approximately 900 m to 1,100 m above sea level. The terrain is gently rolling hill ground, dissected by seasonal streams. The climate is harsh continental type. The temperature range across the year is 30°C to -35°C, the mean temperature in winter is -25°C, and the mean temperature in summer is 32°C. The mean annual precipitation is 544 mm and the rainy season is from April to October. During the winter, the area has snow cover.

SG holds the Tsagaan Chuluut-1 mining licence MV-015436. Details of the mining licence are given in Table ES-1.

Table ES-1: Tsagaan Chuluut-1 mining licence details

Licence Number	Licence Name	Type	Area (ha)	Date of issue	Date of expiry
MV-015436	Tsagaan Chuluut-1	Mining	456.68	25 January 2010	25 January 2040

Geology

The regional geology of the Project area reflects a complex tectonic evolution at the continental margin of Ereendavaa craton of the Amurian palaeocontinent. In terms of the regional geological setting, the Project is located on the margin of a suture zone defining the former Mongol-Okhotsk Ocean (MOO). From the Late Silurian, probably related to back-arc rifting, the MOO opened, resulting in the formation of a Mongolian continent orthogonal to the Siberian margin. From the end of Late Devonian to Early Carboniferous, subduction on the north and south margin of the MOO occurred until the Early Permian. In the Permian to Jurassic, the Mongolian continent was compressed (and uplifted) between the converging Siberian and North China cratons as the Mongol-Okhotsk oceanic basin closed.

In the Late Cainozoic, the amalgamated accretionary orogenic belt underwent transpressional deformation due to northeast-oriented compression. This event reactivated and exploited major Palaeozoic structures resulting in a combination of strike-slip movement and thrusting.

The Neoproterozoic Khachigol Formation comprises marble, amphibolite, schist, gneiss and metamorphosed sandstone. This formation is intruded by Neoproterozoic Phase 1 intrusives of diorite and quartz diorite composition, which are followed by Phase 2 leucogranite, biotitic granite, plagiogranite and gneiss (Figure ES-1 and Figure ES-2). In nearby Russia, uranium-lead zircon dating of biotitic granite and leucogranite yielded ages 740 ± 20 Ma (Bibikova et al.,1979).

The Permian Ulzgol plutonic rocks occur in three phases: Phase 1 mafic – gabbro, diorite and quartz diorite, Phase 2 – biotitic granite, plagiogranite and granodiorite, and Phase 3 – leucocratic granite ± biotite, syenite.

The Late Triassic to Early Jurassic Tsagaan Chuluut Igneous Complex comprises three phases: Phase 1 – gabbro, Phase 2 – diorite and quartz diorite, and Phase 3 – granodiorite and granite.

Middle-Late Jurassic granite porphyry bodies intrude the Late Triassic to Early Jurassic Tsagaan Chuluut Igneous Complex. These intrusions are accompanied by andesite-basalt, andesite-dacite, rhyodacite, rhyolite and their tuff sequences.

Late Jurassic to Early Cretaceous extension is well documented by development of east to northeast-trending graben structures filled by Late Jurassic to Early Cretaceous basal conglomerates, sandstones and rhyolite flows.

Regional northwest and northeast steeply dipping faults occur in the region and are defined, longitudinally as the Bayangolin, Turgenii, Tsagaan Chuluut, Khanangiin and Burged Uul faults. These faults have displaced Late Proterozoic to Mesozoic structures with displacement amplitudes of up to 250–350 m. The Mesozoic intrusives are controlled by the northwest-trending regional Tsagaan Chuluut Fault. SRK interprets the northeast-trending fault system as faults that exploited the inherited structural grain of the MOO subduction zone under the Ereendavaa continental margin. Northwest-trending faults are interpreted to represent early formed transform faults oblique to the subduction zone. Both systems were reactivated during repeated compression and extension since Early Palaeozoic and older faults were rotated to current positions.

The Palaeozoic magmatic complexes typically occur at the intersection of regional northeast- and northwest-trending faults. In addition to the broadly rectilinear fault systems, the region has an abundance of ring structures related to magmatic activity.

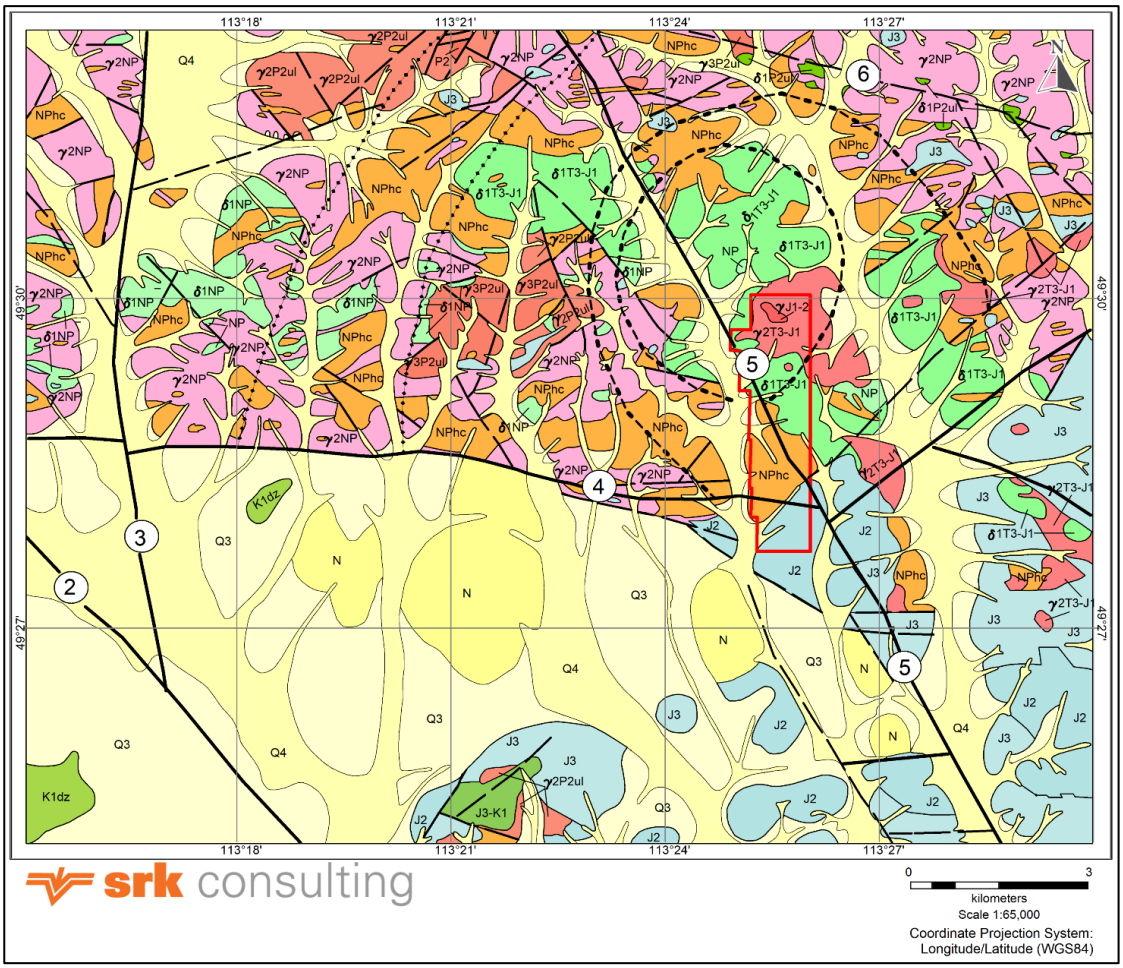

Figure ES-1: Regional geology map with Project location

Source: Ganbaatar (1991)

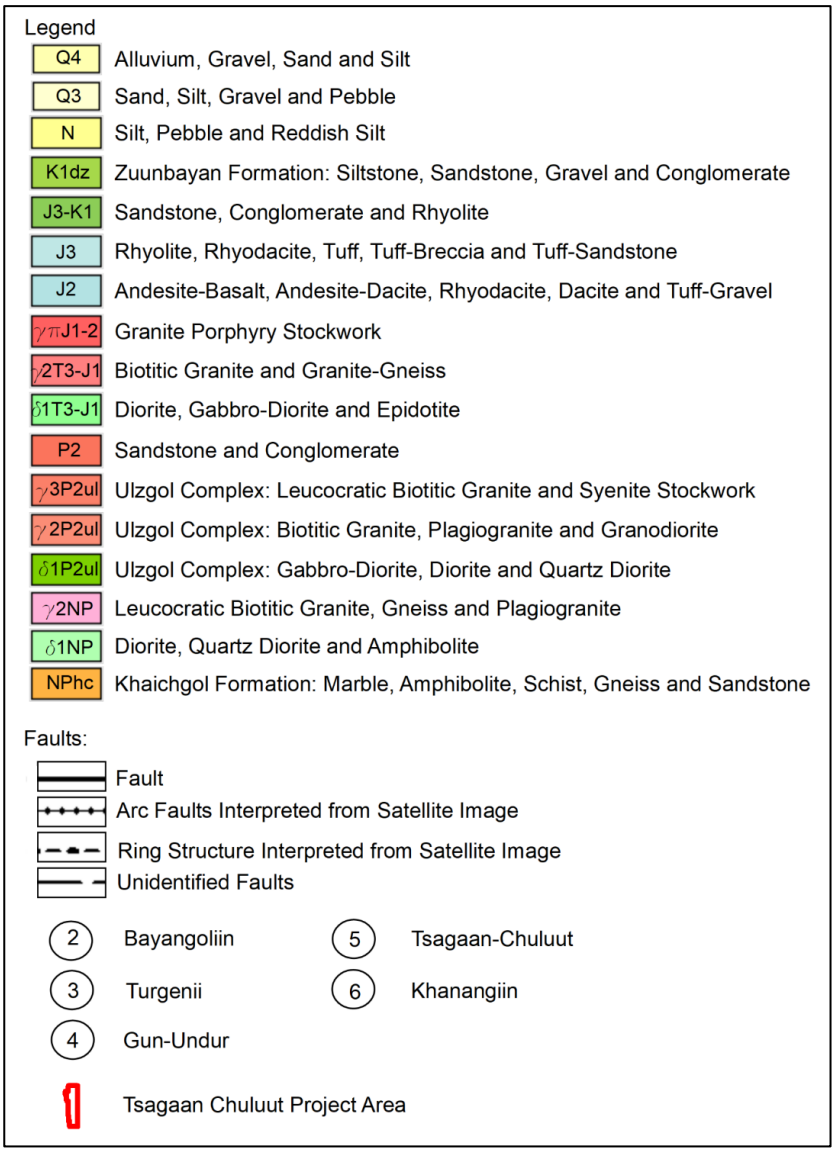

Figure ES-2: Legend to regional geology map

Source: Ganbaatar (1991)

Project geology and mineralisation

Lithology and structure

The local geology is dominated by the Neoproterozoic metasedimentary Khaichgol Formation outcropping in the south of Tsagaan Chuluut area, which has been intruded by the Late Triassic to Early Jurassic Tsagaan Chuluut Igneous Complex. Middle to Upper Jurassic volcanic and granite porphyry units outcrop in the south and north of the Project area, respectively.

The most prominent fault in the tenement is the northwest-trending Tsagaan Chuluut Fault. The Erdene Fault is the most dominant fault proximal to the gold (Au) mineralisation intersected at Tsagaan Chuluut 1 (TC1) deposit in the north sector of tenement, striking northeast through the tenement. SG geologists have identified numerous hydrothermal breccias along the length of the Erdene Fault (Figure ES-3 and Figure ES-4).

The main lithotypes described by SG geologists from core logs are gabbro, diorite, granodiorite, granite, diorite porphyry, quartz diorite porphyry, quartz porphyry, felsic and andesitic volcanics.

SRK has noted that the oldest intrusive samples are gabbrodiorites, which are strongly altered and deformed. These occur in isolated tectonic blocks that were intruded by diorite, diorite porphyry and quartz diorite porphyry. The quartz diorite porphyry intrusion coincides with mineralisation. Diorite, diorite porphyry and quartz diorite porphyry form subvertical stocks, which in plan view are elongated in an east–west direction. Apical parts of intrusive stocks are commonly brecciated, strongly altered and mineralised. The youngest intrusive rocks are granodiorite, granite, granodiorite porphyry and granite porphyry weakly altered by sericite.

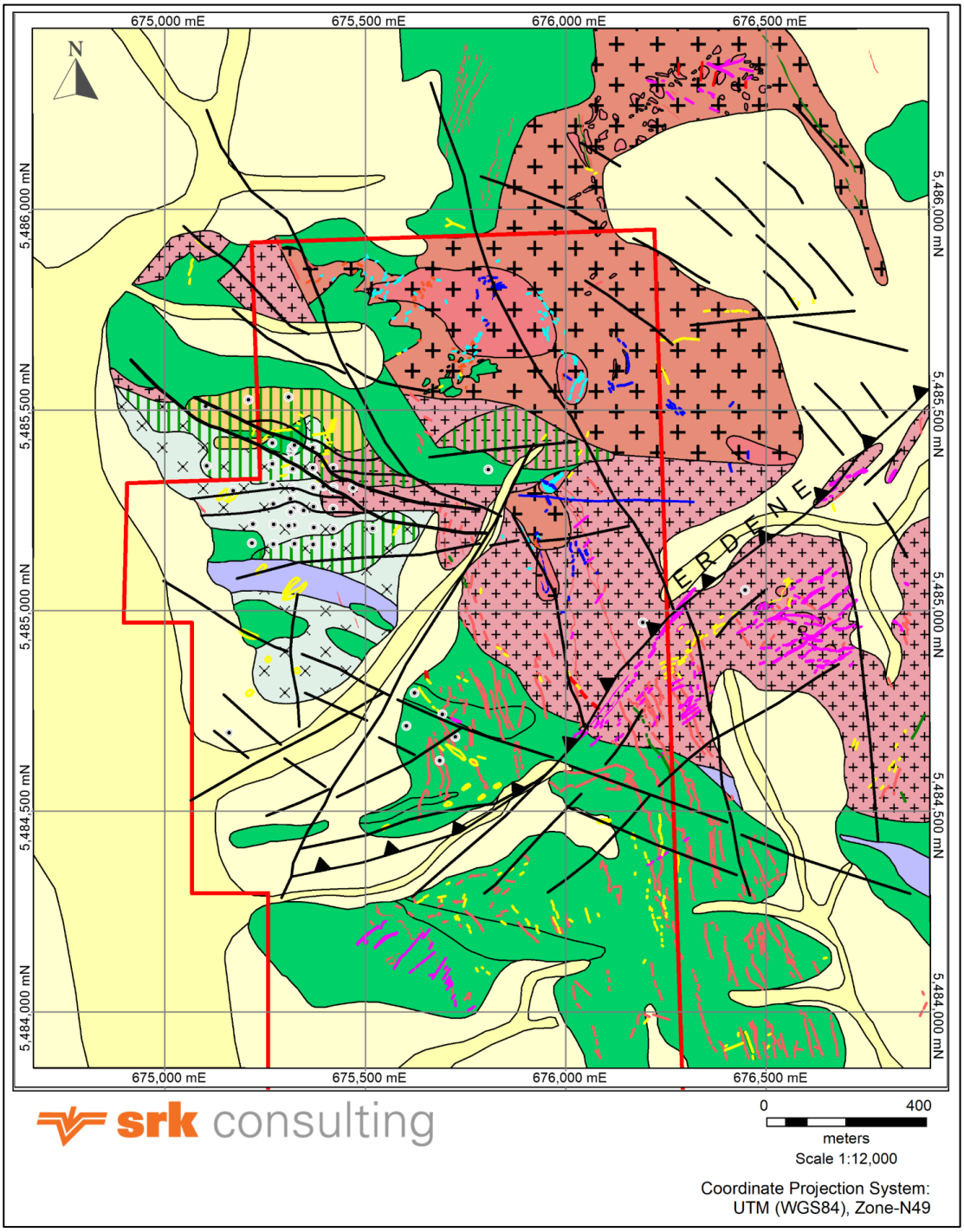

Figure ES-3: Project geology map

Source: SG modified by SRK (2020)

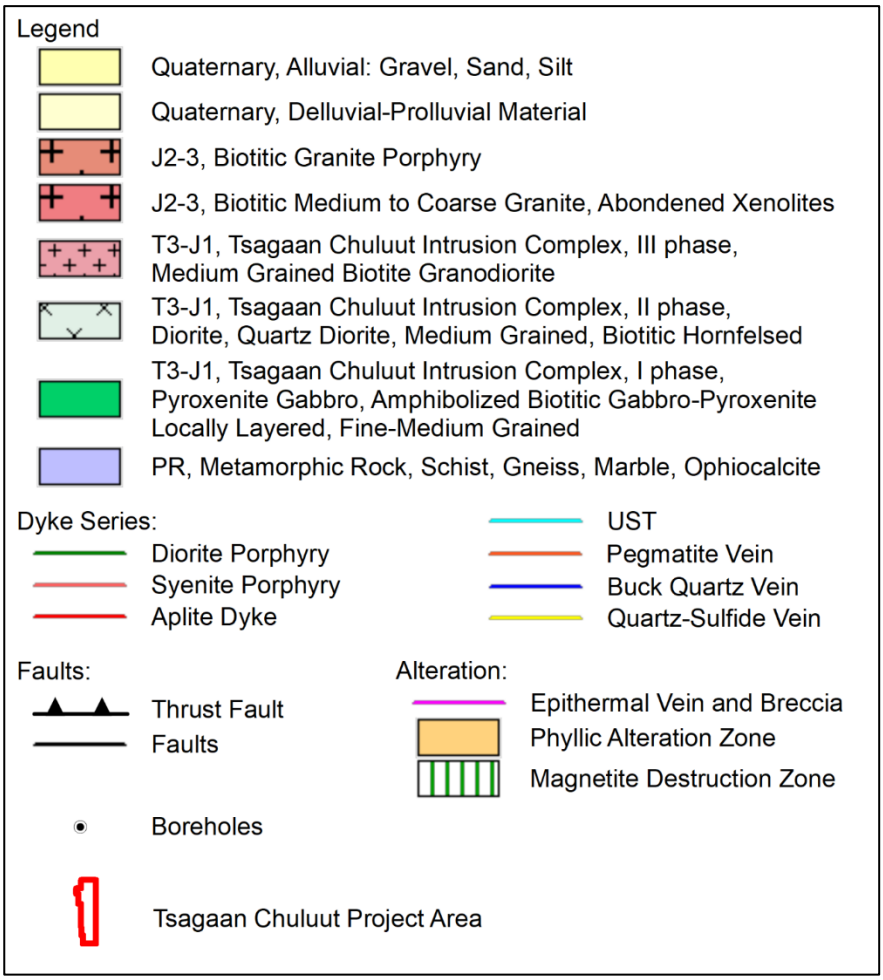

Figure ES-4: Legend of Project geology map

Source: SG modified by SRK

Breccia textures

Breccias are polymictic and occur as several different types. The two main facies are a matrix-supported breccia, open space breccia with granodiorite and an open space breccia with quartz cement. A contact breccia occurs at the contact of granodiorite and is typically matrix supported and dominantly cemented by hydrothermal quartz and occasional large pyrite blebs. Hydrothermal breccias are typically open space (crackle) breccia with quartz cement, occasionally with sulphides and Mn-Fe oxides. Hydrothermal breccias are observed in gabbrodiorite, gabbromonzonite, diorite, diorite porphyry, quartz diorite porphyry and also overprint earlier contact and intrusive breccia bodies.

Alteration

SRK noted that the Tsagaan Chuluut geology map shows a footprint of demagnetised zones, phyllic alteration; however, detailed alteration mapping has not yet been carried out. SRK reviewed alteration records in lithology core logs, observations from the petrology studies and geophysical data images. Based on a review of this data/information, SRK has a low level of confidence in the currently 'mapped' demagnetised zones and phyllic zones. Although areas of epidote and actinolite (propylitic alteration) are mapped, they do not coincide with the main demagnetised zones (as would be expected). The magnetic, resistivity, chargeability and metal factor data suggest intense, multi-stage and extensive alteration. The Project area mainly consists of three igneous rock types, which leads to variations in the magnetic and induced polarisation (IP) responses that reflect original differences in rock composition or intensity of alteration.

The responses reflect variations in three factors:

- Magnetite content
- Presence of sulphide (massive or disseminated)
- Degree of quartz veining.

Based on the petrological description of alteration minerals and core photo reviews, SRK opines that alteration zones of potassic, phyllic and propylitic alteration are present at Tsagaan Chuluut. SRK recommends further alteration evaluation studies, including infrared spectrometry core logging aimed at identification of clay minerals and improved alteration zone mapping, be carried out.

Alteration occurs pervasively through host rocks and/or as selvages/haloes associated with vein development (vein-type). Vein-type alteration and six generations of veining have been described in detail by Bond et al. (2013).

Mineralisation and Deposit Model

Minarco (2011) and Bond et al. (2013) have provided differing genetic deposit models for gold mineralisation at the Project. Minarco (2011) described the following three styles of mineralisation in the Project tenements:

- Porphyry gold-copper mineralisation
- Low sulphidation epithermal gold mineralisation along regional fault structures
- Quartz, sericite, carbonate (ankerite) and pyrite-related)-related gold mineralisation.

Minarco interpreted the mineralisation as a series of sheeted and parallel lower sulphidation, epithermal quartz and sericite veins. Mineralisation in the area is best developed within a brecciated pre-existing bucky quartz vein and in open space breccias aligned with east–west-trending zones dipping to the south at angles ranging from 30° to 40°. The confirmed strike length of the mineralisation zones is over 300 m and mineralisation is open along the flanks. Mineralisation was drill tested to a depth of 300–350 m, which has an approximate elevation ranging from 60 m to 1,000 m. From this drilling, mineralisation is observed to be 120–130 m thick with the grade ranging from 0.81 to 1.96 g/t Au.

Bond et al. (2013) interpreted the Project as a Reduced Intrusion Related Gold System (RIRGS). Bond et al. (2013) described from core samples limited gold mineralisation in third generation beresite veins and majority of gold mineralisation hosted within fifth generation veins. As no core orientation was carried out, Bond et al. (2013) noted that it was not possible to describe the orientation and spatial relationship of veining and mineralisation.

From a review of structural logging and core photos, SRK observes that mineralisation is hosted by quartz diorite porphyry and hydrothermal breccias, with thin quartz veinlets developed locally. SRK noted that the two veinlet systems described by Bond et al. (2013) do not appear to show lateral continuity and opines that both gold-bearing veinlet sets are developed during hydrothermal alteration in breccia bodies. The hydrothermal breccias are spatially related to zones of faulting and shearing. Structure data suggest steep dipping to the southwest and south at angles between 60° and 70°. The continuity, structure and alteration in these zones should be tested by oriented infill drilling to a depth of 200 m.

Within the quartz diorite porphyry system, the drill core highlights quartz vein occurrences typically in the upper part of the system, whereas in the deeper part of the quartz diorite porphyry, diorite and granodiorite, veinlets with carbonate or quartz were only erratically recorded.

SRK favours a gold porphyry model such as described by Sillitoe (2000), associated with the Late Triassic to Early Jurassic Tsagaan Chuluut Igneous Complex, with a hydrothermal alteration and geochemical overprint occurring with the intrusion of later Middle to Late Jurassic granodiorite/s.

Exploration

The several phases of exploration works have been carried out at the Project over a 17-year period between 1997 and 2014. The exploration work has included:

- Topographic survey completed for 105 ha of the Project area
- Geological mapping carried out at 1:5,000 and 1:2,000 scales across 456.68 ha of the Project area
- Geophysical surveys:
  - Ground magnetic survey at 1:5,000 scale – 74.2 line-kilometres with spaced 50 m
  - 20 IP sections at 1:10,000 – 35.0 line-kilometres
- Trenching and drilling including:
  - Trenching – a total length of 1,271.4 m
  - Drilling – 17 reverse circulation (RC) holes for 1,256 m and 35 diamond core drill holes for length of 9,422.9 m
  - All trenches and drill holes were logged and photographed.
- Hydrogeological study
- Sampling:
  - Trench channel – 260 samples
  - Rock chip – 372 samples
  - Soil – 1,050 samples
  - Petrography – 38 samples
  - RC chip – 553 samples
  - Core – 4,533 samples
  - Quality Assurance and Quality Control (QA/QC) samples – 99 blanks, 200 duplicates and 120 certified reference materials (CRMs)
- Laboratory analyses:
  - Fire assay with atomic absorption – 5,505 samples
  - Inductively coupled plasma-optical emission spectrometry (ICP-OES) after 4 acid digest – 5,505 samples
- Density measurements – a total of 1,772 samples.

Mineral Resource estimates

SG supplied two Mineral Resource estimates. The initial Mineral Resource estimate conducted by Micromine (2012) was prepared at the conclusion of an exploration program in 2012 and the second Mineral Resource estimate prepared by Runge Pincock Minarco Ltd (RPM) was carried out in 2014 as an update, following the collection of additional exploration data in 2013.

The Micromine (2012) Mineral Resource estimate, prepared to the JORC Code (2004 Edition)

guidelines, was based on 46 boreholes (17 RC and 29 diamond core drill holes) completed up to 2012. The Mineral Resource estimate is provided in Table ES-2. Micromine did not discuss the reasonable prospects of eventual economic extraction and did not state mining and processing assumptions for determining a cut-off grade for Mineral Resource reporting.

Table ES-2: Mineral Resource statement for the SG Tsagaan Chuluut Project (only Mineral Resources within tenement 15436A are included)

Cut-off grade (ppm Au)	Density (t/m^3)	Volume (m^3)	Mass (t)	Grade (ppm Au)	Contained metal		Classification
					(tr oz)	(t)	
0.3	2.81	4,680,000	13,200,000	0.54	229,000	7.1	Indicated
	2.80	1,880,000	5,350,000	0.52	90,000	2.8	Inferred
	2.80	6,550,000	18,500,000	0.54	319,000	10	Total

Source: Micromine (2012)

For the RPM (2013) Mineral Resource estimate, the total database consisted of 47 boreholes (17 RC and 35 diamond drill holes). The Mineral Resource estimate was based on 3 RC and 24 diamond core drill holes. The Mineral Resource estimate is provided in Table ES-3. As required by the JORC Code (2012), RPM discussed the reasonable prospects of eventual economic extraction and considered lack of infrastructure the main risk for the Project. Mining and processing assumptions used for determining the cut-off grade for Mineral Resource reporting were not stated.

Table ES-3: Mineral Resource estimate as at February 2014

Cut-off grade (ppm Au)	Indicated			Inferred			Total		
	Tonnes (Mt)	Grade (g/t Au)	Metal (oz)	Tonnes (Mt)	Grade (g/t Au)	Metal (oz)	Tonnes (Mt)	Grade (g/t Au)	Metal (oz)
0.7	4.7	1.1	163,500	1.2	1.2	44,600	5.8	1.1	208,200

Source: RPM (2014)

Metallurgy

SRK reviewed metallurgical test reports provided by SG. In 2013, initial, limited or preliminary metallurgical tests were carried out to evaluate the potential for gravity, flotation and cyanide leach processing of the TC1 deposit mineralisation. The initial testing was undertaken by four organisations: Gekko, SGS, Yantai Xinhai Institute and Hepta. In July 2019, a bulk sample was tested by Technology Research Centre of Mongol Alt (MAK) LLC. The results are briefly summarised below.

Gekko (January 2013) gravity and flotation

The combined gravity and flotation testwork indicated a recovery of 87% gold, at a grade of 11.59 g/t Au, and 95.6% of sulphur, at a grade of 12.26% S into a mass yield of 6.8%.

SGS (February 2013)

The ore was amenable to sulphide flotation with high recoveries of gold and sulphur. Gold and sulphur recoveries of 90% to 96%, and >98%, respectively, were achieved into concentrates containing about 4% to 8% of the mass. However, the low grade of the ore samples limited rougher concentrate gold grades to a maximum of 13 g/t Au. It may be possible to upgrade the concentrates further by incorporating cleaning stages into the flotation scheme.

A cyanide leach on the bulk flotation concentrate, which contained 8 g/t Au and 12 g/t Ag, achieved 92% gold and 40% silver recovery. This revealed that the gold present in the ore was not of a refractory nature as had been previously indicated by SG.

Yantai Xinhai Institute (September 2013)

The gold recovery by leaching was up to 73.17% at a particle size of -200 mesh (74 microns). Gold yield improves to 85.41% after application of NaOH (sodium hydroxide).

Hepta (September 2013)

Hepta conducted gravity/flotation testing followed by cyanide roll bottle leach test on a flotation concentrate. The flotation stage yielded a 2.8 kg (yield 2.9%) concentrate with grade of 14.2 ppm Au. In total, 93.8% of gold was recovered by flotation.

The leaching by NaCN (sodium cyanide) indicated a range of 65.6% to 89.1% from the flotation tail.

Technology Centre MAK LLC (July 2019)

The bulk sample, with a total weight of 165.4 kg and a gold grade of 1.05 g/t, was tested by column leach method by solution of NaCN at a concentration of 500 mg/L. After 23 days of leaching, the gold recovery achieved was 74.17% and NaCN consumption was 0.43 kg/t.

SRK Mineral Resource verification

SRK used structurally controlled grade shells generated in Leapfrog™ software to model the domains for constraining the block grade estimation.

RPM prepared mineralisation wireframes as hard boundaries from sectional outlines were manually triangulated to form wireframes. To form ends to the wireframes, the end section strings were copied to a position midway to the next section or to 25 m and adjusted to match the dip, strike and plunge of the zone. The grade cut-off for modelling the wireframes is 0.5 ppm Au in the RPM model.

Mineralisation interpretations were prepared by SRK using a nominal 0.1 g/t Au cut-off grade and a minimum downhole width of 2m.

For blocks in the mineralised domain, block grades and densities were estimated by Ordinary Kriging (OK).

The vast majority of the Tsagaan Chuluut deposit is fresh rock and with a bulk density value 2.84 g/m^3 (Section 7.9). Density was interpolated into the block model using OK. Density values were estimated into 10 × 10 × 5 m parent cells, using a constraint that only density values between 1.5 g/m^3 and 3 g/m^3 be used in the model.

From the block model, the grade-tonnage results were calculated for a series of grade cut-offs (Table ES-4). The curves show that the deposit tonnage is sensitive to cut-off grade, which is demonstrated by a steep decrease of tonnage with increasing grade.

Table ES-4: Grade-tonnage results

Cut-off grade (g/t Au)	Volume (m^3 `000)	Tonnes (kt)	Average grade (g/t Au)	Contained gold	
				(koz)	(t)
0.1	12,816.7	32,082.0	0.48	495.11	15.40
0.2	11,203.9	28,888.2	0.52	467.93	15.02
0.3	8,006.7	21,547.0	0.61	409.42	13.14
0.4	5,623.1	15,162.9	0.72	329.80	10.92
0.5	4,192.6	11,332.6	0.81	295.13	9.18
0.6	3,164.3	8,564.3	0.9	247.82	7.71
0.7	2,434.4	6,594.9	0.98	207.79	6.46
0.8	1,742.2	4,725.9	1.07	162.58	5.06

Cut-off grade (g/t Au)	Volume (m^3 `000)	Tonnes (kt)	Average grade (g/t Au)	Contained gold	
				(koz)	(t)
0.9	1,245.3	3,378.6	1.16	126.01	3.92
1	871.7	2,364.4	1.26	95.78	2.98
1.1	534.1	1,454.5	1.39	65.00	2.02
1.2	374.1	1,017.5	1.5	49.07	1.53
1.3	251.0	682.0	1.63	35.74	1.11
1.4	183.8	498.1	1.73	27.70	0.86
1.5	142.7	387.5	1.82	22.68	0.71
1.6	102.1	277.6	1.93	17.23	0.54
1.7	71.0	193.3	2.05	12.74	0.40
1.8	51.8	141.3	2.17	9.86	0.31
1.9	38.9	105.9	2.28	7.77	0.24
2	30.7	83.7	2.37	6.38	0.20

Estimated blocks were classified based on criteria derived from variography. The principal criterion for assigning the Mineral Resource classification was the maximum drill hole spacing compared with the gold variogram range.

Classification was based on the following criteria:

- In the block between 675250E and 675440E, where the closer-spaced drilling exists, all wireframes were treated as semi-soft boundaries (higher-grade to lower-grade domains as soft and lower-grade to higher-grade domains as hard). For all estimation purposes, the Mineral Resources inside the 0.1 ppm Au domains and above an elevation of 750 m above sea level were classified as Indicated.
- In the block outside the 675250E-675440E, where drilling is sparser, the Mineral Resources inside the 0.1 ppm Au domains were classified as Inferred.

To assess reasonable prospects of eventual economic extraction, SRK applied the following assumptions:

- Mining cost (open pit mining) US$2.5/t
- Processing Cost (gravity/flotation) US$13/t
- Gold price US$38.5/g
- Processing yield 82%
- Water availability from adjacent streams, where placer mines are operating.

The Mineral Resource estimates for the Tsagaan Chuluut deposit are reported at a cut-off grade of 0.4 ppm Au.

Cut-offs were calculated using the following formula:

Cut-off = Processing cost (US$/t ore)/(Recovery * Gold price (US$/g))

0.4 ppm Au = (US$13/t ore)/(82% * US$38.5/g))

The results of SRK's verification of the Tsagaan Chuluut Gold Project Mineral Resource estimates are shown in Table ES-5.

Table ES-5: Tsagaan Chuluut deposit verification estimate as at May 2020

Category	Cut-off grade (g/t Au)	Volume (m^3 `000)	Tonnes (kt)	Average grade (g/t Au)	Contained gold	
					(koz)	(t)
Indicated	0.4	4,556.5	12,278.5	0.73	298.83	9.00
Inferred		1,053.5	2,847.3	0.69	65.10	1.96
Total		**5,610.0**	**15,125.8**		**363.93**	**10.96**

In summary, at the same cut-off grade, the RPM (2014) model shows a lower volume and tonnage, a higher average grade and a lower tonnage of contained gold metal whereas the SRK model shows a higher volume and tonnage, a lower average grade and a higher tonnage of contained gold metal. The deposit remains open along the flanks.

The SRK model differs from RPM model in structural control, natural cut-off 0.1 ppm Au grade shell and modelled bulk density with exclusion of densities below 1.5 t/m^3 and above 3 t/m^3.

A comparison between the 2014 RPM estimate and 2020 SRK estimate is shown in Table ES-6.

Table ES-6: Summary of Mineral Resource estimation comparison – RPM vs SRK

Cut-off grade (g/t Au)	2014 RPM estimate			2020 SRK estimate		
	Average grade (g/t Au)	Contained gold		Average grade (g/t Au)	Contained gold	
		(koz)	(t)		(koz)	(t)
0.40	1.05	224.68	6.68	0.72	329.80	10.92
0.50	1.05	223.78	6.62	0.81	295.13	9.18
0.60	1.07	219.79	6.4	0.90	247.82	7.71
0.70	1.11	208.18	5.84	0.98	207.79	6.46

Exploration upside

SRK opines that Tsagaan Chuluut Gold Project has significant exploration upside. Based on SRK's assessment of the Project area, several target areas were highlighted for follow-up investigation. Targeting was based on a combination of geological, geochemical and geophysical vectors and the limited drilling data provided by SG.

RPM (2013) considered the western continuation of TC1 deposit as an Exploration Target and estimated a target range for the grades and tonnages. In addition to the TC1 West target, RPM (2014) reports quartz-sulphide mineralisation of lesser intensities in the Altan Chuluut area exposed in marmot holes and hand-dug trenches. One DD (diamond) and 10 RC holes have been drilled at this target, with results being 80 m at a grade of 0.47 g/t Au. The RPM Exploration Targets are summarised in Table ES-7.

Table ES-7: RPM Exploration Targets

TC1 West		
	Low grade	**High grade**
Tonnage (Mt)	18.5	8.5
Grade (g/t Au)	0.5	1.5
Gold (t)	10	13
Altan Tsagaan Chuluut		
	Low grade	**High grade**
Volume of Target Model (Mm^3)	11.5	11.5
Proportion mineralised	Two thirds	One third
Volume of Target Model Mineralised (Mm^3)	7.6	3.8
Density	2.83	2.83
Tonnage of Target Model Mineralised (Mt)	21.7	10.8
Grade (g/t Au)	0.5	2.5
Gold (t)	11	27

SRK's review of the Project has highlighted a strong regional northwest-striking control to the mineral potential of the region associated with the Tsagaan Chuluut Fault and subparallel subordinate faults, as well as the related east–west faults and breccia zones. Zones of intersecting northeast-striking structures are additionally considered to be important structural features to the mineral potential. Gold mineralisation is primarily hosted within a quartz diorite porphyry intrusion as well as in hydrothermal breccias. Quartz and quartz-sulphide veins additionally provide indication of gold mineralisation and potentially indicate high-grade zones. Preliminary alteration of potassic, phyllic and argillic alteration indicate potential target zones. Propylitic alteration is considered a marker for the more distal parts of the mineralised system. A combination of these vectors/exploration criteria were used to identify targets during a phase of mineral potential analysis for follow-up investigation.

The relative importance of each of these exploration criteria to the mineralisation potential was then ranked from 1 to 2, with 2 being the highest.

Based on the available data and rankings applied to the key exploration criteria, areas in the northern part of the licence show the highest mineralisation favourability, while areas to the south and outside of the lease extents are shown to have lower mineralisation favourability. It should be noted that data coverage is variable over the licence and surrounding area, which leads to lower exploration favourability for this review.

From the mineral potential mapping, 15 target areas worthy of follow-up field-based exploration were identified (see Figure ES-5). Each of these targets has been ranked as Priority 1 or Priority 2 targets based on the derived mineral favourability in these areas (warmer colours). Each of the coincident exploration criteria observed to occur in each target area is summarised in Table ES-8, indicating the criteria are enclosed within the target area ['P' denotes a partial overlap within that target area].

Table ES-8: Summary of exploration target areas

Target ID	1	2	3	4	5	6	7	8	9	10	11	12	13	14	15
Target rank	1	1	1	1	2	2	2	2	2	2	2	2	2	2	2
Resistivity margin	Y	P	P	P	Y	Y		Y							
Chargeability margin	P	Y	Y	P	P	Y		P							
Demagnetised zone	Y	Y		P											
50 m of local faults	P	Y	P	P	P	Y	P								
Regional faults (100 m)									P	P	P	P	P		
Regional faults (300 m)	P			P				Y			P	P	P	P	
Favourable lithology	Y	P	Y	Y	Y		Y	Y		Y	Y	Y	Y	Y	Y
Favourable alteration	Y	Y	Y		P	Y	Y	Y							
Hydrothermal breccia	P														
Intrusive breccia	P														
Quartz veining	Y	P	P	Y	Y	P	Y		Y	Y					Y
Au geochemistry	P			P				Y	P					Y	
Cu geochemistry			P				Y		Y						
Pb geochemistry		P	Y		Y										
Zn geochemistry	P			P	Y						Y	P			Y

Targets 1 to 4 are shown to have the highest mineral potential and occur in the northern part of the Project area. Each of these four targets show several overlapping favourable exploration criteria inclusive of proximity to faults, presence of favourable alteration, favourable host lithology, geochemical signatures in soils (e.g. Au, Cu, Pb or Zn) as well as the presence of quartz veining at surface. Each of these Priority 1 targets occurs at least in part along the margin of coincident IP chargeability and resistivity anomalies, which are interpreted to be favourable indicators for mineralisation. Targets 5 and 6 show many of these same exploration features, but rank slightly lower based on the derived maps with fewer overlapping criteria defined.

Targets 9 to 15 lie outside of the extents of the current IP and magnetic datasets and these exploration criteria therefore cannot be applied in these zones. These targets show favourable geochemistry, lithological host and structural features, which highlight their potential.

The target locations are shown on Figure ES-5.

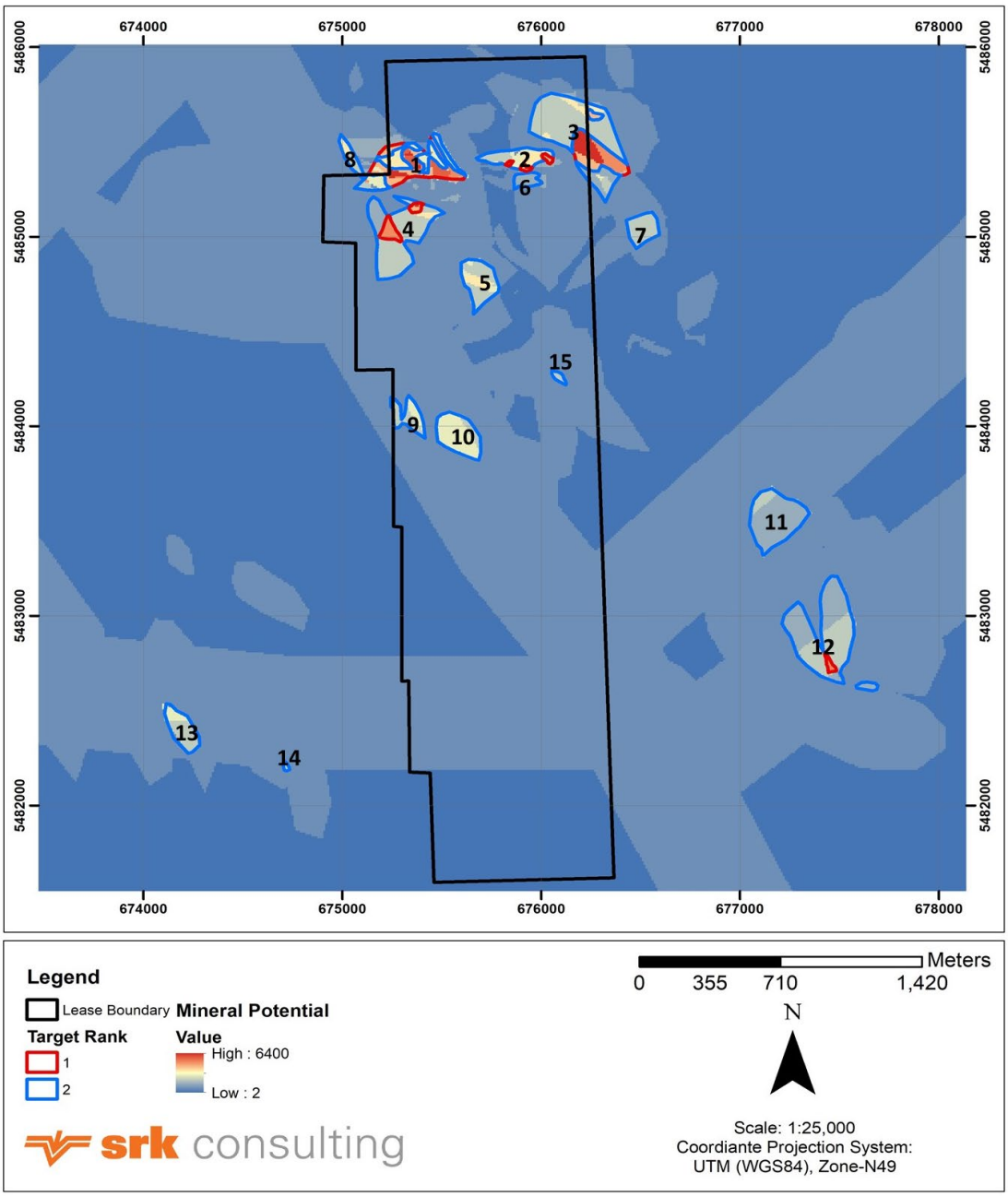

Figure ES-1: Tsagaan Chuluut derived exploration mineral potential map

Conclusion and recommendations

The Tsagaan Chuluut is an advanced exploration project with an identified Indicated and Inferred Mineral Resources. SRK estimated an Indicated Mineral Resource of 12,278 kt grading at 0.72 g/t Au, containing 8.84 t of gold metal (293.8 koz) and an Inferred Mineral Resource of 2,847 kt grading at 0.69 g/t Au, containing 1.96 t of gold metal (65.26 koz). The Total Mineral Resource is 15,125 kt containing 10.81 t of gold metal (358.94 koz). The TC1 deposit remains open along the flanks.

In addition to the Mineral Resource, SRK identified an additional 15 exploration targets which warrant further evaluation.

SRK makes the following recommendations:

TC1 deposit – High-grade test drilling

- Conduct an two phase infill fully cored drilling program aimed at testing high-grade structures/zones, with target depths of 135 m to 250 m from an initial 6,360 m drill program. The infill drill holes should be oriented.
- Conduct a structural study of the new drill holes and across the broader TC1 area.
- Log the additional drill holes by infrared spectrometry in order to identify alteration minerals and better define zones of alteration.
- Conduct additional petrology studies from drill hole samples in the high-grade zones.

Table ES-9: Proposed infill drilling – Phase 1

Borehole ID	X	Y	Z	Designed depth (m)	Azimuth (°)	Dip (°)
DDH20_001	675443.17	5485310.29	982.14	140	0	60
DDH20_002	675441.93	5485282.07	977.60	190	0	60
DDH20_003	675418.67	5485282.60	978.39	150	0	60
DDH20_004	675421.51	5485326.63	986.42	135	0	60
DDH20_005	675396.83	5485331.60	990.23	155	0	60
DDH20_006	675396.30	5485308.16	984.83	180	0	60
DDH20_007	675395.59	5485285.80	980.35	185	0	60
DDH20_008	675396.30	5485259.52	974.74	225	0	60
DDH20_009	675370.02	5485287.22	982.65	205	0	60
DDH20_010	675368.60	5485336.58	994.73	155	0	60
DDH20_011	675342.68	5485333.03	998.25	180	0	60
DDH20_012	675344.46	5485306.03	989.82	220	0	60
DDH20_013	675345.17	5485282.25	981.81	240	0	60
DDH20_014	675323.14	5485284.02	980.71	240	0	60
DDH20_015	675318.89	5485332.32	995.63	200	0	60
DDH20_016	675293.67	5485339.77	990.41	200	0	60
Total				**3,000**		

Table ES-10: Proposed infill drilling – Phase 2

Borehole ID	X	Y	Z	Designed Depth (m)	Azimuth (°)	Dip (°)
DDH20_017	675444.00	5485257.00	973.65	200	0	60
DDH20_018	675444.00	5485233.00	970.38	200	0	60
DDH20_019	675419.38	5485233.60	970.27	200	0	60
DDH20_020	675395.23	5485236.80	970.57	210	0	60
DDH20_021	675372.15	5485239.64	971.33	250	0	60
DDH20_022	675293.67	5485288.28	979.65	240	0	60
DDH20_023	675294.73	5485311.72	985.92	200	0	60
DDH20_024	675294.73	5485363.92	989.09	185	0	60
DDH20_025	675314.98	5485376.70	989.26	135	0	60
DDH20_026	675266.68	5485389.49	984.69	155	0	60
DDH20_027	675268.46	5485344.74	986.92	210	0	60
DDH20_028	675269.88	5485293.60	977.73	200	0	60
DDH20_029	675241.12	5485293.25	974.83	200	0	60
DDH20_030	675243.25	5485318.11	980.60	230	0	60
DDH20_031	675245.37	5485346.51	984.84	200	0	60
DDH20_032	675246.80	5485369.60	985.01	180	0	60
DDH20_033	675243.96	5485387.71	983.56	165	0	60
Total (m)				**3,360**		

Exploration target areas

- Conduct alteration mapping of the target areas.
- Carry out age dating of the intrusive rocks, whole-rock analyses and inductively coupled plasma-mass spectrometry (ICP-MS) geochemical and rare earth element (REE) analysis of the intrusive rock suite to improve understanding of intrusive events, magma composition and classification and understanding of geotectonic affinity.
- Conduct structural geology mapping.
- Based on alteration and structural mapping and intrusive rock studies, update the current exploration target evaluations, then design and carry out a scout drilling program.
- Apply for (or acquire) additional exploration tenure on the western and eastern flanks of the Project to extend coverage over currently defined exploration targets.

Table of Contents

Executive Summary ii
Disclaimer xxv
List of Abbreviations xxvi
1 Introduction and Scope of Report 1
2 Program Objectives and Work Program 2
2.1 Program objectives 2
2.2 Reporting standard 2
2.3 Work program 2
2.4 Project team 3
2.5 Statement of SRK independence 3
3 Project General Description 4
3.1 Licence 5
4 Regional Geology 7
4.1 Mongol-Okhotsk Ocean 7
4.1 Regional Geology of Tsagaan Chuluut Gold Project 10
5 Local Geology 14
5.1 Stratigraphy 14
5.2 Magmatism 14
5.3 Structure and Tectonics 15
5.4 Project area geology 16
5.4.1 Structure 16
5.4.2 Lithology descriptions 18
5.4.3 Alteration 26
5.4.4 Alteration with veining 29
6 Mineralisation 41
6.1 Porphyry – epithermal mineralisation system (Minarco, 2011) 41
6.2 Reduced Intrusion Related Gold System 43
6.3 TC1 deposit area 43
6.3.1 Mineralogy and Geochemistry 50
6.4 Genetic Model summary 55
7 Exploration 56
7.1 Geology mapping 56
7.2 Topographical survey 57
7.3 Geophysical survey 58
7.4 Surface geochemical mapping 59
7.5 Trenching 59
7.6 Drilling 60

7.7 Sampling 68
7.8 Analytical methods 71
7.9 Density data 71
7.10 Quality Assurance/Quality Control and Data Verification 73
8 Mineral Resource Estimate Review 84
8.1 Micromine 2012 Mineral Resource estimate 84
8.2 RPM 2014 Mineral Resource estimate 84
8.2.1 Geology interpretation, wireframes and digital terrain models 84
8.2.2 Domain statistics and geostatistics 86
8.2.3 Block Model 89
8.2.4 Density and Material Type 90
8.2.5 Model Validation 90
8.2.6 Mineral Resource Classification 90
8.2.7 Reasonable Prospects of Eventual Economic Extraction 91
8.2.8 Mineral Resource Reporting 91
8.3 Metallurgy 92
8.3.1 Gekko (January 2013) 92
8.3.2 SGS (February 2013) 93
8.3.3 Yantai Xinhai Institute (September 2013) 94
8.3.4 Hepta (September 2013) 94
8.3.5 Technology Research Centre MAK LLC 94
8.4 SRK Mineral Resource verification on TC1 94
8.4.1 Modelling of the mineralisation domain 94
8.4.2 Grade shell thresholds 95
8.4.3 Weathering Wireframes 96
8.4.4 Geostatistical Estimation 97
8.4.5 Statistical analysis 97
8.4.6 Variogram Modelling 99
8.4.7 Block Model 100
8.4.8 Ordinary Kriging 100
8.4.9 Validation 101
8.4.10 Density Estimate 103
8.4.11 Grade-tonnage results 103
8.4.12 Verification estimate categories 105
8.4.13 Tsagaan Chuluut Project Verification estimate 106
9 Exploration Upside 108
9.1 Exploration vectors for porphyry-style mineralisation 108
9.1.1 Geological vectors 108
9.1.2 Geochemical vectors 108
9.1.3 Geophysical vectors 108

9.2 Exploration Potential 108
9.3 Exploration Potential Mapping 109
10 Conclusions and Recommendations 116
11 References 119

List of Tables

Table 2-1: SRK Project team 3
Table 3-1: Tsagaan Chuluut-1 mining licence details 5
Table 3-2: Coordinates of the Tsagaan Chuluut-1 mining licence 5
Table 5-1: Petrology study results (2002) 22
Table 5-2: Petrology study results - breccia (Stockley, 2002) 23
Table 5-3: Petrology study results - intrusive (Stockley, 2002) 23
Table 5-4: Petrology study results (Batulzi, 2005) 24
Table 5-5: Petrology study results (Bond et al., 2013) 25
Table 5-6: Mineral paragenesis in veins 29
Table 6-1: Statistics of selected elements 50
Table 6-2: Correlation of selected elements 51
Table 6-3: Selected elements normalised value 51
Table 6-4: Mineralogical composition from mineralised rock submitted for metallurgical testing 52
Table 6-5: Statistics of selected elements for hydrothermal, intrusive and contact breccia types 53
Table 6-6: Statistics of selected elements for rock types 54
Table 7-1: Summary of RC holes drilled in 2005 62
Table 7-2: Summary of drill holes drilled in 2012 63
Table 7-3: Summary of drill holes drilled in 2013 and 2014 64
Table 7-4: Attributes recorded in geological and geotechnical logging sheets 67
Table 7-5: Number of samples in 2012 and 2014 69
Table 7-6: Incorrect density values for rock types 73
Table 7-7: Summary of QA/QC samples from the 2005 and 2012 exploration drilling programs 73
Table 7-8: Certified values of CRMs and sample numbers from the 2012 exploration drilling program 75
Table 8-1: Mineral Resource statement for the Tsagaan Chuluut Gold Project TC1 Area (only Mineral Resources within tenement 15436A included) 84
Table 8-2: Grade-tonnage table using varying cut-off grades (only Mineral Resources within Tenement 15436A are included) 84
Table 8-3: Summary statistics for 1 m composites 86
Table 8-4: Summary of top-cuts applied 87
Table 8-5: Kriging parameters applied in Mineral Resource estimation 88
Table 8-6: Block model parameters 89
Table 8-7: Search and kriging parameters 90
Table 8-8: Mineral Resource estimate as at February 2014 92
Table 8-9: Leapfrog parameters of Au 0.1 ppm domain 96

Table 8-10: Summary statistics for composites and capped composites (ppm) 97
Table 8-11: Variogram model parameters 100
Table 8-12: Block model dimensions 100
Table 8-13: Kriging neighbourhood parameters 101
Table 8-14: Statistics for estimated block grades vs composites at zero cut off 101
Table 8-15: Grade-tonnage results 103
Table 8-16: Tsagaan Chuluut verification estimate as at May 2020 107
Table 8-17: Comparison between RPM and SRK Mineral Resource estimates 107
Table 9-1: RPM exploration target areas 109
Table 9-2: Exploration criteria and applied weight 111
Table 9-3: Exploration Target summary 113
Table 10-1: Proposed infill drilling – Phase 1 116
Table 10-2: Proposed infill drilling – Phase 2 117

List of Figures

Figure ES-5: Tsagaan Chuluut derived exploration mineral potential map xvi
Figure 3-1: Project location map 4
Figure 3-2: Licence Map 6
Figure 4-1: Project location in CAOB context 9
Figure 4-2: Mongolia terrane subdivision with project location 10
Figure 4-3: Regional geology map with Project location 12
Figure 4-4: Legend to regional geology map 13
Figure 5-1: Local geology map 15
Figure 5-2: Interpreted faults on the RTP magnetic image 16
Figure 5-3: Project geology map 17
Figure 5-4: Legend of Project geology map 18
Figure 5-5: Main lithotypes of Tsagaan Chuluut Project 19
Figure 5-6: Breccia types 21
Figure 5-7: Alteration map of project area 27
Figure 5-8: Alteration styles 28
Figure 5-9: Gold distribution in soil and rock chips samples 31
Figure 5-10: Silver distribution in soil and rock chips samples 32
Figure 5-11: Arsenic distribution in soil and rock chips samples 33
Figure 5-12: Bismuth distribution in soil and rock chips samples 34
Figure 5-13: Copper distribution in soil and rock chips samples 35
Figure 5-14: Molybdenum distribution in soil and rock chips samples 36
Figure 5-15: Lead distribution in soil and rock chips samples 37
Figure 5-16: Antimony distribution in soil and rock chips samples 38
Figure 5-17: Tungsten distribution in soil and rock chips samples 39
Figure 5-18: Zinc distribution in soil and rock chips samples 40

Figure 6-1: Exploration targets identified by Minarco 42
Figure 6-2: 3D distribution of gold mineralisation as well as hydrothermal breccia (black) and porphyry distributions (pink) 44
Figure 6-3: 3D distribution of hydrothermal breccia development (black) and faults (tan)....45
Figure 6-4: TC1 deposit geology map 46
Figure 6-5: TC1 deposit - Section CS3 47
Figure 6-6: TC1 deposit - Section CS4 47
Figure 6-7: TC1 deposit - Section CS5 48
Figure 6-8: TC1 deposit - Section CS6 48
Figure 6-9: TC1 deposit - Section CS7 49
Figure 6-10: TC1 deposit - Section CS8 49
Figure 7-1: Location of area of topographic and ground magnetic survey areas and IP dipole-dipole profiles across the TC1 deposit area 57
Figure 7-2: Total magnetic intensity map 58
Figure 7-3: Locations of geochemical samples and trenches 60
Figure 7-4: Location of RC and core drill holes at Tsagaan Chuluut Gold Project 61
Figure 7-5: Twinned holes with gold grade on Section 6 64
Figure 7-6: Collars of TCDD-028 and TCDD-040 (facing north) 65
Figure 7-7: 3D view of TCDD-019 and TCDD-041 (facing north) 66
Figure 7-8: Histogram for sample interval length 69
Figure 7-9: Histogram for bulk density of measured samples 72
Figure 7-10: Performance of blanks 74
Figure 7-11: Performance of OREAS-501 76
Figure 7-12: Performance of OREAS-502 76
Figure 7-13: Performance of OREAS-503 77
Figure 7-14: Performance of OREAS-504 77
Figure 7-15: Performance of CRM OREAS-901 78
Figure 7-16: Performance of OREAS-70P 78
Figure 7-17: Performance of RC duplicates in 2005 79
Figure 7-18: Performance of core duplicates in 2012 80
Figure 7-19: Performance of pulp duplicates at ActLabs (gold) 80
Figure 7-20: Performance of SGS's internal CRMs – OxC44 and OxH52 81
Figure 7-21: Performance of ActLabs' internal CRMs – CGS-24 and GS-P7H 82
Figure 7-22: Performance of ActLabs' internal repeats 83
Figure 8-1: Log histogram and log probability plot of raw samples at Tsagaan Chuluut 85
Figure 8-2: 2014 Mineral Resource estimate wireframes in section 675,325mE (facing west) 85
Figure 8-3: Log histogram and log probability log of 1 m composite data – Domain 1 87
Figure 8-4: Downhole and directional semi variograms – Domain 1 88
Figure 8-5: Tsagaan Chuluut 2014 Mineral Resource Classification (facing 245°) (green Indicated and Red Inferred Resource) 91
Figure 8-6: Grade-tonnage curves 92
Figure 8-7: Au 0.1 ppm domain boundary analysis 95

Figure 8-8: View of mineralisation domains from southwest 96
Figure 8-9: Log-transformed histogram – Gold, all data 98
Figure 8-10: Cumulative probability plot of composite grades – all data....99
Figure 8-11: Primary direction variograms for gold 100
Figure 8-12: Section 5 with sample and block grades....102
Figure 8-13: Section 6 with sample and block grades....103
Figure 8-14: Grade vs tonnage curve – gold....104
Figure 8-15: Grade vs troy ounces curve – gold 105
Figure 8-16: Mineral Resource Classification (view from southwest) 106
Figure 9-1: Example exploration criteria used in mineral potential mapping: A) proximity to regional faults, B) alteration style, C) surface geochemical signature, D) chargeability and/or resistivity margin 110
Figure 9-2: Map showing mineral potential at Tsagaan Chuluut....112
Figure 9-3: Geology map of Project area with exploration targets draped....114
Figure 9-4: Legend to geology map of Project area with exploration targets draped 115

List of Appendices

Appendix A: Mining Licence Copy

Disclaimer

The opinions expressed in this Report have been based on the information supplied to SRK Consulting MGL LLC (SRK) by the SG Gold Mining LLC (SG). The opinions in this Report are provided in response to a specific request from SG to do so. SRK has exercised all due care in reviewing the supplied information. While SRK has compared key supplied data with expected values, the accuracy of the results and conclusions from the review are entirely reliant on the accuracy and completeness of the supplied data. SRK does not accept responsibility for any errors or omissions in the supplied information and does not accept any consequential liability arising from commercial decisions or actions resulting from them. Opinions presented in this Report apply to the site conditions and features as they existed at the time of SRK's investigations, and those reasonably foreseeable. These opinions do not necessarily apply to conditions and features that may arise after the date of this Report, about which SRK had no prior knowledge nor had the opportunity to evaluate.

List of Abbreviations

Abbreviation	Meaning
°	Degree (angle)
°C	Degree (Celsius)
3D	Three-dimensional
3SD	Three Standard Deviations
AAS	Atomic absorption spectroscopy
Ag	Silver
ALS	ALS Group Laboratory
As	Arsenic
ASTER	Advanced Spaceborne Thermal Emission and Reflection
Au	Gold
Bi	Bismuth
CAOB	Central Asian Orogenic Belt
CRM	Certified reference material
Cu	Copper
gr	Grams
ha	Hectares
ICP-AES	Inductively coupled plasma-atomic emission spectrometry
ICP-MS	inductively coupled plasma-mass spectrometry
ICP-OES	Inductively coupled plasma-optical emission spectrometry
IP	Induced polarisation
ITR	Independent Technical Review
JORC Code	Australasian Code for Reporting of Exploration Results, Mineral Resources and Ore
koz	Thousand ounces
kt	Thousand tonnes
m	Metres
M	Millions
m^3	Cubic metres
Mo	Molybdenum
MOO	Mongol-Okhotsk Ocean
MRAM	Mongolian Mineral Resources Agency
Mt	Million tonnes
oz	Ounces
Pb	Lead
QA/QC	Quality Assurance and Quality Control
RIRGS	Reduced Intrusion Related Gold System
RPM	Runge Pincock Minarco Ltd
RQD	Rock quality designation
RTP	Reduced to pole
Sb	Antimony
SG	SG Gold Mining LLC
SG Group	SG Group LLC
SGS	SGS-IMME Laboratory
SRK	SRK Consulting MGL LLC
TMI	Total Magnetic Intensity
TC1	Tsagaan Chuluut 1
W	Tungsten
WGS	World Geodetic Survey
Zn	Zinc

1 Introduction and Scope of Report

SG Gold Mining LLC (SG, the Client or the Company) requested SRK Consulting MGL LLC (SRK) to undertake an Independent Technical Review (ITR) on the geology and Mineral Resources of the Tsagaan Chuluut Gold Project (the Project) located in the Dornod Province of Mongolia. SRK was advised that the Report will be initially used for the Company's internal assessment of the Project. As part of the scope of work, SRK was requested to include recommendations for future work that will enable SG, potential equity investors and possible future shareholders to assess the Project..

2 Program Objectives and Work Program

2.1 Program objectives

The objective of the ITR is to provide unbiased assessment of Project's exploration potential, current Mineral Resource estimate and work required to improve the Mineral Resources and progress the Project to next stage of project development.

2.2 Reporting standard

This Report is an Independent Technical Assessment – it is not a Valuation Report and does not express an opinion as to the value of mineral assets, nor to the 'fairness and reasonableness' of any transactions. Aspects reviewed in this Report do include product prices, socio-political issues and environmental considerations; however, SRK does not express an opinion regarding the specific value of the assets and tenements involved.

In this Report and supporting compiled data, where identified, Mineral Resources are quoted using categorisation in accordance with the JORC Code (2012) or equivalent and in some instances earlier superseded Resource Code editions (e.g. JORC Code, 2004). The Mineral Resource estimate verification work undertaken for this review has been done in accordance with the Australian Code for the reporting of Exploration Results, Mineral Resources and Ore Reserve (The JORC Code) 2012 edition (JORC, 2012).

This Report has been prepared as an internal Report only and has not been prepared for publication. Should a Report in accordance with the VALMIN Code be required for general publication, SRK reserves the right to upgrade this Report to the necessary standards at cost. At this stage, SRK grants no permission to publish this Report. It should be noted that the authors of this Report are Corporate Members of The AusIMM and, as such, are bound by the VALMIN Code.

2.3 Work program

SRK has undertaken the scope of work as follows:

- A site visit undertaken by a Senior Geologist to review the site geological conditions, deposit structure, bore core handling and storage practices, geological logging and sampling methods, onsite data management and any other site-based activities relevant to the reporting of Mineral Resources.
- Reviewed the exploration drilling database, geophysical and geochemical data, the geological model and Mineral Resource estimate/s provided by SG, incorporating SRK's in-house knowledge of the region.
- Interpreted the ground geophysical survey data.
- Reviewed the exploration philosophy and priorities for the Project, including any proposed exploration programs, to determine their suitability for the deposit in order to upgrade the Mineral Resources.
- Discussed any material issues regarding the assets with SG's technical staff.
- Formed an independent opinion and provided comments (or feedback) to SG regarding the Project's additional exploration potential and assessment of current Mineral Resources and their reasonable prospects of eventual economic extraction.
- Provided recommendations on further exploration and Project development, where appropriate.
- Prepared an ITR under the guidelines of the JORC Code – an initial draft for SG's review, follow-up discussion and further analysis on key issues of concern, as required, followed by a final report.

Ganzorig Tuvshinbayar visited the site between 1 and 3 May 2020. This report details the results of this review conducted between April and June 2020.

2.4 Project team

The SRK project team for this commission together with their areas of responsibility are listed in Table 2-1.

Table 2-1: SRK Project team

Name	Designation	Area of Responsibility
Petr Osvald	Principal Consultant (Geology and Mining)	Project management; Geology and Mineral Resource estimate review
Ganzorig Tuvshinbayar	Senior Consultant (Geology)	Geology and data review
Bayasgalan Erdenechuluun	Consultant (Geology)	Geological model and Mineral Resource estimate review
Sarantungalag Garamjav	Consultant (Geology)	Geology and data review
Ben Jupp	Senior Consultant (Geology)	Geological model and targeting
Danny Kentwell	Principal Consultant (Resource)	Mineral Resource estimate evaluation
Peter Stuart-Smith	Principal Consultant (Geology)	Structural geology review/interpretation
Chris Woodfull	Corporate Consultant (Geology)	Peer review

2.5 Statement of SRK independence

Neither SRK nor any of the authors of this Report have any material present or contingent interest in the outcome of this Report, nor do they have any pecuniary or other interest that could be reasonably regarded as being capable of affecting their independence or that of SRK.

SRK has no prior association with SG regarding the mineral asset – Tsagaan Chuluut, that is the subject of this Report. SRK has no beneficial interest in the outcome of the technical assessment being capable of affecting its independence.

SRK's fee for completing this Report is based on its normal professional daily rates plus reimbursement of incidental expenses. The payment of that professional fee is not contingent upon the outcome of the Report.

3 Project General Description

The Tsagaan Chuluut Gold Project is located in Eastern Province, northeast Mongolia, some 600 km west of the capital Ulaanbaatar (Figure 3-1). The nearest village to the Project area is Bayandun Soum, about 30 km away. The Project is about 180 km away Choibalsan, the capital of the Eastern Province. The Project is situated 40 km south of the Russian border and 200 km east of Manzhouli (a city in the Inner Mongolia Autonomous Region, China). The distance by road between Ulaanbaatar and the Project is approximately 740 km and includes 540 km of asphalted road and 200 km of gravel road. The road is relatively flat, and the transportation is convenient.

The Project is about 900 m to 1,100 m above sea level, where the terrain comprises gently rolling hills slightly dissected by seasonal streams. The climate is harsh continental. Due to the high altitude, the temperature is typically not high and the temperature range between day and night can be large. The temperature range across the year is 30°C to -35°C, the mean temperature in winter is -25°C, and the mean temperature in summer is 32°C. The mean annual precipitation is 544 mm and the rainy season is from April to October. During winter, the area has snow cover.

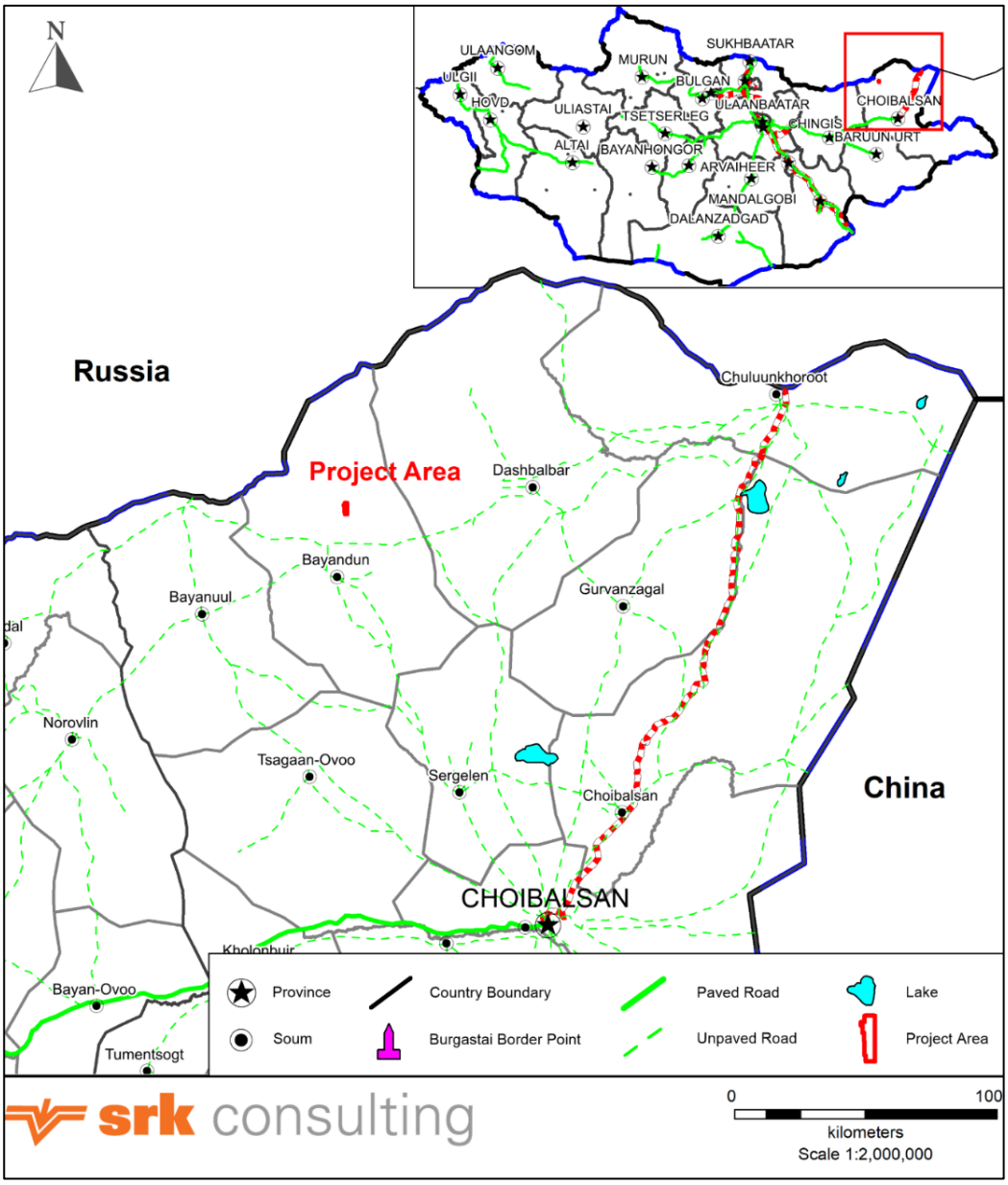

Figure 3-1: Project location map

3.1 Licence

SG holds the Tsagaan Chuluut-1 mining licence MV-015436 (Figure 3-2).

The Tsagaan Chuluut-1 mining licence was originally granted to the SG Group LLC (SG Group) on 25 January 2010. SG Group transferred ownership of the licence to SG on 12 June 2015. The mining licence MV-015436 covers an area of 456.68 ha and is valid until 25 January 2040. Details of the mining licence are given in Table 3-1.

Table 3-1: Tsagaan Chuluut-1 mining licence details

Licence Number	Licence Name	Type	Area (ha)	Date of Issue	Date of Expiry
MV-015436	Tsagaan Chuluut-1	Mining	456.68	January 25, 2010	January 25, 2040

Mining licence MV-015436 has 16 vertices, with coordinates provided in Table 3-2. The coordinate projection system is Longitude/Latitude World Geodetic Survey 1984 (WGS 84).

Table 3-2: Coordinates of the Tsagaan Chuluut-1 mining licence

Vertex ID	Longitude			Latitude		
	Degrees	Minutes	Seconds	Degrees	Minutes	Seconds
1	113	26	2.1	49	27	41.95
2	113	26	1.96	49	30	2.01
3	113	25	12.01	49	30	2.01
4	113	25	12.11	49	29	42.95
5	113	24	55.62	49	29	42.95
6	113	24	54.66	49	29	31.7
7	113	25	3.1	49	29	31.52
8	113	25	2.03	49	29	9.72
9	113	25	11.46	49	29	9.54
10	113	25	10.15	49	28	42.81
11	113	25	12.17	49	28	42.77
12	113	25	10.83	49	28	16.58
13	113	25	12.81	49	28	16.54
14	113	25	12.03	49	28	0.7
15	113	25	17.49	49	28	0.58
16	113	25	17.11	49	27	41.95

Copies of the MV-015436 mining licence are included in Appendix A.

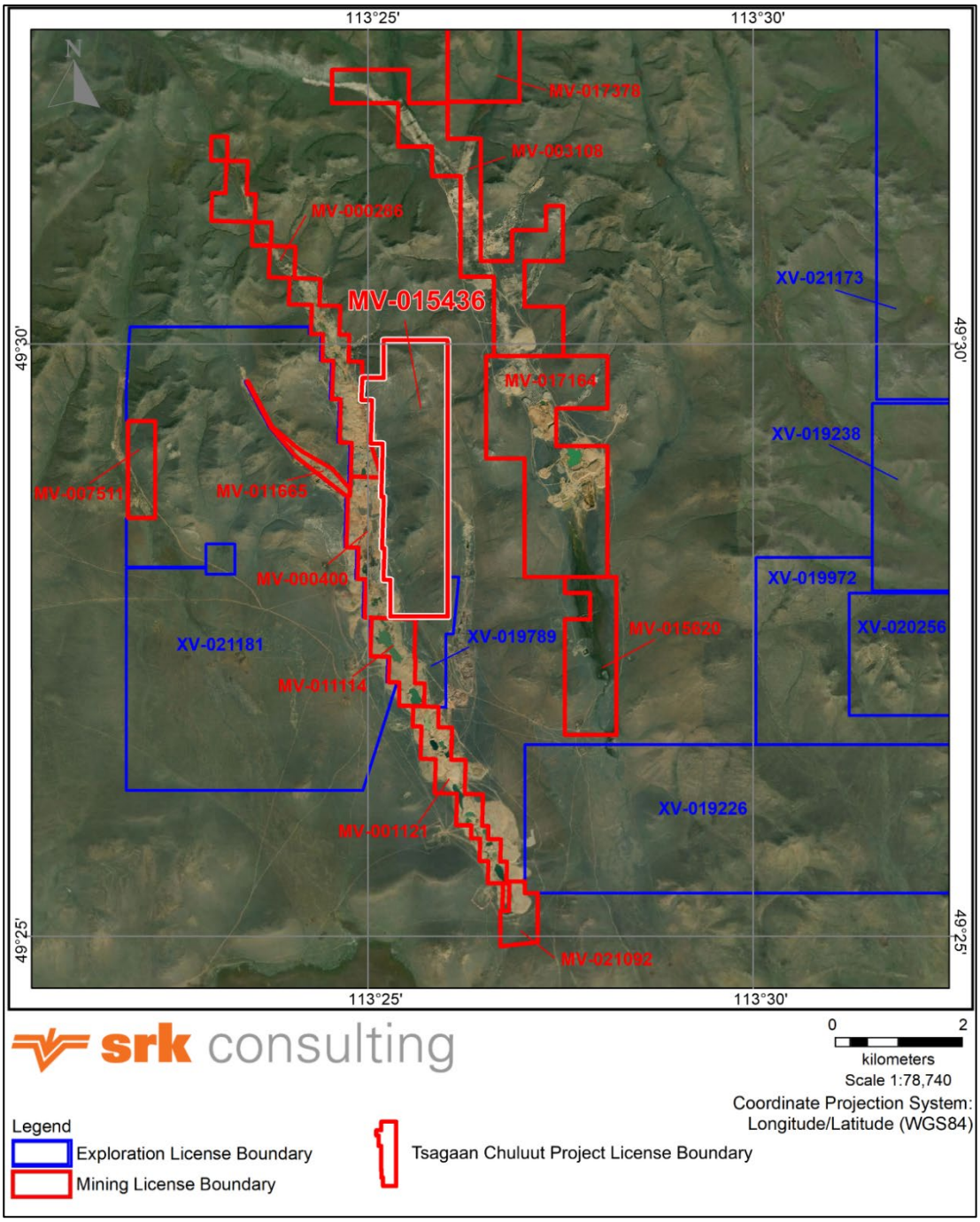

Figure 3-2: Licence Map

4 Regional Geology

Mongolia is part of the Central Asian Orogenic Belt (CAOB), which extends from the Pacific coast to the Ural Mountains. The Mongolian tract of the CAOB (Figure 4-1) has been formed by the accretion of Neoproterozoic, Cambrian, Ordovician and Devonian–Carboniferous arcs, back-arcs and accretionary wedges and Archaean to Neoproterozoic (early Tonian) microcontinents associated with three major accretionary events:

1. Late Proterozoic–Early Cambrian amalgamating continental fragments and accreting oceanic domains, which formed ophiolite sheets
2. Late Cambrian–Early Ordovician forming the island arc of the Siberian continent in the north, which collided with Gondwana-derived microcontinents (this was accompanied by a magmatic and high temperature/low pressure metamorphic event)
3. Late Devonian–Early Carboniferous convergent accretion, shortening the external oceanic crust and forming vast oceanic domains south of the continental margins with accreted microcontinents.

From the Late Silurian, the Mongol-Okhotsk Ocean (MOO) opened, resulting in the formation of a Mongolian continent, orthogonal to the Siberian margin. From the end of Late Devonian–Early Carboniferous accretion until the Early Permian, the whole system rotated clockwise. In the Permian to Jurassic, the Mongolian continent was compressed (and uplifted) between the converging Siberian and North China cratons as the Mongol-Okhotsk oceanic basin closed.

In the Late Cainozoic, the amalgamated accretionary orogenic belt underwent transpressional deformation due to northeast-oriented compression. This event reactivated and exploited major Palaeozoic structures, resulting in a combination of strike-slip movement and thrusting.

4.1 Mongol-Okhotsk Ocean

Bussien et al. (2011) speculate that the MOO may have opened by back-arc spreading during the Late Silurian by cutting into the Early Palaeozoic domain (north of Main Mongolian Lineament) in Mongolia. Later subduction of MOO lithosphere toward the north and south is corroborated by the observation that in both margins, continental volcanic arcs penetrate and overlie deformed rocks of the Early Palaeozoic domain. In the north, the continental igneous activity is recognised/preserved as the Middle Carboniferous to Triassic Selenge arc and the Angar–Vitim granitoids in Transbaikalia (340–280 Ma), e.g. Mazukabzov et al. (2010). The southern continental arc is located in the Middle Carboniferous–Triassic Middle Gobi volcanic–plutonic belt (Badarch et al., 2002), which includes Carboniferous–Jurassic granitoids in the Kherlen Depression (Murao et al., 1998).

Bussien et al. (2011) interpret the MOO fringed to the north and south by active continental margins but depict slightly different periods of subduction-related volcanism. Along the northern margin (the Hangai–Hentei margin), during the Devonian and Early Carboniferous, northward subduction of MOO lithosphere and continental arc magmatism prevailed, which was re-initiated during the Permian.

The contemporaneous Silurian–Devonian southern margin (the Ereendavaa terrane and Middle Gobi volcanic–plutonic belt, Figure 4-2) presumably represented an extension of the continental margin of Amurian continent (Figure 4-1) on which clastics from the erosion of Early Palaeozoic domain were deposited. The southern margin changed to an active continental margin later in the Carboniferous as indicated by initiation of input of magmatic arc zircon grains. Continued southward subduction is evidenced by the occurrence of Permian and Triassic zircons in coeval sedimentary rocks (Bussien et al., 2011).

On both margins, Triassic and Jurassic continental sedimentary sequences unconformably overlie tectonically deformed forearc and accretionary wedge sequences (Badarch et al., 2002).

Permian–Triassic marine (turbiditic) sedimentary rocks from the MOO basin included in the suture zone (Adaatsag and Dochgol terranes, Figure 4-2) are composed of mostly (reworked) Permian volcanic–plutonic source rocks together with older reworked continental basement. A Jurassic post-collisional continental sandstone is composed of locally reworked subduction-related volcanic rocks of Triassic–Early Jurassic (Rhaetian) age. The closure of the MOO is interpreted to have occurred after the deposition of the continental sandstone sequence in the Jurassic. Bussien et al. (2011) summarises key regional features and events:

1. The opening of the MOO occurred post-Ordovician, within the Early Palaeozoic collage of the CAOB, probably through back-arc spreading, due to protracted northward subduction of Palaeo-Asian oceanic lithosphere under the Early Palaeozoic margin of the newly formed Mongolia, which fringed the North Asia Craton (Siberia) to the south. SRK suggests the MOO represented a shorter-lived side branch of the Palaeo-Pacific Ocean as recently outlined by Parfenov et al. (2010).
2. Soon after the development of oceanic basin spreading during the Silurian–Devonian, the northern margin of the MOO turned to subduction accretion and the development of continental volcanic arcs (correlated with the Zaamar granite and Selenge volcanic–plutonic belts). Coeval Devonian sedimentary sequences deposited on the southern margin (Ereendavaa–Middle Gobi) do not yet prove the existence of continental volcanic arc source rocks, and a protracted extensional margin regime can be inferred for this period.
3. The establishment of a volcanic–plutonic arc along the southern margin of the MOO during the Carboniferous and Permian. Continental margin arcs present in the Middle Gobi volcanic belt and Kherlen depression formed through southward subduction of the MOO lithosphere.
4. Intensive reworking of Permian volcanic arc sequences in the Permian and Triassic, preserved as marine sandstones of the MOO domain (Adaatsag–Dochgol terrane) and in coeval continental sandstones of the Ereendavaa–Middle Gobi belt, document a major Permian subduction pulse. In contrast, along the northern margin (Hangai–Hentei), evidence suggests Permian volcaniclastic sedimentation was minor.
5. Discordant, Jurassic continental facies sandstones of the southern margin (Ereendavaa–Middle Gobi) contain mainly Triassic volcanic-plutonic zircons and few Jurassic zircons. Therefore, the collision of the margins and suturing should have occurred after the Triassic. This is corroborated by the persistence of Triassic marine turbidite deposition in the Adaatsag–Dochgol terrane. On a regional scale, the MOO was finally formed by the post-Triassic collision of two opposing active continental margins as inferred by Zorin et al. (1999). However, an equivalent of the suggested intra-oceanic Onon arc in adjacent Siberia (Zorin et al., 1999) could not be found. In the present model, continental blocks as acquired during the Early Palaeozoic orogeny and newly formed accretionary complexes collided after the bivergent subduction of the intervening oceanic domain. A similar process of accretionary wedge collision was suggested by Xiao et al. (2003) for the latest Permian closure of the Palaeo-Asian ocean leading to the Sulinheer suture in southernmost Mongolia. The MOO, therefore, represented the last step of consolidation of the CAOB on Mongolian territory.

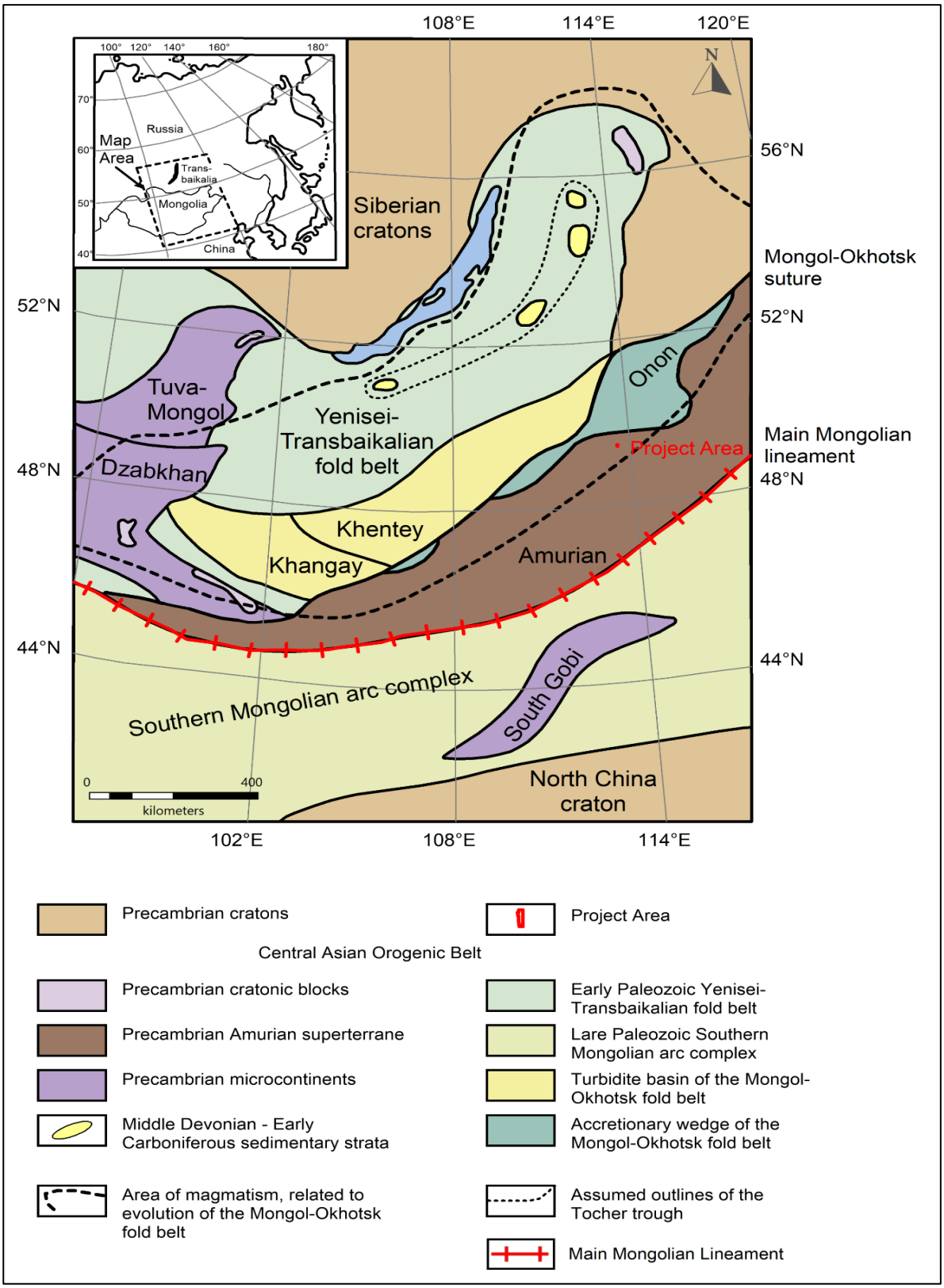

Figure 4-1: Project location in CAOB context

Source: Mossakovsky et al. (1993)

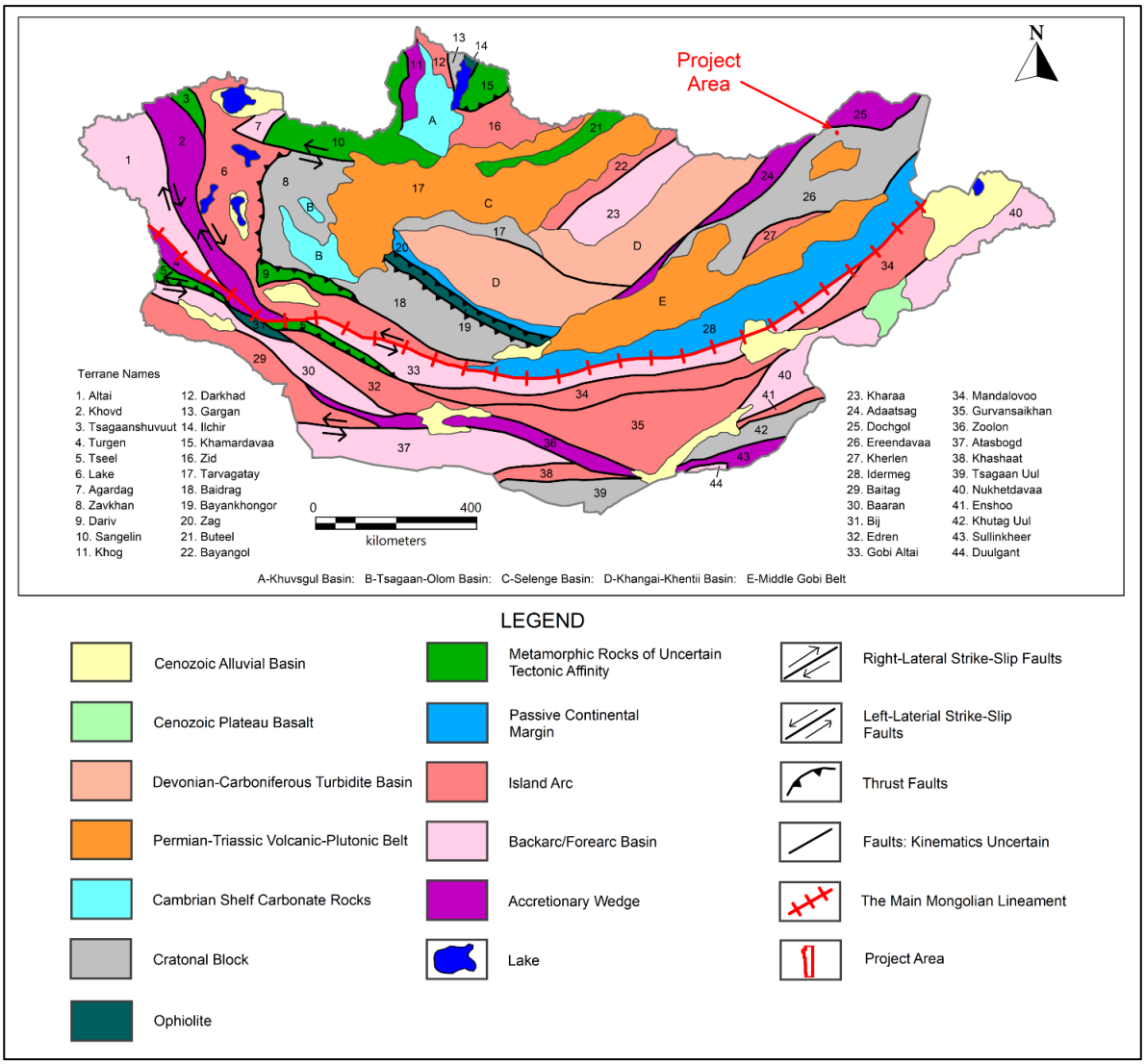

Figure 4-2: Mongolia terrane subdivision with project location

Source: Badarch, et al. 2002

4.1 Regional Geology of Tsagaan Chuluut Gold Project

Geology

The regional geology of the Tsagaan Chuluut Project reflects a tectonic evolution at the continental margin of Ereendavaa craton of the Amurian palaeocontinent (Figure 4-1). The Neoproterozoic Khaichgol Formation comprises marble, amphibolite, schist, gneiss and metamorphosed sandstone. This formation is intruded by Neoproterozoic Phase 1 intrusives of diorite and quartz diorite composition, which are followed by Phase 2 leucogranite, biotitic granite, plagiogranite and gneiss (Figure 4-3 and Figure 4-4). In nearby Russia, dating of biotitic granite and leucogranite by uranium-lead zircon suggested an age of 740 ± 20 Ma (Bibikova et al., 1979).

The Permian Ulzgol plutonic rocks occur in three phases: Phase 1 – mafic gabbro, diorite and quartz diorite, Phase 2 – biotitic granite, plagiogranite and granodiorite and Phase 3 – leucocratic granite ± biotite, syenite (Figure 4-3 and Figure 4-4).

The Late Triassic–Early Jurassic Tsagaan Chuluut Igneous Complex comprise three phases: Phase 1 – gabbro, Phase 2 – diorite and quartz diorite and Phase 3 – granodiorite and granite (Figure 4-3 and Figure 4-4).

Middle–Late Jurassic granite porphyry bodies intrude the Late Triassic–Early Jurassic Tsagaan Chuluut Igneous Complex (Figure 5-1). These intrusions are accompanied with andesite-basalt, andesite-dacite, rhyodacite, rhyolite and their tuff sequences.

The Late Jurassic–Early Cretaceous extension is well documented by development of east- to northeast-trending graben structures filled by Late Jurassic–Early Cretaceous basal conglomerates, sandstones and rhyolite flows.

Structure

Ganbaatar (1991) describes a number of thrust faults and a prominent ring structure, which coincides with outcrop of the Tsagaan Chuluut Igneous Complex and Middle–Late Jurassic granite porphyry.

Regional northwest- and northeast-trending, steeply dipping faults occur within the region and are defined, longitudinally as Bayangol, Turgen, Tsagaan Chuluut, Khanangiin and Burged Uul. These faults have displaced Late Proterozoic–Mesozoic structures with displacement amplitudes of 250–350 m.

SRK interprets the northeast-trending fault system as faults that exploited the inherited structural grain of the MOO subduction zone under the Ereendavaa continental margin. Northwest-trending faults are interpreted to represent reactivated transform faults that formed oblique to the subduction zone. Both systems have undergone repeated compression and extension since Early Palaeozoic, and older faults have been rotated to current positions.

Magmatic complexes occur typically along the northwest-trending regional Tsagaan Chuluut Fault (Figure 4-3 and Figure 4-4).

Ganbaatar (1991) interpreted the ring structures to have formed during Jurassic plutonic and volcanic activity, forming as a result of hydrothermal fracturing and alteration caused by upwelling solutions derived from or circulated by underlying intrusions. SRK opines that ring structures formed, in part, as a result of updoming, followed by the (periodic) withdrawal of magma (and resultant volcanism), and potentially further updoming of a late-stage granite. In contrast to Ganbaatar (1991), SRK opines that ring structures originated during intrusion of the Triassic multi-phase Tsagaan Chuluut Igneous Complex and were later exploited and overprinted by a Jurassic magmatic event.

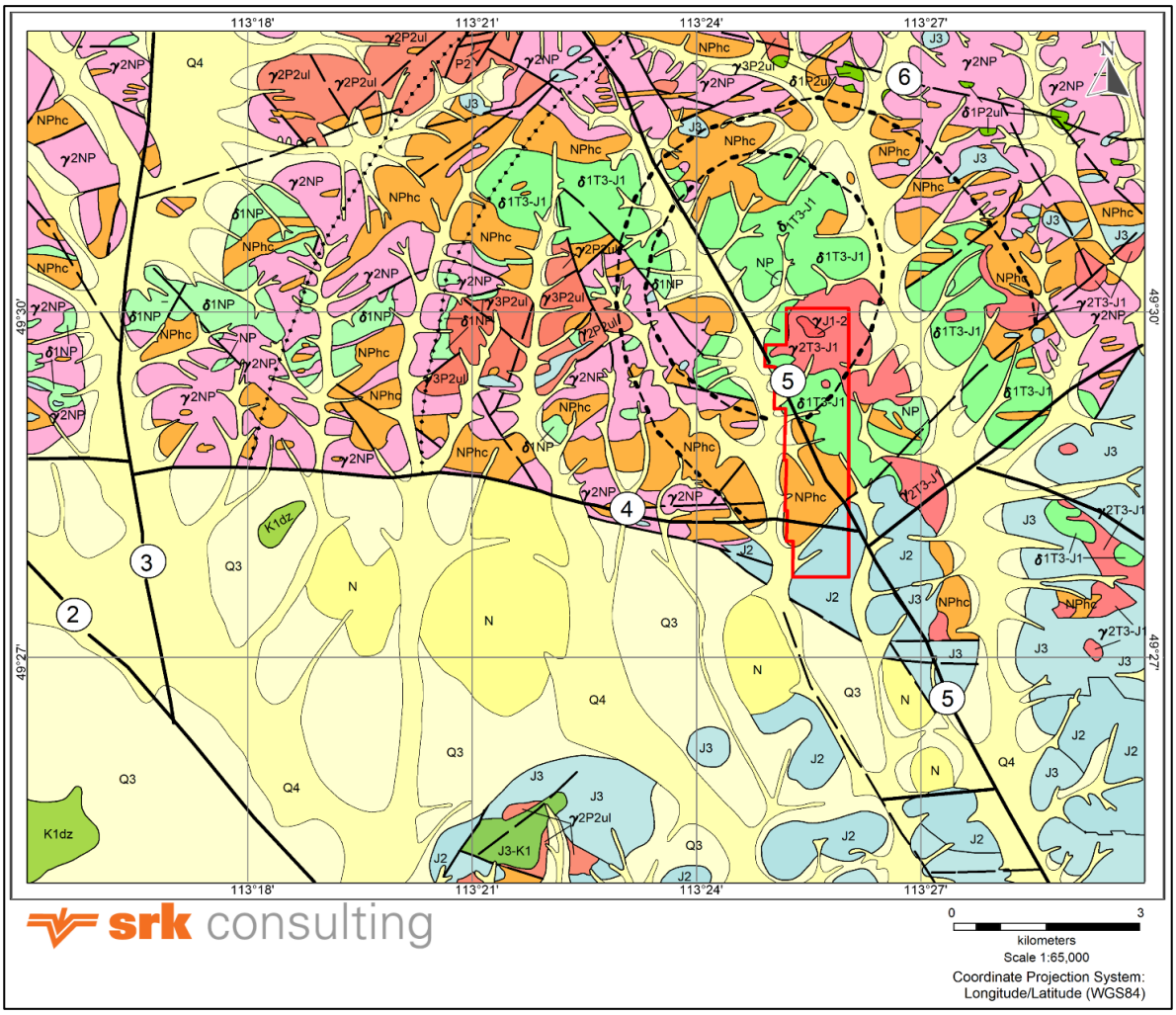

Figure 4-3: Regional geology map with Project location

Source: Ganbaatar (1991)

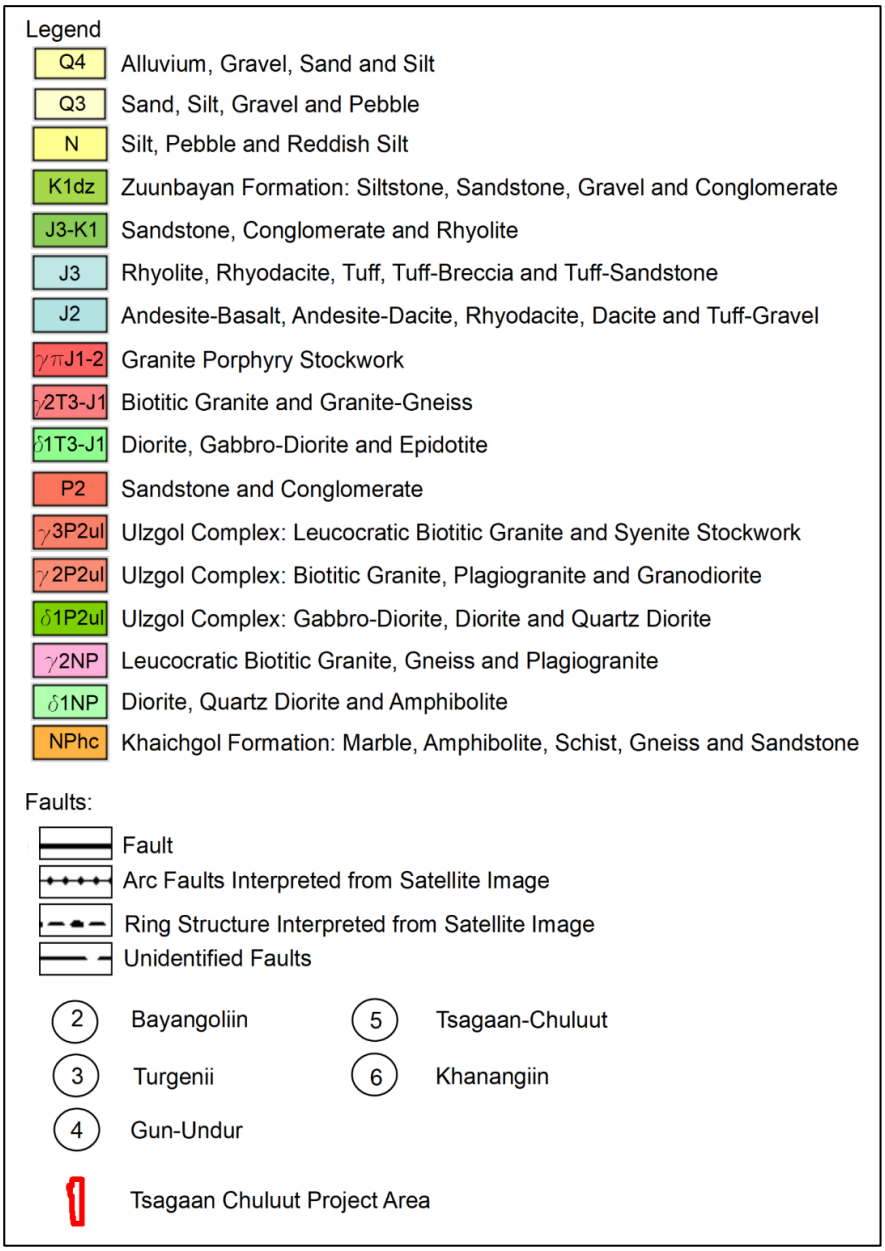

Figure 4-4: Legend to regional geology map

Source: Ganbaatar (1991)

5 Local Geology

The local geology is dominated by the Neoproterozoic metasedimentary Khaichgol Formation outcropping in the south of Tsagaan Chuluut area, which has been intruded by the Late Triassic–Early Jurassic Tsagaan Chuluut Igneous Complex, composed of gabbro, diorite and granodiorite. Middle–Upper Jurassic volcanic and granite porphyry units outcrop in the south and north of the project area, respectively (Figure 5-1). A brief overview of the local geology follows.

5.1 Stratigraphy

Neoproterozoic Khaichgol Formation is distributed in the south of the Project area and comprises sedimentary rocks metamorphosed to biotite-muscovite, amphibole, amphibole-pyroxene and pyroxene-biotite gneiss. The metamorphic rocks are strongly deformed with mica-rich units preserving a schistosity, which trends east–west (Figure 5-1).

Middle–Upper Jurassic volcanic strata, composed of intermediate and felsic volcanics outcrop in the southern sector of the Project area.

Quaternary is mainly alluvium and colluvium deposits preserved in the topographic lows.

5.2 Magmatism

In the Project area, the following intrusive rocks, from oldest to the youngest, occur:

- Late Triassic–Early Jurassic Tsagaan Chuluut Igneous Complex ($\gamma\delta$T3-J1 cc) – see Figure 5-1
- Middle–Late Jurassic granite porphyry
- Middle–Late Jurassic dykes.

The Late Triassic–Early Jurassic Tsagaan Chuluut Igneous Complex ($\gamma\delta$T3-J1 cc) is divided into three phases:

- **Phase 1** – outcrops in the northwest and central part of the Project area (Figure 5-1). Phase 1 is composed of medium-grained pyroxenite gabbro (later petrology studies describe this gabbro as gabbrodiorite) and amphibole biotite gabbro-pyroxenite. The pyroxenite gabbro is typically altered by chlorite-epidote-actinolite. The Phase 1 rocks are intruded by diorite, granite, rhyolite porphyry and diorite porphyry dykes.
- **Phase 2** – outcrops rarely and is composed of fine- to medium-grained biotite-quartz diorite. Diorite has undergone phyllic (quartz, sericite, pyrite, carbonate) alteration, and demagnetisation has also occurred as a result of (hydrothermal) alteration. **Based on evidence from mapping and core drilling, Phase 2 is likely to be associated with the mineralisation.**
- **Phase 3** – outcrops in the northeast of the Tsagaan Chuluut area and is composed of medium-grained granodiorite which is intruded by granite. The granodiorite is weakly porphyritic with typically biotite and orange feldspar phenocrysts. The granodiorite intrudes the Proterozoic metamorphic rocks and is intruded by granite porphyry dykes. The granodiorite has undergone strong alteration and is overprinted by quartz-sulphide veins.

Middle–Late Jurassic granite porphyry bodies intrude the Late Triassic–Early Jurassic Tsagaan Chuluut Igneous Complex (Figure 5-1). Clusters of porphyry stocks have been identified in the wider Project area. Well-preserved unidirectional solidification textures observed in outcrops suggest these outcropping areas represent the apical part of porphyry stocks.

Middle–Late Jurassic dykes comprising rhyolite porphyry, syenite porphyry and diorite porphyry have intruded the Tsagaan Chuluut Igneous Complex granodiorite, diorite and gabbrodiorite.

5.3 Structure and Tectonics

The Project area is situated on the prominent ring structure, which is bisected by the northwest-trending Tsagaan Chuluut Fault. Further south are several mapped northeast-trending faults along which graben structures filled with Jurassic volcanics are developed (Figure 5-1).

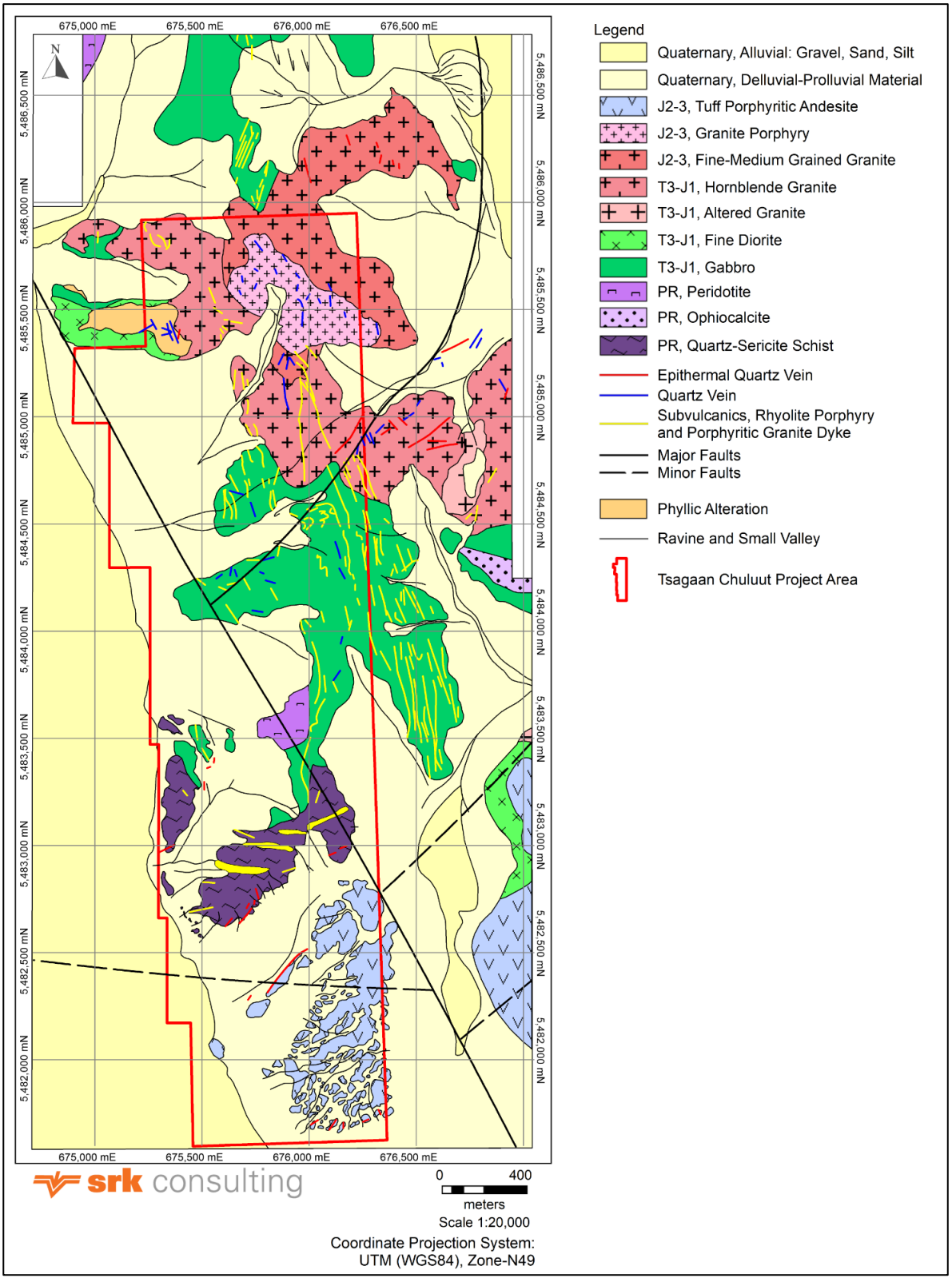

Figure 5-1: Local geology map

Source: SG and Ganbaatar (1991)

5.4 Project area geology

5.4.1 Structure

The most prominent fault in the tenement is the northest-trending Tsagaan Chuluut Fault (Figure 4-3, Figure 4-4 and Figure 5-1). The northeast-striking Erdene Fault is the most dominant fault proximal to the gold mineralisation at Tsagaan Chuluut 1 (TC1) deposit, in the northern sector of tenement (Figure 5-2 and Figure 5-3). Numerous hydrothermal breccias are evident along the length of the Erdene Fault (Bat-Erdene, Enkhbayar and Arvinzen, 2006). The northern block, which contains the mineralisation, has been uplifted (Figure 5-3 and Figure 5-4) and Ganbaatar (1991) interpreted the Erdene Fault as a reverse fault. SRK interpreted faults from the ground magnetic survey (Reduced to Pole (RTP) image) and from core logs and photos. SRK's fault interpretation is provided in Figure 5-2.

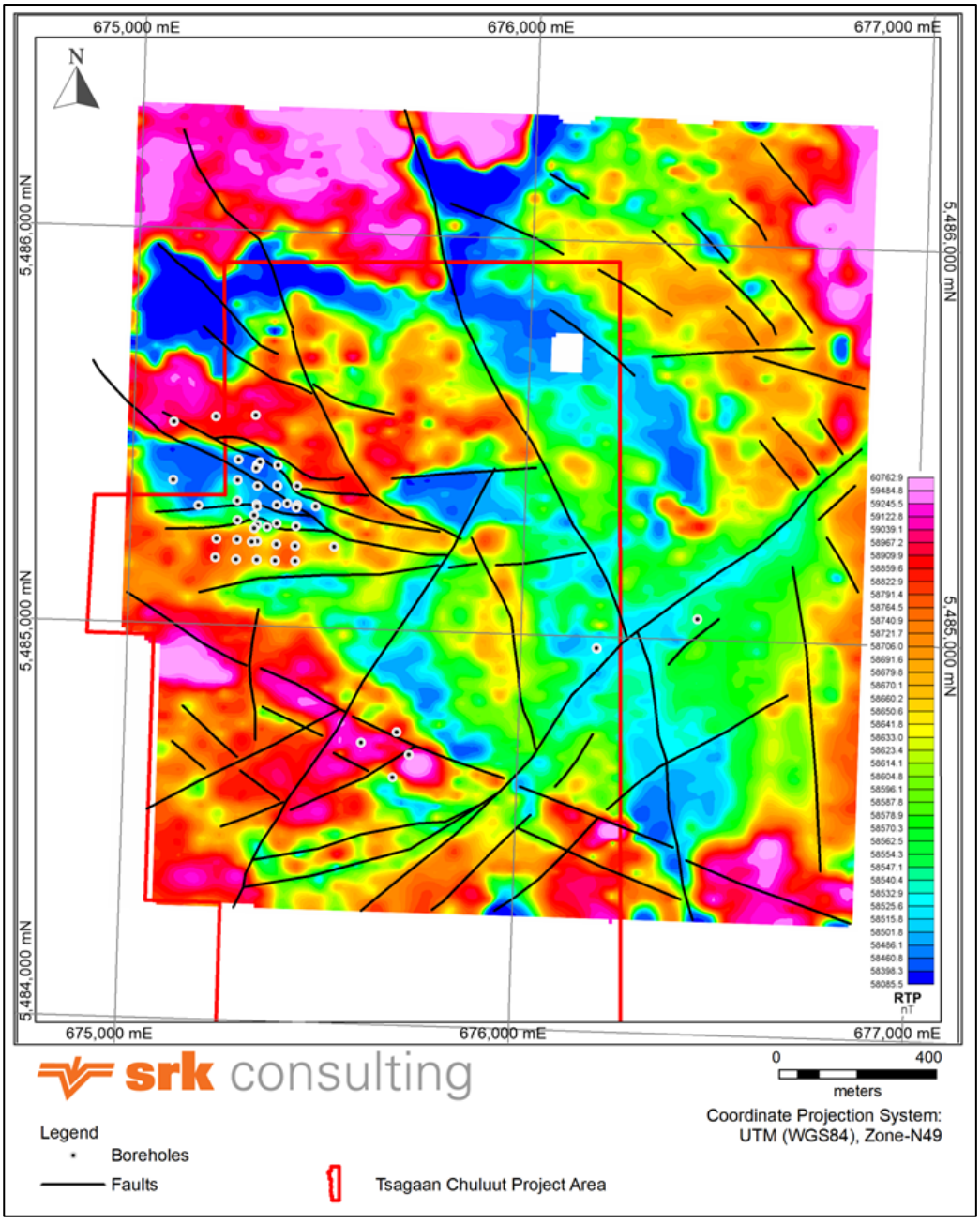

Figure 5-2: Interpreted faults on the RTP magnetic image

Source: SRK (2020)

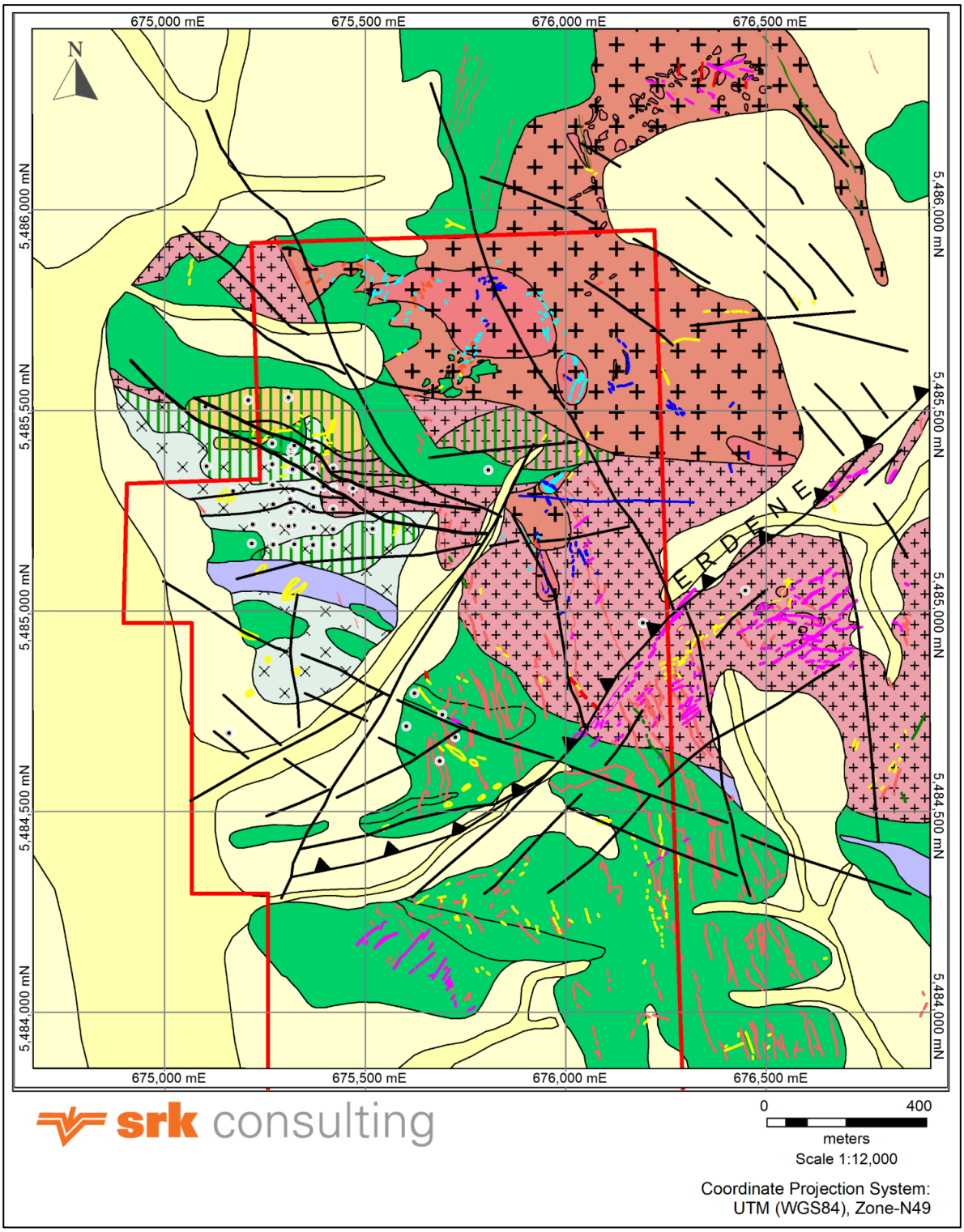

Figure 5-3: Project geology map

Source: SG modified by SRK (2020)

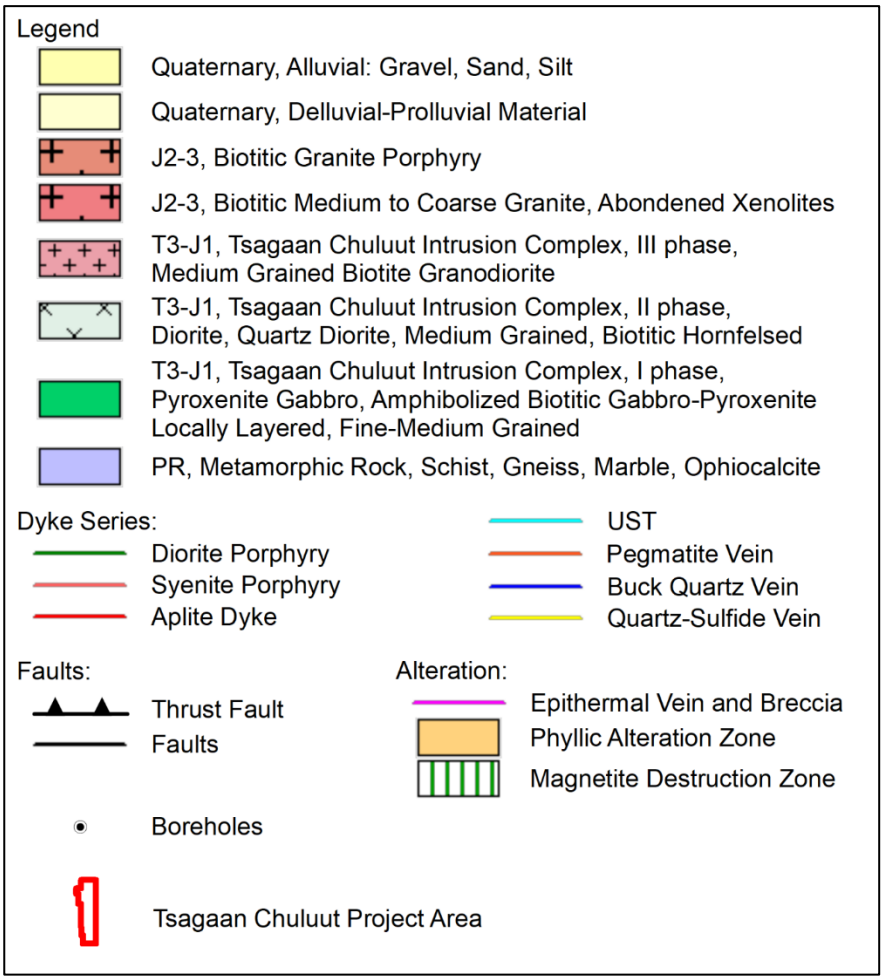

Figure 5-4: Legend of Project geology map

Source: SG modified by SRK

5.4.2 Lithology descriptions

The main lithotypes described by SG geologists from core logs are gabbro, diorite, granodiorite, granite, diorite porphyry, quartz diorite porphyry, quartz porphyry, felsic and andesitic volcanics. Photographic images of each of the main lithotypes are presented in Figure 5-5.

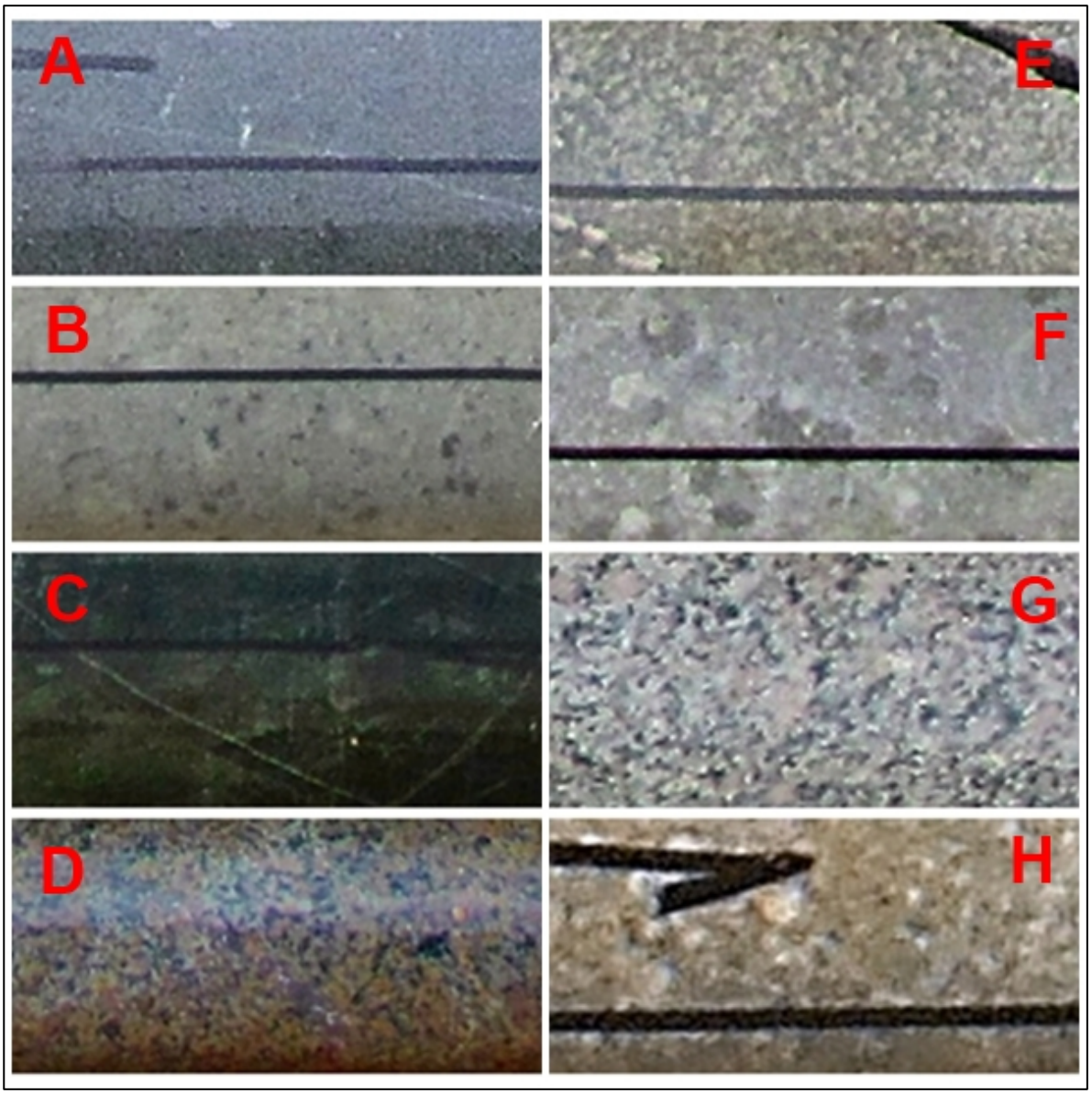

Figure 5-5: Main lithotypes of Tsagaan Chuluut Project

Note: A – TCDD-010 (373.1–380.5 m) – volcanic dyke, B – TCDD018 (278.0–286.0 m) – quartz diorite porphyry, C – TCDD021 (46.7–53.5 m) – gabbro, D – TSDD026 (102.7–110.6 m) – granite, E – TCDD027 (86.8–93.75 m) – diorite porphyry, F – TCDD028 (126.25–133.0 m) – quartz diorite porphyry, G – TCDD028 (189.8–197.3 m) – granodiorite, H – TCDD035 (271.8–279.45 m) – quartz porphyry.

SRK was given copies of with the following four petrology studies carried out on Tsagaan Chuluut rock samples:

1. The initial study was carried out in 2002 (SRK was not provided with the author of the study) on 12 rock samples collected from outcrops (Table 5-1).
2. Stockley (2002) carried out study on a 7 samples collected from the Project and identified breccia in 5 samples and altered igneous rock in 2 samples (Table 5-2 and Table 5-3). However, this report does not provide sample locations.
3. Batulzi (2005) studied 9 core samples collected from mineralised intervals (Table 5-4).
4. During an exploration program in 2013, a petrology study was conducted by Bond et al.(2013) on 10 core samples from mineralised intervals (Table 5-5).

SRK reviewed all four studies and noted that, based on regional field mapping and supported by observation from core drilling, the oldest intrusive samples are gabbrodiorite that is strongly altered

and deformed. These occur in isolated tectonic blocks, which were intruded by diorite, diorite porphyry and quartz diorite porphyry. The quartz diorite porphyry intrusion coincides with mineralisation. Diorite, diorite porphyry and quartz diorite porphyry form subvertical stocks, which in plan view, are elongated in an east–west direction. Apical parts of intrusive stocks are commonly brecciated, strongly altered and mineralised.

Primary and alteration rutile was observed, which Bond et al. (2013) considers is an indication of a Reduced Intrusion Related Gold System (RIRGS). The Bond et al. (2013) petrology study does not report magnetite; however, metallurgical tests report magnetite yield from processed metallurgical samples. Magnetite content in a mineralised quartz diorite porphyry suggests a more oxidised intrusion (or that some trapped fluids were more oxidising than others).

The youngest intrusive rocks are granodiorite, granite, granodiorite porphyry and granite porphyry weakly altered by sericite.

Breccias

Breccias are polymictic and occur as several different types. There are two main types:

- Matrix-supported breccia (Figure 5-6 C and D)
- Open-space breccia with granodiorite (Figure 5-8 E) and open-space breccia with quartz cement (Figure 5-8 A, B and F).

Corbett (2018) classifies breccias in genetic order from deep to shallow crustal levels as there is a progressive decline in the magmatic and increase in the meteoric contributions to the breccia: contact → intrusion → magmatic/hydrothermal (containing intrusion and collapse) →phreatomagmatic → phreatic breccias.

The location of the breccias at Tsagaan Chuluut suggests that in the vicinity of the youngest granodiorite and granite intrusion are developed contact and intrusion breccias.

Magmatic brecciation is typically matrix supported, cemented by hydrothermal quartz and occasional large pyrite blebs. Breccia clasts comprise a wide variety of rocks (Table 5-2), including diorite, fragments of K-feldspar (Figure 5-6 C), sedimentary rock fragments and (earlier) breccias. The matrix is commonly intensively altered rock flour often cemented by quartz (Figure 5-6 D). These breccias are in position of deeper crustal level similar to the contact and intrusion breccia of Corbett (2018) classification.

Hydrothermal breccias are typically open space (crackle) breccia with quartz cement, and occasionally with sulphides and Mn-Fe oxides. Hydrothermal breccias are observed in gabbrodiorite, gabbromonzonite, diorite, diorite porphyry, quartz diorite porphyry and also overprint earlier contact and intrusive breccia bodies.

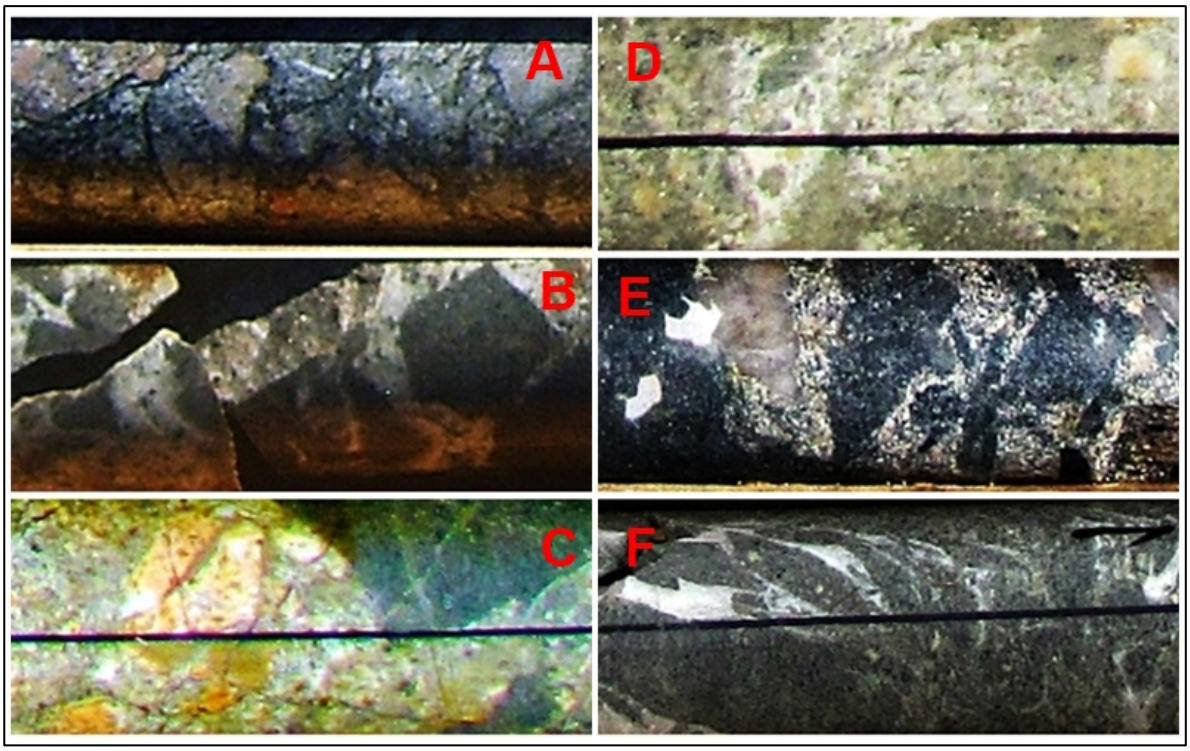

Figure 5-6: Breccia types

Note: A – TCDD-01 (120.0 m) – hydrothermal breccia, B – TCDD01 (134.0 m) – hydrothermal breccia, C – TCDD028 (64.0 m) – contact breccia, D – TSDD028 (68.0 m) – contact breccia, E – TCDD028 (247.0 m) – contact breccia, F – TCDD029 (207.0 m) – hydrothermal breccia.

Table 5-1: Petrology study results (2002)

No.	Sample ID	Field Description	Microscopic Description	Major	Minor	Accessories	Phenocrysts	Structure	Texture	Alteration	Mineralisation
1	1	Fine-grained granite porphyry	Fine-grained granite porphyry - granite syenite	Quartz (Q) 20% Plagioclase (Pl) 40% K-feldspar (K-feldspar) 30-35%	Biotite + hornblende (Bi + Hrb) 12-20%	Apatite, sphene, monazite		Hypidiomorphic	Porphyritic	Sericite	Pyrite
2	12	Granite porphyry dyke	Granodiorite porphyry	Plagioclase (Pl) 70-80% K-feldspar (K-feldspar) 10-15% Quartz (Q) 10-5%	Biotite		Plagioclase	Cryptogranular	Porphyritic	Sericite, chlorite	Pyrite
3	14	Dark green laminated peridotite	Amphibolite	Amphibole (Am) 60%	Plagioclase (Pl)			Hypidiomorphic	Massive - banded	Chlorite, sericite amphibole, actinolite	Haematite
4	16	Fine-grained granite porphyry	Fine-grained granite	K-feldspar (Ê-felspar) 25-30% Plagioclase (Pl) 25-30% Quartz (Q) 20-25%	Biotite + Hornblende (Bi + Hrb) 15-20%	Apatite, sphene, ore minerals		Hypidiomorphic	Massive	Sericite	Pyrite
5	17	Granite porphyry	Granite porphyry	Plagioclase (Pl) 30% K-feldspar (K-feldspar) 30% Quartz (Q) 30%	Biotite (Bi) 10%		Quartz (Q), plagioclase (Pl), K-feldspar, biotite (Bi)	Microhypidiomorphic	Porphyritic	Sericite	Sulphide minerals
6	20	Microdiorite dyke	Metadolerite (diabase)	Plagioclase (Pl), pyroxene				Hypidiomorphic			
7	32	Fine-grained, blue grey diorite	Fine-grained diorite	Plagioclase (Pl) 55-60% Biotite + Hornblende (Bi + Hrb) 35-40%	Pyroxene (Pyx) Quartz (Q) 2%	Apatite, ore minerals, sphene		Prismatic	Porphyritic like, massive	Sericite, chlorite, epidote	Pyrite
8	9230	Fine-grained gabbro	Gabbrodiorite (gabbro) - monzodiorite	Plagioclase (Pl) 50% Hornblende (Hrb) 40%	K-feldspar (K-felspar) 30% Quartz (Q) 5-6%	Sphene, rutile		Hypidiomorphic	Massive	Sericite, chlorite, carbonate, epidote,	
9	9241	Diorite that has undergone strong quartz-sericite (beresite) alteration, with oxidised pyrite	Quartz-sericite metasomatite	Quartz (Q) 20-25% Sericite (Se) 75-80%	Pyrite	Rutile, apatite		Metasomatic	Massive	Quartz-sericite, pyrite, hematite	Pyrite
10	9243	Diorite that has undergone strong quartz-sericite (beresite) alteration, with oxidised pyrite	Diorite that has undergone quartz-sericite alteration	Quartz (Q) 30-40% Sericite (Se) 20-30%	K-feldspar 30-40%	Rutile, apatite		Metasomatic	Massive	Quartz-sericite, haematite after pyrite	Pyrite
11	TC1	Strong quartz-sericite altered rock	Quartz-sericite metasomatite	Quartz (Q) 30-40% Sericite (Se) – 60-70%		Rutile, apatite		Metasomatic	Massive	Quartz-sericite, haematite after pyrite	Pyrite
12	TCH1	Strong quartz-sericite altered rock with oxidised pyrite	Quartz-sericite metasomatite	Quartz (Q) 75-80% Sericite (Se) 20-25%		Rutile, apatite		Metasomatic	Massive	Quartz-sericite, haematite	Haematite chalcedony veinlet with pyrite

Table 5-2: Petrology study results - breccia (Stockley, 2002)

No.	Sample ID	Description	Support	Clasts		Matrix	Cement
				Composition	Shape		
1	9362	Silicified and sericite altered hydrothermal breccia	Matrix	Sedimentary rock, chert, quartz with sericite, K-feldspar	Angular	Quartz	Quartz
4	9368	Quartz cemented heterolithic breccia	Matrix	Pyroclastic, breccia, rhyolite, porphyry	Angular		Quartz
5	9371	Quartz cemented breccia	Matrix	Shale, quartz	Angular		Quartz
6	9378	Heterolithic breccia	Matrix	Sedimentary rocks and breccia			Quartz
7	9381	Heterolithic breccia	Matrix	Fragments of igneous rock	Angular	Microphenocryst-sized K-feldspars in the fine Ti oxide replete groundmass	Quartz, fluorite

Table 5-3: Petrology study results - intrusive (Stockley, 2002)

No.	Sample ID	Description	Major	Minor	Accessories	Phenocrysts	Structure	Texture	Alteration
2	9366	Sericite altered and oxidised quartz syenite	K-feldspar sericite	Goethite	Rutile quartz, Mn oxides		Hypidiomorphic	Porphyritic	Sericite, goethite
3	9367	Quartz microsyenite	K-feldspar quartz	Muscovite, carbonate	Rutile, goethite	K-feldspar	Hypidiomorphic, allotriomorphic	Aplitic, porphyritic	Mica, calcite, goethite

Table 5-4: Petrology study results (Batulzi, 2005)

No.	Hole ID	Depth (m)	Field Description	Microscopic Description	Major	Minor	Accessories	Phenocrysts	Structure	Texture	Alteration
1	TCDD-010	156.9	Diorite	Altered monzodiorite	Plagioclase pyroxene hornblende quartz and K-feldspar			Plagioclase pyroxene hornblende quartz and K-feldspar	Idiomorphic and hypidiomorphic	Porphyritic	Carbonate, chlorite, epidote, saussurite
2	TCDD-031	289.4	Diorite porphyry	Altered granite porphyry	Quartz 28-30% Plagioclase 43-45% K-feldspar 20-22% Biotite 5-7%	Magnetite approx. 2%	Sphene, epidote	Plagioclase, K-feldspar and biotite	Idiomorphic and hypidiomorphic	Porphyritic	Carbonate, sericite, chlorite, epidote
3	TCDD-010	233.0	Quartz diorite porphyry	Altered muscovite granite	Quartz 30% Plagioclase 43-45% K-feldspar-20-22%	Muscovite 2-3%, Magnetite approx.2%	Sphene	plagioclase K-feldspar quartz and muscovite	Hypidiomorphic	Porphyritic	Muscovite
4	TCDD-010	372.7	Gabbro	Biotite granite	Quartz 30% Plagioclase 33-35% K-feldspar 30-32%	Muscovite 3% Magnetite 2%	Sphene, zircon	Plagioclase K-feldspar quartz and biotite		Porphyry	Calcite, epidote, chlorite
5	TCDD-010	217.0	Diorite porphyry	Pegmatitic granite	Quartz 30-32% K-feldspar 50-52% Albite 15%	Biotite 3%				pegmatitic	Sericite, chlorite
6	TCDD-010	183.4	Quartz diorite porphyry	Altered muscovite granite	Plagioclase square K-feldspar muscovite and quartz			K-feldspar, muscovite and quartz		Porphyritic	Muscovite, carbonate
7	TCDD-011	259.0	Diorite	Muscovite granite	Plagioclase K-feldspar biotite quartz		Sphene, zircon	Plagioclase, K-feldspar, quartz and few muscovite		Porphyritic	Calcite, epidote, chlorite
8	TCDD-018	48.0	Diorite	Altered quartz monzodiorite	Pyroxene 20-22% Hornblende 13-15% Biotite 5-7% Plagioclase 45-47% K-feldspar 8-10% Quartz 7-10%			Pyroxene, plagioclase, hornblende and biotite	Hypidiomorphic	Porphyritic	Carbonate, albite
9	TCDD-022	304.8	Diorite	Altered muscovite granite	Remnants are quartz and muscovite						Carbonate, smectite, kaolinite, muscovite

Table 5-5: Petrology study results (Bond et al., 2013)

No.	Sample ID	Hole ID	Depth (m)	Field Description	Microscopic Description	Major	Minor	Accessories	Alteration	Ore minerals
1	10369	TCDD-011	155	Quartz diorite porphyry	Strong K-altered rock	K-feldspar sericite illite	Ankerite dolomite	Monazite, zircon, apatite	K-feldspar sericite illite	Pyrite, galena, tetrahedrite, gold
2	10797A	TCDD-014	68	Gabbro	Strong K-altered rock	K-feldspar, sericite illite	Ankerite dolomite	Rutile, apatite	K-feldspar sericite illite	Pyrite, chalcopyrite, sphalerite
3	10797B	TCDD-014	68	Gabbro	Strong altered rock - quartz and albite remnants	Sericite dolomite ankerite K-feldspar and secondary quartz	Primary quartz and albite	Rutile	Sericite, dolomite, ankerite K-feldspar and secondary quartz	Pyrite, chalcopyrite, sphalerite, galena, tetrahedrite, Bi-Cu sulphide
4	10797C	TCDD-014	68	Gabbro	Strong altered rock - quartz and albite remnants	Sericite dolomite ankerite and quartz	Primary quartz and feldspar	Zircon, monazite, rutile	Sericite, dolomite, ankerite and quartz	Pyrite, tetrahedrite, minor chalcopyrite
5	11685	TCDD-028	69	Gabbro	Strong altered rock - quartz and albite remnants	Sericite dolomite ankerite and quartz	Primary quartz and feldspar	Zircon, monazite, rutile barite	Sericite, dolomite, ankerite and quartz	Pyrite, gold, goethite
6	11834A	TCDD-017	77	Gabbro	Strong altered rock - quartz and albite remnants	Sericite K-feldspar and quartz	Dolomite ankerite	Calcite, rutile, monazite, zircon	Sericite K-feldspar and quartz	Pyrite chalcopyrite and tetrahedrite
7	11834B	TCDD-017	77	Gabbro	Strong altered rock - quartz and albite remnants	Sericite quartz and K-feldspar	Ankerite calcite	Rutile, monazite, apatite, zircon	Sericite quartz and K-feldspar	Pyrite, chalcopyrite
8	12162	TCDD-024	99	Quartz diorite porphyry contact with diorite	Altered quartz diorite porphyry	Quartz albite sericite	Ankerite calcite	Rutile, apatite	Quartz albite sericite	Pyrite, galena, gold, emplectite
		TCDD-024	100		Strongly altered diorite	sericite quartz and K-feldspar	Dolomite ankerite	Rutile, monazite, zircon	Sericite quartz and K-feldspar	Pyrite, tetrahedrite
9	12649	TCDD-018	127	Quartz diorite porphyry	Strongly altered quartz diorite porphyry	Sericite quartz and K-feldspar	Plagioclase ankerite dolomite	Rutile, apatite	Sericite quartz and K-feldspar	Pyrite, chalcopyrite galena, tetrahedrite gold
10	13118	TCDD-029	114	Quartz diorite porphyry	Strongly altered quartz diorite porphyry	Quartz K-feldspar sericite	Plagioclase ankerite dolomite	Rutile, apatite zircon	Quartz K-feldspar sericite	Pyrite, tetrahedrite chalcopyrite

5.4.3 Alteration

SRK noted that the Tsagaan Chuluut geology map shows a footprint of phyllic alteration; however, detailed alteration mapping was not carried out. SRK reviewed alteration records in lithology core logs and observations from the petrology studies. Based on SRK's review, SRK has low confidence in the demagnetised and phyllic zones presented on the SG geology map and recommends a more detailed assessment of alteration across the Project area be carried out, including targeted alteration mapping.

Although there is mapped epidote and actinolite (propylitic alteration), these do not coincide with the main demagnetised zones (as would be expected). The magnetic, resistivity, chargeability and metal factor data suggest intense, multi-stage and extensive alteration. The area contains three main igneous rock types, which leads to variations in the magnetic and induced polarisation (IP) responses that reflect original differences in rock composition or intensity alteration. The responses reflect variations in three factors:

- Magnetite content
- Presence of sulphide (massive or disseminated)
- Degree of quartz veining.

Using the geophysical properties, SRK has variously classified a number of different alteration zones (Figure 5-7). Each zone is given a potential identifier based on the type of alteration. However, this is very conjectural as other data such as Advanced Spaceborne Thermal Emission and Reflection (ASTER) data or field observations are needed to calibrate the different zones. The identified zones need to be treated with caution and are preliminary.

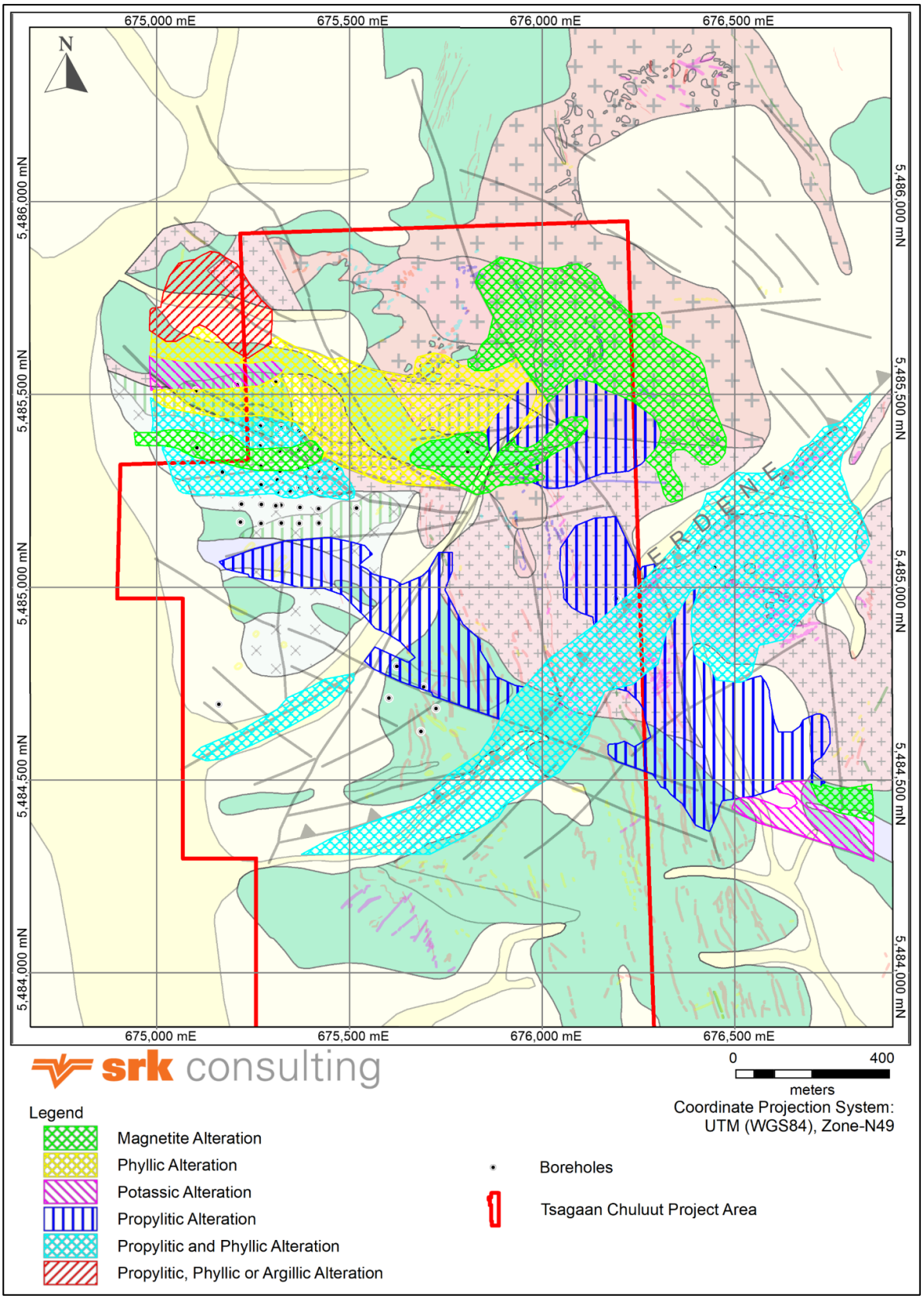

Figure 5-7: Alteration map of project area

The dominant alteration minerals spatially related to gold mineralisation (Table 5-5) are K-feldspar, sericite and quartz. These major alteration minerals are accompanied by carbonates, such as dolomite, ankerite and calcite. Alteration by carbonate, chlorite and epidote is more widespread in diorite and granite type rocks (Table 5-4). Saussurite, carbonate, chlorite and epidote alteration was observed in diorite rocks; amphibolite exhibits chlorite, sericite, amphibole and actinolite alteration, while gabbrodiorite typically exhibits sericite, chlorite, carbonate and epidote alteration. Propylitic alteration is described by Batulzi (2005) in samples showing an alteration mineral association of chlorite-epidote-calcite-saussurite.

Based on the review of geophysical image data, the petrological description of alteration minerals and core photo reviews, SRK opines that alteration zones of potassic, phyllic and propylitic alteration are present at Tsagaan Chuluut. As noted above, SRK recommends further alteration evaluation studies, including infrared spectrometry core logging aimed at identification of clay minerals and improved alteration zone mapping, be carried out.

Alteration occurs pervasively through host rocks and/or is more discretely associated with vein development (vein type).

Pervasive alteration occurs in different lithotypes. K-feldspar, sericite and quartz alteration in quartz diorite porphyry is shown on Figure 5-8B; the same alteration occurs in a quartz diorite breccia shown on Figure 5-8F and Figure 5-8H and in a gabbrodiorite (Figure 5-8C).

Quartz veining with a potassic alteration halo is shown on Figure 5-8A, cross cutting veins of quartz, sericite and K-feldspar with oxidised pyrite is shown on Figure 5-8E and a vein of K-feldspar and quartz cut by a younger carbonate veinlet is shown on Figure 5-8D.

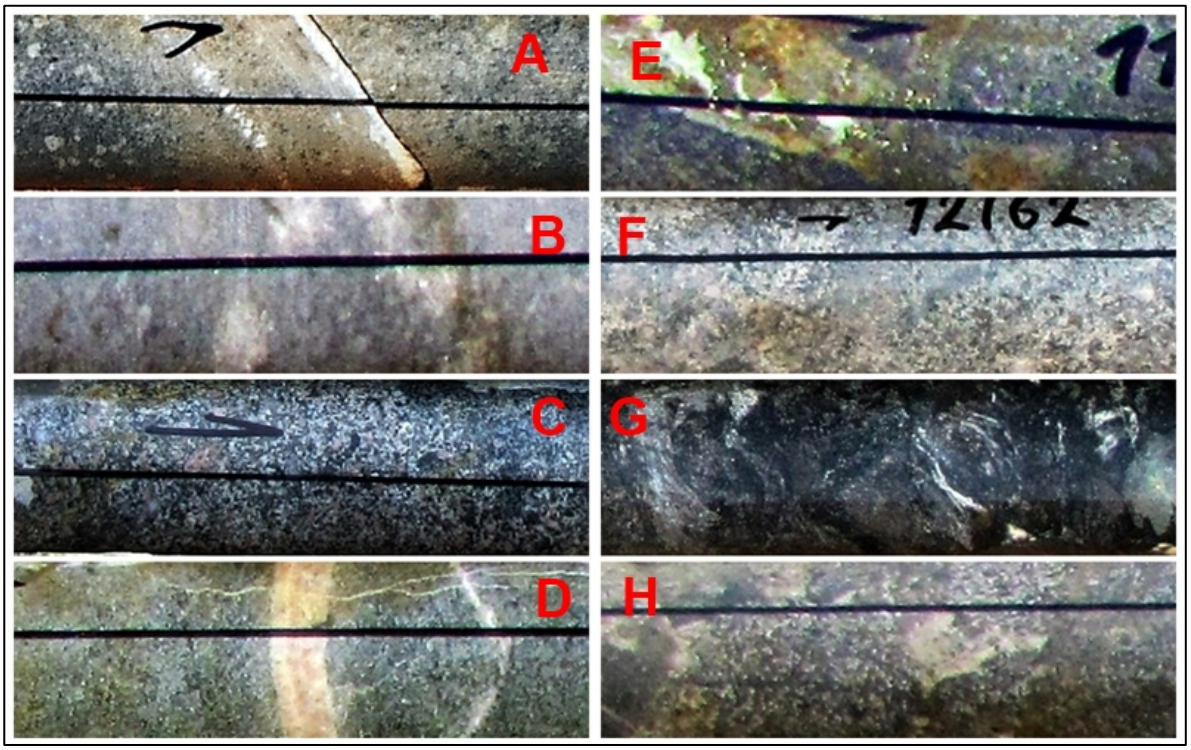

Figure 5-8: Alteration styles

Note: A – TCDD-032 (241.0 m), B – TCDD011 (165.0 m), C – TCDD011 (292.0 m), D – TSDD014 (68.0 m), E – TCDD017 (77.0 m), F – TCDD021 (99.0 m), G – TCDD028 (193.0 m), H – TCDD029 (114.0 m)

5.4.4 Alteration with veining

Vein-type alteration and six vein generations are described in detail by Bond et al. (2013). The generations of veins identified by Bond et al. (2013) and associated vein mineralogy are summarised in Table 5-6.

Table 5-6: Mineral paragenesis in veins

Vein/Alteration	Generation						
Mineral	**1**	**2**	**3A**	**3B**	**4**	**5**	**6**
Quartz							
K-feldspar							
Dolomite/Ankerite							
Sericite							
Albite							
Rutile							
Monazite							
Apatite							
Zircon							
Sphalerite							
Pyrite							
Chalcopyrite							
Tetrahedrite							
Galena							
Gold							
Barite							
Bi-Cu-Sulphide							
Calcite							
Goethite							

Note: Magenta – strong, green – moderate, pink – weak
Source: Bond et al., 2013

First generation veins are up to 25 mm in width. The veins are composed of K-feldspar with approximately 30% quartz and minor biotite, are not mineralised and are not associated with strong wall-rock alteration seen in other generations.

Second generation veins occur as isolated quartz crystals and less commonly narrow quartz veins approximately 1 mm across. Quartz crystals are mostly euhedral, suggesting growth into open space originated in extension ruptures. The quartz is often surrounded by third generation ankerite and dolomite and in places has been partially destroyed by sericite.

Third generation A ‘beresite’ veins are composed dominantly of carbonate (ankerite/dolomite) with minor sericite and quartz and, importantly, are mineralised. The ore minerals are dominated (>95%) by pyrite. The pyrite is hosted in the wall-rock and veins and contain inclusions of monazite, apatite, rutile and zircon, which also occur in the wall-rock. Intense wall-rock replacement surrounding these veins is dominated by quartz and sericite to approximately 25 mm in width. Rare gold mineralisation exists in this generation as round inclusions of gold within the pyrite.

Third generation B veins are composed of quartz, sericite and pyrite and are accompanied by strong wall-rock potassic alteration with coarse sulphide blebs.

Fourth generation veins are narrow bands of pyrite coated by calcite, which is coated by quartz.

Fifth generation veins are gold-bearing quartz veins observed primarily as narrow quartz veins. Quartz of this generation is also observed infilling space around euhedral ankerite crystals. In addition to quartz, the gangue material contains sericite and rare albite and calcite. Ore mineralogy consists of pyrite, free gold, tetrahedrite, galena, chalcopyrite, barite and rare emplectite ($CuBiS_2$). Ore minerals are commonly hosted in fractures within third generation pyrite. Gold mineralisation is dominantly associated with tetrahedrite and galena, and also occurs in pyrite fractures and rarely as free gold mineralisation within fifth generation quartz.

Sixth generation veins are goethite alteration veins that occur as a coating on pyrite grains, within fractures in pyrite grains and between bladed sericite crystals. Goethite has also grown between sericite crystals and has coated a gold grains associated with fifth generation quartz veining.

Geochemical Survey Results

SRK reviewed geochemical data from soil and rock chip survey and prepared maps of distribution of gold (Figure 5-9), silver (Figure 5-10), arsenic (Figure 5-11), bismuth (Figure 5-12), copper (Figure 5-13), molybdenum (Figure 5-14), lead (Figure 5-15), antimony (Figure 5-16), tungsten (Figure 5-17) and zinc (Figure 5-18).

SRK makes the following observations:

- Gold distribution in soil samples indicates elevated gold in the western sector of the Project overlapping with mapped outcrops of Tsagaan Chuluut Igneous Complex and elongated in a northwest direction along Tsagaan Chuluut Fault. Gold decreases over Middle–Late Jurassic granite porphyry outcrops. Rock chips suggest clustering of elevated gold plotting over the Tsagaan Chuluut Igneous Complex and along east to east–northeast-trending structures transecting a Middle–Late Jurassic granite intrusion.
- Within the licence boundary, the silver signature in soil samples is weak and slightly increases along over a granodiorite outcrop of the Tsagaan Chuluut Igneous Complex as well as its contact with Middle-Late Jurassic granite porphyry. Rock chip samples shows a few scattered samples with silver over 10 ppm.
- Soil sample results show elevated silver as a wide aureole over outcrops of igneous rocks. The soil samples for silver broadly define outcrops of intrusive rocks.
- Soil sample results shows elevated bismuth over a Middle–Late Jurassic granite intrusion and related contact aureole. Rock chips with bismuth over 100 ppm also occur along an outcrop of granite intrusion and associated with Jurassic dykes.
- Soil sample results indicate increased copper in gabbro and Middle–Late biotitic granite. Elevated copper also occurs along east–northeast-trending structures and coincides with elevated gold in rock chips.
- A cluster of elevated molybdenum occurs in soils sampled in the eastern sector of the licence and the cluster trends north to north-northeast. It appears to be related to a Middle–Late Jurassic granite intrusion. Rock chips with over 500 ppm Mo coincide with the east–northeast-trending structures along with elevated gold and copper levels.
- Lead in soil samples suggest a prominent maximum over a Middle–Late Jurassic granite intrusion and rock chips with over 500 ppm Pb occurring along east–northeast-trending structures.
- Elevated antimony levels in soil samples occur along the contact of a Middle–Late Jurassic granite intrusion. Only a few rock chips with levels over 100 ppm Sb occur in Project area, typically occurring where gold mineralisation was drilled.

- Elevated tungsten levels in soil samples occur over the outcropping Middle–Late Jurassic granite intrusion as well as over the outcrop of numerous Jurassic dykes in an area southeast of the granite intrusion. Rock chips with over 100 ppm W cluster along a contact of the Tsagaan Chuluut Igneous Complex with a Middle–Late Jurassic granite and along east–west-trending structures.
- Elevated zinc levels in soil samples occur in a southeast-trending zone which starts close to the drilled gold mineralisation at TC1 and extends along outcrops of Jurassic dykes.

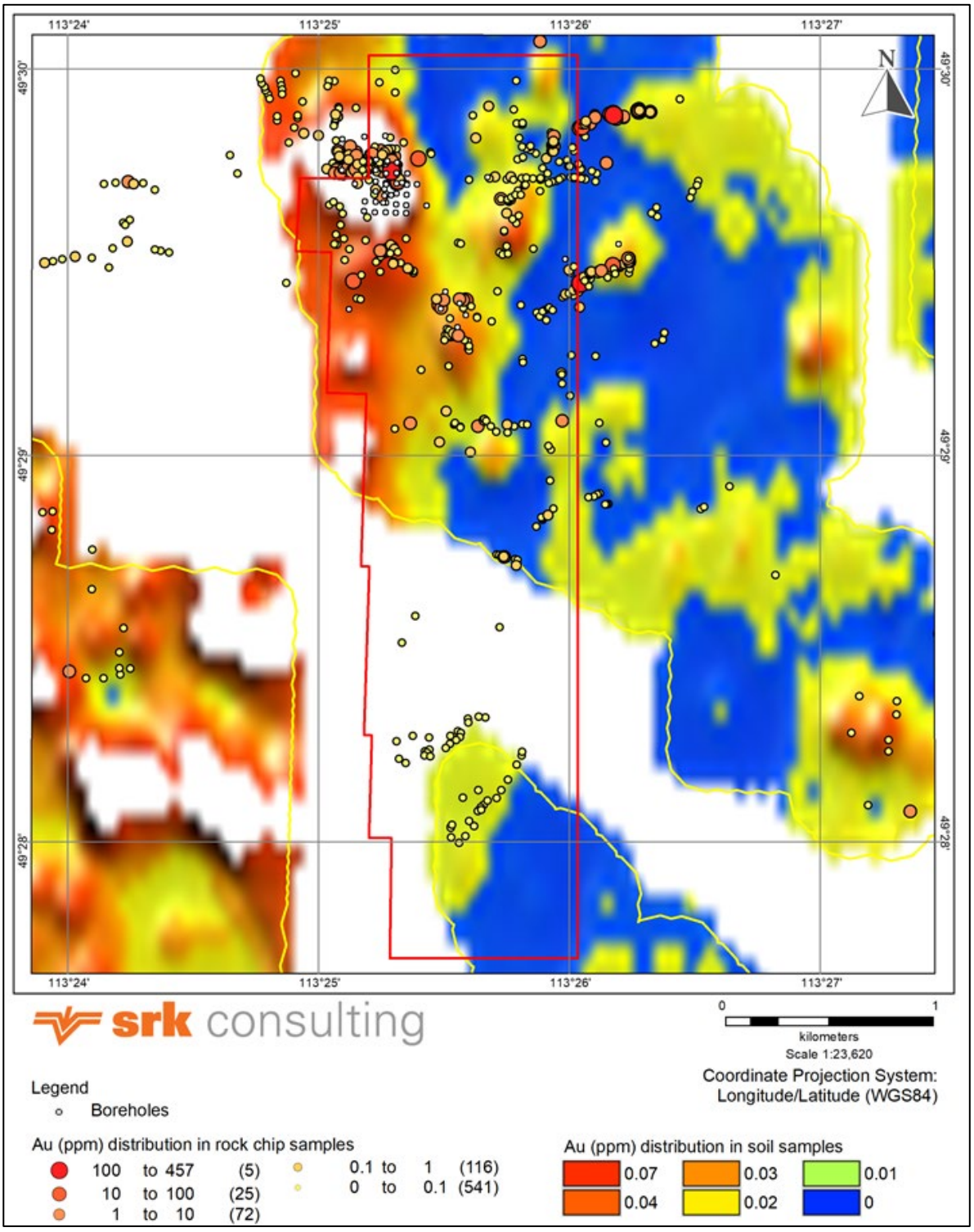

Figure 5-9: Gold distribution in soil and rock chips samples

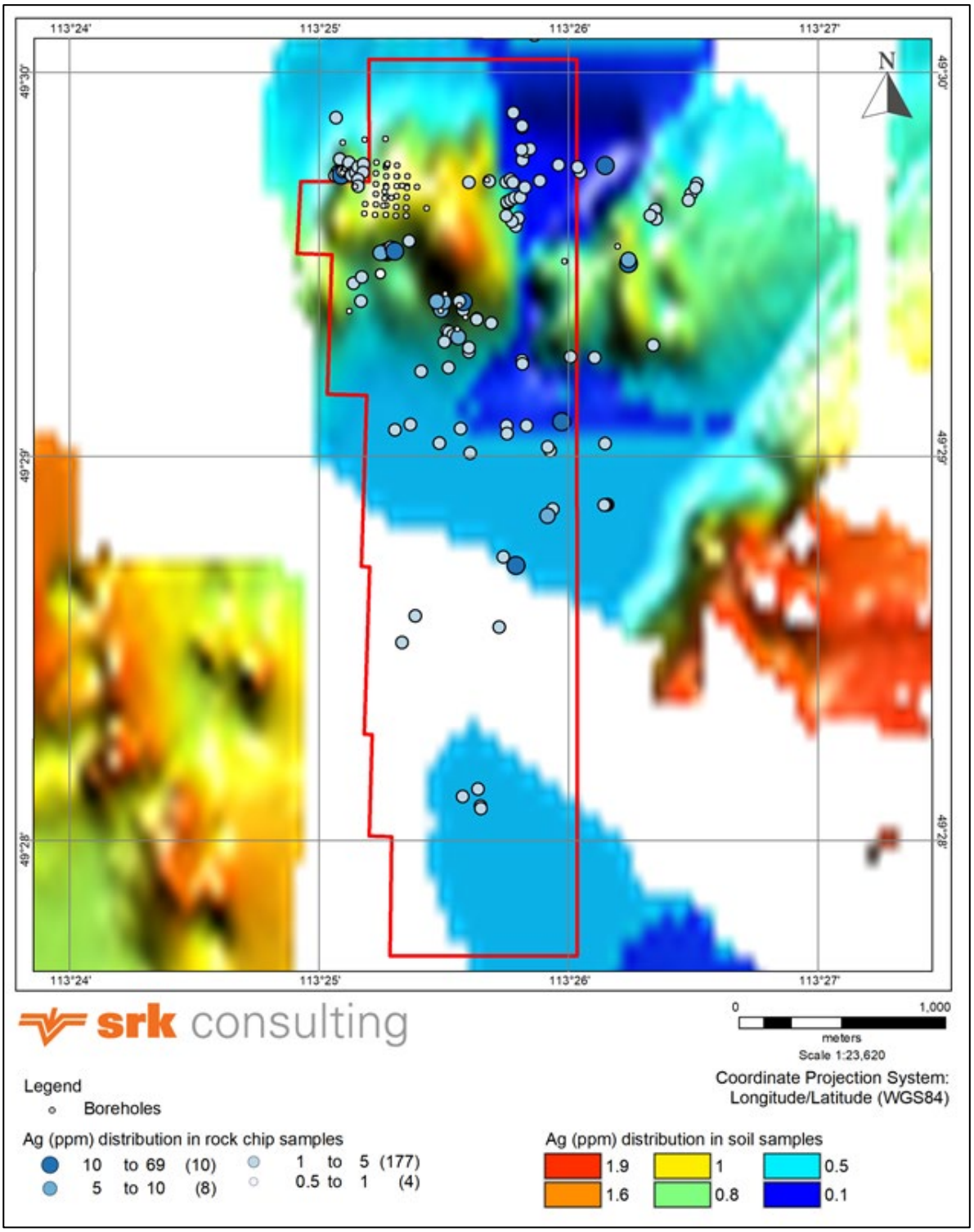

Figure 5-10: Silver distribution in soil and rock chips samples

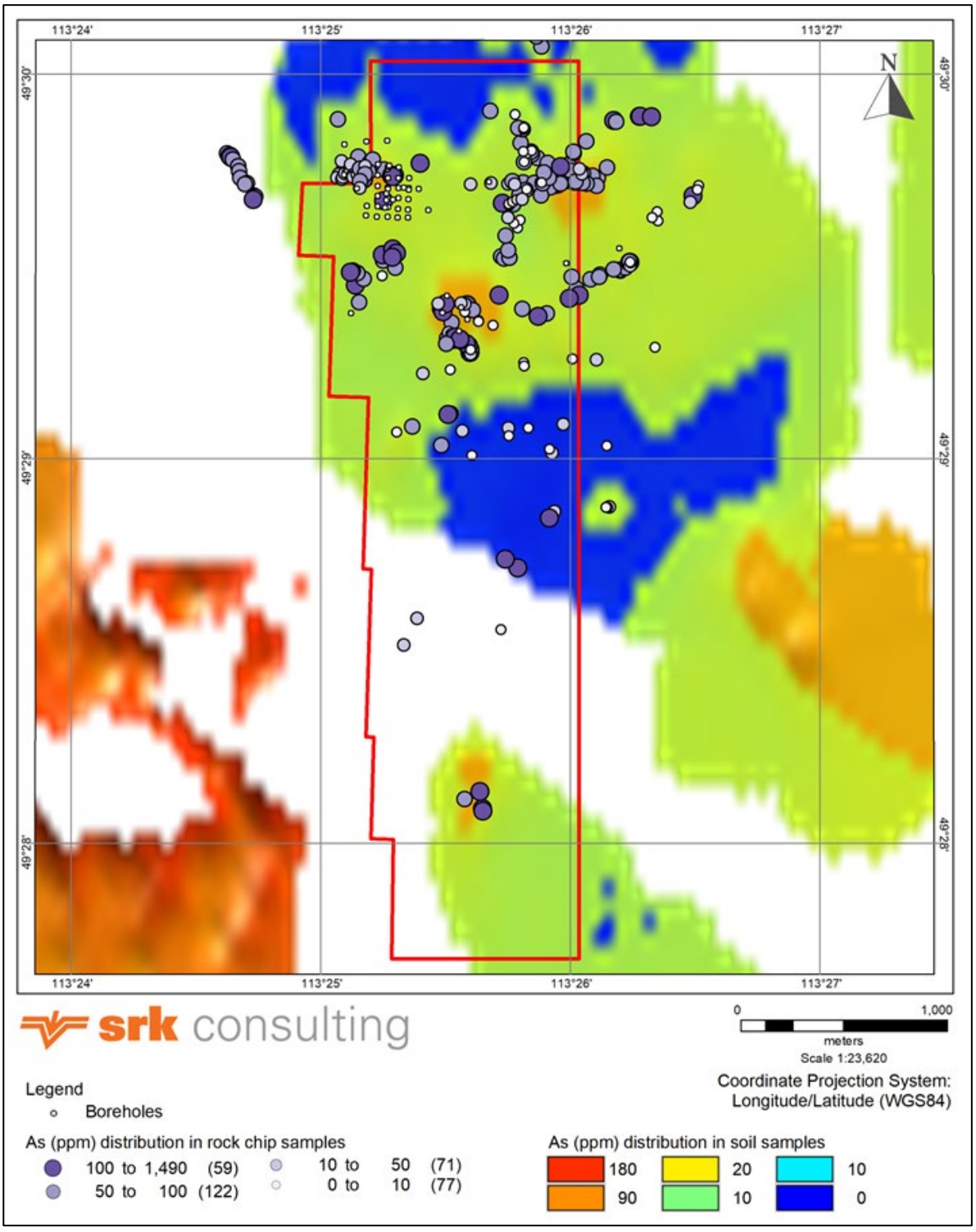

Figure 5-11: Arsenic distribution in soil and rock chips samples

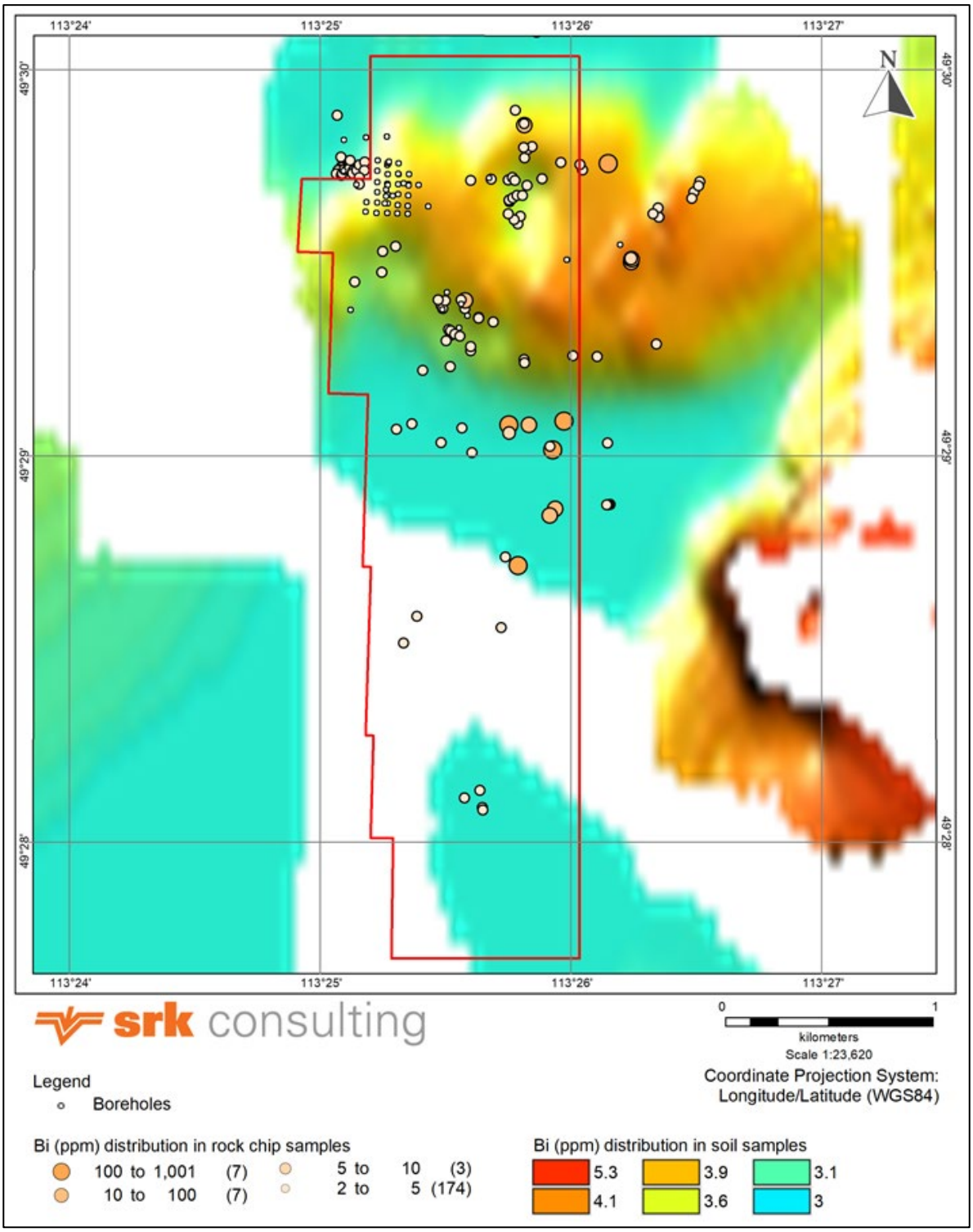

Figure 5-12: Bismuth distribution in soil and rock chips samples

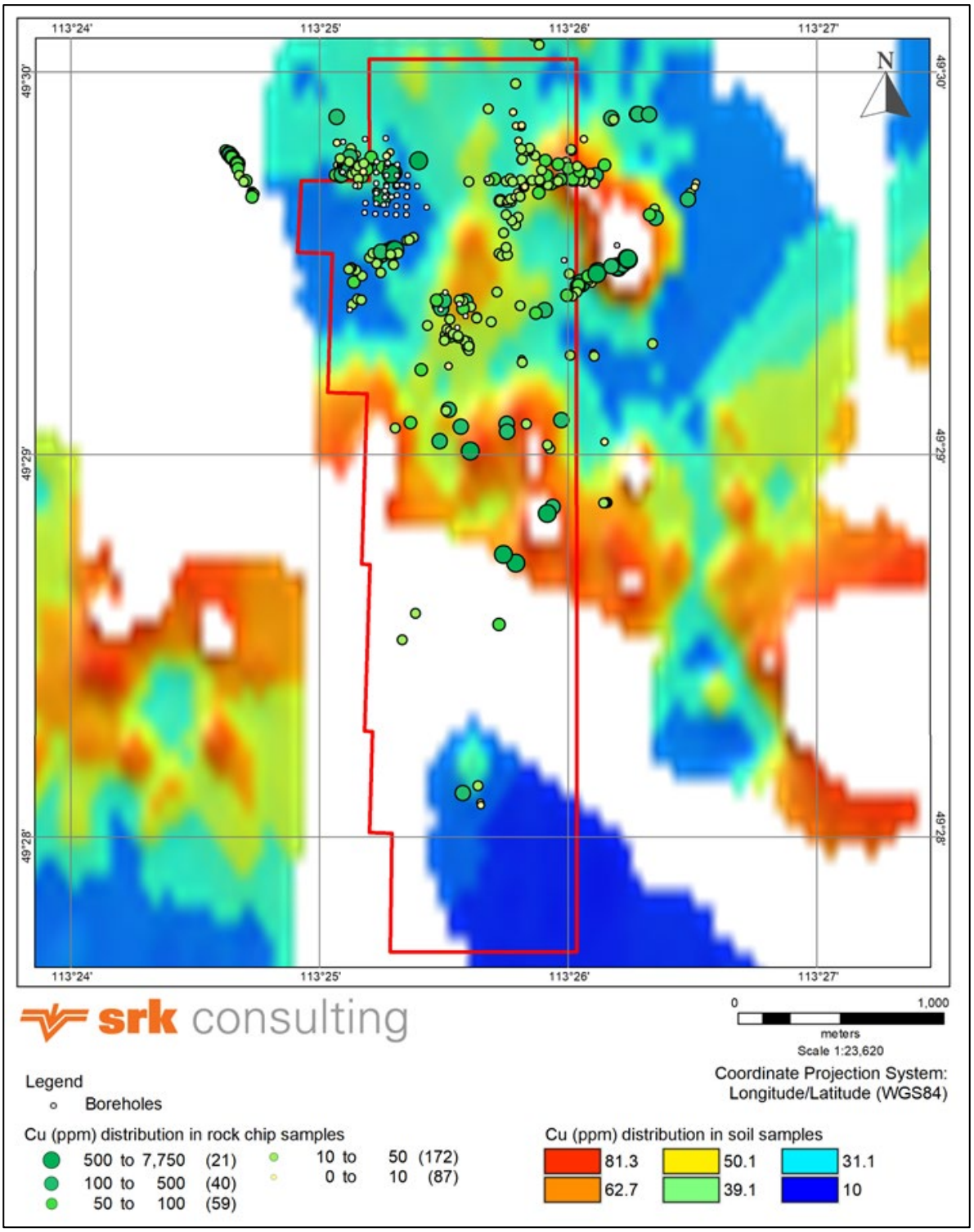

Figure 5-13: Copper distribution in soil and rock chips samples

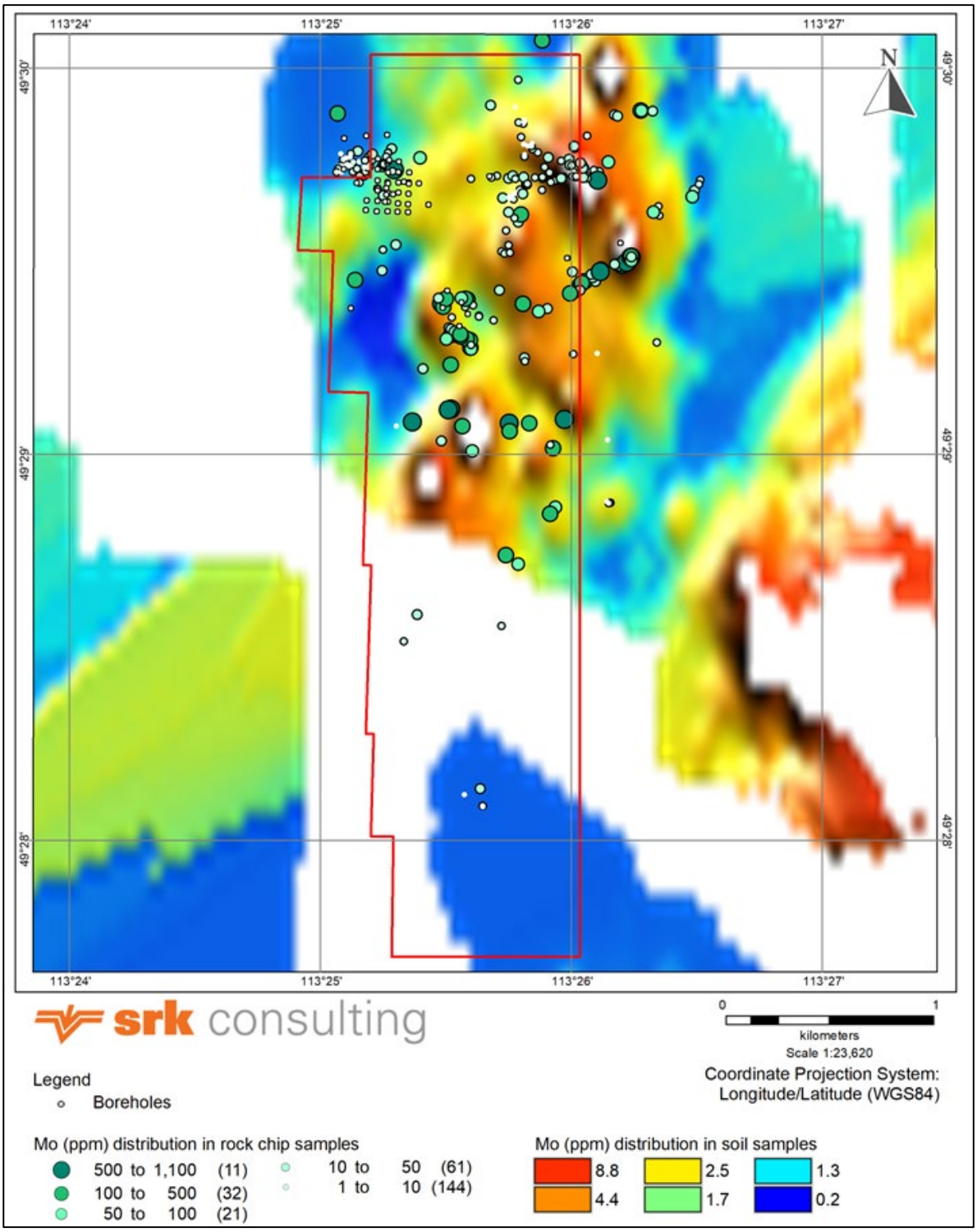

Figure 5-14: Molybdenum distribution in soil and rock chips samples

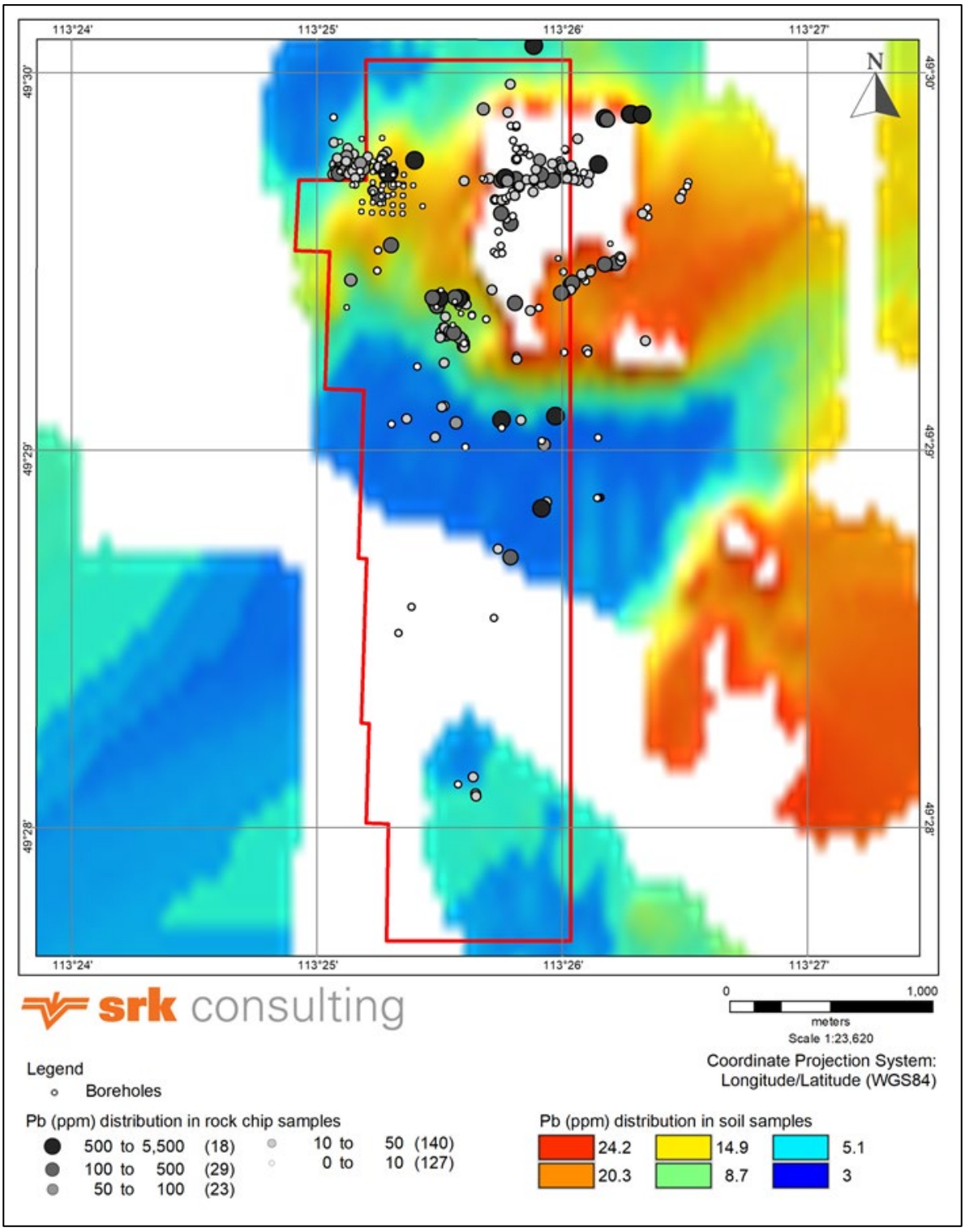

Figure 5-15: Lead distribution in soil and rock chips samples

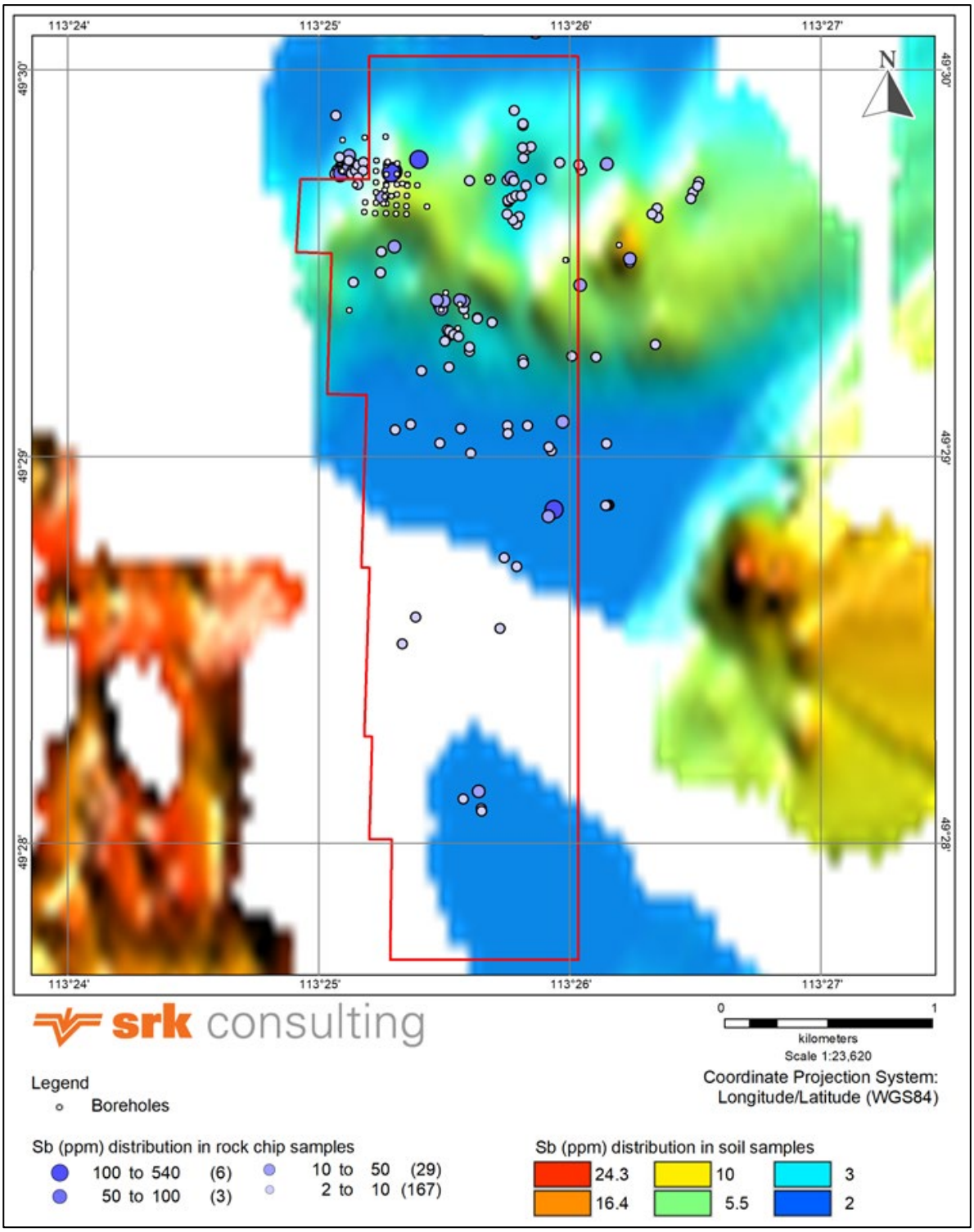

Figure 5-16: Antimony distribution in soil and rock chips samples

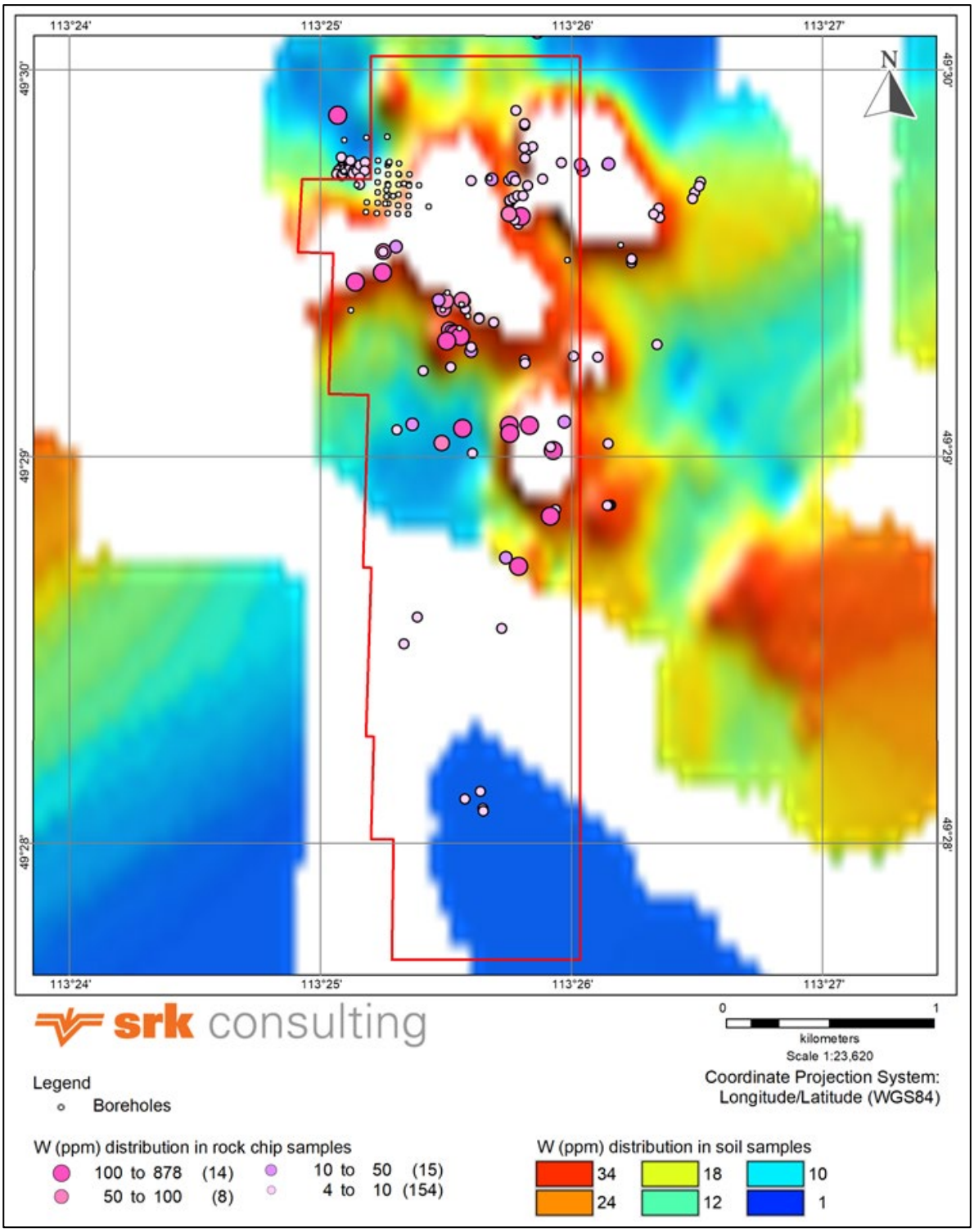

Figure 5-17: Tungsten distribution in soil and rock chips samples

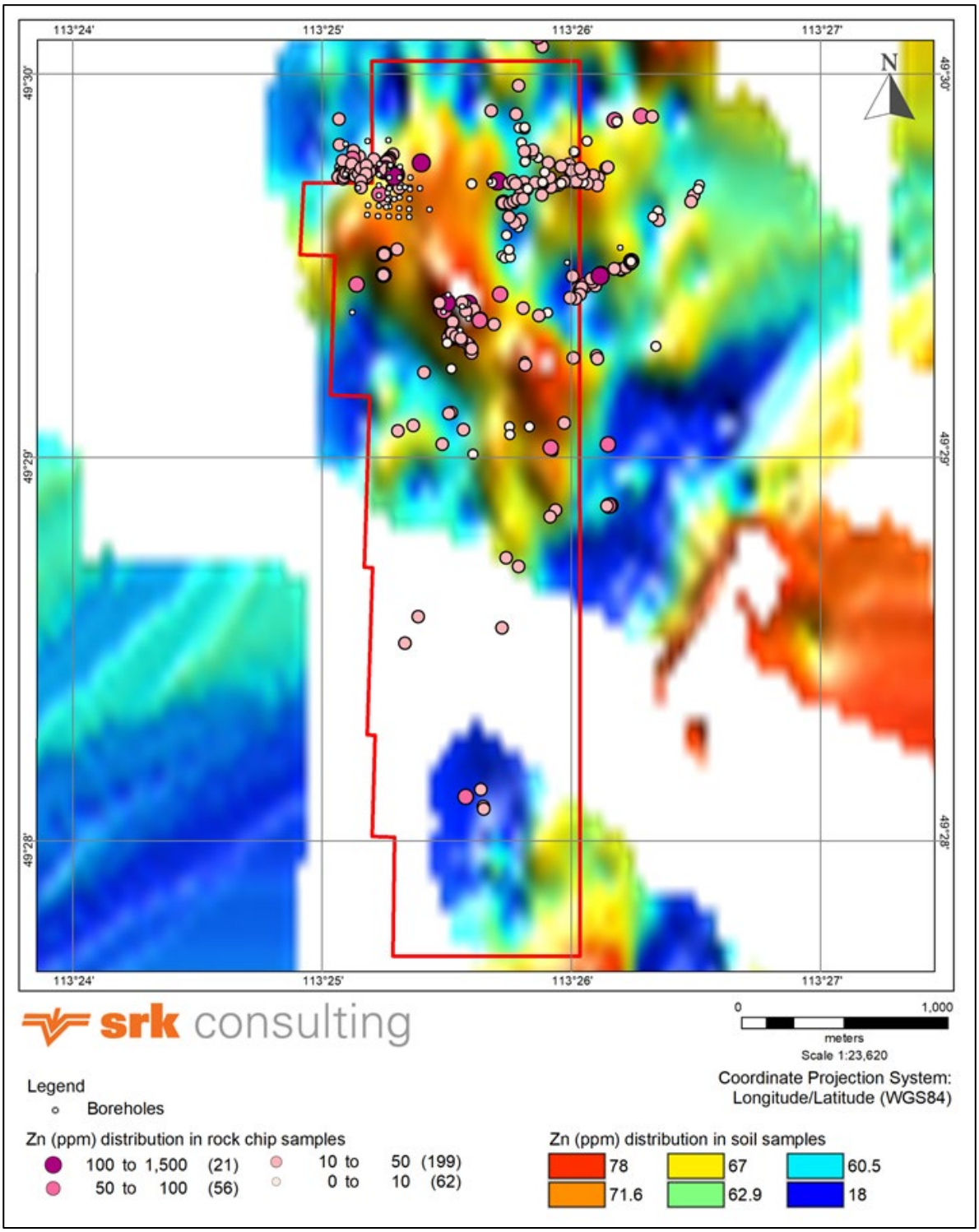

Figure 5-18: Zinc distribution in soil and rock chips samples

6 Mineralisation

SRK notes that two main genetic deposit models have been postulated for mineralisation identified at the Tsagaan Chuluut Gold Project: initially by Minarco (2011) and then by Bond et al. (2013).

6.1 Porphyry – epithermal mineralisation system (Minarco, 2011)

Minarco (2011) describes three styles of mineralisation in the Project tenements as follows:

- Porphyry gold-copper targets
- Low-sulphidation epithermal gold mineralisation along regional fault structures
- Phyllic (or beresite)-related gold mineralisation, which is associated with the TC1 deposit.

Minarco opines that Tsagaan Chuluut Gold Project is large deep-seated gold-copper porphyry system, with epithermal gold mineralisation developed in palaeo sub-surface levels, while the beresite-related mineralisation is an interpreted phyllic alteration in shallower parts of the system. Minarco speculated that a hypothetical gold-copper porphyry target lies beneath the beresite mineralisation. Minarco interpreted the total magnetic imagery (TMI) survey and identified several potential porphyry targets as shown on Figure 6-1.

SRK supports the Minarco model in principle, but opines that these targets need refining using satellite image interpretation, more-detailed structural geological and alteration mapping supported by infrared spectrometry, a more-detailed study of the breccias and magma fertility studies.

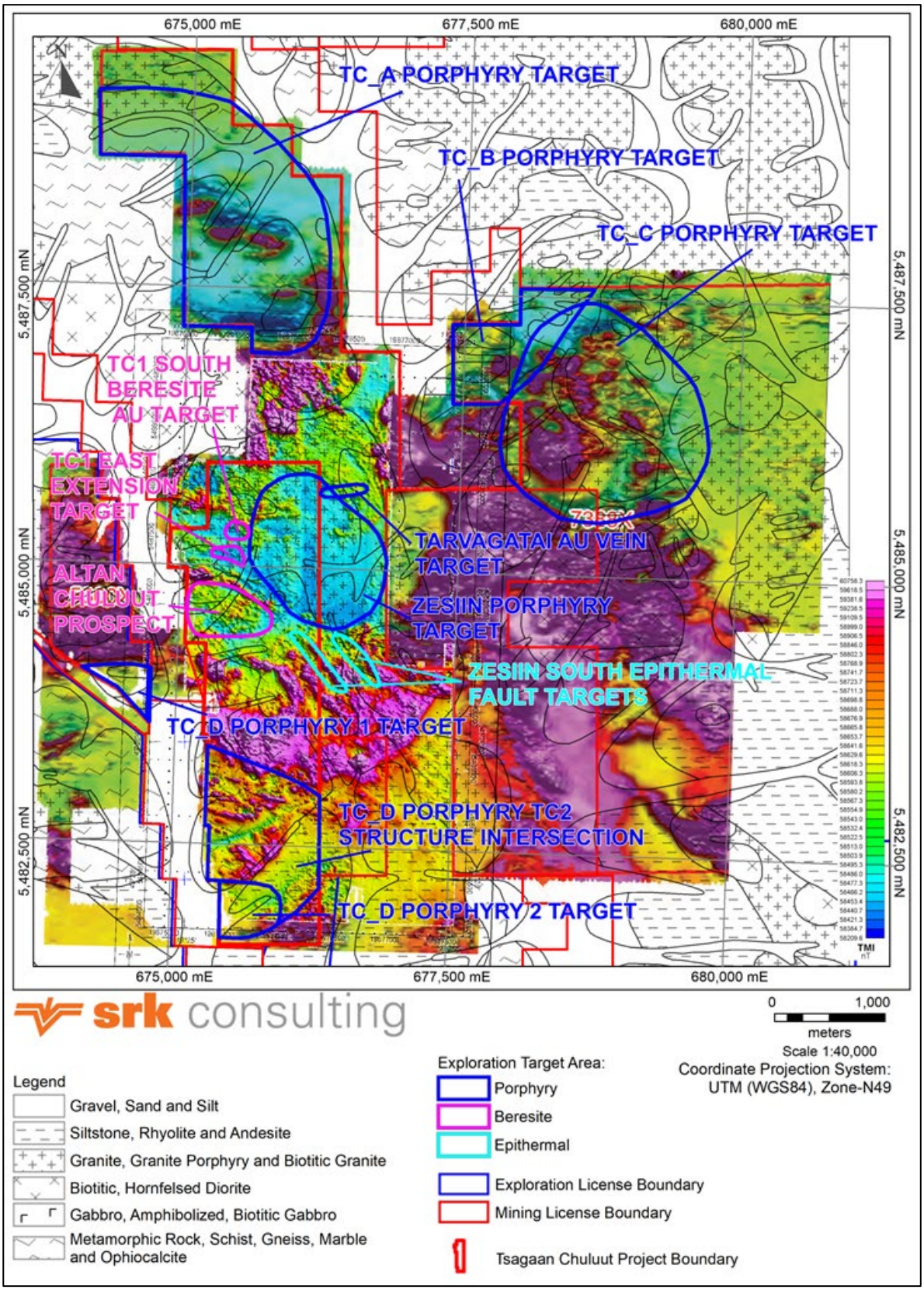

Figure 6-1: Exploration targets identified by Minarco

Source: Minarco, 2011

6.2 Reduced Intrusion Related Gold System

Bond et al. (2013) speculated that the Tsagaan Chuluut Gold Project is either a Reduced Intrusion Related Gold System (RIRGS), low-sulphidation epithermal system or an orogenic gold system. According to their petrological and geochemical study, Bond et al. (2013) opined that the mineralisation texture, orebody form and geochemical signatures of an RIRGS closely match those at the TC1 deposit. However, the mineral assemblage observed at TC1 almost perfectly matches what would be expected with a low-sulphidation epithermal deposit but lacks the high gold grades associated with this style of deposit and has none of the expected free silver or silver tellurides. However, the TC1 deposit would not be a conventional RIRGS because at least part of the gold mineralisation appears to be due to beresite metasomatism that predates the main mineralising phase.

Bond et al. (2013) describe two types of gold mineralisation. Type I comprises earlier round inclusions of gold within third generation pyrite. The Type II is prevalent at TC1 as gold filling later stage fractures in third generation pyrite associated with fifth generation quartz veining. It is the fifth generation quartz veining which contains Type A, CO_2-bearing fluid inclusions and these fluid inclusions appear to be the result of hydrothermal alteration from a reduced source, which is interpreted to be a reduced granitoid body. Although emplectite (Bi-Cu-S) and bismuth-bearing galena were observed at the TC1 deposit, as were very rare tellurides, the suite was not enriched in bismuth or tellurium minerals to the extent expected in an RIRGS.

Bond et al. (2013) opined that the chemical elevations and mineralisation assemblage at TC1 suggests it lies within the arsenic-gold zone of an RIRGS. In this middle zone, the TC1 deposit is still moderately enriched in tungsten and shows enrichment in antimony, evidenced by abundant tetrahedrite, which is a feature of the next zone (distally). Although a Mid-Jurassic granite outcrops relatively close to the TC1 deposit, there is no higher-grade gold recorded between the TC1 deposit and the Mid-Jurassic granite.

The presence of unidirectional solidification textures within the granite may suggest it to be an apical part of a deeper intrusive system.

According to Bond et al. (2013), the first generation K-feldspar and biotite veins (which Bond et al. (2013) called ‘granitoid’ veins), occurring earlier than the fifth generation silicification, leads to an interpretation that the granite outcropping at the TC1 deposit was responsible for the first generation granitoid veins only, and fifth generation gold mineralisation is therefore the result of an undiscovered reduced granitoid body at depth in an RIRGS. The source of the third generation beresitising fluids is unknown, but upwelling fluids could have been focused through the intrusives, as in the Berezovskoe deposit, Kryazhev et al. (2009). In the formation of the Berezovskoe deposit, the local granite previously thought to be the source of the mineralising fluids was merely a pathway of least resistance that focused gold-bearing orogenic fluids, Kryazhev et al. (2009).

6.3 TC1 deposit area

Minarco (2011) interpreted mineralisation as a series of sheeted and parallel lower sulphidation, epithermal quartz and sericite veins. Mineralisation in the area is best developed within a brecciated pre-existing bucky quartz vein and in open space breccias aligned with east–west-trending zones dipping to the south at angle ranging from 30° to 40°. The confirmed strike length of the mineralisation zones is over 300 m and mineralisation is open along the flanks. Mineralisation was drill tested to a depth of 300–350 m, which has an approximate elevation ranging from 700 to 1000 m above sea level. From this drilling, mineralisation is observed to be 120–130 m thick, with grade ranging from 0.81 to 1.96 g/t Au.

Bond et al. (2013) describe, from selected core samples, limited gold mineralisation in third generation beresite veins and the majority of gold mineralisation occurring with the fifth generation quartz veins. Since the drill core was not oriented, Bond et al. noted that it was not possible to define the orientation and spatial relationship of the fifth generation veins (Bond et al., 2013).

Based on SRK's observations from structural logging and core photos provided by SG, the mineralisation occurs with, or is hosted by, hydrothermal breccias with thin quartz veinlets developed locally within or associated with the hydrothermal brecciation. This is illustrated in Figure 6-2 with a strong spatial correlation noted between the hydrothermal breccia and gold distribution based on 3D modelling in Leapfrog™. SRK notes that both veinlet (third and fifth generation gold hosting) systems described by Bond et al. (2013) do not show lateral continuity and opines that both gold-bearing veins are developed during hydrothermal alteration within breccia bodies, which are closely spatially related with zones of faulting and shearing (Figure 6-3).

Quartz veins recorded in core are typically in upper part of the quartz diorite porphyry system. In the deeper part of the quartz diorite porphyry, diorite and granodiorite veinlets with carbonate or quartz have been recorded, but only erratically.

An updated geology map of TC1 deposit area is provided in Figure 6-4 and cross sections are shown in Figure 6-5, Figure 6-6, Figure 6-7, Figure 6-8, Figure 6-9 and Figure 6-10.

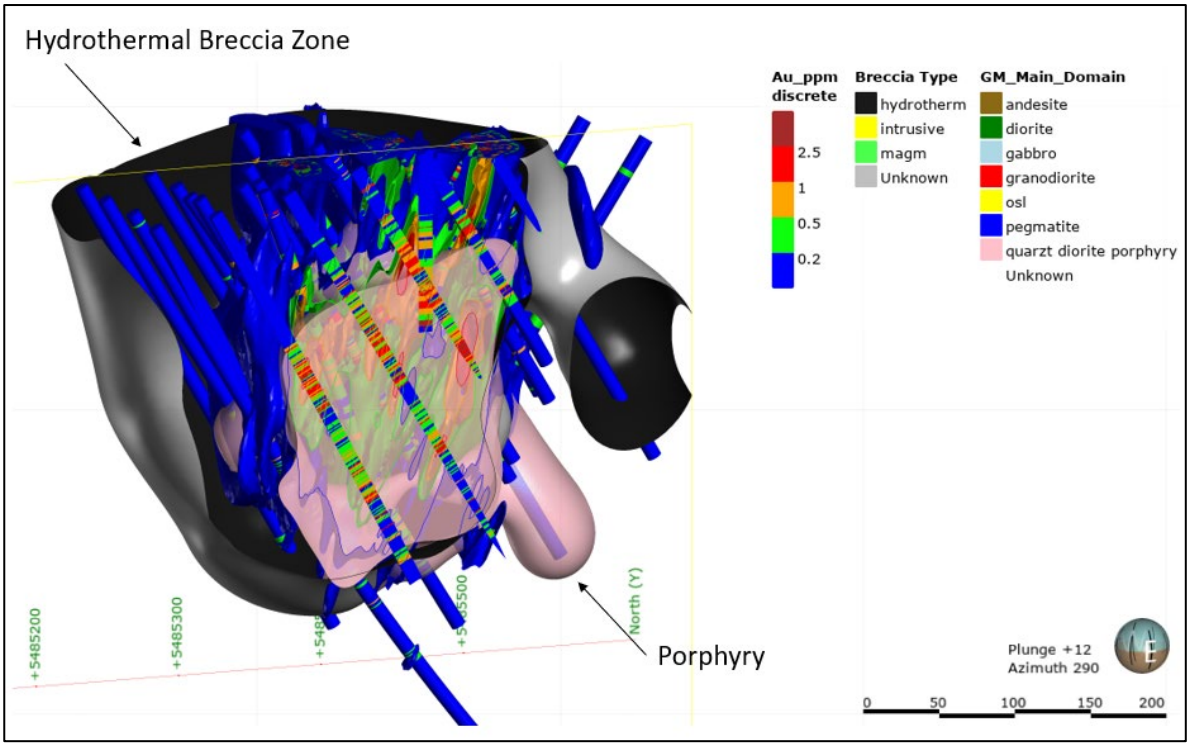

Figure 6-2: 3D distribution of gold mineralisation as well as hydrothermal breccia (black) and porphyry distributions (pink)

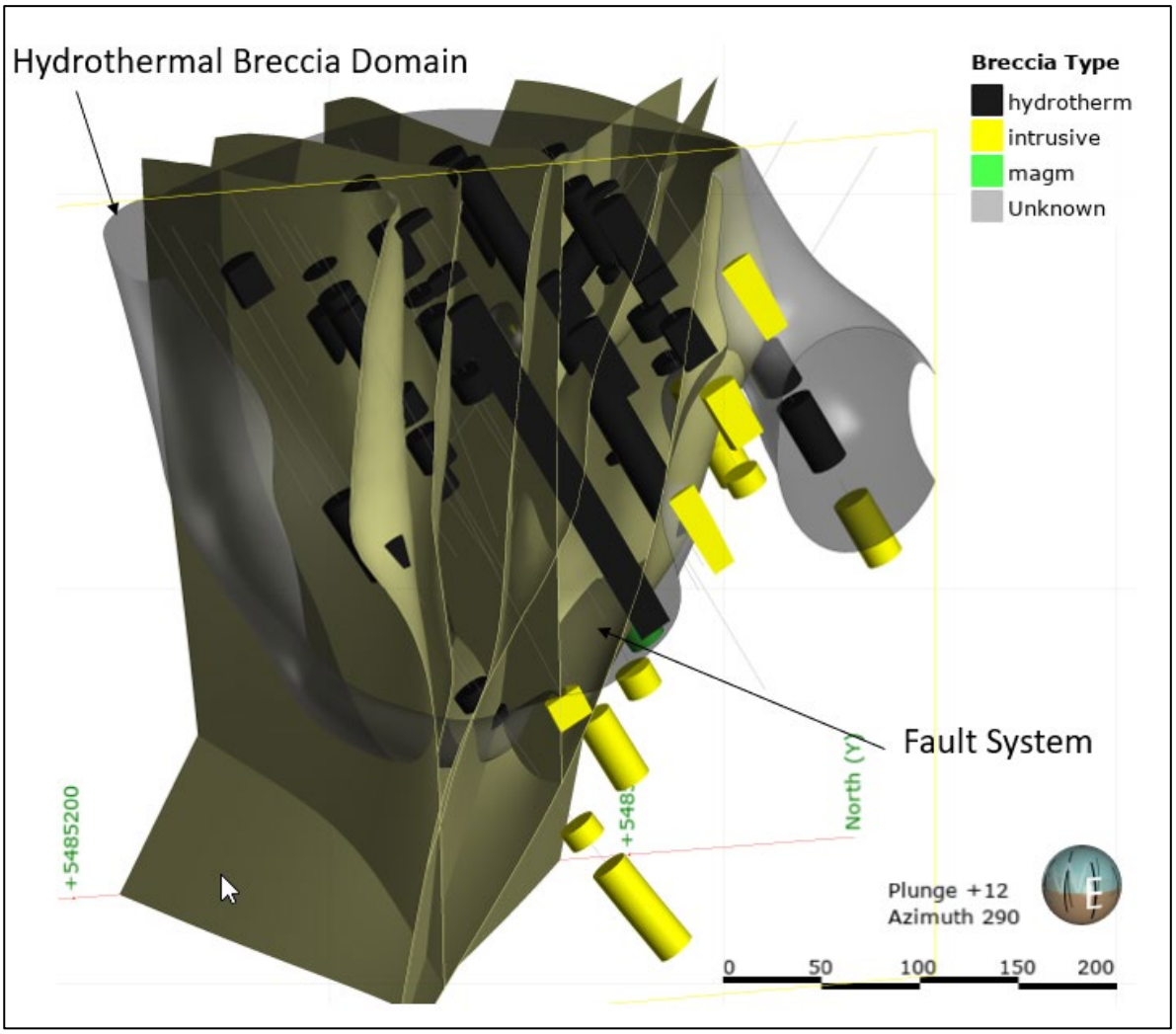

Figure 6-3: 3D distribution of hydrothermal breccia development (black) and faults (tan)

Note: On boreholes are hydrothermal breccia intervals marked black, intrusive breccia intervals marked yellow and other magmatic breccias in green

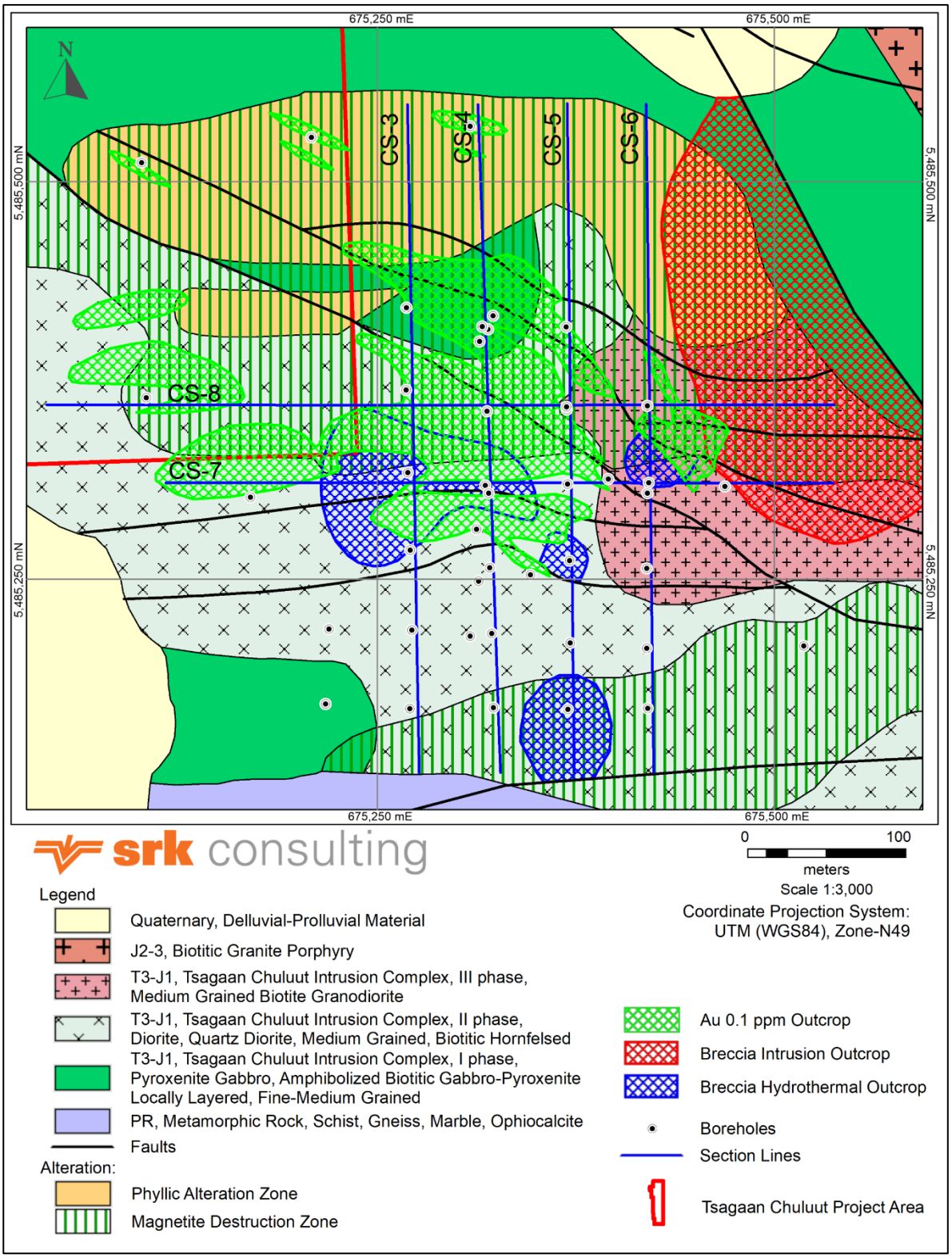

Figure 6-4: TC1 deposit geology map

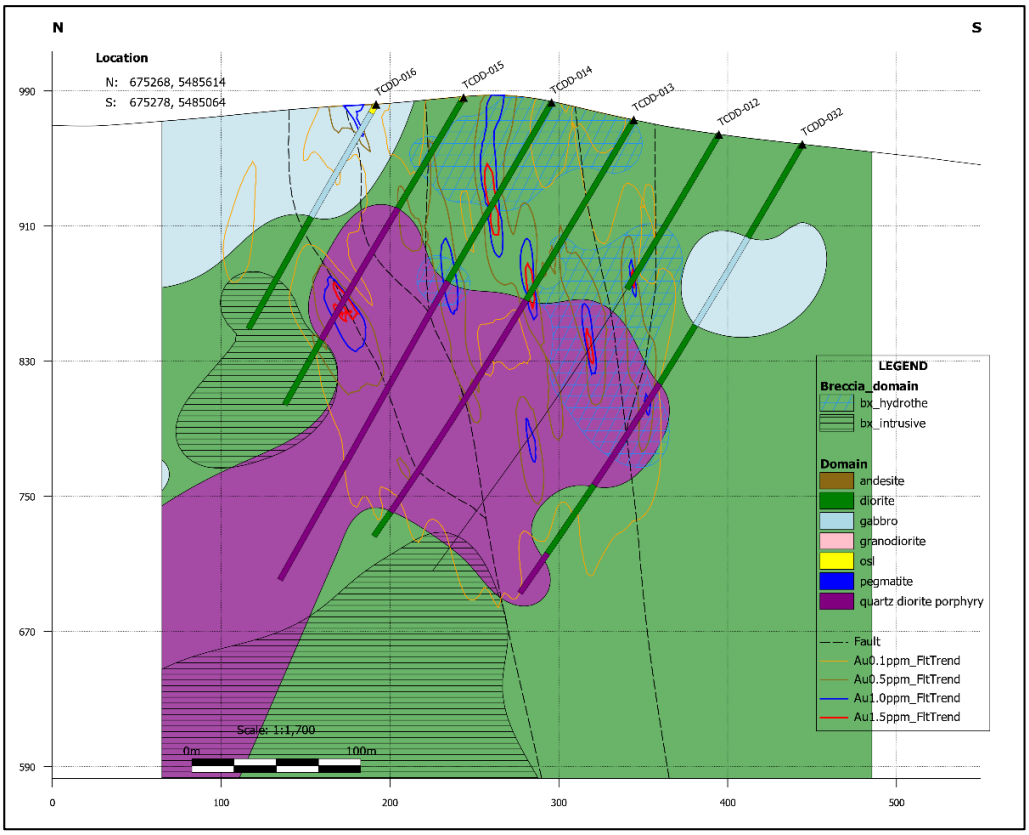

Figure 6-5: TC1 deposit - Section CS3

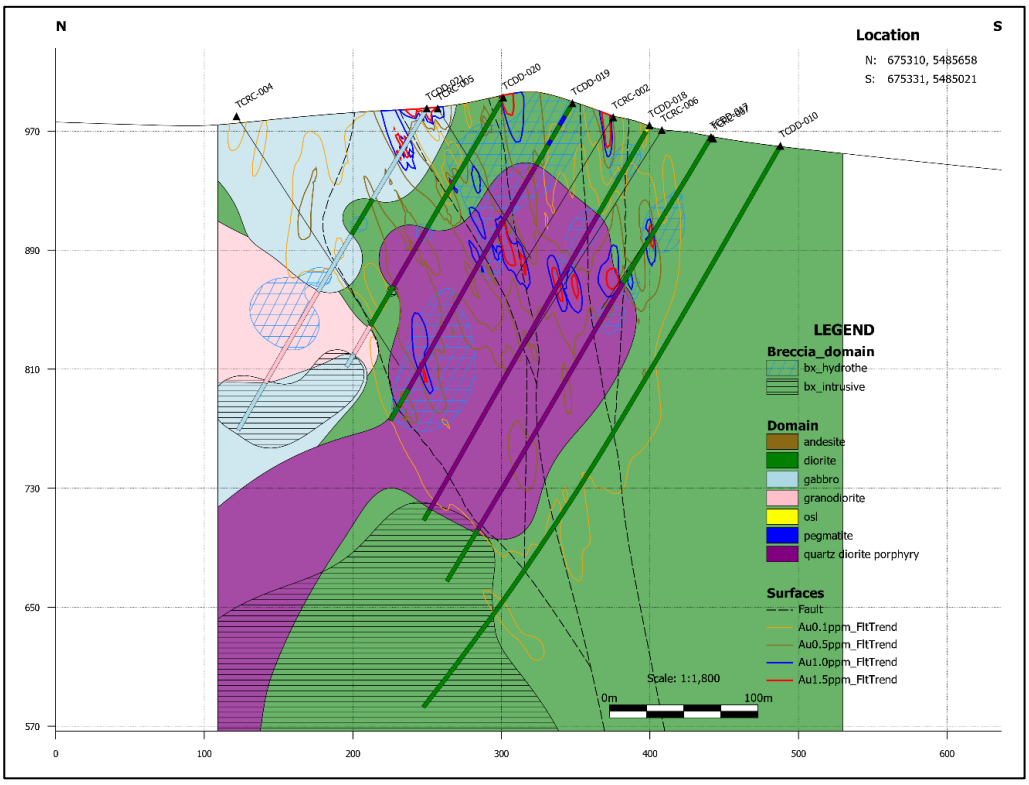

Figure 6-6: TC1 deposit - Section CS4

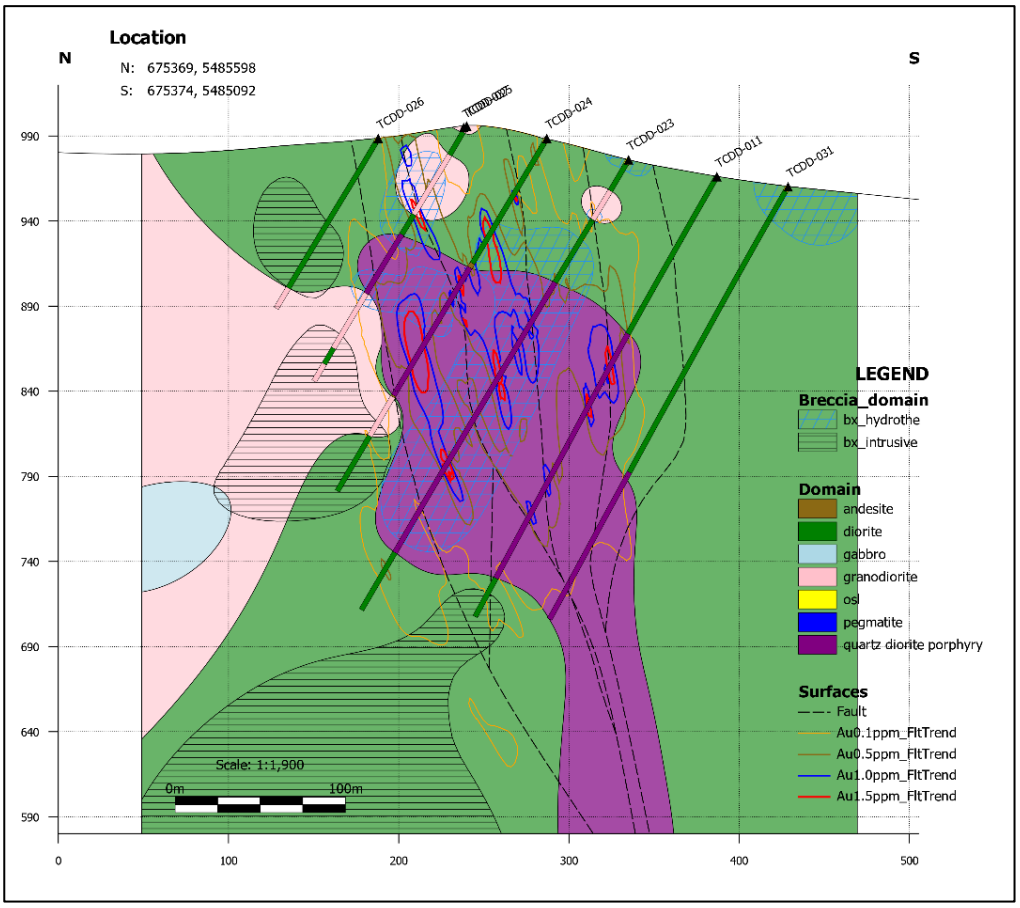

Figure 6-7: TC1 deposit - Section CS5

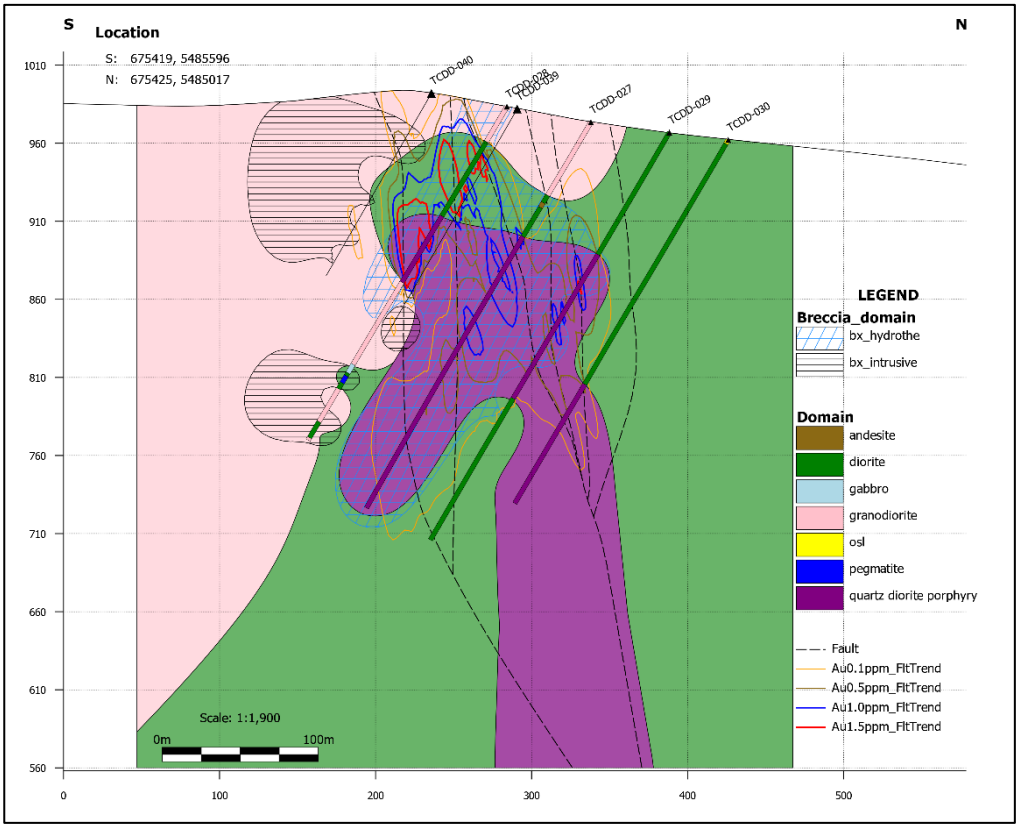

Figure 6-8: TC1 deposit - Section CS6

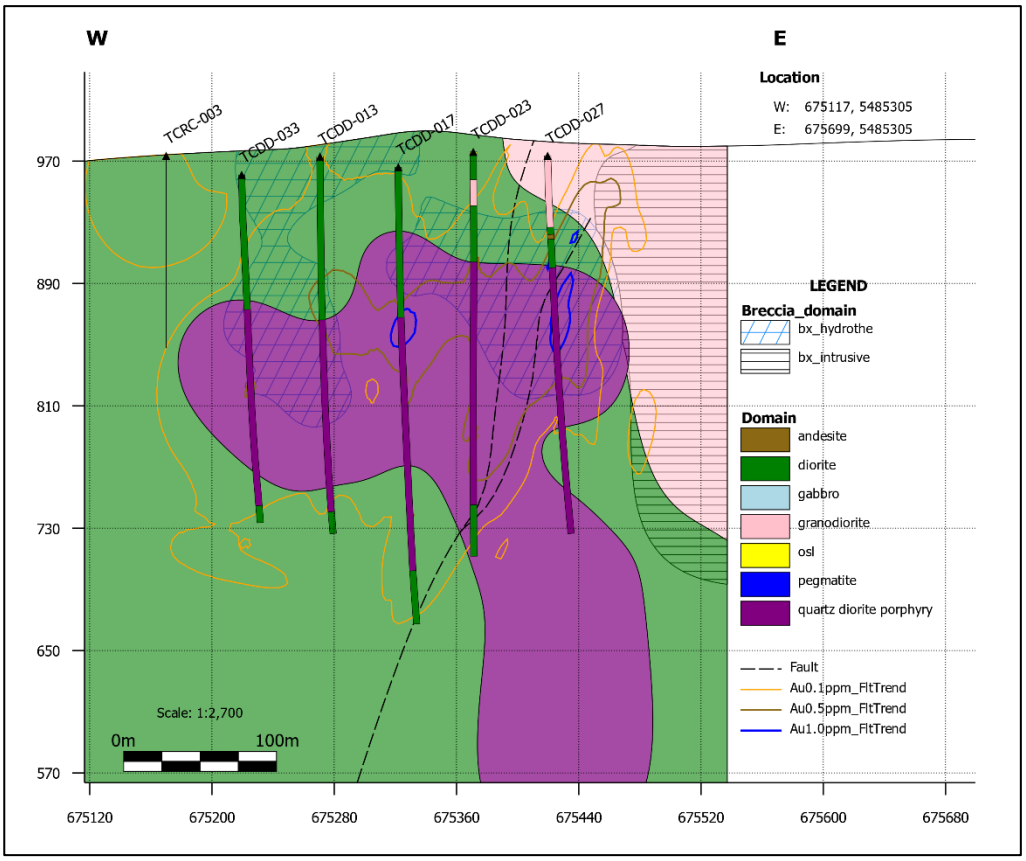

Figure 6-9: TC1 deposit - Section CS7

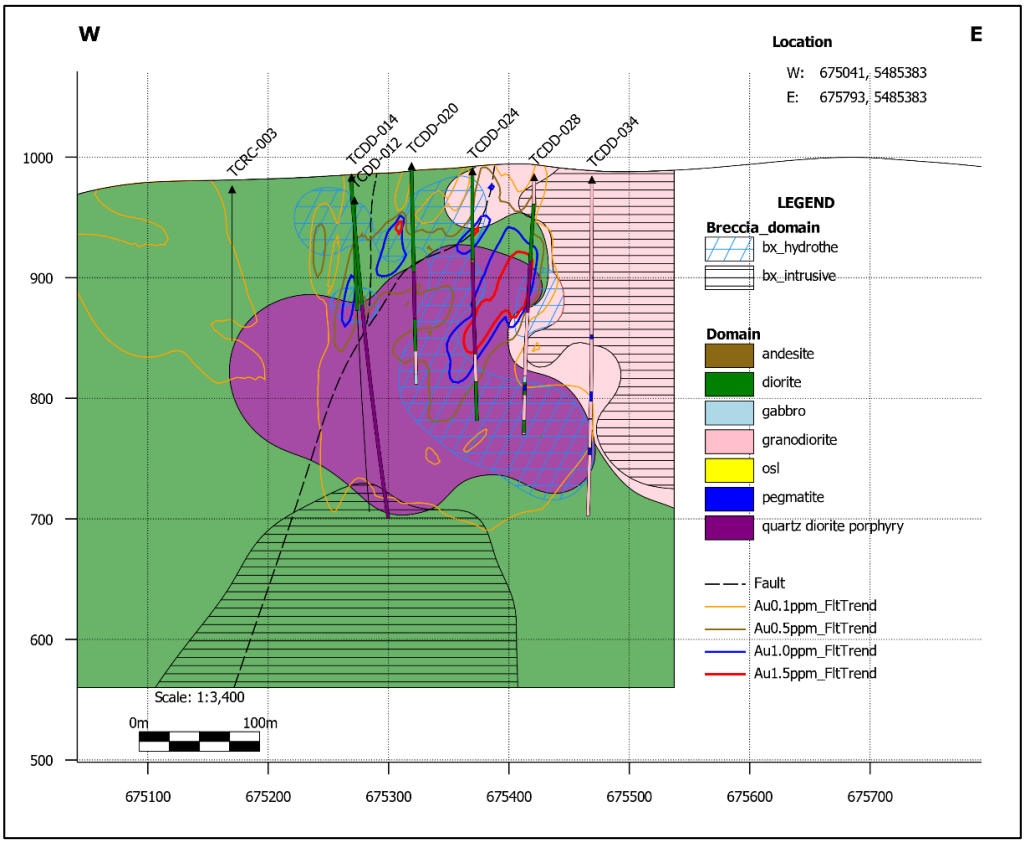

Figure 6-10: TC1 deposit - Section CS8

6.3.1 Mineralogy and Geochemistry

SRK reviewed core sample assay data and carried out basic statistics of selected elements as provided in Table 6-1 and a correlation table of selected elements is provided in Table 6-2. In order to assess elevated elements, SRK normalised selected elements typically related to either porphyry, RIRGS or low-sulphidation epithermal mineralisation using Rudnick's composition of upper continental crust as provided in Table 6-3 (Rudnick, 2014). SRK noted that the elements typically related to a gold porphyry system and an RIRGS are both elevated, but tellurium, which would be expected in an inner zone of an RIRGS, occurs in traces. In addition, Table 6-2 shows moderate to good correlation of Sb, As, Ag, Bi with Cu, which is more suggestive of a porphyry system origin.

Table 6-1: Statistics of selected elements

	Au	Ag	As	B	Ba	Bi	Ce
Min.	0.00	0.10	0.00	0.00	6.45	0.00	1.60
Max.	28.90	30.60	390.00	2050.00	4060.00	1180.00	93.50
Avg	0.41	2.97	12.99	98.39	492.79	9.39	43.10
Median	0.17	0.70	0.00	40.00	490.00	0.00	40.70
Std Dev	0.96	4.95	22.46	143.88	234.55	77.87	12.07
CV	2.33	1.66	1.73	1.46	0.48	8.30	0.28
Count	4669	298	2079	720	1718	1152	979
	Co	**Cr**	**Cu**	**Mn**	**Mo**	**Nb**	**Pb**
Min.	0.00	0.00	0.00	89.00	0.00	0.00	0.00
Max.	140.00	600.00	958.00	5760.00	140.00	110.00	1680.00
Avg	12.72	82.64	32.51	889.01	2.94	2.43	17.14
Median	10.00	30.00	12.00	750.50	0.00	0.00	6.00
Std Dev	11.38	103.80	61.72	557.03	8.30	6.13	72.18
CV	0.89	1.26	1.90	0.63	2.82	2.52	4.21
Count	1715	1717	2089	1718	2075	1681	1883
	Sb	**Sn**	**Sr**	**Te**	**V**	**W**	**Zn**
Min.	0.00	0.00	30.00	0.00	0.00	0.00	0.00
Max.	444.00	520.00	1020.00	1.20	355.00	2580.00	1230.00
Avg	8.19	0.44	299.39	0.00	114.57	18.54	39.21
Median	0.00	0.00	254.50	0.00	100.00	0.00	30.00
Std Dev	27.18	13.22	168.05	0.06	44.73	98.09	64.51
CV	3.32	30.29	0.56	15.82	0.39	5.29	1.65
Count	1681	1673	1718	953	1718	1682	1886

CV = coefficient of variation

Table 6-2: Correlation of selected elements

	Au	Ag	As	Ba	Bi	Co	Cu	Li	Mo	Pb	Sb	V	W
Ag	0.13												
As	0.16	0.29											
Ba	-0.30	-0.09	-0.22										
Bi	0.43	0.39	0.52	-0.22									
Co	0.52	0.11	0.31	-0.22	0.50								
Cu	0.33	0.73	0.56	-0.21	0.53	0.38							
Li	0.28	-0.08	-0.03	-0.48	-0.07	0.12	-0.15						
Mo	0.27	0.16	0.18	-0.10	0.16	0.16	0.31	0.05					
Pb	0.37	0.29	0.46	-0.09	0.83	0.37	0.43	-0.13	0.26				
Sb	0.15	0.73	0.53	-0.12	0.65	0.25	0.71	-0.09	0.08	0.51			
V	0.03	0.15	0.51	-0.25	-0.10	0.09	0.20	0.11	0.02	-0.12	0.12		
W	0.16	0.08	0.15	-0.06	-0.06	0.31	0.47	-0.04	0.49	0.02	0.04	0.00	
Zn	-0.07	0.33	0.13	-0.18	0.01	0.06	0.31	-0.08	0.13	0.20	0.30	0.28	0.17

Note: green indicates the highest correlation; red indicates the lowest correlation.

Table 6-3: Selected elements normalised value

	Au	Ag	As	Ba	Bi	Ce
Avg	0.41	2.97	12.99	492.79	9.39	43.10
Rudnick	0.00	0.05	4.80	624.00	0.16	63.00
CV	274.02	56.12	2.71	0.79	58.66	0.68
	Co	**Cr**	**Cu**	**Mo**	**Nb**	**Pb**
Avg	12.72	82.64	32.51	2.94	2.43	17.14
Rudnick	17.30	92.00	28.00	1.10	12.00	17.00
CV	0.74	0.90	1.16	2.67	0.20	1.01
	Sb	**Sn**	**Sr**	**V**	**W**	**Zn**
Avg	8.19	0.44	299.39	114.57	18.54	39.21
Rudnick	0.40	2.10	320.00	97.00	1.90	67.00
CV	20.48	0.21	0.94	1.18	9.76	0.59

The average Ag/Au ratio is 8.4, the Cu(%)/Au(ppm) ratio is 0.03 and the Cu/Mo ratio is 12, which is more consistent with a gold±copper porphyry system.

Bismuth and tungsten are strongly elevated as indicated in Table 6-1 and Table 6-3, which is an association described in the upper parts of porphyry systems and a pluton-proximal RIRGS.

The mineralogical descriptions in various geology, resource and petrology reports are limited. The most comprehensive description provided in Bond et al. (2013) deals mainly with vein mineralogy. The most comprehensive mineralogical description of mineralised rocks is provided in the Hepta metallurgical test report (Hepta, 2013) and reproduced in Table 6-4. The mineralogy of the one tested sample indicates the presence of magnetite and secondary rutile and the absence of ilmenite, which is consistent with an oxidised fluid.

In summary, the data to date are more characteristic of mineralisation/metal transport in an oxidised hydrothermal fluid associated with an intrusion/porphyry system.

Table 6-4: Mineralogical composition from mineralised rock submitted for metallurgical testing

Product	Concentrate	Intermediate Product		Waste-2		Waste-3	
Fraction size (µm)	-	74	-74	74	-74	74	-74
Fraction yield (%)		86.8	13.2	49	50.9	72.2	27.8
Total (g)	**26.14**	**34.69**	**5.58**	**22**	**22.3**	**33.8**	**12.3**
Minerals							
Gold (number of grains)	-	-	-	-	-	-	-
Amphibole	0.55	0.79	0.21	0.6	0.6	2	0.3
Amphibole-Chlorite-Carbonate-quartz veins-aggregate with pyrite	0.54						
Anatase	mn	mn	mn	mn	few	mn	mn
Apatite	0.02	0.03	0.01	0	mn	mn	mn
Galena	mn	mn	mn	mn	mn	mn	-
Garnet	mn	-	few	-	mn	mn	-
Lepidolite	0.04	0.02	mn	0	0.01	0.3	0.01
Secondary minerals of copper	0.02	0.01	mn	mn	mn	mn	mn
Carbonate-siderite	2.41	15.27	3.96	7.7	15.3	21.3	9.78
Quartz	0.86	10.16	0.3	10	4	4.2	1.2
Magnetite	0.2	5.54	0.1	1	0.1	3	0.1
Monazite	mn	mn	0.01	mn	mn	mn	mn
Pyrite	19.4	1.5	0.81	0.1	0.13	0.18	0.2
Zircon	0.04	0.06	0.02	0	mn	mn	mn
Rutile	mn	mn	mn	mn	few	mn	few
Sphene	0.12	0.05	0.03	0	0.01	0.01	0.01
Iron	0.79	0.12	mn	mn	mn	0.03	mn
Iron oxide	0.35	0.11	0.02	0.1	0.08	0.1	0.01
Fluorite	0.1	0.11	0.01	mn	mn	0.01	0.01
Chalcopyrite	mn	0.01	-	-	-	mn	mn
Chlorite	0.25	0.22	0.02	0.2	0.1	1	0.2
Feldspar	0.35	0.6	0.05	2.3	2	1.6	0.4
Zircon	0.05	0.01	0.01	mn	mn	0.01	0.01
Epidote	0.05	0.01	0.01	mn	mn	0.01	0.01

Note: few -few granular (number of 1-10 grains)
mn -abundant grains (more than 10 grains)

Source: Hepta (2013)

SRK extracted assays of selected elements from samples within modelled hydrothermal, intrusive and contact breccias. The approach adopted was similar to the approach for lithology types. Statistics of selected elements from breccia- and lithology-type samples suggest that hydrothermal breccia and quartz diorite porphyry are the primary host rocks of gold mineralisation as shown in Table 6-5 and Table 6-6. SRK opines that this supports a porphyry-type mineralisation model at the TC1 deposit.

Table 6-5: Statistics of selected elements for hydrothermal, intrusive and contact breccia types

	Hydrothermal			Intrusive			Contact		
	Mean	Min.	Max.	Mean	Min.	Max.	Mean	Min.	Max.
Ag (ppm)	0.36	0.01	50	0.10	0.01	2	0.01	0.01	0.01
As (ppm)	20.33	2.5	158	5.56	2.5	70	12.21	2.5	60
Au (ppm)	0.52	0.005	17.26	0.05	0.005	2.01	0.09	0.005	0.19
Bi (ppm)	0.50	0.01	8	0.23	0.01	2.5	0.01	0.01	0.01
Cu (ppm)	38.26	1	958	31.66	1	180	6.14	1	10
Li (ppm)	26.41	0.5	100	29.61	3	117	17.71	10	20
Mo (ppm)	3.49	1	112	8.10	1	70	1.00	1	1
Ni (ppm)	56.38	4	270	25.66	1	71	27.63	1	40
Pb (ppm)	20.62	1	965	9.60	1	90	13.23	1	60
W (ppm)	3.41	0.01	160	7.50	0.01	440	38.71	5	180
Zn (ppm)	39.21	2.5	169	54.51	2.5	190	38.71	2.5	50

Table 6-6: Statistics of selected elements for rock types

	Andesite			Diorite			Gabbro			Granodiorite			Pegmatite			Quartz Diorite Porphyry		
	Mean	Min.	Max.	Mean	Min.	Max.	Mean	Min.	Max.	Mean	Min.	Max.	Mean	Min.	Max.	Mean	Min.	Max.
Ag (ppm)				1.30	1	50	1.10	1	17	1.00	1	1	1.00	1	1	2.03	1	30
As (ppm)				13.26	2.5	390	15.12	2.5	114	4.19	2.5	18	2.50	2.5	2.5	8.22	2.5	70
Au (ppm)	0.11	0.005	0.44	0.26	0.005	10.05	0.33	0.005	5.39	0.12	0.005	3.98	0.09	0.005	0.87	0.49	0.005	17.26
Bi (ppm)				2.50	2.5	2.5	2.50	2.5	2.5	2.50	2.5	2.5	2.50	2.5	2.5	2.54	2.5	8
Cu (ppm)				25.34	1	740	19.13	1	293	35.35	1	313	5.60	2	9	39.72	1	569
Li (ppm)				28.19	0.5	117	27.53	8	77	25.00	6	82	6.60	3	8	23.83	0.5	640
Mo (ppm)				4.47	1	140	6.40	1	112	12.62	1	92	6.60	5	7	1.99	1	40
Ni (ppm)				55.33	1	270	33.79	3	111	24.90	6	51	5.00	1	7	13.12	1	190
Pb (ppm)				12.96	1	965	12.81	1	149	11.74	6	17	9.80	5	15	22.49	1	1190
W (ppm)				27.80	5	1690	19.45	5	130	18.45	5	130	5.00	5	5	17.02	5	1480
Zn (ppm)				47.97	2.5	510	56.55	18	98	28.52	11	58	8.50	2.5	11	35.27	2.5	1230

6.4 Genetic Model summary

SRK notes that the following genetic models for the Tsagaan Chuluut Gold Project have been postulated by Minarco (2011) and Bond et al. (2013) as part of their respective Mineral Resource estimate and petrological Project work:

- Minarco (2011) proposes that a magnetic low is indicative of demagnetised zones surrounding a porphyry intrusion and quartz-sericite-pyrite-carbonate alteration is interpreted as phyllic alteration in the upper crustal levels of porphyry systems.
- Bond et al. (2013) proposes that reduced granodiorite is the primary host of the gold mineralisation and the geochemical signature described as elevated gold, arsenic, tungsten and low copper indicates an RIRGS system.

SRK favours a gold porphyry model such as described by Sillitoe (2000), associated with the Late Triassic to Early Jurassic Tsagaan Chuluut Igneous Complex, with a hydrothermal alteration and geochemical overprint occurring with the intrusion of later Middle to Late Jurassic granodiorite/s on the basis of:

- The primary host of gold mineralisation is a quartz diorite porphyry of Tsagaan Chuluut Igneous Complex of Late Triassic–Early Jurassic age, when subduction under the Ereendavaa terrane was still active.
- The geochemical signature of TC1 deposit fits the gold porphyry model and is similar to an RIRGS, which are similar but TC1 is deficient in tellurium.
- Alteration patterns described from geophysical and core data support potassic, phyllic and argillic zones which are expected to develop in porphyry system.

Further work is required to confirm this mineralisation model.

7 Exploration

Several phases of exploration work were carried out at the Tsagaan Chuluut Gold Project in the period between 1997–2014 by the following organisations/companies:

- Russian Exploration Team (1973–1985)
- Java Gold Corporation (1997)
- Troy Mongolia Alt Resource (Troy) LLC (2002–2006)
- SG (2011–2014).

This work is briefly summarised below and within the following section:

- Topographic survey – 105 ha (Figure 7-1)
- Geological mapping at 1:5,000 and 1:2,000 scales – 456.68 ha
- Geophysical survey:
  - Ground magnetic survey at 1:5,000 scale – 74.2 line-kilometres at 50 m spacing (Figure 7-1)
  - 20 IP sections at 1:10,000 – 35.0 line-kilometres (Figure 7-1)
- Trenching and drilling, including:
  - Trenching – a total length of 1,271.4 m
  - Drilling – 17 reverse circulation (RC) holes for 1.256 m and 35 diamond core drill holes for length of 9,422.9 m
  - All trenches and drill holes were logged and photographed.
- Hydrogeological study
- Sampling:
  - Trench channel – 260 samples
  - Rock chip – 372 samples
  - Soil – 1,050 samples
  - Petrography – 38 samples
  - RC chip – 553 samples
  - Core – 4,533 samples
  - Quality Assurance and Quality Control (QA/QC) samples – 99 blanks, 200 duplicates and 120 certified reference material (CRMs)
- Laboratory analyses:
  - Fire assay with atomic absorption – 5,505 samples
  - Inductively coupled plasma-optical emission spectrometry (ICP-OES) after 4-acid digest – 5,505 samples
- Density measurements – a total of 1,772 samples.

7.1 Geology mapping

Two periods of geological mapping have been carried out across the Project area:

- In 1997, geology mapping and reconnaissance work at a 1:10,000 scale by Java Gold Corporation.
- In 2002–2006, detailed geology mapping at 1:10,000, 1:5,000 and 1:2,000 scales by Troy.

7.2 Topographical survey

In March 2012, Bayasakh Survey LLC carried out a ground topographic survey. Topographic mapping at a 1:2,000 scale was implemented across 105 ha of the northern area of the Tsagaan Chuluut-1 mining licence (MV-015436) as shown in Figure 7-1. The survey was carried out with DGPS (Differential Global Positioning System) equipment using the Leica TC-800 instrument and SDR Mapping Design software. The contour interval in the resulting topographic map is 1.0 m and the point accuracy is reported to be between 2 cm and 2.5 cm.

The survey data were provided to SRK in a digital format.

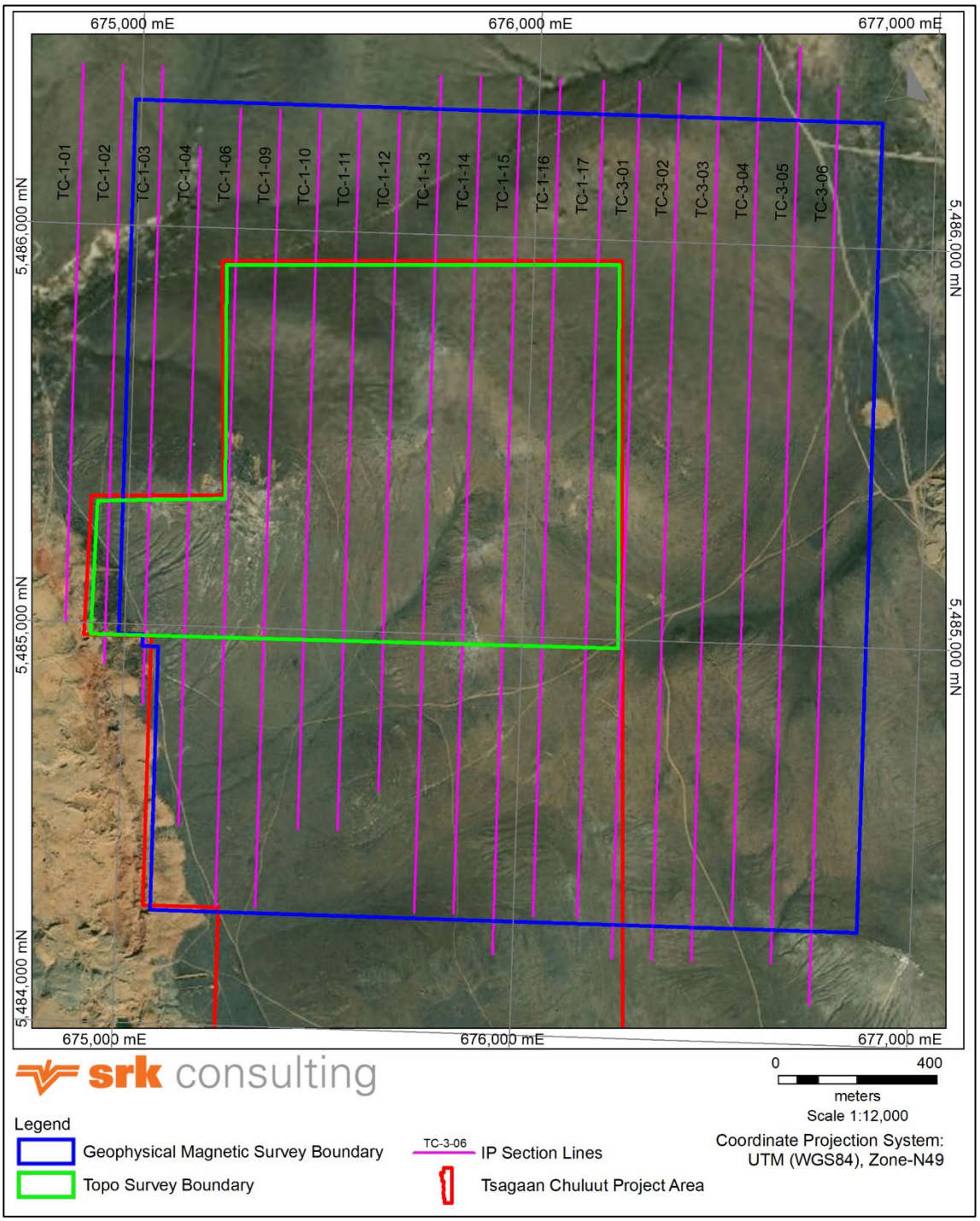

Figure 7-1: Location of area of topographic and ground magnetic survey areas and IP dipole-dipole profiles across the TC1 deposit area

7.3 Geophysical survey

In 1997, Java Gold Corporation conducted a ground magnetic survey in the 2.09 km^2 area of the Tsagaan Chuluut-1 mining licence and adjacent licences. A total magnetic intensity (TMI) map is illustrated in Figure 7-2.

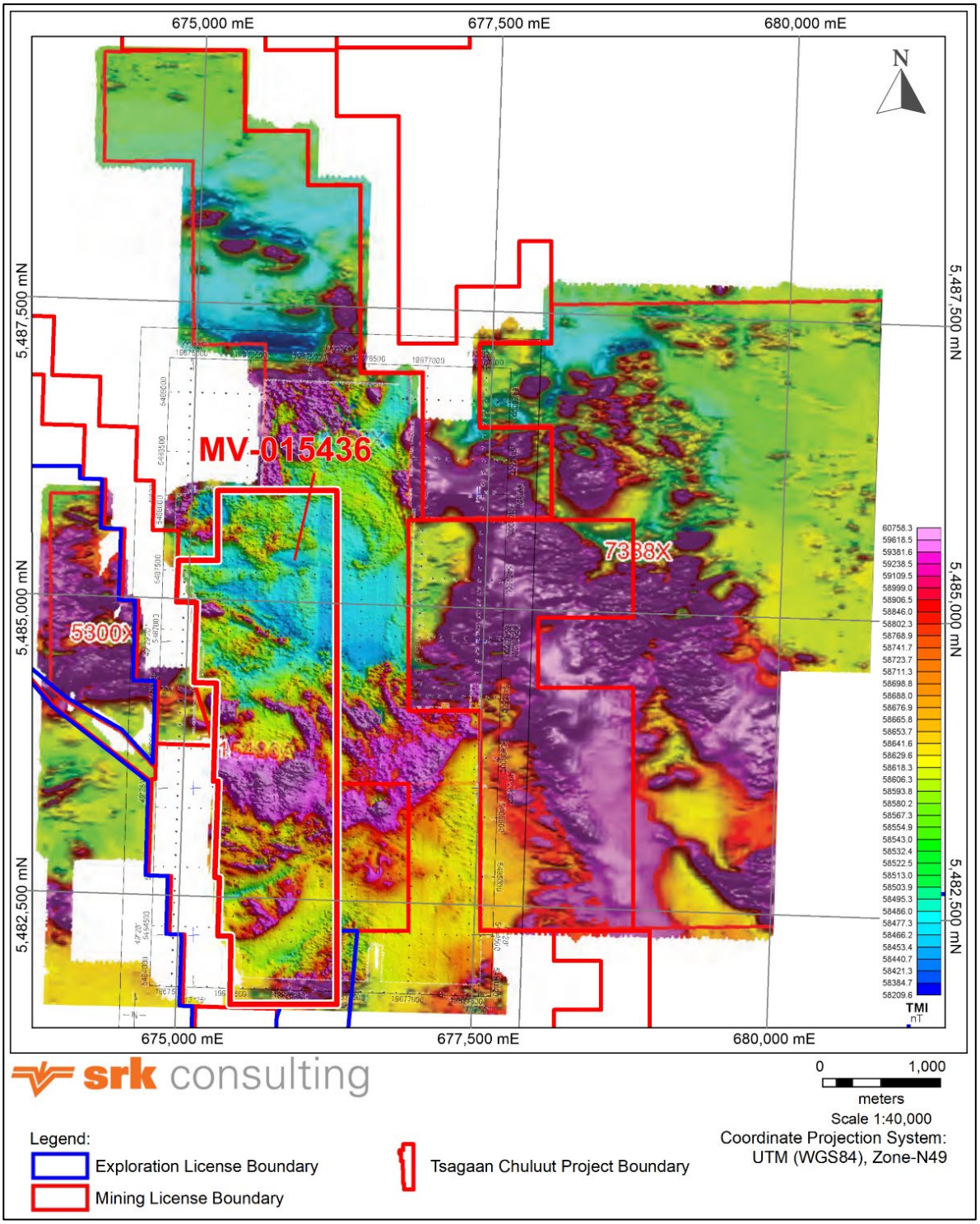

Figure 7-2: Total magnetic intensity map

Source: SG modified by SRK

In 2011, SG commissioned DashMagEng LLC to conduct a geophysical survey program comprising ground magnetics and IP gradient chargeability and resistivity and IP dipole-dipole profiles in the Tsagaan Chuluut deposit area. Figure 7-1 illustrates the area of the ground magnetic survey and the location of IP profiles.

The ground magnetic survey was undertaken at a 50 m line spacing, with 10 m station spacing along the lines, for a total survey length of 74.2 line-kilometres. DashMagEng processed the raw data to provide TMI, Reduced to Pole (RTP), Residual and Tilt Derivative (TDR) maps. SRK reviewed and interpreted the ground magnetic datasets (refer to Section 5.4).

DashMagEng LLC conducted IP dipole-dipole profiling along 20 lines (Figure 7-1), with a total length of 35 line-kilometres, and 2D chargeability and resistivity grids/images were generated at a 1:10,000 scale and reviewed by SRK.

7.4 Surface geochemical mapping

Troy conducted surface-related geochemical surveys in 2002 and 2006 as part of geological mapping work. A total of 372 rock chip samples were collected from the altered and mineralised outcrop.

Soil sampling was also conducted on 50 m × 50 m grids. A total of 1,050 soil samples were collected. The locations of all geochemical sampling are shown in Figure 7-3.

7.5 Trenching

During Troy's exploration programs in 2002 and 2004, five trenches were excavated for a total length of 1,271.4 m and 260 samples were collected. Trench lengths, ranging from 5 m to 170 m, were excavated to a depth of 1.5–3 m. Samples were collected from trench floor areas where bedrock was exposed. Samples were collected as 0.5–3 m long continuous channel samples from intervals where mineralisation was observed. The coordinates of all trenches were not provided to SRK.

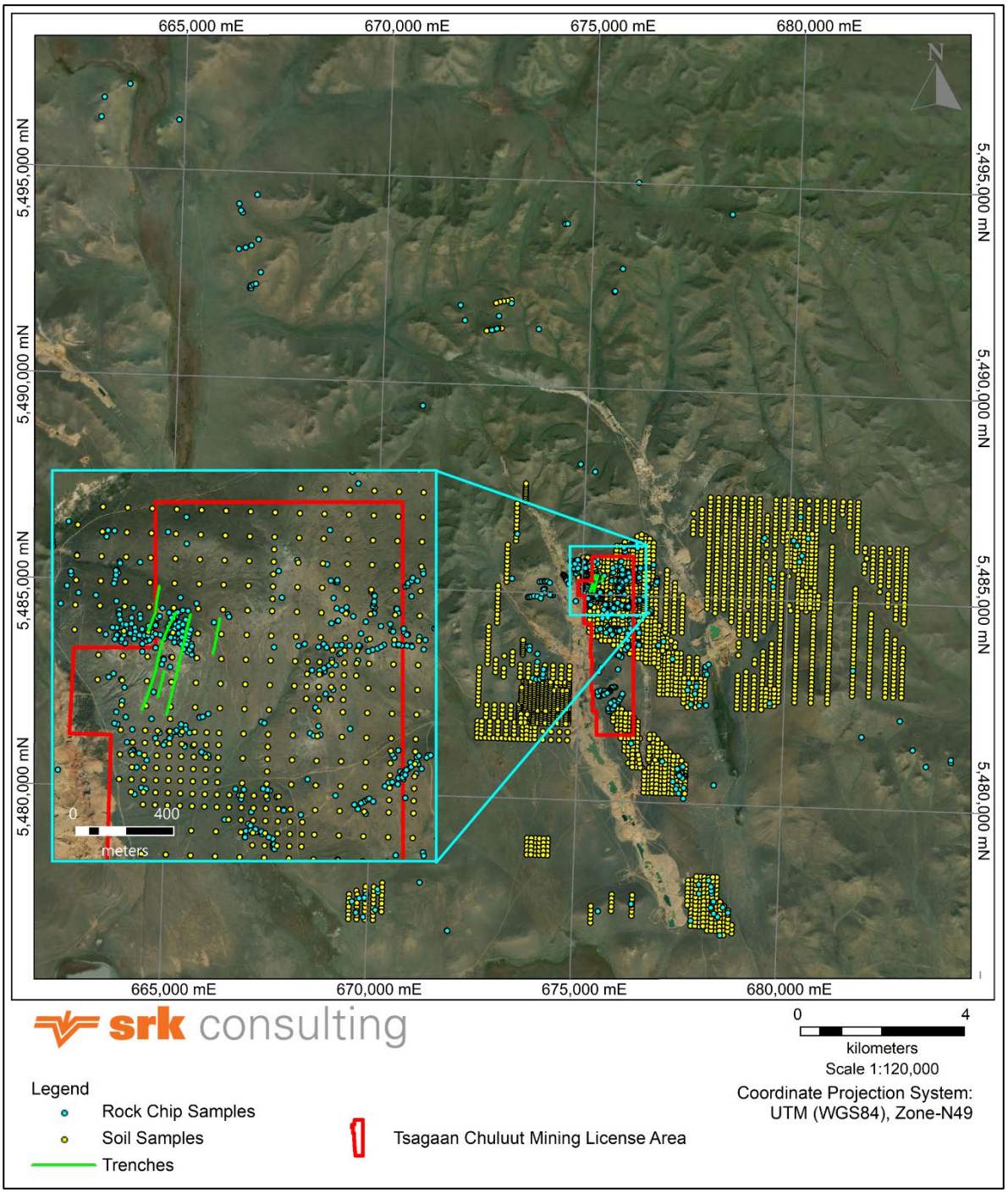

Figure 7-3: Locations of geochemical samples and trenches

7.6 Drilling

The following four generations of drilling have been completed at the Project:

- 5 diamond drill holes completed by a Russian exploration team in 1973–1985
- 3 diamond drilled holes by Java Gold Corporation in 1997
- 17 reverse circulation (RC) holes drilled by Troy in 2005
- 29 diamond drill (DD) holes completed by SG in 2012–2014.

Only drilling results from the campaigns period between 2005 and 2014 (namely Troy's and SG's) were provided to SRK for review.

The 2005 Troy RC drill holes were drilled on a line spacing between 100 m and 120 m. The second generation of drilling by SG in 2012 was designed on a 50 m × 50 m grid. The highest density of drilling is located in the central part of the Tsagaan Chuluut deposit and test holes have also been drilled to the south and east. The location of the all drill holes is shown in Figure 7-4.

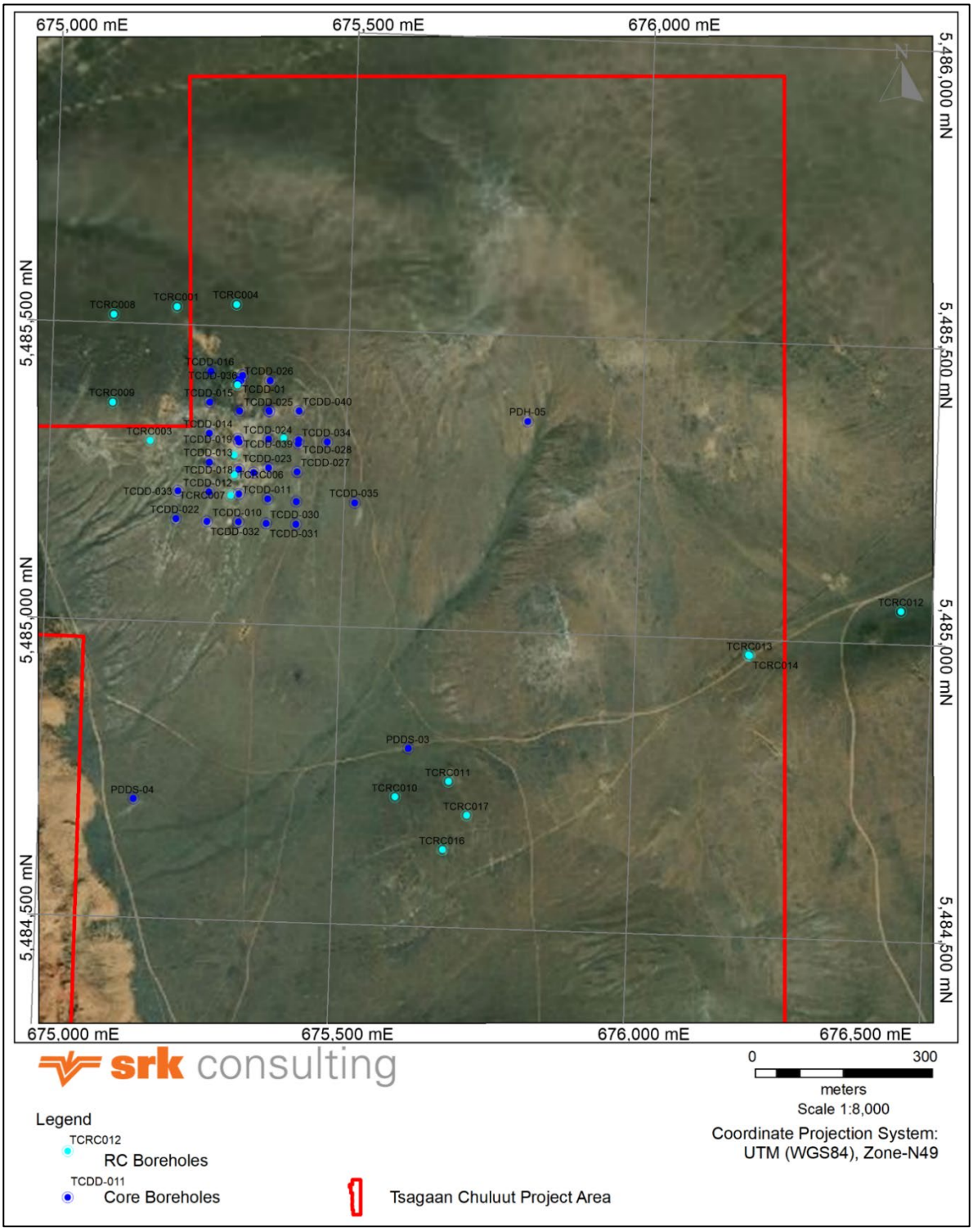

Figure 7-4: Location of RC and core drill holes at Tsagaan Chuluut Gold Project

In 2005, a 17-hole RC drilling program for 2,156 m was carried out under the supervision of Troy's geologists, John Stockley and Bat-Erdene. Troy targeted three areas with this drilling campaign (Figure 7-4). Of the drill holes, 10 were targeted at the Tsagaan Chuluut Project, while the remaining holes tested nearby prospects. The 10 drill holes totalled 1,532 m of drilling. All drill holes were drilled vertically, with depths ranging between 60 m and 200 m and an average depth of 127 m. The drilling was conducted by Major Drilling using a P-50 rig. Details of the 2005 RC drilling program are given in Table 7-1.

Table 7-1: Summary of RC holes drilled in 2005

Hole ID	Easting (m)	Northing (m)	Elevation (m)	Depth (m)	Azimuth (°)	Dip (°)
TCRC001	5485528.99	675208.44	973	180	0	-90
TCRC002	5485282.42	675312.55	979.39	126	0	-90
TCRC003	5485302.47	675170.04	973.41	150	0	-90
TCRC004	5485535.98	675308.4	980	200	0	-90
TCRC005	5485400.67	675314.36	985.32	120	0	-90
TCRC006	5485249.64	675313.72	970.75	198	0	-90
TCRC007	5485215.02	675308.46	965.21	138	0	-90
TCRC008	5485513	675101.48	945	150	0	-90
TCRC009	5485365.06	675104.48	963	120	0	-90
TCRC010	5484716.3	675602.55	935.53	78	0	-90
TCRC011	5484745.37	675692.32	944.98	96	0	-90
TCRC012	5485055.16	676446.92	940	156	0	-90
TCRC013	5484973.2	676194.02	968	60	0	-90
TCRC014	5484974.2	676192.02	968	90	0	-90
TCRC015	5485314.08	675395.36	970	150	0	-90
TCRC016	5484630.05	675685.58	942.9	84	0	-90
TCRC017	5484689.33	675724.21	945	60	0	-90

In 2012, SG carried out diamond drilling programs in the Tsagaan Chuluut area under supervision of Micromine.

The 2012 drill holes were completed initially by Erd Geo LLC using two types of drilling rigs: a Hanjing Power 7000 and a ZIF 640M. An additional three rigs were sourced from Kali Khakkin LLC: two Hanjing Power 9000 and a YDX-3G type rigs. All rigs used a conventional wire-line diamond drilling technique, with a single core barrel inside the drilling rods. The majority of the 2012 drilling was carried out with HQ-sized diamond core with water circulation. PQ-sized rods and casing were used at the top of the holes to stabilise the collars. A total of 29 diamond core drill holes for a total length of 8,252.7 m were completed. Core recovery exceeded 92.6% for all 2012 drill holes. The drill holes details are provided in Table 7-2.

Table 7-2: Summary of drill holes drilled in 2012

Hole ID	Easting (m)	Northing (m)	Elevation (m)	Depth (m)	Azimuth (°)	Dip (°)	Core Recovery (%)
TCDD-010	5485170	675323	960.17	450	0	-60	92.66
TCDD-011	5485211	675371.5	966.1	295	0	-60	93.01
TCDD-012	5485219	675271.6	964.28	310	0	-60	98.14
TCDD-013	5485269	675270.7	972.97	291	0	-60	97.4
TCDD-014	5485318	675269.2	983.21	327	0	-60	98.31
TCDD-015	5485370	675268.1	986.14	210.4	0	-60	99.31
TCDD-016	5485422	675268.4	982.1	153.2	0	-60	97.25
TCDD-017	5485217	675322	966.03	348	0	-60	96.9
TCDD-018	5485258	675320.7	973.88	306	0	-60	96.34
TCDD-019	5485310	675317.9	988.8	247	0	-60	96.61
TCDD-020	5485357	675319.1	992.71	209.7	0	-60	97.21
TCDD-021	5485408	675319.7	985.34	251	0	-60	97.68
TCDD-022	5485172	675217.3	955.49	351.5	0	-60	97.73
TCDD-023	5485263	675371	976.01	307.5	0	-60	97.79
TCDD-024	5485311	675369.7	988.52	241	0	-60	98.69
TCDD-025	5485358	675369.4	995.86	175	0	-60	96.59
TCDD-026	5485410	675368.9	988.55	116.5	0	-60	95.33
TCDD-027	5485258	675419.6	973.46	286.4	0	-60	96.79
TCDD-028	5485312	675421	983.46	248.8	0	-60	97.48
TCDD-029	5485207	675419.7	966.88	303	0	-60	97.82
TCDD-030	5485170	675420.3	962.2	270	0	-60	95.07
TCDD-031	5485169	675370	960.15	291	0	-60	95.99
TCDD-032	5485169	675270.3	958.46	315	0	-60	97.27
TCDD-033	5485219	675219.4	960.98	267	0	-60	96.97
TCDD-034	5485309	675468.9	981.46	321.5	0	-60	97.44
TCDD-035	5485209	675518.5	967.5	317.2	0	-60	97.45
PDDS-03	5484798	675622.4	936.44	394	210	-60	
PDDS-04	5484700	675160.7	910.13	340	0	-90	
PDH-05	5485355	675806.3	987.31	309	0	-90	

In 2013 and 2014, SG carried out a verification drilling program of six drill holes at the Tsagaan Chuluut deposit for a total length of 1,170.2 m, with depths ranging between 120 m and 195 m. A drilling procedure and rig type description for these verification drill holes were not provided to SRK for review. A summary of the verification drill holes is shown in Table 7-3.

Table 7-3: Summary of drill holes drilled in 2013 and 2014

Hole ID	Easting (m)	Northing (m)	Elevation (m)	Depth (m)	Azimuth (°)	Dip (°)
TCDD-036	5485417	675322.9	985	300	180	-70
TCDD-037	5485359	675369.1	995	120	0	-90
TCDD-038	5485254	675346.3	973.5	180	180	-60
TCDD-041	5485305	675320	987	262.7	0	-60
TCDD-039	5485305	675420	982	172.5	0	-60
TCDD-040	5485360	675420	992	135	0	-60

Drill hole TCDD-039 is a twin of TCDD-028 (Figure 7-5 and Figure 7-6). SRK notes that the gold grade continuity and distribution are similar and therefore highlight reasonable repeatability for these twinned holes.

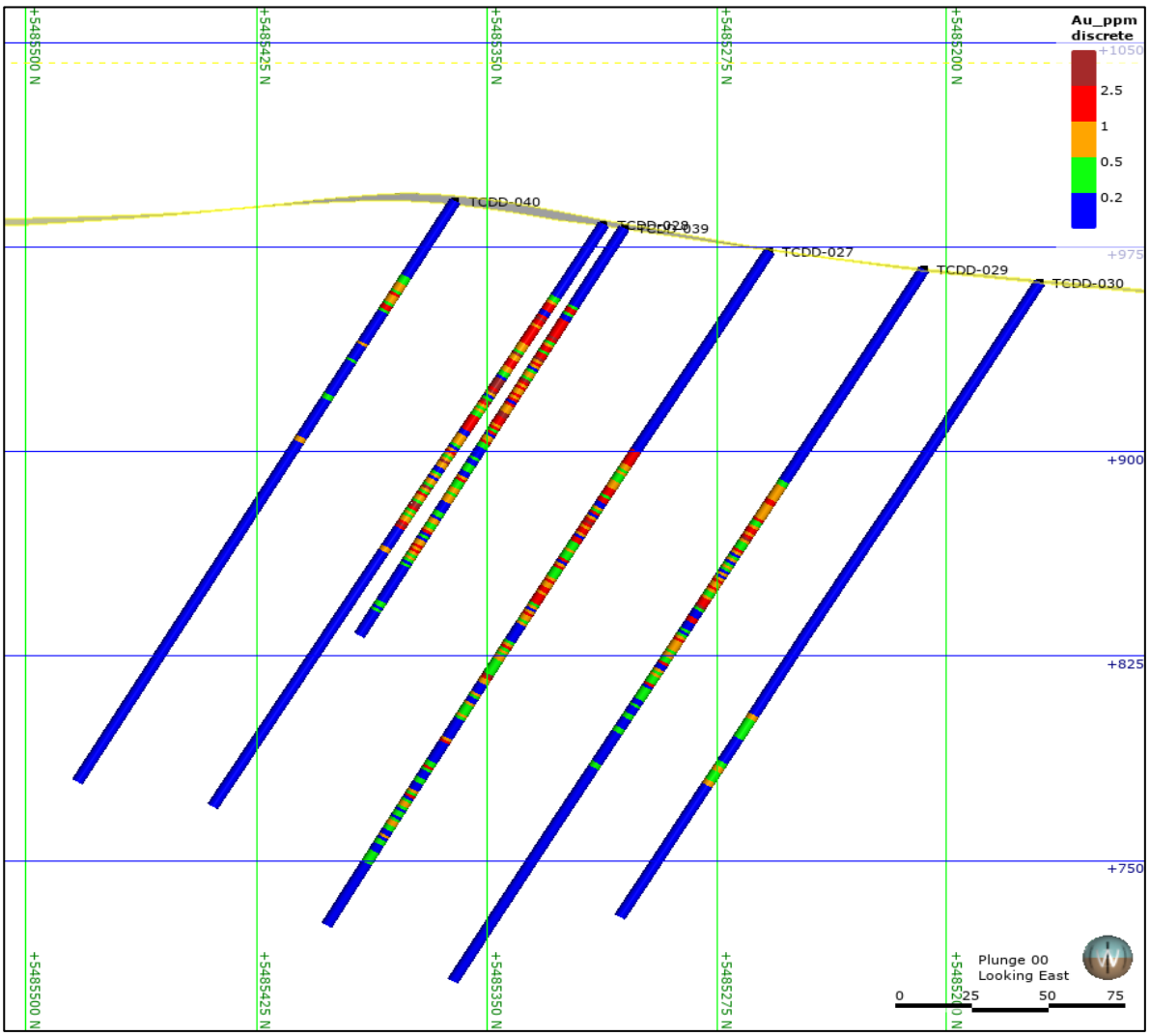

Figure 7-5: Twinned holes with gold grade on Section 6

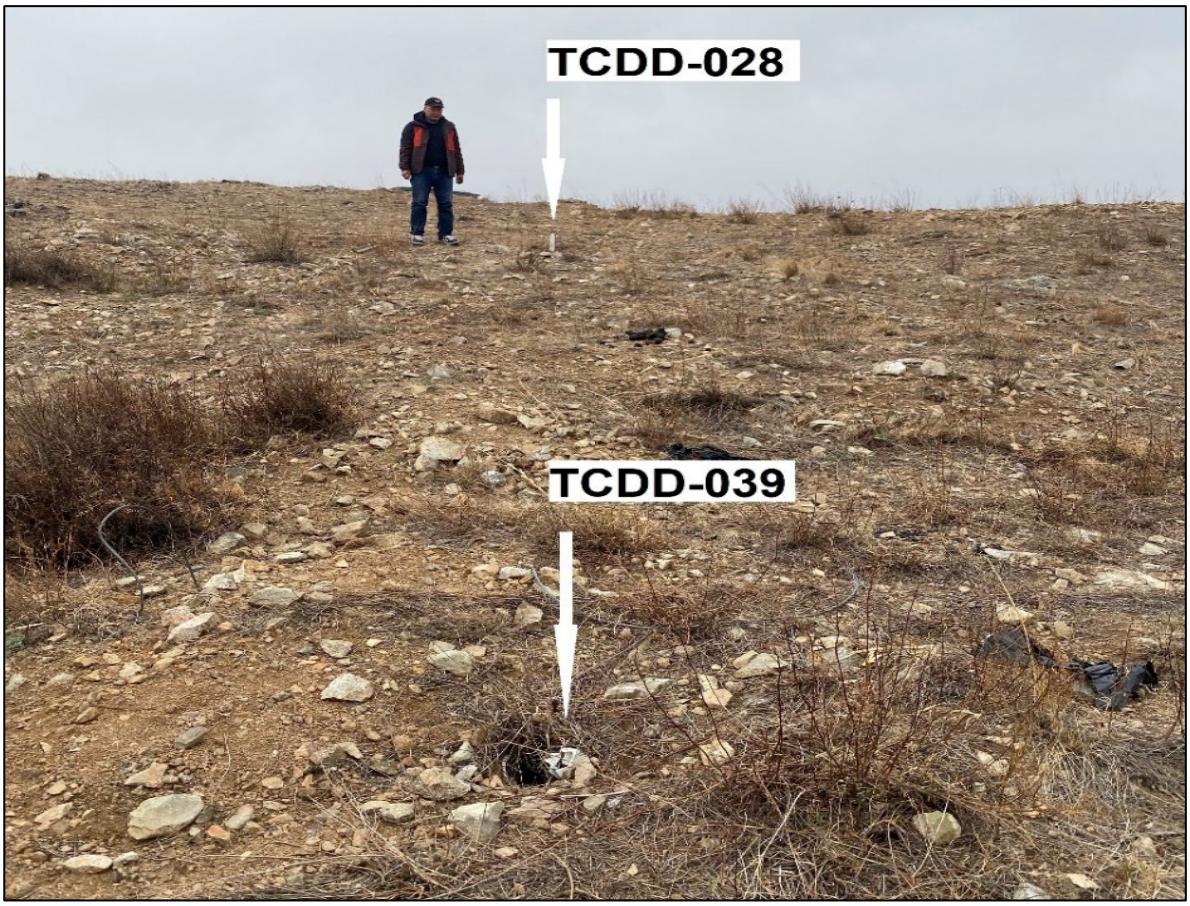

Figure 7-6: Collars of TCDD-028 and TCDD-040 (facing north)

Drill holes TCDD-041 and TCDD-19 were drilled with same angle on the same section, but the holes are not actually twins. There is a 16 m difference between the final depths of those drill holes (Figure 7-7).

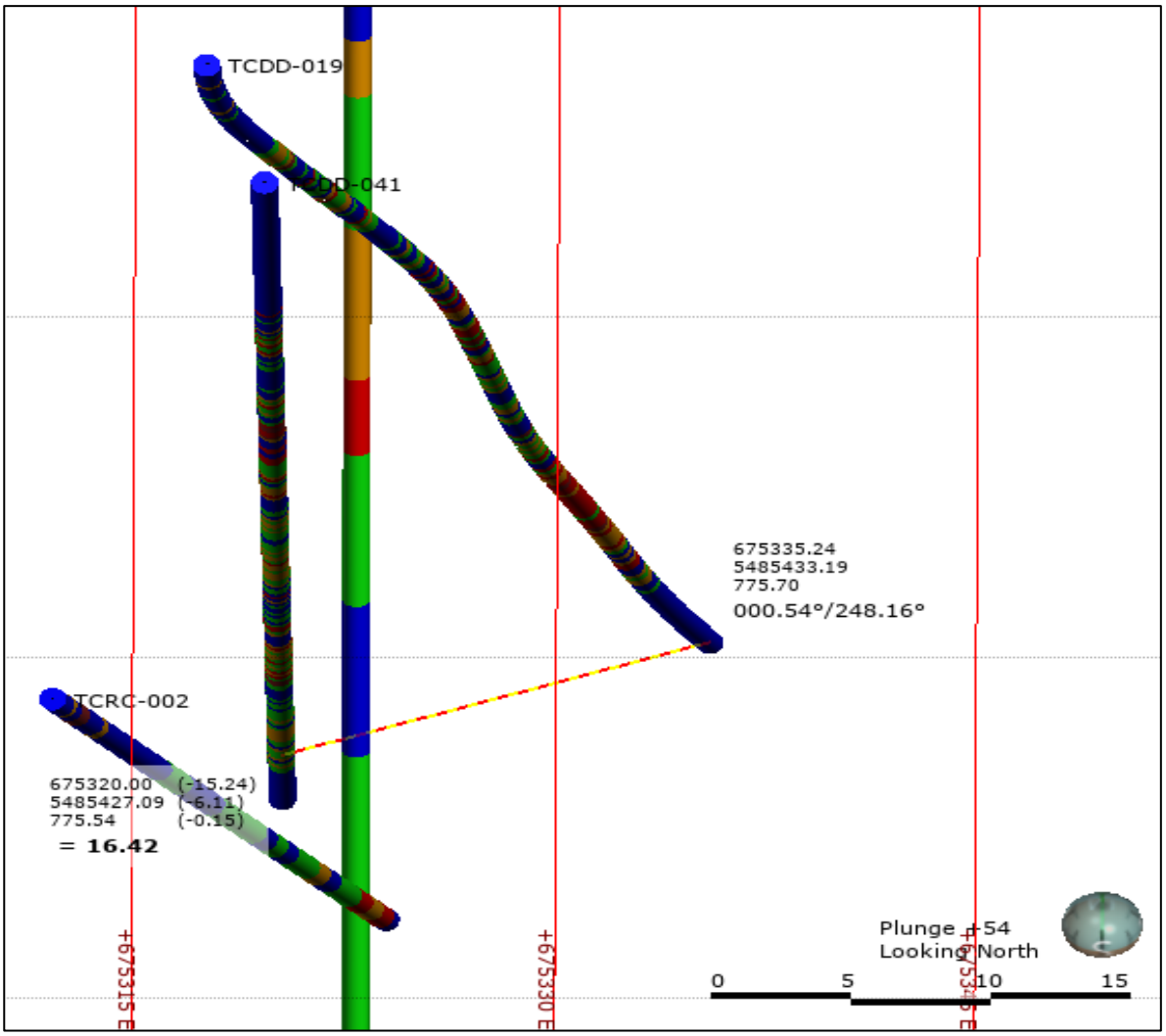

Figure 7-7: 3D view of TCDD-019 and TCDD-041 (facing north)

Drill hole collar survey

All drill hole collars positions from the 2005, 2012 and 2013 programs have been accurately surveyed by a contract surveyor, Bayasakh Survey LLC, with a Leica TC-800 instrument using the Universal Transverse Mercator (UTM), WGS84, Zone 49 North system data. The historical drill holes (49 out of 52) surveyed in local grid have been transformed into WGS84. SRK received hand-held GPS (global positioning system) coordinates only for three of the verification drill hole collars drilled in 2014.

Downhole survey and core orientation

All of the diamond drill holes drilled in 2012, 2013 and 2014 were generally inclined at 60°–70° and reached depths of between 116.5 m and 450.0 m. All drill holes drilled in 2012 were downhole surveyed with a Reflex EZ-SHOT™ camera at 30 m intervals. As holes were aligned to an azimuth of true north, the drill rig was set up using the GPS to ensure the rig was aligned correctly. SRK was provided with downhole survey logs.

The 2013 and 2014 diamond verification drill holes were not downhole surveyed.

Drill core orientation was not undertaken for any of the diamond drill holes.

Geological logging

RC chips

In 2005, all RC holes were geologically logged by Troy geologists in the field. The only detail recorded from these chips was a major rock code with the data entered into Microsoft Excel spreadsheets and imported into a Microsoft Access database. Every sample (1–2 m interval) was sieved and washed then stored in chip trays for future reference.

Core

SRK was provided with the Standard Operating Procedures (SOPs) and a system for logging core records (lithology, mineralisation, alteration, weathering, colour, core recovery, rock quality designation (RQD) and other primary features) of the core samples for diamond drilling programs in 2012 and 2013. Micromine provided customised logging sheets to the SG geologists to use for collecting data during the drilling campaign. Logging sheets consist of the information shown in Table 7-4.

Table 7-4: Attributes recorded in geological and geotechnical logging sheets

Geological Logging	Geotechnical Logging
Major Lithology Code	Run Length
Secondary Lithology Code	Length Recovered
Weathering	Recovery
Colour	Number of pieces >10 cm
Grainsize	Longest Length
Texture	Sum of Total Pieces >10 cm
Vein Texture	RQD
Vein Minerals	Rock Strength
Vein %	Number of Fractures
Alteration	
Alteration Intensity	
Pyrite %	
Arsenopyrite %	
Chalcopyrite %	
Gold %	
Copper %	
Molybdenum %	
Haematite %	
Sphalerite %	

All drill holes were logged in full, to the end of hole by an SG geologist. Core was routinely photographed digitally and measured for core recovery and RQD.

The procedure required that core recovered from the core barrel was geologically logged and photographed. After logging, the field geologists selected the intervals for sampling. Core samples were then split into halves using a diamond saw; one half-core sample was packed into fabric bags for analysis. All records were entered in an electronic database and all electronic data, including geological logging, core photographs and assays, are stored in a Microsoft Access database.

The logging workflow consisted of joining the core so that there were no large gaps between pieces

of core, then labelling the depth of the core at each metre using a permanent marker. Any variation between the core blocks and the actual length of core in the core tray was resolved in conjunction with the driller and drilling supervisor.

SRK was provided with core photography and lithology, core recovery, RQD, alteration, mineralisation and downhole survey log data entered into Microsoft Excel spreadsheets and imported into a Microsoft Access database.

7.7 Sampling

Methodology

RC chip samples

Major Drilling used a sample splitter during the 2005 RC drilling program. RC chip samples were packed in green plastic bags and sampled by hand spear by Troy geologists. RC chip samples were taken as 1 m intervals where mineralisation was observed and as 2 m intervals where no mineralisation was evident.

A total of 595 samples during RC drilling were collected and submitted for laboratory analysis, consisting of and 553 primary (RC chip) samples, 28 duplicate samples and 14 blanks.

Core samples

On completion of the drill hole core logging and photography, the geologist on site selected and marked the sample intervals on the core and recorded the details on the sample sheet. The marked core samples were then cut into two equal halves along the length of the core using a core saw with a diamond-tipped blade. One half of the core was sampled and packed into fabric sample bags marked with the sample ID. The fabric bags were then placed into large sacks marked with the sample numbers and the laboratory name and address, for submission to the laboratory. The other core halves were retained and stored in core boxes at the project site. Field duplicate samples were taken from quartering the retained half-core.

For core from the 2012 and 2013 drilling program, nominal 1 m length samples were taken for assay, with a small number sampled at shorter intervals ranging between 0.2 m and 6.5 m lengths, depending on the width of mineralisation the width of veining and/or alteration. SRK noted that some samples from drill holes TCDD-036, TCDD-037 and TCDD-038 have variable sample lengths, including sample intervals greater than or equal to 4 m. The samples with lengths over 4 m are not mineralised.

The histogram for the core and trench sample interval lengths is provided in Figure 7-8.

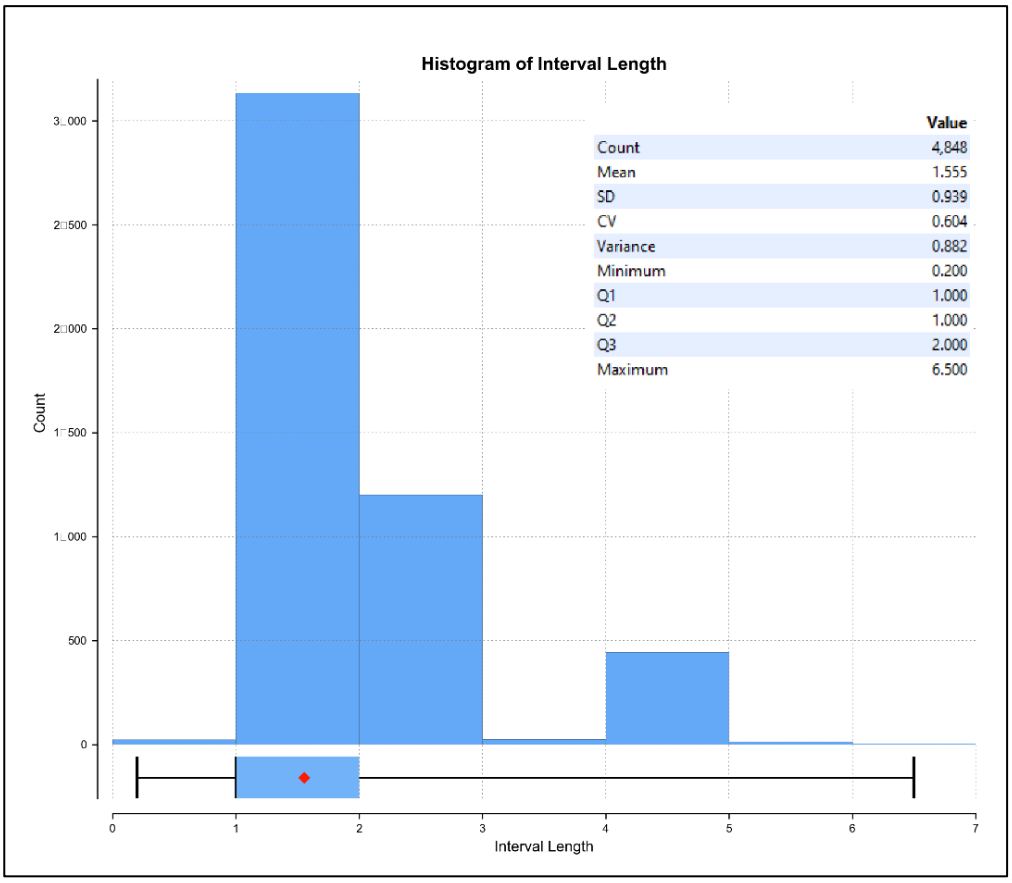

Figure 7-8: Histogram for sample interval length

A total of 4,533 core and 377 quality control (CRM, blank, duplicate and umpire) samples were analysed during the SG exploration program between 2012 and 2014.

The number of drill hole sample numbers per drill hole and QA/QC samples submitted for analysis in Tsagaan Chuluut Project are summarised in Table 7-5.

Table 7-5: Number of samples in 2012 and 2014

Hole ID	No. of samples	No. of QA/QC samples			Total no. of samples
		Blanks	CRMs	Duplicates	
TCDD-010	295		16	8	319
TCDD-011	184		9	5	198
TCDD-012	214	6	12	6	238
TCDD-013	241	1	13	6	261
TCDD-014	213	6	12	6	237
TCDD-015	162	5	8	4	179
TCDD-016	34	1	2	1	38
TCDD-017	286	8	15	8	317
TCDD-018	230	6	13	6	255
TCDD-019	233	6	13	6	258
TCDD-020	109	3	6	3	121
TCDD-021	148	4	8	4	164
TCDD-022	41	1	2	1	45

Hole ID	No. of samples	No. of QA/QC samples			Total no. of samples
		Blanks	CRMs	Duplicates	
TCDD-023	248	7	13	7	275
TCDD-024	168	5	9	4	186
TCDD-025	90	2	5	3	100
TCDD-026	7		1		8
TCDD-027	186	5	10	5	206
TCDD-028	110	2	3	2	117
TCDD-029	117	3	6	3	129
TCDD-030	50	1	3	1	55
TCDD-031	61	2	3	2	68
TCDD-032	102	3	5		110
TCDD-033	158	4	9		171
TCDD-035	59	2	3	2	66
TCDD-036	83				83
TCDD-037	49				49
TCDD-038	75				75
TCDD-039	120				120
TCDD-040	75				75
TCDD-041	211				211
TCRC001	45	2		3	49
TCRC002	46	2		4	50
TCRC003	38	1		2	41
TCRC004	51	1		1	54
TCRC005	30	1		1	32
TCRC006	50	1		2	53
TCRC007	35	1		1	37
TCRC008	38	1		3	41
TCRC009	30	1		2	33
TCRC010	26			1	27
TCRC011	14				15
TCRC012	39	1			42
TCRC013	15			1	16
TCRC014	22	1		1	25
TCRC015	38	1		3	41
TCRC016	21	1		1	23
TCRC017	15			1	16
PDDS-03	15				15
PDDS-04	53				53
PDH-05	11	1	1		13
TCDD-01	95				95
Total	**5,086**	**99**	**200**	**120**	**5,505**

Sample preparation

RC chip (in 2005) and core samples (in 2013 and 2014) were sent to SGS Laboratory in Ulaanbaatar, Mongolia. When received, samples were sorted and then dried in ovens at 70°C. The samples were then crushed to greater than 75% of the sample passing a size fraction of -3.35 mm. Crushed samples were then split using a Jones riffle splitter. The split sample of up to 500 g in weight was then pulverised to greater than 90% of the sample passing a size fraction of 75 µm. Pulverised samples were retained for analyses, while the remaining coarse reject samples were stored.

For the 2013 verification drilling program, core samples and external repeats were sent to ActLabs in Ulaanbaatar, Mongolia. Sample preparation involved weighing the sample, followed by crushing in a jaw crusher to a 2 mm size fraction up to 90% passing. After crushing, the samples were screened and split followed by 250 g being pulverised to 95% passing 105 µm.

7.8 Analytical methods

All samples were analysed by fire assay with atomic absorption spectroscopy (AAS) for gold and by inductively coupled plasma-atomic emission spectrometry (ICP-AES) methods for a suite of 33 other elements, in internationally accredited laboratories (SGS and ActLabs), both of which are in Ulaanbaatar. Silver was analysed during this multi-element sweep using AAS.

SGS used ICP-40B, AAS22S and FAA505 procedures. The ICP-40B procedure involved a four-acid digest of nitric, hydrofluoric, perchloric and hydrochloric acid prior to analysis of the solution by the ICP machine for the suite of 33 elements. Samples which recorded assays over the upper detection limit for the method of 1,000 ppm Au were re-assayed using the atomic absorption spectrometry (AAS) 22S method to define the higher grades.

In ActLabs, the samples underwent a similar multi-acid digestion followed by 1A2-30 – gold fire assay AA30g and 1EM – aqua regia AAS for Au, Ag, Cu, Mo, Pb and Zn. The sample was mixed with fire assay fluxes (borax, soda ash, silica and litharge) and with silver added as a collector, and the mixture was placed in a fire clay crucible. The mixture is preheated at 850°C, intermediate 950°C and finish 1060°C, with the entire fusion process lasting 60 minutes.

At the time of the production of the assay results, all the laboratories used were accredited to ISO/IEC 17025:2005 (MNS ISO/IEC 17025:2007), ISO ILAC-IAF 2009 and LQSi 2012 standards.

7.9 Density data

In the SG 2012 drilling program, bulk density measurements were carried out in the field. Bulk density was estimated from density measurements carried out on 1,772 samples from 23 drill holes using the Archimedes method of dry weight versus weight in water. The Archimedes principle postulates that the apparent weight of an object immersed in a liquid decreases by an amount equal to the weight of the volume of the liquid it displaces. Most samples were taken from fresh rock as the majority of the Tsagaan Chuluut deposit is fresh rock.

Micromine's 2012 report noted that after cutting the core on site, the half-core samples were put into bags and then the bagged sample was used to measure bulk density. When weighing the dry sample, the weight of the bag was subtracted from the weight of the core for increased accuracy. When weighing the wet sample, care was taken to ensure all air bubbles were let out of the bag so that the measured weight was accurate. The bag weight in water was not subtracted from the wet weight, as there is no significant weight difference. A barrier was built around the weighing table to prevent wind affecting the measurements. The wind can affect measurements by ±30 g.

The weight in water was then recorded, and the weight of the empty bucket in water was subtracted. The bulk density was then calculated according to the following formula:

Specific gravity = Weight in air/(Weight in air – Weight in water)

The results of the bulk density testwork include several exceedingly large values. After removing data greater than 6.0 t/m^3, SRK produced the histogram shown in Figure 7-9. The mean bulk density of the data is 2.84 t/m^3. The histogram shows the main population is around the main peak at 2.84 t/m^3 and number of small populations are clustered at 3.8 t/m^3, 4.8 t/m^3 and 5.2 t/m^3. These populations are considered incorrect for rock types encountered at TC1.

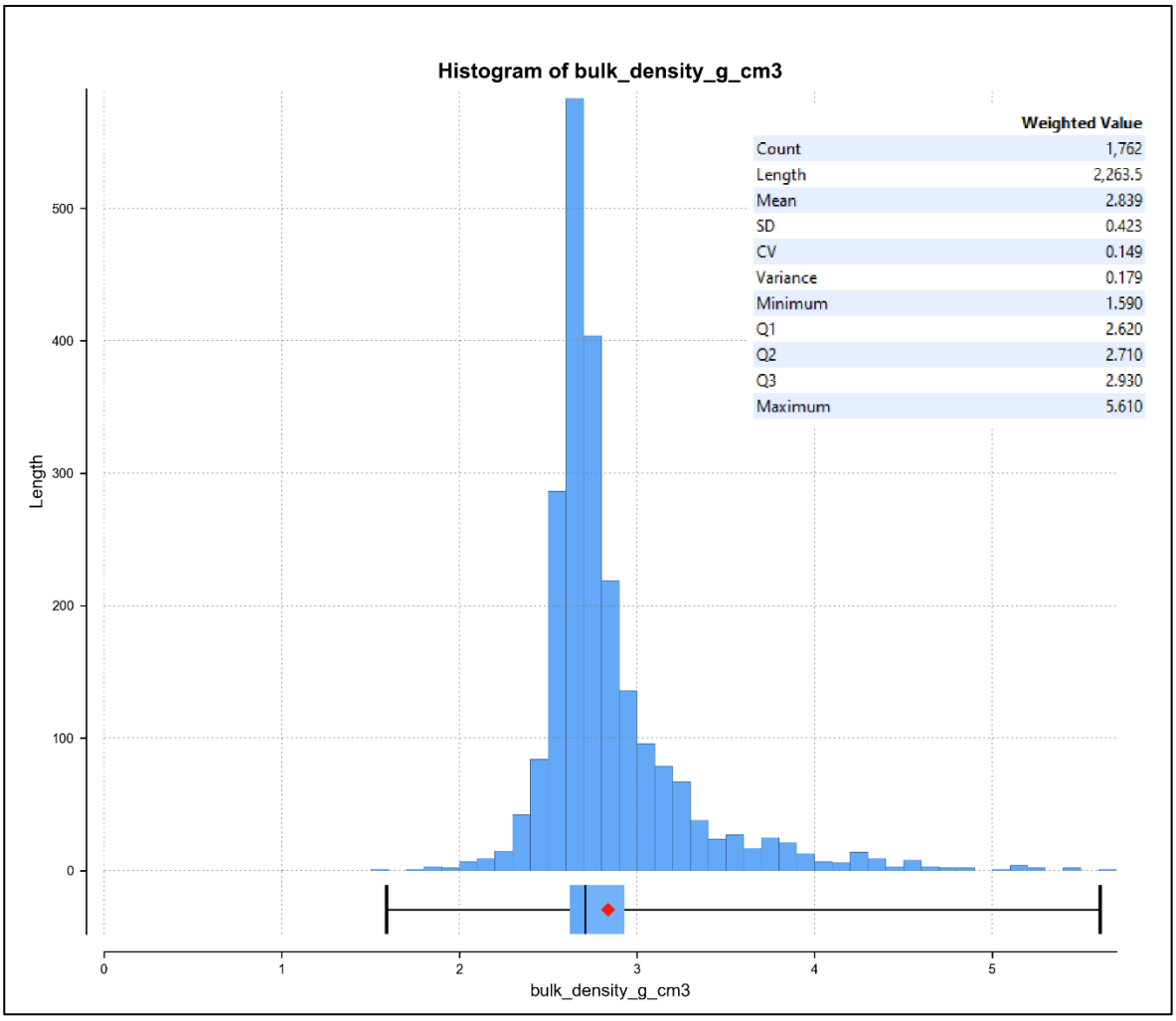

Figure 7-9: Histogram for bulk density of measured samples

In order to check bulk density measurements, SRK has reviewed the bulk density measurement results, separated density data by modelled lithology domain and carried out basic statistics of density for each lithology type. The incorrect values less than 2 t/m^3 or greater than 3 t/m^3 are listed in Table 7-6.

Table 7-6: Incorrect density values for rock types

Rock type	Number of samples	
	<2 t/m^3	>3 t/m^3
Quartz Diorite Porphyry	6	144
Granodiorite	1	14
Diorite		141
Gabbro		38
Total	**7**	**337**

SRK notes that the performance of bulk density of measurement was incorrectly performed and 19% of total measured samples have values of greater than 3 t/m^3 or less than 2 t/m^3.

SRK opines that bulk density values between 1.5 t/m^{3}and 2 t/m^3 may be due to the effect of strong alteration on the rock, while bulk density values above 3 t/m^3 are considered incorrect.

7.10 Quality Assurance/Quality Control and Data Verification

SRK was provided with a core recovery record and was satisfied that core recovery is typically over 92.6%.

For every sampling program, a series of QA/QC samples needs to be analysed to ensure accuracy and measure the precision of the final dataset. The QA/QC program needs to answer the following four questions:

- Is the sampling process reproducible?
- Is the assay process reproducible?
- Is there bias in the assay results?
- Is there any cross contamination between samples?

The QA/QC data provided to SRK included the result of CRMs, blanks and duplicate samples and also the laboratories' internal control data.

The QA/QC program was set up by Troy for the 2005 exploration program. Duplicate samples were taken at a rate of 1:20 samples, and blanks were inserted at a rate of 1: 30 samples before dispatch to the laboratory and analysed for QA/QC purposes (Table 7-5). No CRMs were used during the 2005 RC drilling program.

The 2012 QA/QC program was designed and implemented by Micromine. The analytical bias and assay precision were monitored using CRMs and duplicates, respectively. Blanks were also inserted. A combination of either blanks, CRMs, or duplicates was performed for 25 drill holes drilled in 2012 (Table 7-5).

In 2013, SG completed independent and external checks on 29 pulp duplicate samples from the 2012 drilling program.

The QA/QC samples used in 2018 and 2019 are summarised in Table 7-7.

Table 7-7: Summary of QA/QC samples from the 2005 and 2012 exploration drilling programs

QA/QC	Blanks	CRMs	Duplicates	Assays	CRMs (%)	Blanks (%)	Duplicates (%)
Internal	99	200	120	4,310	4.6	2.3	2.8
External	-	-	29		-	-	0.8

For core from the 2013 and 2014 verification drilling programs, SG did not conduct any QA/QC checks.

Performance of blanks in 2005 and 2012

During the 2005 RC drilling, 15 blank samples were taken from a white quartz vein from the Tsagaan Chuluut area and crushed to smaller than 1 cm. The white buck quartz vein where the blank sample materials were taken is 1–1.5 wide and more than 110 m long.

During the 2012 core drilling, blanks were created on site using barren rhyolite and inserted into the sample sequence at a rate of 1:40 samples. A total of 84 blanks were assayed.

A total of 99 blank samples were inserted throughout the 2005 and 2012 drilling programs. SRK reviewed the performance of blank samples subjected to fire assay testing and noted that two samples showed 0.03 ppm Au. SRK speculates that these two blanks could have been contaminated. SRK concluded that, overall, the blanks showed good performance and most of the results show blanks assaying at close to zero levels and below the minimum detection limit (<0.01 ppm). The performance of blanks from the SGS laboratory is provided in Figure 7-10.

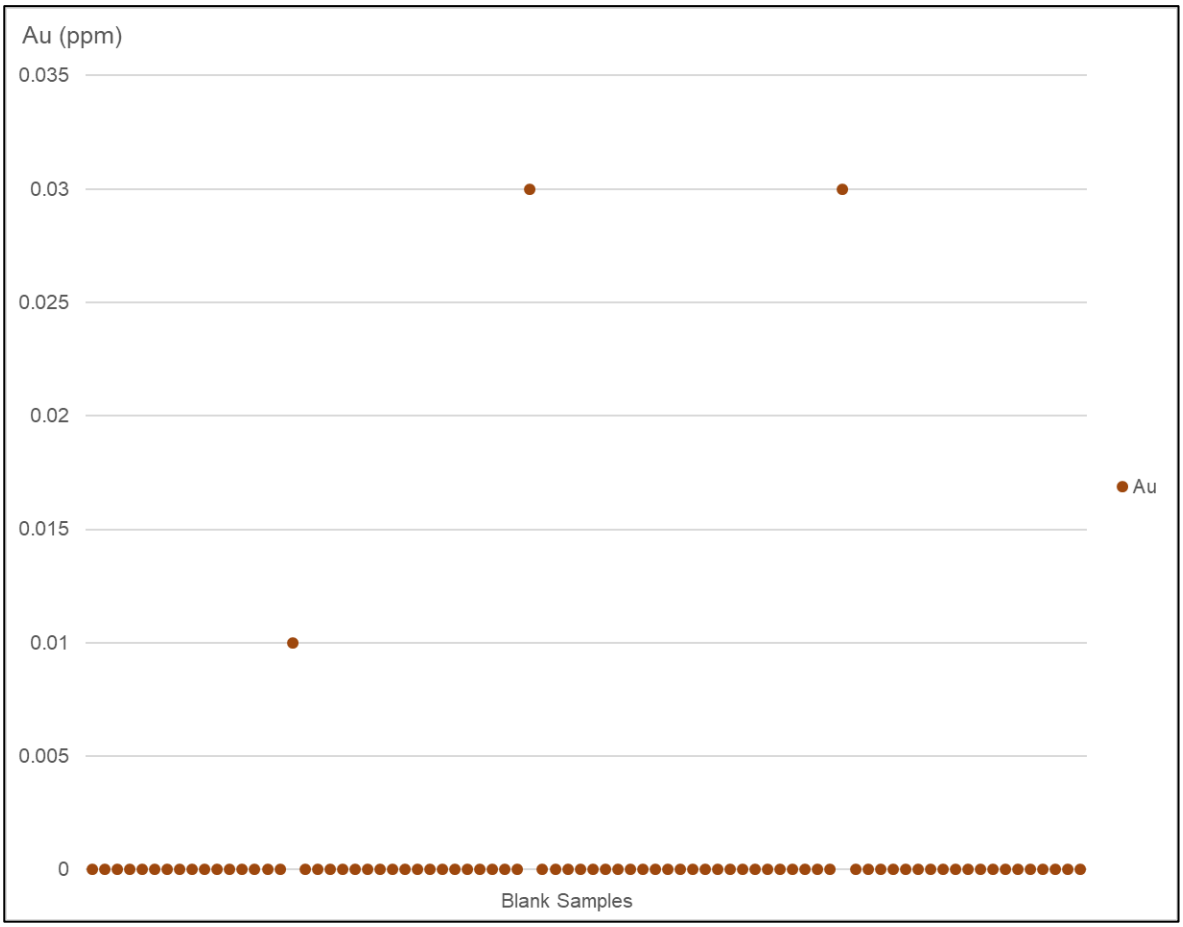

Figure 7-10: Performance of blanks

Performance of CRMs in 2012

In 2012, SG used six different types of CRMs: OREAS-501, 502, 503, 504, 901 and 70P for gold analyses, which were sourced and certified by OREAS.

In all, 200 CRMs have been analysed and the certified values and first standard deviations are provided in Table 7-8.

Table 7-8: Certified values of CRMs and sample numbers from the 2012 exploration drilling program

CRMs		Au (ppm)		No. of samples
		Certified value	Std Dev	
Central Geological Laboratory OREAS	OREAS-70P	0.013	0.002	28
	OREAS-501	0.204	0.011	37
	OREAS-901	0.363	0.0183	34
	OREAS-502	0.491	0.02	31
	OREAS-503	0.687	0.024	34
	OREAS-504	1.48	0.04	36
Total				**200**

SRK has checked all cases and noted that there were isolated outliers and that other CRMs inserted in the same sample batch performed well. SRK notes that, in general, the performance of the CRMs is reasonable. Out of 200 CRMs inserted, only 4 did not perform within the limits of 3 Standard Deviations (3SD) (action line).

- The OREAS-501, OREAS-502 and OREAS-503 plots indicate that all results fall within the 3SD acceptable limits.
- Analysis of the OREAS-70P plot indicates the majority of results are within acceptable limits and only two sample are slightly above the 3SD limit.
- The OREAS-504 and OREAS-901 plots indicates that the majority of results fell within the 3SD limits and are scattered around mean values, but one result of each CRM was outside the 3SD limit.

SRK plotted the performance of all CRMs; the results are provided in Figure 7-11, Figure 7-12, Figure 7-13, Figure 7-14, Figure 7-15 and Figure 7-16.

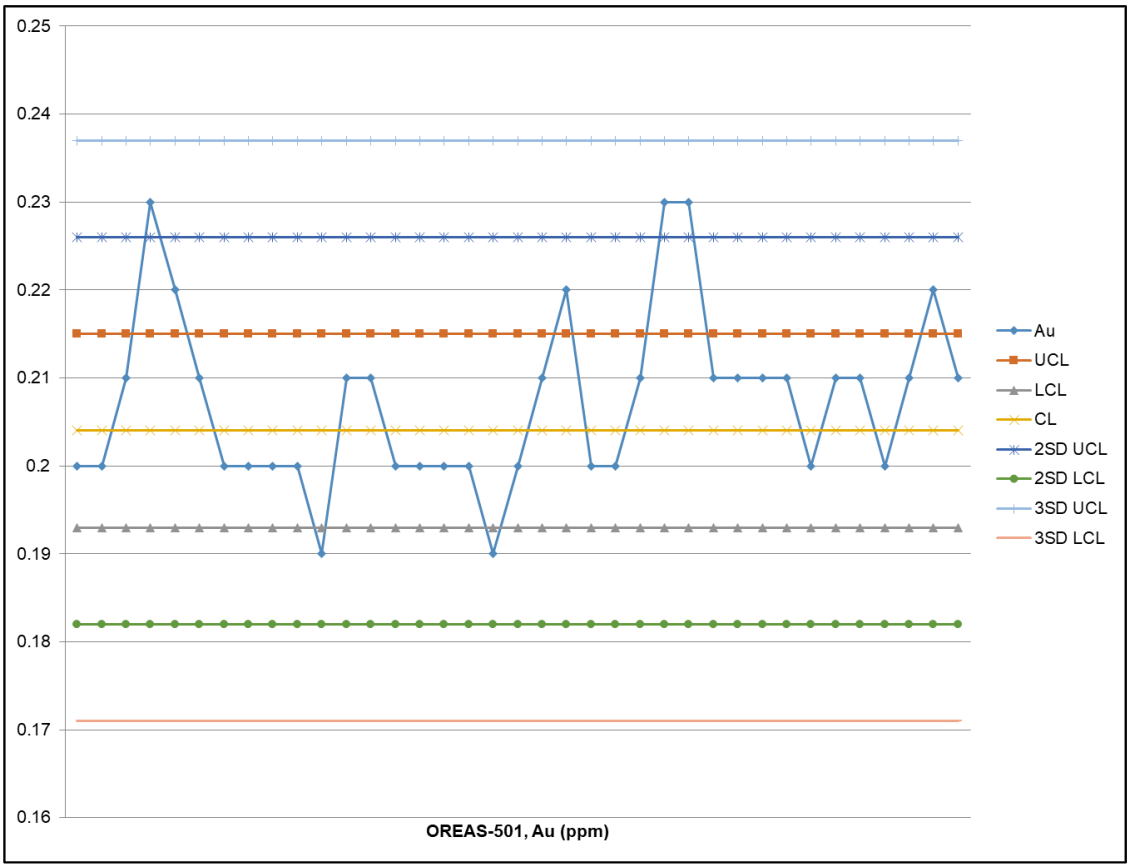

Figure 7-11: Performance of OREAS-501

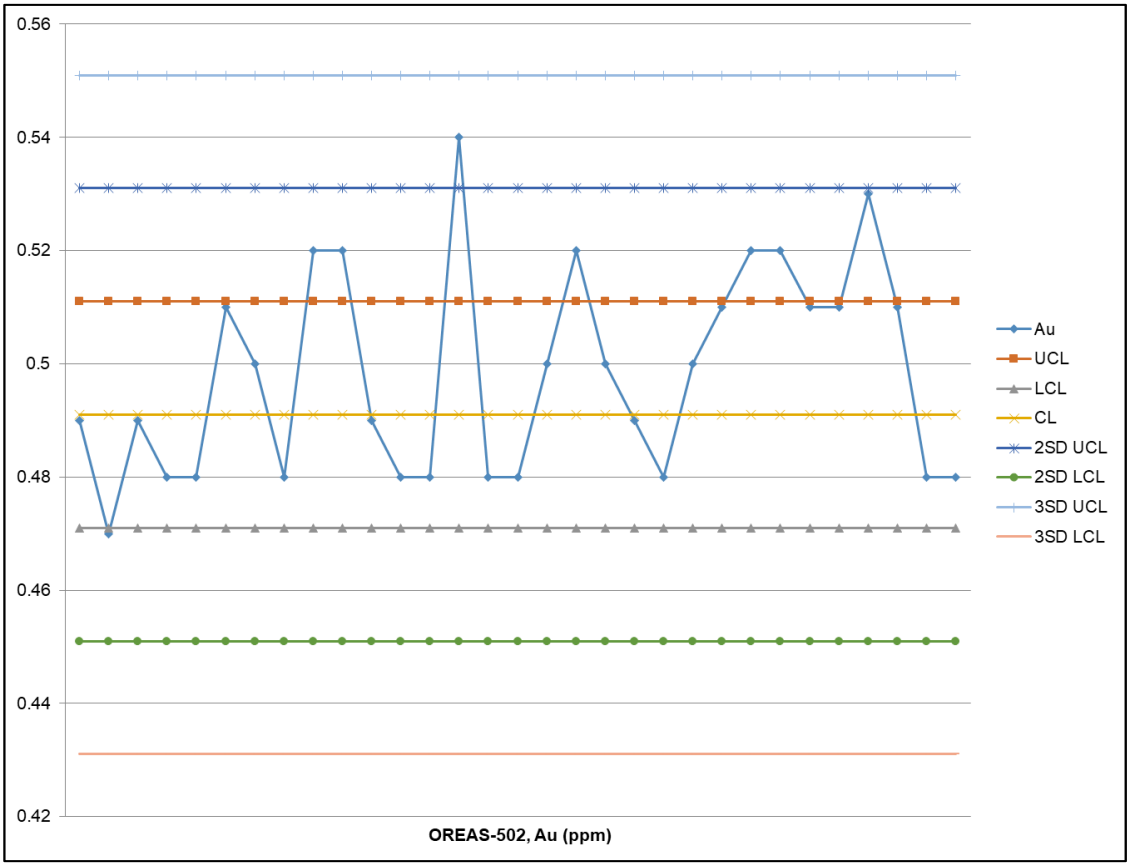

Figure 7-12: Performance of OREAS-502

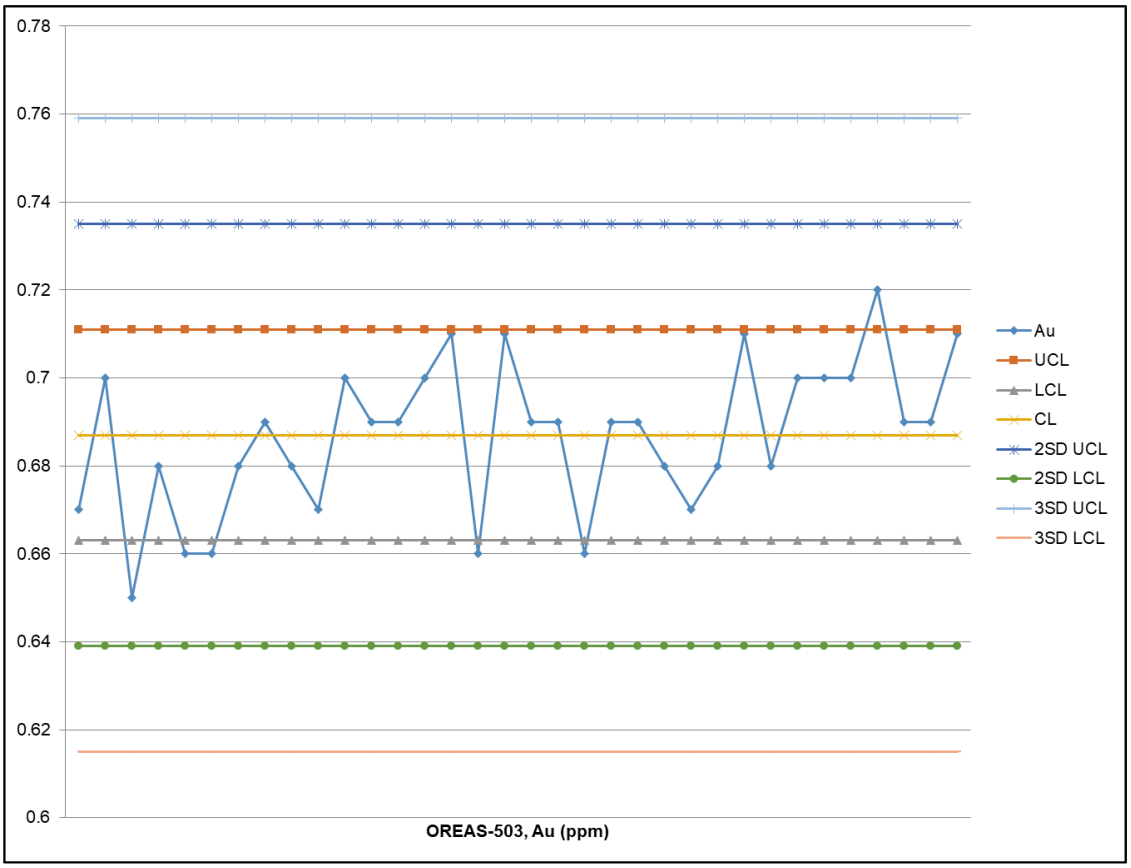

Figure 7-13: Performance of OREAS-503

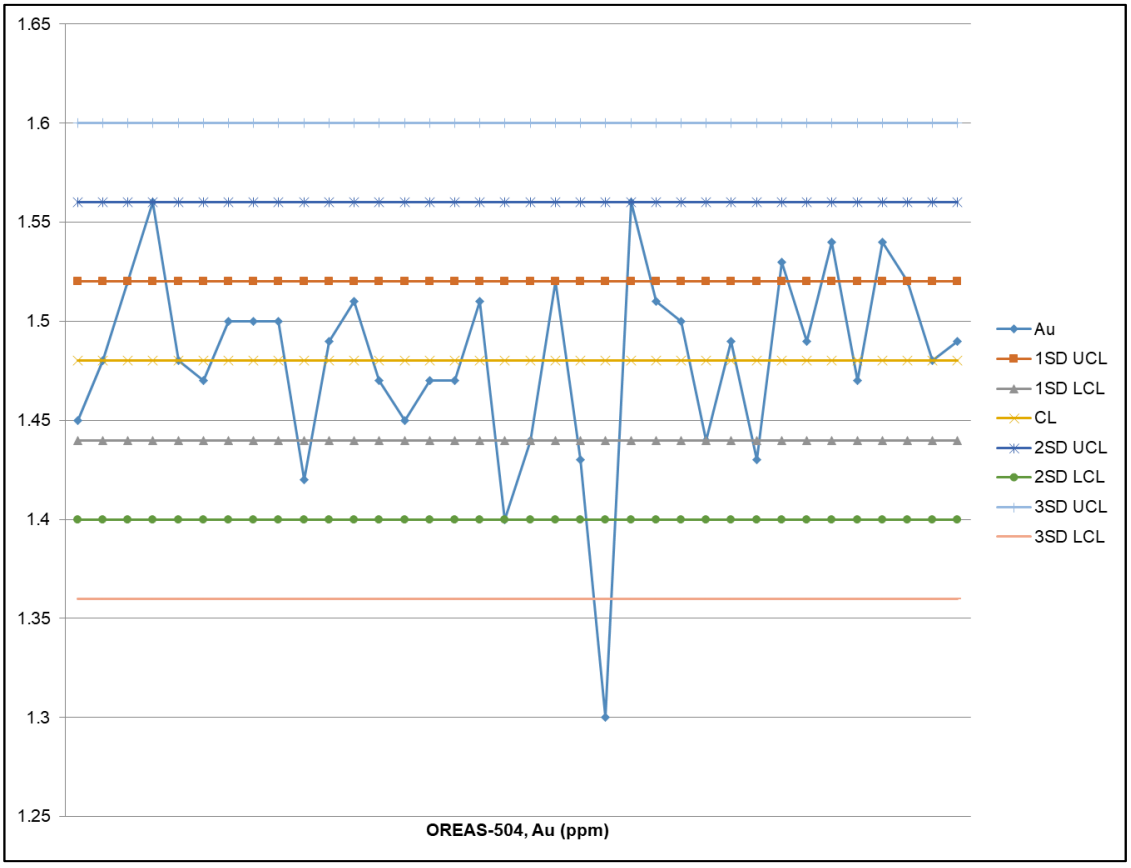

Figure 7-14: Performance of OREAS-504

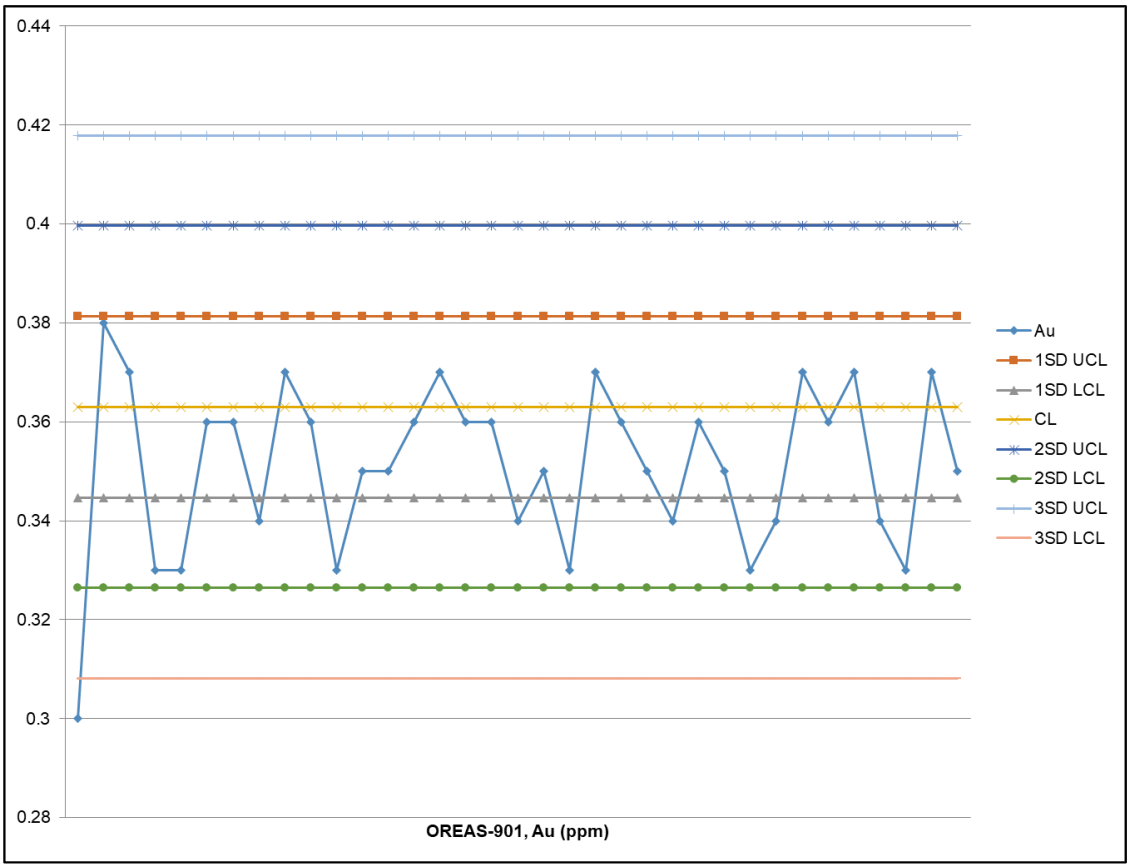

Figure 7-15: Performance of CRM OREAS-901

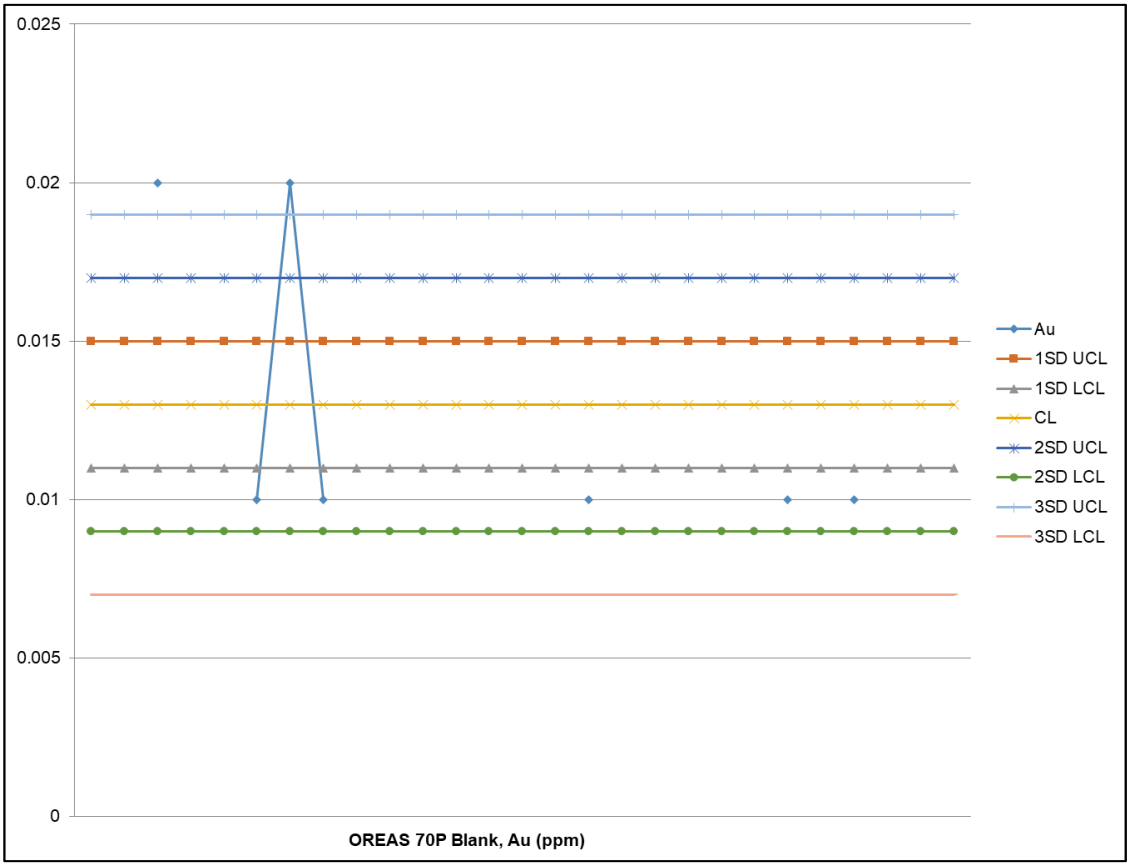

Figure 7-16: Performance of OREAS-70P

Performance of duplicates in 2005 and 2012

A total of 120 duplicate samples consisting of either the quarter-core sample from the retained (or unsampled) core half or RC chips were analysed during the 2005 and 2012 exploration programs. SRK checked sample batches and noted outliers in for core duplicate samples in 2012 results, however no reproducibility limits are defined. SRK opines that few observed outliers indicated coarse gold in 2012.

RC chip duplicates 2005

A total of 27 duplicate samples were prepared from RC chip material and analysed in 2005. The RC chip duplicates' performance is provided in Figure 7-17. In general, RC duplicates show reasonable repeatability and performed well. Analysis of these plots indicates that almost all of the results are aligned along the x=y line. This indicates that the laboratory sample preparation procedures are of a high standard, with good assay repeatability.

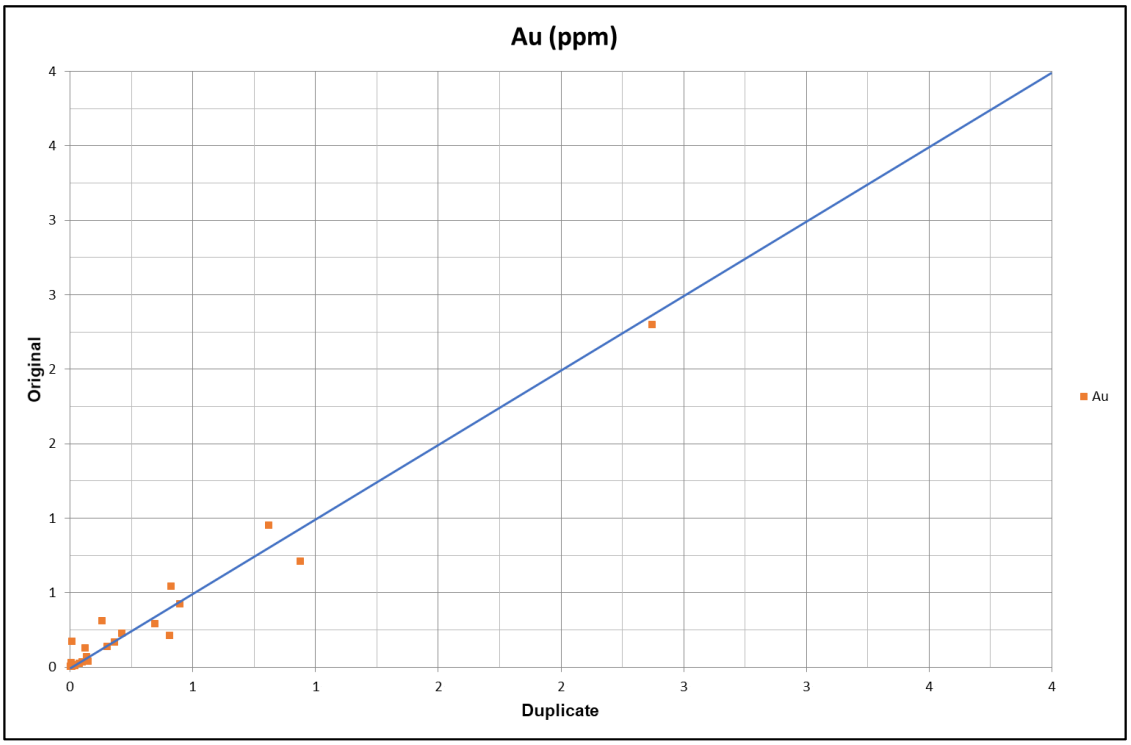

Figure 7-17: Performance of RC duplicates in 2005

Core duplicates 2012

A total 93 duplicate samples were prepared from quarter-core samples in 2012.

The performance results for core duplicates are provided in Figure 7-18. An analysis of the plots indicates reasonable for half-/quarter-core gold splits. SRK notes that core duplicates do not indicate any bias and core duplicates, unlike homogenised RC duplicates normally display a high degree of scatter as the two sides of the core are actually different samples. Observed scatter is likely caused by a moderate natural variability or 'nugget effect' typical at a high grade of gold deposits.

RPM also noted that the relatively poor correlation and given the nature of the sample (quarter coring) and the style of mineralisation (RPM, 2014).

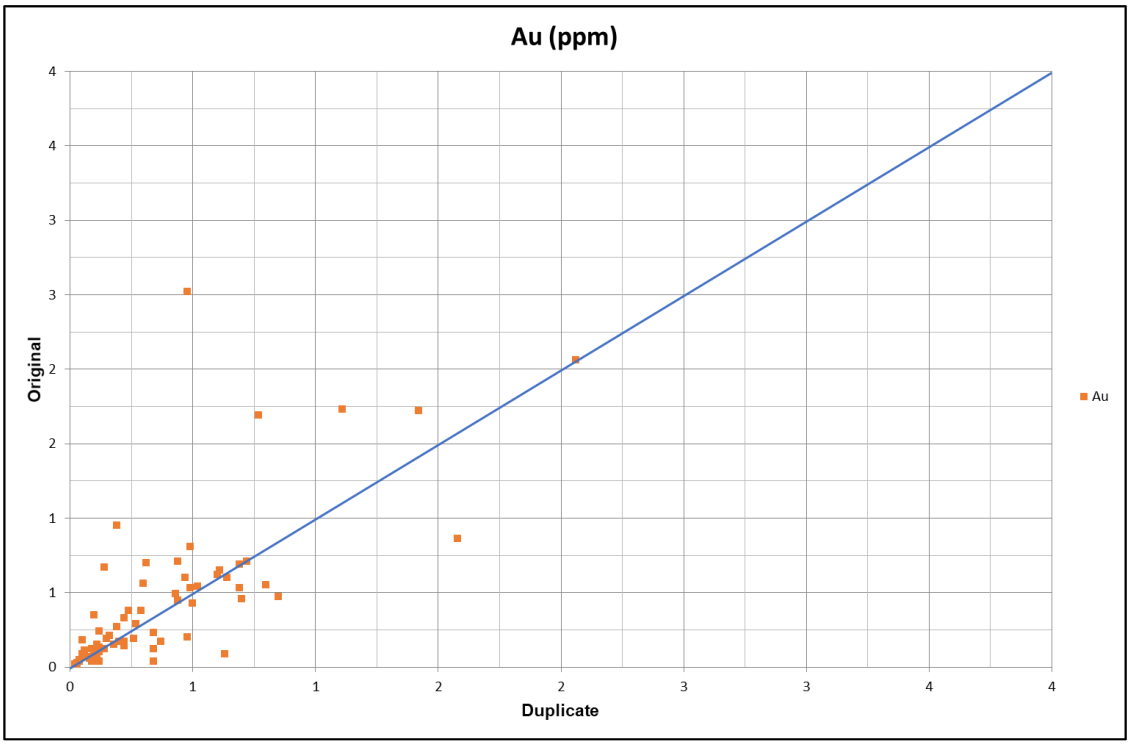

Figure 7-18: Performance of core duplicates in 2012

External laboratory pulp duplicates

In 2013, SG completed independent and external checks on 29 randomly selected pulp duplicate samples from the 2012 drilling program. Original pulp samples from the SGS laboratory were reanalysed by ActLabs.

The performance results for pulp duplicates by external checks are provided in Figure 7-19. Analysis of this plots indicates poor repeatability but no noticeable bias.

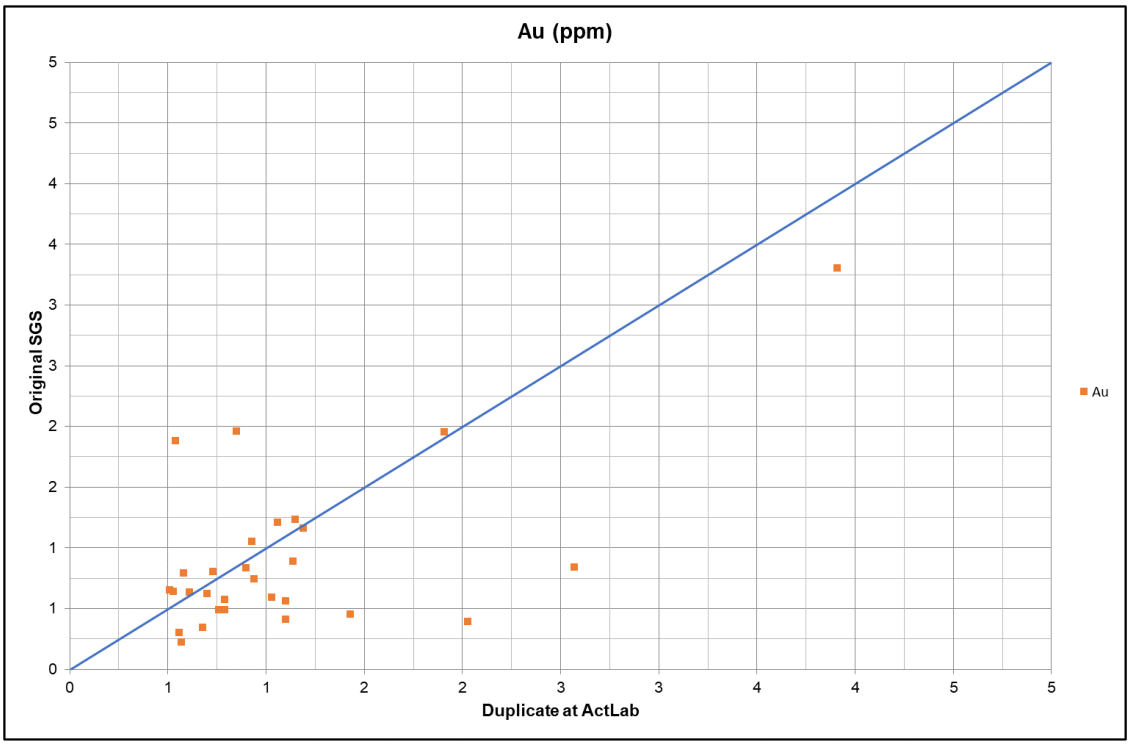

Figure 7-19: Performance of pulp duplicates at ActLabs (gold)

SGS and ActLabs Laboratories – Internal Control

In 2012 and 2013, SGS and ActLabs both inserted 5% CRMs, blanks and repeats as part of their internal quality control (QC) procedures and QA/QC plots are provided as Figure 7-20, Figure 7-21 and Figure 7-22.

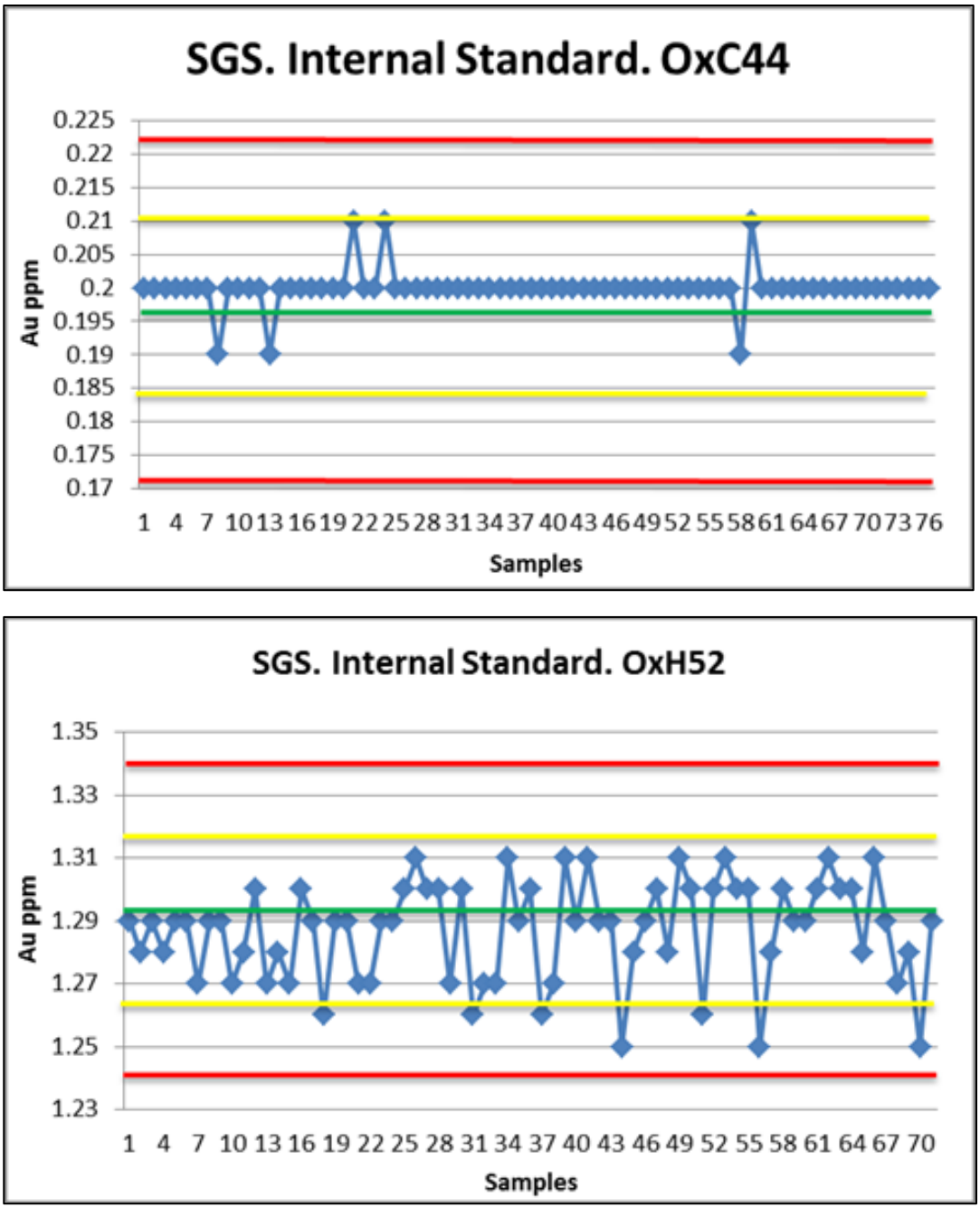

Figure 7-20: Performance of SGS's internal CRMs – OxC44 and OxH52

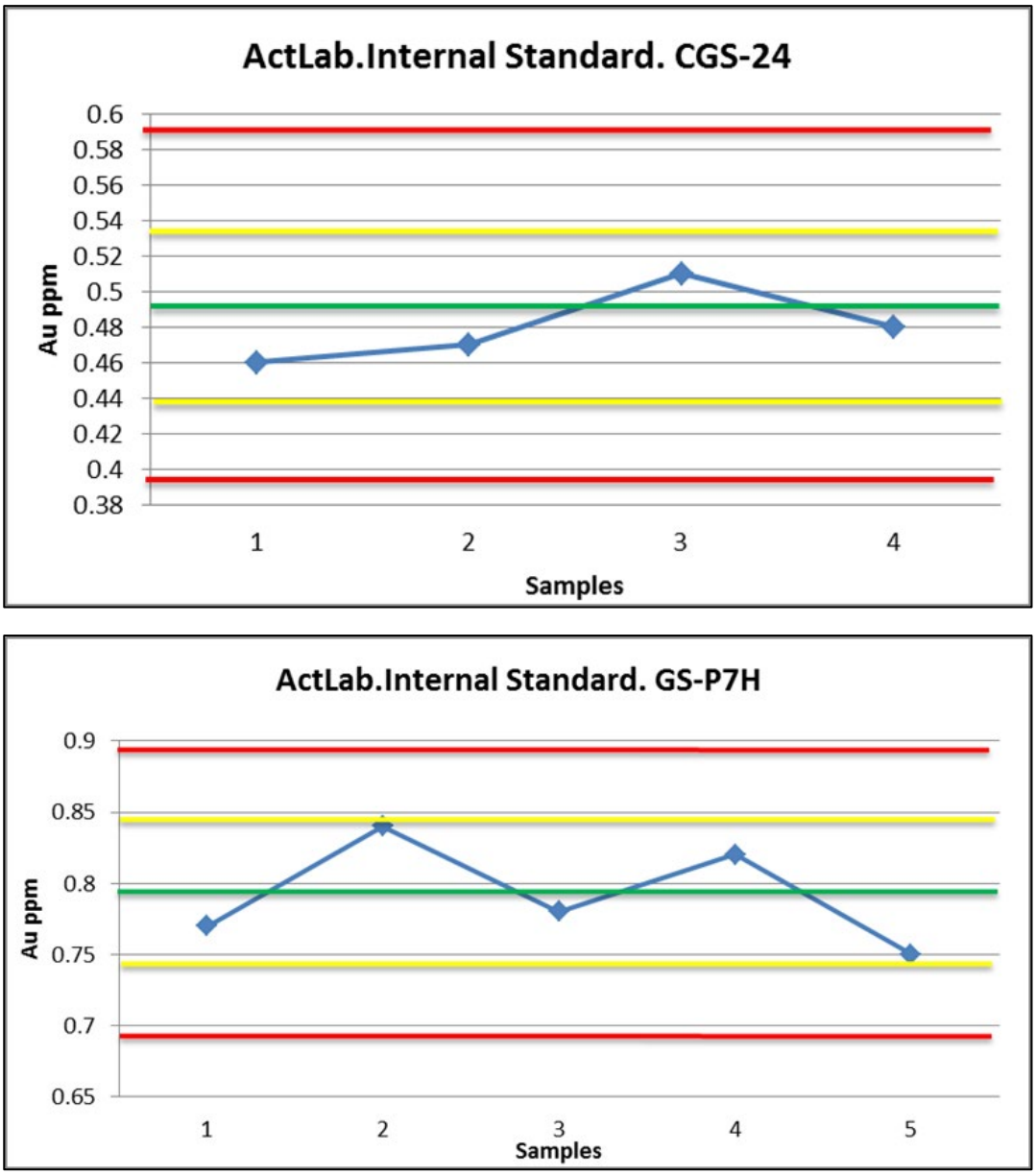

Figure 7-21: Performance of ActLabs' internal CRMs – CGS-24 and GS-P7H

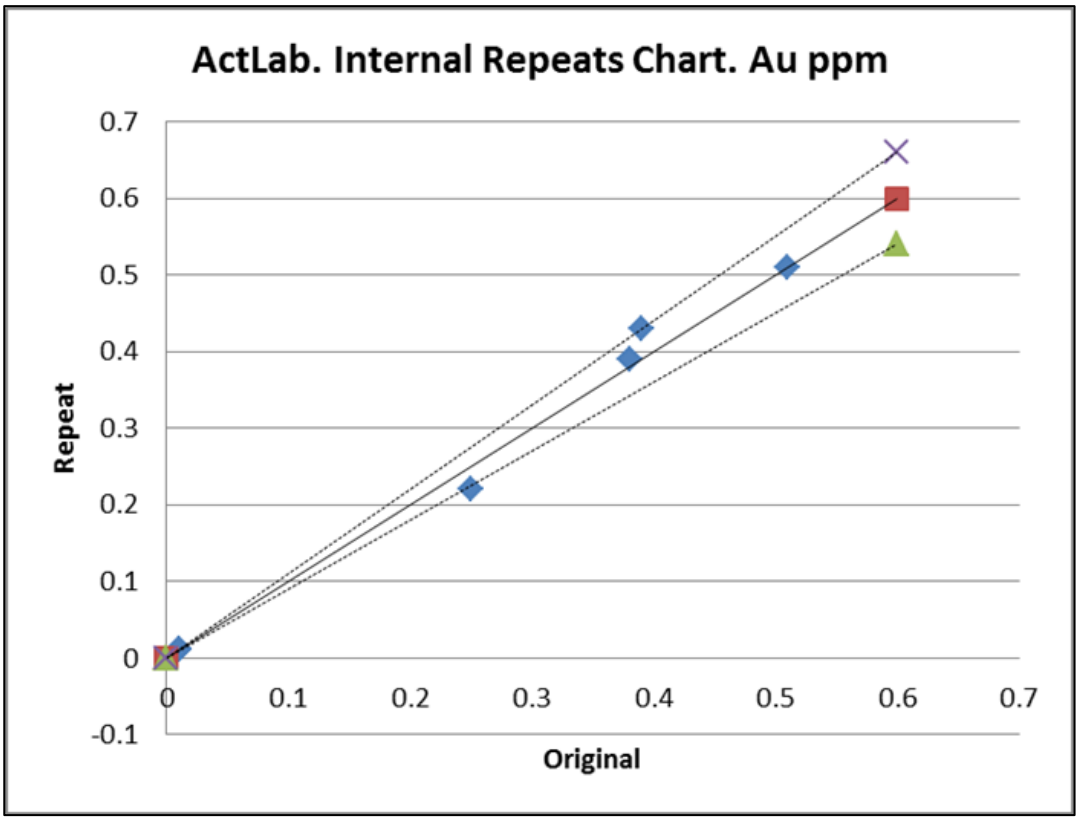

Figure 7-22: Performance of ActLabs' internal repeats

SRK notes that the samples assayed are representative and there is no sampling bias. Overall, the internal quality control QA/QC results of both laboratories were satisfactory and reliable.

8 Mineral Resource Estimate Review

SRK was provided with two Mineral Resource estimates on TC1 area to review. The maiden Mineral Resource estimate was conducted by Micromine at the conclusion of the 2012 exploration program and the second estimate, which was carried out in 2014 as a Mineral Resource update that included exploration data collected in 2013, was done by RPM.

8.1 Micromine 2012 Mineral Resource estimate

Micromine completed the first Mineral Resource estimate on Tsagaan Chuluut Gold Project. The Mineral Resource was based on 46 boreholes (17 RC and 29 core drill holes) completed for the Project up to and including the 2012 program. The results are shown in Table 8-1.

Table 8-1: Mineral Resource statement for the Tsagaan Chuluut Gold Project TC1 Area (only Mineral Resources within tenement 15436A included)

Cut-off grade (ppm Au)	Density (t/m^3)	Volume (m^3)	Mass (t)	Grade (ppm Au)	Contained Metal		Classification
					(troy oz)	(t)	
0.3	2.81	4,680,000	13,200,000	0.54	229,000	7.1	Indicated
	2.80	1,880,000	5,350,000	0.52	90,000	2.8	Inferred
	2.80	6,550,000	18,500,000	0.54	319,000	10	Total

Source: Micromine (2012)

Micromine's grade-tonnage curves indicate a low-grade gold deposit with spotty high-grade pods (Table 8-2).

Table 8-2: Grade-tonnage table using varying cut-off grades (only Mineral Resources within Tenement 15436A are included)

Cut-off grade (ppm Au)	Density (t/m^3)	Volume (m^3)	Mass (t)	Grade (ppm Au)	Contained Metal	
					(troy oz)	(t)
1.0	3.04	157,000	477,000	1.08	17,000	0.5
0.7	2.85	1,290,000	3,710,000	0.86	102,000	3.2
0.5	2.84	2,960,000	8,450,000	0.70	191,000	5.9
0.3	2.80	6,550,000	18,500,000	0.54	319,000	10.0
0.1	2.80	7,600,000	21,400,000	0.50	342,000	11.0
0.0	2.82	7,600,000	21,400,000	0.50	342,000	11.0

Source: Micromine (2012)

8.2 RPM 2014 Mineral Resource estimate

8.2.1 Geology interpretation, wireframes and digital terrain models

RPM used Surpac™ software for 3D modelling and the Mineral Resource estimate.

At SG's request, RPM prepared wireframes using a 0.5 g/t Au cut-off grade and a 2 m minimum downhole width of mineralisation. A total of 31 wireframes were created. The mineralisation wireframes were treated as hard boundaries, which means that only assays from within each wireframe were used to estimate blocks within that wireframe. No weathering surface or line of oxidation was created. RPM adjusted the surveyed surface to cover the extents of the block model. Fixed length – 1 m downhole – composites within the intervals inside wireframes were extracted. After validation of composites (checks for spatial correlation with the domains, the location of the rejected

composites and zero composite values), composite files for the individual domains were separated.

SRK opines that an artificial 0.5 ppm Au cut-off is too high, which create false continuation of the high grade. Histogram (Figure 8-1) suggest a natural cutoff at about 0.1 ppm Au. RPM wireframes (Figure 8-2) are constructed by connecting drilled intervals with a 0.5 ppm Au cut-off and geological and structural data are not used for wireframe control.

Based on geology, core logs, structural logs and core photo review, SRK opines that presence of moderately dipping breccia structures is not supported by the geology and structural data. SRK recommends conducting infill drilling with core orientation in order to capture appropriate structural data and thereby improve the understanding of the geology and structural controls on mineralisation.

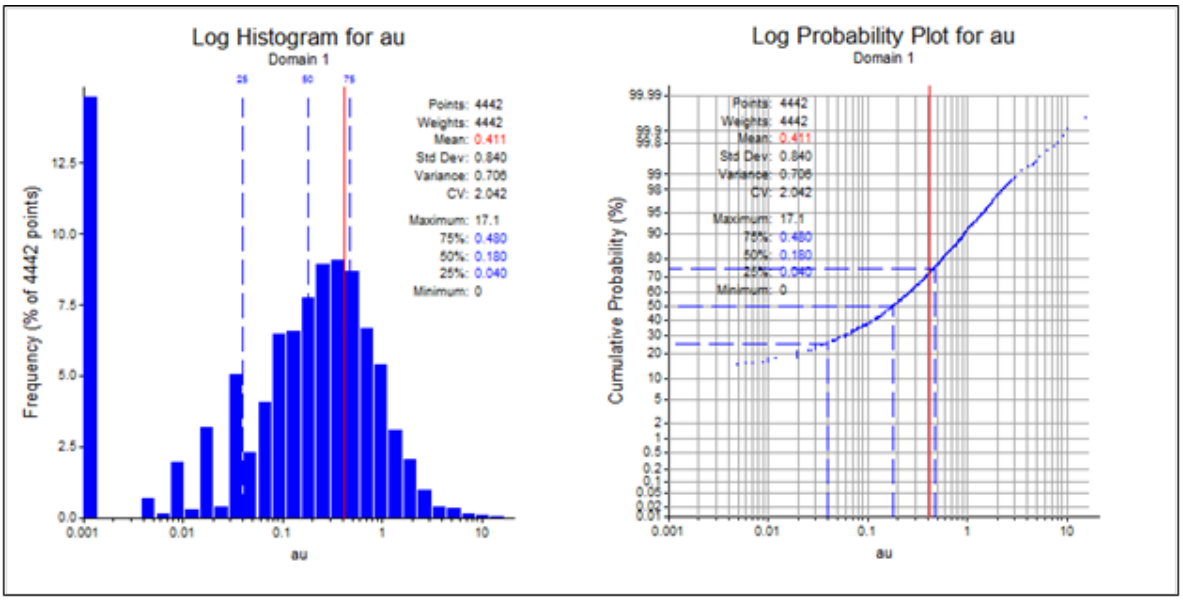

Figure 8-1: Log histogram and log probability plot of raw samples at Tsagaan Chuluut

Source: RPM (2014)

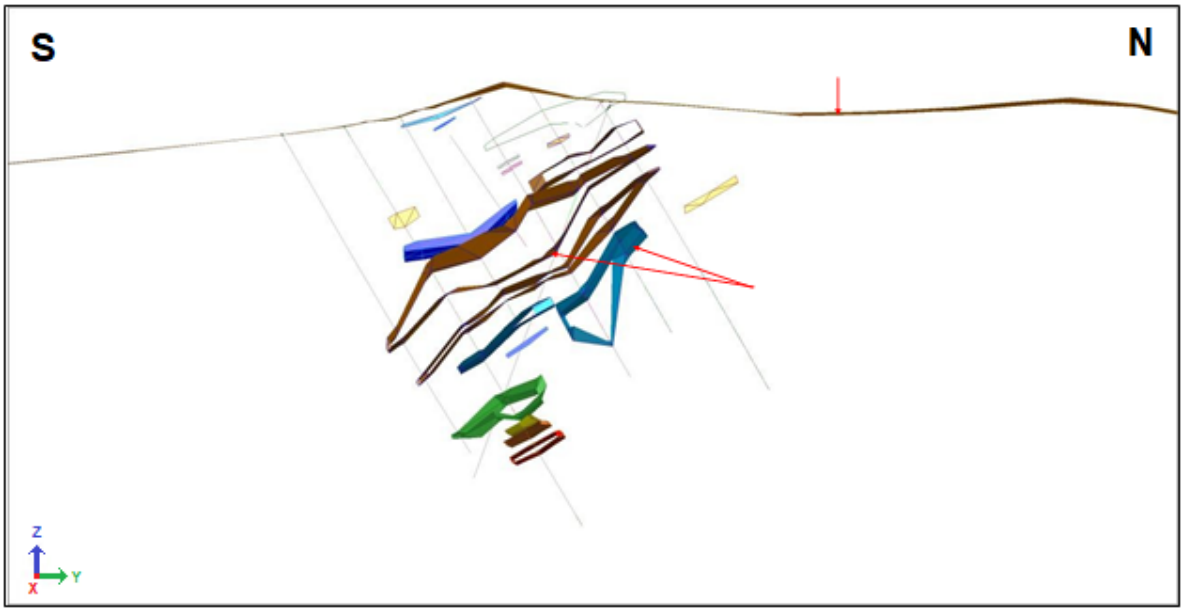

Figure 8-2: 2014 Mineral Resource estimate wireframes in section 675,325mE (facing west)

Source: RPM (2014)

8.2.2 Domain statistics and geostatistics

RPM imported the 1 m composite data into Supervisor software for the domain statistics and reported statistics for the three largest domains, Domain 1, Domain 3 and Domain 40 (Table 8-3).

Table 8-3: Summary statistics for 1 m composites

Parameter	All Domains	Domain 1	Domain 3	Domain 40
Samples	1,501.0	887.0	127.0	110.0
Minimum	0.0	0.0	0.1	0.0
Maximum	17.1	17.1	6.4	9.1
Mean	1.0	1.0	1.2	1.2
Std Dev	1.4	1.4	1.0	1.5
CV	1.3	1.4	0.8	1.3
Variance	1.8	2.0	1.0	2.2
Percentiles				
10.0%	0.24	0.22	0.30	0.29
20.0%	0.42	0.38	0.53	0.43
30.0%	0.53	0.50	0.73	0.60
40.0%	0.61	0.59	0.81	0.70
50.0%	0.71	0.70	0.90	0.80
60.0%	0.83	0.84	1.11	0.89
70.0%	0.99	1.00	1.43	1.00
80.0%	1.29	1.30	1.74	1.39
90.0%	1.91	1.83	2.43	2.63
95.0%	2.82	2.57	3.01	3.15
97.5%	4.67	4.16	3.44	5.76
99.0%	7.73	7.73	4.96	9.11

Source: RPM (2014)

RPM used Supervisor software to produce log histograms and log probability plots for each wireframe domain. The log histogram and log probability plot for the main domain (Domain 1) is shown in Figure 8-3. RPM decided to apply a top-cut of 9 g/t Au to three individual domains only (Table 8-4). No top-cut was applied to the remaining domains.

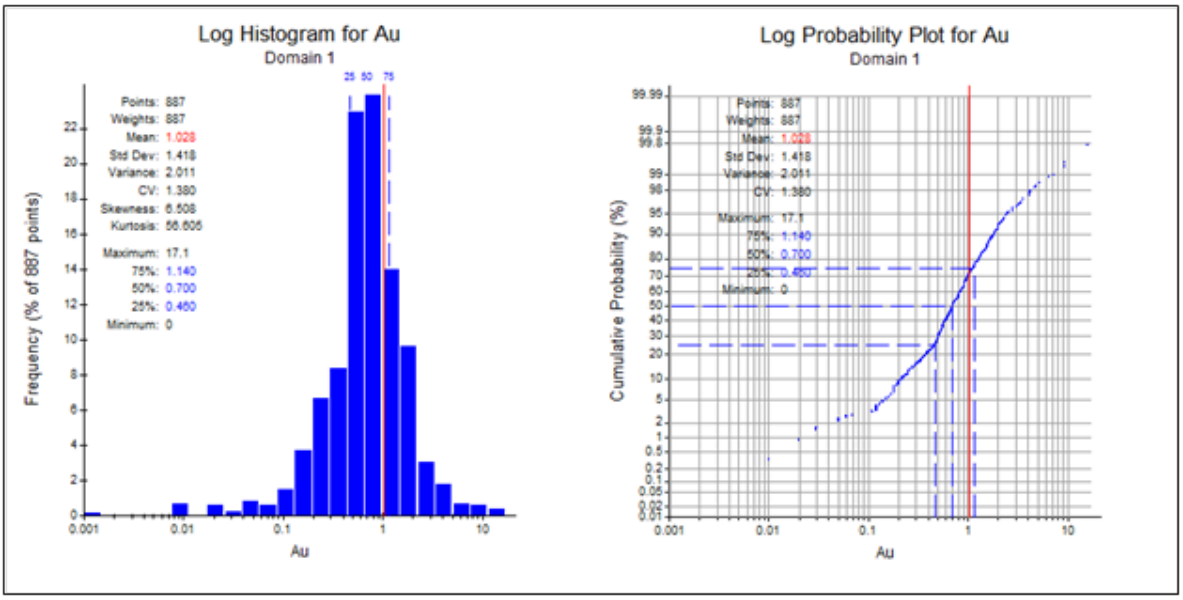

Figure 8-3: Log histogram and log probability log of 1 m composite data – Domain 1

Source: RPM (2014)

SRK notes the extreme middle bin frequencies and diminished left hand side frequencies. This suggests to that the 0.5 ppm Au cut-off is not a geological break and that lower grades are being artificially excluded. In practical terms the modelled continuity at 0.5 ppm Au is unlikely to be real or achievable and lower grade (background) metal is not being captured in the estimate. SRK opines that application of a 0.5 ppm Au cut-off introduces a false continuity of moderate to high grade mineralisation into the model.

Table 8-4: Summary of top-cuts applied

Domain	High grade cut (g/t Au)	Number of cut samples	Uncut mean (g/t Au)	Cut mean (g/t Au
1	9	10	1.03	1.00
26	9	1	1.65	1.65
40	9	1	1.18	1.18

Source: RPM (2014)

Geostatistical Analysis

RPM has calculated experimental variograms for the main lode (Domain 1).

The 1 m composite sample data were imported into Supervisor software for analysis. A two-structure nested spherical model was found to model the experimental variogram reasonably well. The downhole variogram provides the best estimate of the true nugget value, which was 0.4 for Domain 1. RPM modelled the downhole and three orthogonal variograms for Domain 1. The variograms displayed reasonable structure. The directional variograms for Domain 1 are shown in Figure 8-4.

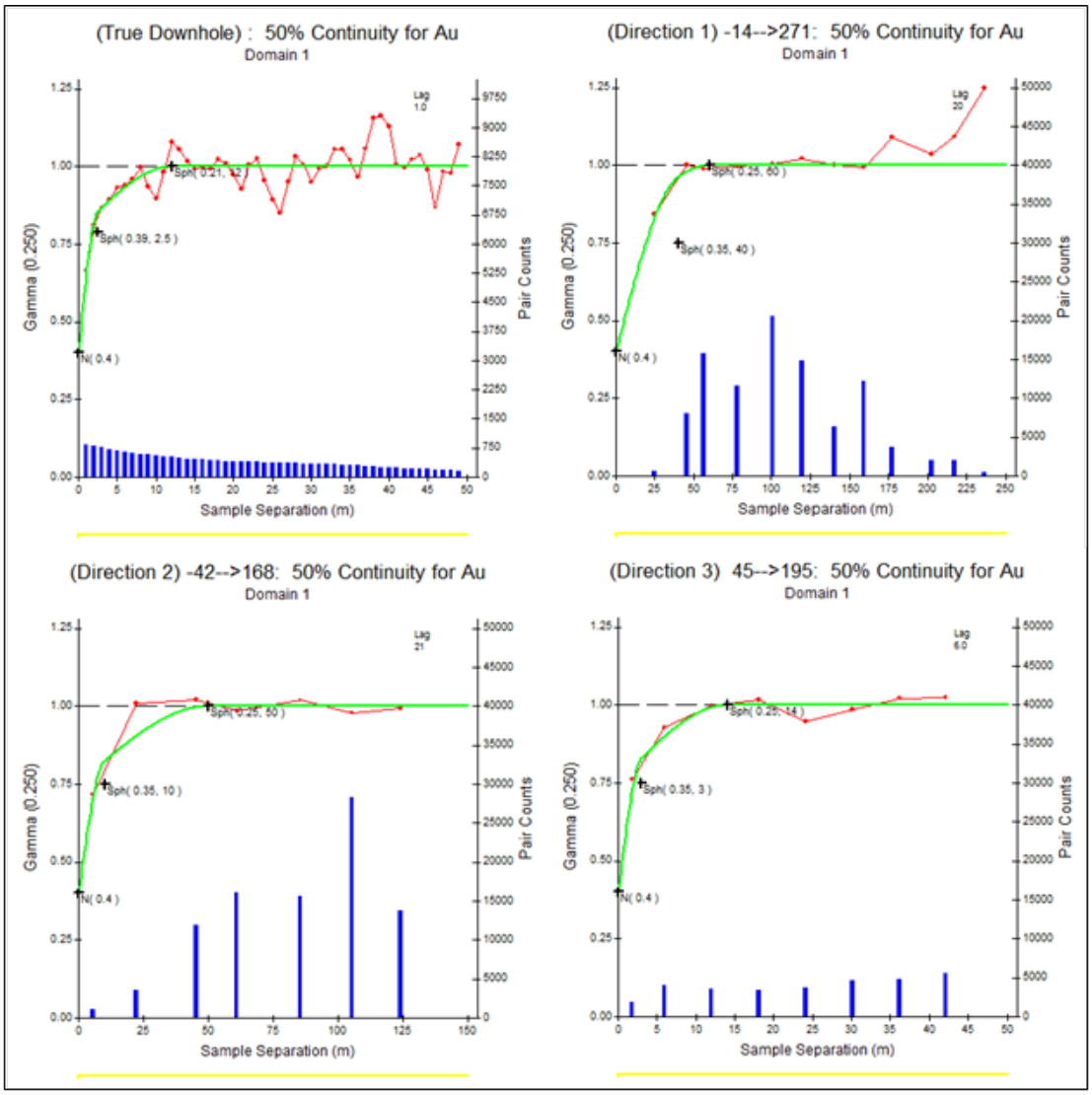

Figure 8-4: Downhole and directional semi variograms – Domain 1

Source: RPM (2014)

The gold grades were interpolated in a Surpac™ block model using the ordinary kriging (OK) with parameters provided in Table 8-5.

Table 8-5: Kriging parameters applied in Mineral Resource estimation

Structure	Parameter	Value
	Major Direction	**-14-->271**
1	Nugget	0.4
	Sill C1	0.35
	Reach	40
	Major/Semi-major	4
	Major/Minor	13.3
2	Sill C1	0.25
	Reach	60
	Major/Semi-Major	1.2
	Major/Minor	4.3

Source: RPM (2014)

8.2.3 Block Model

The parameters used in creating a Surpac™ block model are listed in Table 8-6.

The parent block size was selected on the basis of 50% of the average drill hole spacing of the Project, while dimensions in other directions were selected to provide sufficient resolution to the block model in the across-strike and down-dip direction.

Table 8-6: Block model parameters

Model name	tsagaan_chuluut_ok_20140124.mdl		
	Y	X	Z
Minimum coordinates	5,485,000	675,000	550
Maximum coordinates	5,485,600	675,600	1,150
Block size (sub-blocks)	25 (3.125)	25 (3.125)	5 (0.625)
Rotation		**none**	
Attributes:			
au_uncut	Estimated block uncut gold grade		
au_cut	Estimated block gold grade using cut grades - Reported		
min_dis	Distance to nearest sample		
ave_dis	Average distance to samples		
num_sam	Number of samples used for block grade interpolation		
Class	mes, ind, inf, minpot		
class_code	mes = 1, ind = 2, inf = 3, minpot = 4		
est_type	Estimation method e.g. ok, id2 or ave		
kvar_au_cut	Kriging variance for au_cut		
Bd	Bulk density		
Type	air, ox, tr, fr air= air, ox= oxide, tr= transitional, fr= fresh		
Lease	y or n		
Pass	1 = interpolated in first pass, 2 = second pass, 3 = third pass		
Pod	Domain number		
Mined	y or n		

Source: RPM (2014)

The grade interpolation was conducted using Ordinary Kriging (OK), with the wireframes acting as a hard boundary of each domain. Variography parameters from Domain 1 were used for definition of search ellipsoid used for all domains. Three interpolation passes were used for the interpolation. Over 97 of blocks was informed in Pass 1 and 2. The kriging parameters are listed in Table 8-7. There was no limit applied to the maximum number of samples used per hole in the estimate due to the relatively thin nature of the mineralised units.

Table 8-7: Search and kriging parameters

Parameter	Pass 1	Pass 2	Pass 3
Search type	Ellipsoid	Ellipsoid	Ellipsoid
Bearing	270° to 271°	270° to 271°	270° to 271°
Dip	30° to 43°	30° to 43°	30° to 43°
Plunge	-14° to 0°	-14° to 0°	-14° to 0°
Major to Semi-Major ratio	1.2	1.2	1.2
Major to Minor ratio	4	4	4
Search radius	80	80	200
Minimum samples	10	6	2
Maximum samples	32	32	32
Maximum samples per hole	8	8	8
Block Discretisation	4X by 4Y by 2Z	4X by 4Y by 2Z	4X by 4Y by 2Z
Percentage blocks filled	93%	4%	<1%

Source: RPM (2014)

A single drill hole intersected a total of 17 domains, therefore, average grades exported from Supervisor were assigned to these domains; 3% of the blocks in the block model were assigned average grades.

8.2.4 Density and Material Type

Bulk density was estimated from density measurements carried out on 1,772 samples from 23 drill holes using the Archimedes method of dry weight versus weight in water. RPM opined that the majority of the TC1 deposit is fresh rock; therefore, the average value of 2.83 t/m^3 was assigned to all material below the topographic surface.

RPM does not provide any commentary regarding how samples with bulk density over 3 t/m^3 were treated in the database.

8.2.5 Model Validation

RPM used the following three validation techniques:

- Visual check on cross sections
- Comparison of the average gold grades of the composite file input against the gold block model output for all the resource objects
- Trend analysis by comparing the interpolated blocks to the sample composite data. The trend analysis was completed for 50 m eastings and for elevation in 20 m bench heights for all domains.

8.2.6 Mineral Resource Classification

RPM classified the Mineral Resource in the Indicated and Inferred Mineral Resource categories based on data quality, sample spacing, and lode continuity. The Indicated Mineral Resource was defined within areas of close-spaced diamond and RC drilling of less than 50 m by 50 m, and where there was good continuity and predictability of the lode positions. The Inferred Mineral Resource was assigned to areas of the deposit where drill hole spacing was greater than 50 m by 50 m, where small isolated pods of mineralisation occur outside the main mineralised zones, and to geologically complex zones.

A model showing the Mineral Resource classification is shown in Figure 8-5.

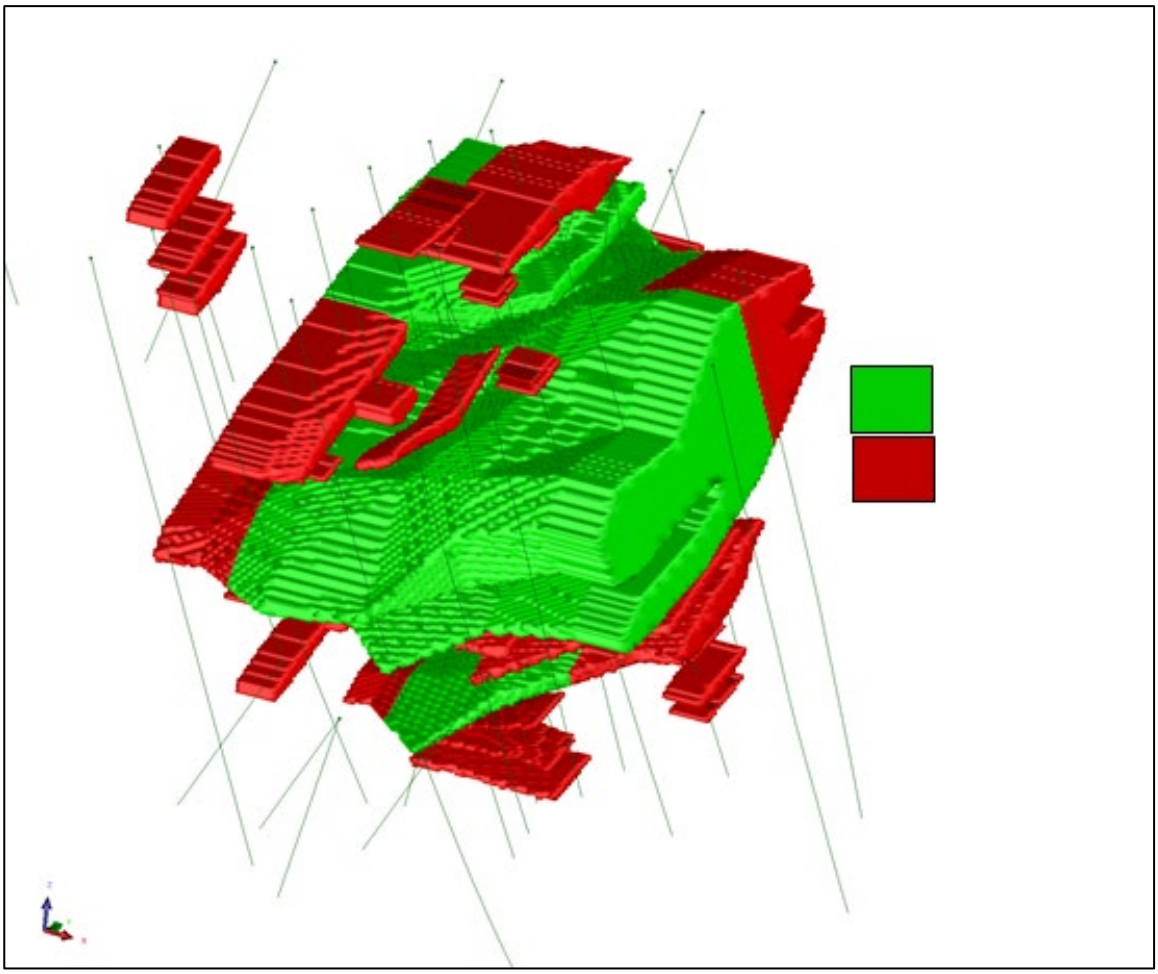

Figure 8-5: Tsagaan Chuluut 2014 Mineral Resource Classification (facing 245°) (green Indicated and Red Inferred Resource)

Source: RPM (2014)

8.2.7 Reasonable Prospects of Eventual Economic Extraction

RPM (2014) considered that limited infrastructure is a major risk for the Project.

According to the RPM (2014), the key consideration for development of the Project is the provision of adequate supplies of water for the proposed processing plant. There are no supplies of permanent surface water in the area and further hydrogeological survey work (to at least pre-feasibility study level) will be required. To date, only a limited hydrogeological survey around the Nogtot prospect has been completed. Significant quantities of water would be required for the operation of a processing plant at the Project.

RPM did not state any mining and metallurgical assumptions for Tsagaan Chuluut Gold Project.

8.2.8 Mineral Resource Reporting

RPM recommended reporting the Tsagaan Chuluut Mineral Resource with a 0.7 g/t Au cut-off grade. The Mineral Resource estimate is shown in Table 8-8.

The grade-tonnage curve for the entire Mineral Resource is shown in Figure 8-6.

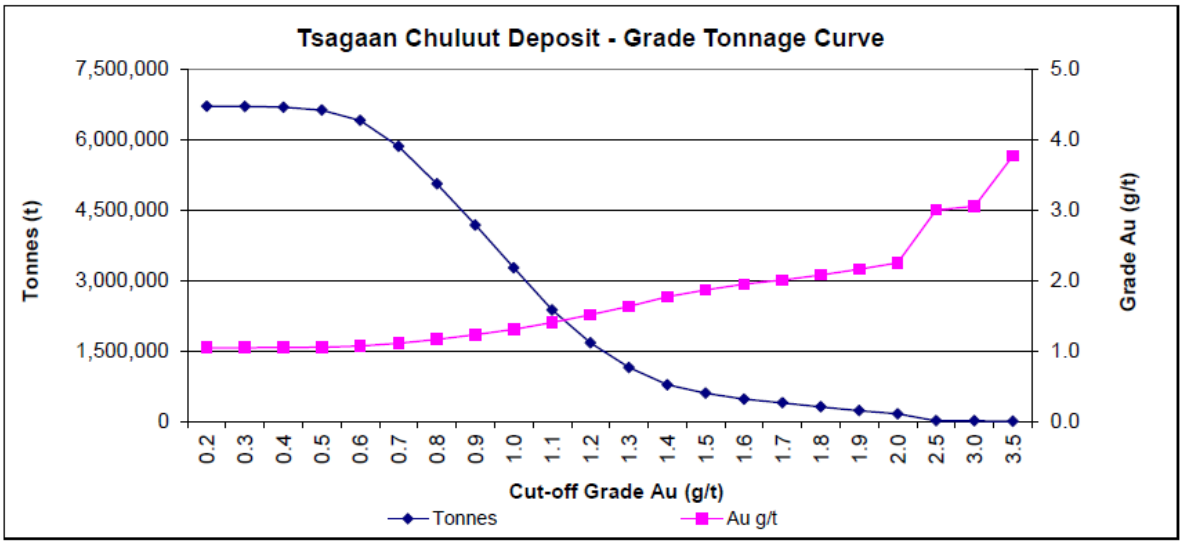

Figure 8-6: Grade-tonnage curves

Source: RPM (2014)

Table 8-8: Mineral Resource estimate as at February 2014

Cut-off grade	Indicated			Inferred			Total		
0.7 g/t Au	Tonnes (Mt)	Grade (g/t Au)	Contained Metal Au (Oz)	Tonnes (Mt)	Grade (g/t Au)	Au Ounces	Tonnes (Mt)	Grade (g/t Au)	Contained Metal Au (Oz)
	4.7	1.1	163,500	1.2	1.2	44,600	5.8	1.1	208,200

Source: RPM (2014)

8.3 Metallurgy

In 2013, the following initial, limited metallurgical tests were undertaken on Tsagaan Chuluut gold mineralisation:

- Gekko was commissioned to provide a preliminary understanding of the ore's response to gangue rejection, vertical shaft impact crushing, gravity separation and flotation, all of which are key components of Python pre-concentration processing.
- SGS' objective was to determine the potential for the recovery of gold from the ore by a sequential process involving flotation, bacterial oxidation and cyanide leaching.
- Hepta was commissioned to carry out the gravity and flotation test work and to determine the gold yield from flotation concentrate by means of cyanide leaching under optimised conditions.
- Yantai was commissioned to conduct gold ore metallurgical tests, aiming to provide the basis for processing design and future production of the mine.

In July 2019, SG commissioned Technological Research Centre of Mongol Alt (MAK) LLC to conduct column leaching test on a bulk sample (total weight of 165.4 kg).

8.3.1 Gekko (January 2013)

Gekko's testwork was aimed at testing the suitability of Python processing technology for TC1 gold ore processing. The results are summarised below:

- The Bond Abrasion Index is 0.2004, indicating that the tested sample is slightly abrasive.
- The average assayed head grade of the sample received was 0.93 g/t Au and 0.89% S, while

calculated head grades were determined from the various tests, with the sample having an average calculated head grade of 0.88 g/t Au and 0.90% S.

- No preferential distribution of gold or sulphur with particle size occurs with crushing to 100% passing 11.2 and 1.18 mm.
- It appeared that post Vertical Shaft Impact (VSI) crushing showed 80% of the gold was in approximately 45% of the mass, which may provide an opportunity to reject 55% of the mass not including the fines screened out before VSI crushing.
- The sample had a moderate amenability to VSI crushing for a product size of 100% passing 1.18 mm. The single pass produced 27% minus 1.18 mm, and even with a circulating load this remained 27%, indicating relatively consistent hardness throughout the sample.
- The sample was amenable to pre-concentration by gravity with 73% of the contained gold and 83% of the contained sulphur recovered into a 5.6% mass yield. The grade of this cleaner concentrate was 12 g/t Au and 13% S. This corresponds to an upgrade ratio of 13 and 14 for gold and sulphur, respectively.
- In the final gravity tail, approximately 60% of the unrecovered gold and 85% of the unrecovered sulphur was reported in the minus 106 µm fraction, which is the size fraction that recovery by continuous gravity begins to decrease.
- Flotation on a composite of the CGR cleaner and rougher table tail was able to recover 54% of the gold and 77% of the sulphur into a 1.59% mass yield after 2 minutes of flotation. The grade of this flotation concentrate was 9 g/t Au and 7.6% S.
- The deportment of gold, with particle size, in the flotation tail was predominately reporting to the coarser size (plus 106 µm) fractions. This indicates a finer grind may be required to increase liberation and hence recovery.
- The combined gravity and flotation recovered 87% of the gold, at a grade of 11.59 g/t, and 95.6% sulphur, at a grade of 12.26% into a mass yield of 6.8%.

8.3.2 SGS (February 2013)

The objective metallurgical testwork undertaken by SGS was to determine the potential for the recovery of gold from the ore by a sequential process involving flotation, bacterial oxidation and cyanide leaching.

The metallurgical sample was prepared from four composite samples collected from four different drill holes. The four composite samples were of equal weight, and had the following gold grades:

- TCDD-014: 0.60 g/t
- TCDD-024: 0.24 g/t
- TCDD-028: 0.62 g/t
- TCDD-033: 0.38 g/t.

The TCDD composite grade was 0.42 g/t.

The main conclusions were:

- The ore samples were low grade containing approximately 0.2 to 0.6 g/t Au.
- There was negligible arsenopyrite, which is typically present in refractory ore types. The arsenic grade in the composite sample was 21 ppm.
- The ore was amenable to sulphide flotation with high recoveries of both gold and sulphur. Gold and sulphur recoveries of 90%–96%, and >98%, respectively, were achieved into concentrates containing approximately 4%–8% of the mass. However, the low grade of the ore samples limited

rougher concentrate gold grades to a maximum of 13 g/t. It may be possible to upgrade the concentrates further by incorporating cleaning stages into the flotation scheme.

- A cyanide leach on the bulk flotation concentrate, which contained 8 g/t Au and 12 g/t Ag, achieved 92% Au and 40% Ag extraction. This suggest that the gold present in the ore was not of a refractory nature as had been previously indicated by the Client to SGS.

8.3.3 Yantai Xinhai Institute (September 2013)

The Yantai Xinhai Institute tested Tsagaan Chuluut ore in order to design processing plant. The sample grades were 0.41 g/t Au, 0.2 g/t Ag, 0.63% S, 0.009% As and 0.013% Sb. Ore minerals identified were pyrite, hematite and magnetite. Gangue minerals were quartz, sericite, muscovite, potassium feldspar and calcite.

The Yantai Xinhai Institute concluded that cyanide leaching process is suitable for gold recovery – up to 73.17% at particle size of minus 200 mesh (74 µm). After applying NaOH as a protection alkali with dosage of 5 kg/t and NACN dosage of 2 kg/t, the recovery reached 85.41%.

8.3.4 Hepta (September 2013)

- Hepta conducted a gravity/flotation test and cyanide roll bottle leach test on a flotation concentrate. The test was carried out on a 96 kg sample grading at 0.46 ppm Au.
- The sample was crushed and ground till 65% of the sample mass was minus 74 µm (-200 mesh).
- Flotation was carried out using soda ash to maintain a pH of 9.5, copper sulfate as activator at 100 g/t, 50 g/t PAX (potassium amyl xanthate) and 25 g/t AERO® 8045 used as collector. OREPREP® X-133 was used as a frother. The flotation time was 8 minutes to recover a concentrate and then the tail was floated for an additional 4 minutes to recover gold in tail.
- The flotation stage yielded 2.8 kg (yield 2.9%) concentrate with a grade of 14.2 ppm Au. In total, 93.8% of gold was recovered by flotation.
- The leaching by NaCN indicated a recovery range 65.6% to 89.1%.

8.3.5 Technology Research Centre MAK LLC

A bulk sample, weighing 165.4 kg and grading at 1.05 g/t Au, was tested by the column leach method using a solution of NaCN at a concentration 500 mg/L.

The sample was homogenised and split by a rotary sample divider. The mass of the sub-sample was 10 kg, which was crushed to top size 5 mm (-5 mm). The crushed sub-sample was then grinded and sieved by a 1 mm size screen to generate two fractions with different grain size ranges: the first fraction -1 mm and second fraction -5 to +1 mm. Fractions were properly homogenised and split by rotary sample divider to obtain a subsample for analysis and the bulk sample for the column leach testing was reconstituted from both fractions.

After 23 days of leaching, the gold recovery achieved was 74.17% and the NaCN consumption was 0.43 kg/t.

8.4 SRK Mineral Resource verification on TC1

8.4.1 Modelling of the mineralisation domain

SRK used grade shells generated in Leapfrog™ software to model the domains for constraining a block grade estimate. The SRK-reviewed structural logs and data indicate that the gold mineralisation is located within breccia bodies with hydrothermal alteration, which are spatially related to zones of faulting and shearing. Quartz veins are developed locally in the upper level of the quartz porphyry

intrusion and do not show continuity. In comparison with the RPM model, the fault zones are oriented northwest and east–west and dip steeply to the southwest and to the south at an angle of 60°–70°.

Mineralisation interpretations were prepared by SRK using a nominal 0.1 g/t Au cut-off grade and a minimum downhole width of 2 m.

8.4.2 Grade shell thresholds

The SRK-interpreted faults trend approximately northwest–southeast to east–west. Modelling of the mineralisation contact itself was based on a grade shell for the 0.1 ppm Au threshold. The 0.1 ppm threshold was chosen as the best compromise between being selective enough to exclude substantial barren zones, while maintaining reasonable continuity between mineralised intersections. The gold threshold wireframes of the mapped and logged fault architecture were used as an input for a 'structural trend' (FaultTrend) in Leapfrog™ (Figure 8-8). The wireframes were treated as soft boundaries for estimation purposes (Figure 8-7).

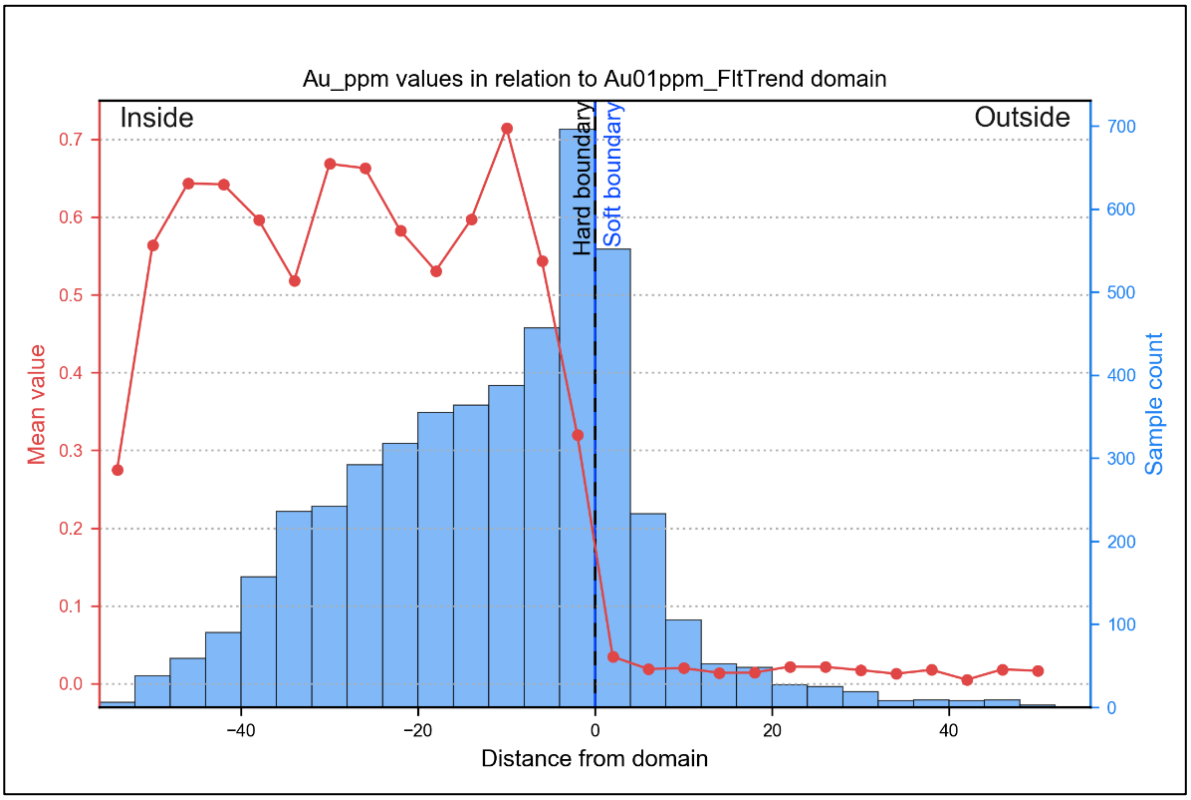

Figure 8-7: Au 0.1 ppm domain boundary analysis

The other Leapfrog™ settings for generating the 0.1 ppm grade shells are given in Table 8-9. The final mineralised domain models in Figure 8-8 were produced after the following manual edits to the wireframe model:

- Excessive extrapolation was trimmed in areas with little or no drill hole or trench information.
- Minor, isolated volumes based on single intersections were deleted.

The final domains were exported to GEOVIA Surpac™ software, validated and used for coding the drill holes and constraining the block model.

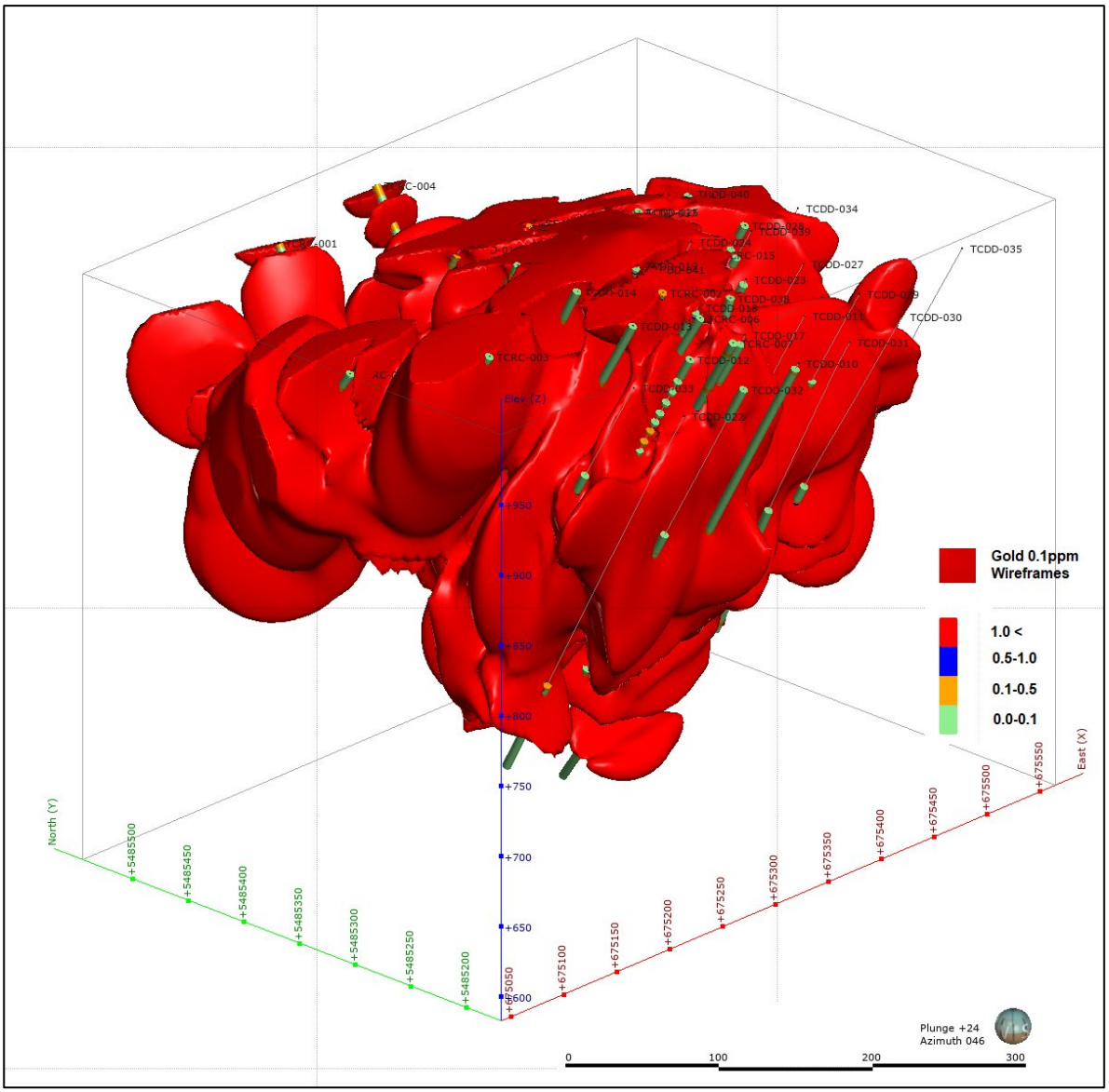

Figure 8-8: View of mineralisation domains from southwest

Table 8-9: Leapfrog parameters of Au 0.1 ppm domain

Variable modelled	Au
Grade threshold	0.1 ppm
Composite length	1 m
Grade transformation	Log
Variogram model	Spheroidal
Variogram sill	0.7
Variogram range	60 m
Base range	60 m
Resolution	5

8.4.3 Weathering Wireframes

Weathering surfaces were not prepared by SRK as the vast majority of the Tsagaan Chuluut mineralisation is fresh rock.

8.4.4 Geostatistical Estimation

Compositing

The raw sample length ranged from 0.2 m to 6.5 m, with an average of 2.0 m. The majority of samples were 1m in length (Figure 7-8), but longer sample lengths were used during the 2013 drilling program.

The samples within the individual mineralisation domains were independently composited to 2 m for gold assay and bulk density determination, with compositing starting and finishing at the domain contacts. Compositing was done in Surpac™, using the 'best fit' option, which allows small deviations from the set 0.5 m length to be made, in order to avoid creating short, residual composites at the end of drill hole intersections.

The 1 m length was also found to produce a set of composites that were sufficiently numerous for variogram modelling, yet with some of the extreme variability from the raw samples smoothed out.

8.4.5 Statistical analysis

Summary statistics of the composite grades are presented in Table 8-10.

Table 8-10: Summary statistics for composites and capped composites (ppm)

Variable	2 m Composite	Capped 2 m Composite
Min.	0.005	0.005
Max.	11.65	8.85
Avg	0.54	0.53
Median	0.33	0.33
Std Dev	0.76	0.69
CV	1.41	1.3
Count	2,687	2,687

The 0.1 ppm cut-off was used for modelling. The histogram is shown in Figure 8-9.

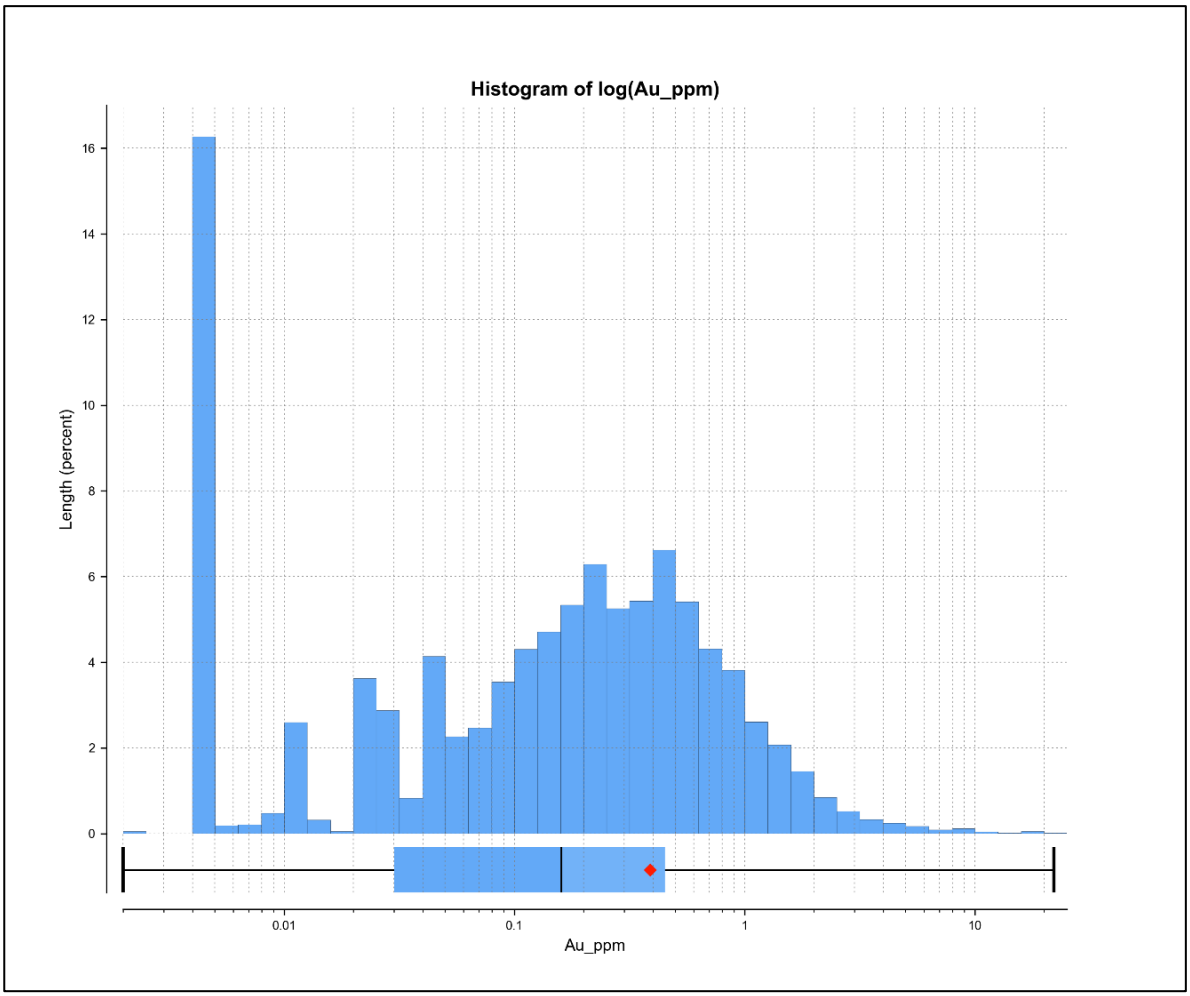

Figure 8-9: Log-transformed histogram – Gold, all data

The grades for top-capping were based on the grade at which the high tail of the grade distribution starts to break up and become erratic (Figure 8-10).

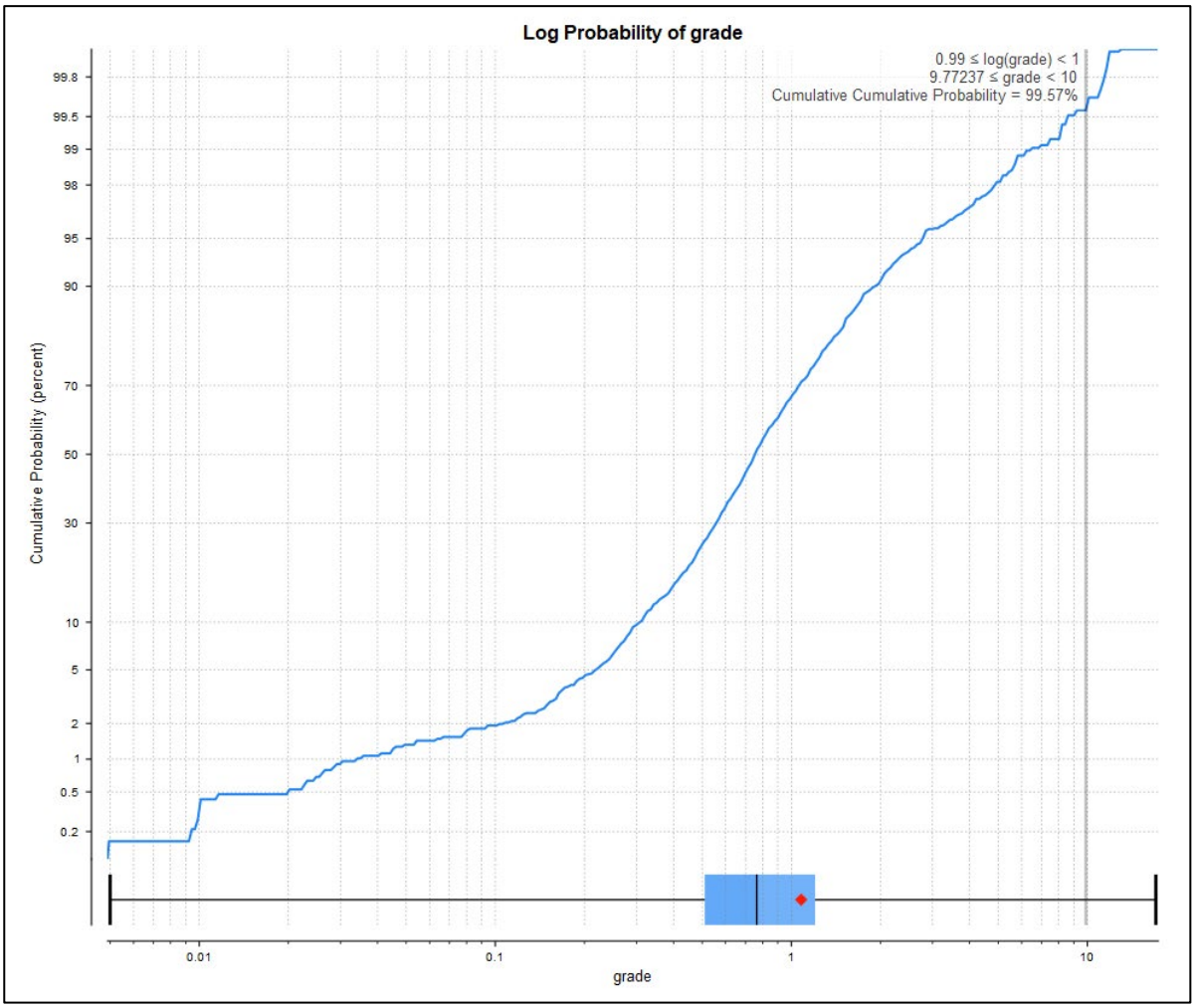

Figure 8-10: Cumulative probability plot of composite grades – all data

The high-grade cuts at 10 ppm were applied to 8 samples for the variogram modelling composites.

8.4.6 Variogram Modelling

Understanding the grade continuity and determining its extent and orientation is achieved through interpreting and modelling the experimental variogram. Variogram models were fitted using GEOVIA Surpac™ software. The nugget components of the variogram models were interpreted from constructing downhole variograms.

The experimental and modelled variograms are shown in Figure 8-11.

The parameters of the variogram models are given in Table 8-12.

Table 8-11: Variogram model parameters

Model	Parameters		Au	Bulk Density
Au0.1ppm	Principal directions of anisotropy (plunge ≥ azimuth, negative plunge is down)	Major (U)	56 ≥ 267	-53 ≥ 342
		Semi-Major (V)	0 ≥ 177	0 ≥72
		Minor (W)	34 ≥ 87	-37 ≥ 162
	Nugget		0.18	0.01
	Sill		0.29	0.01
	Ranges (U/V/W) of first structure (m)		20/20/20	80/63/63

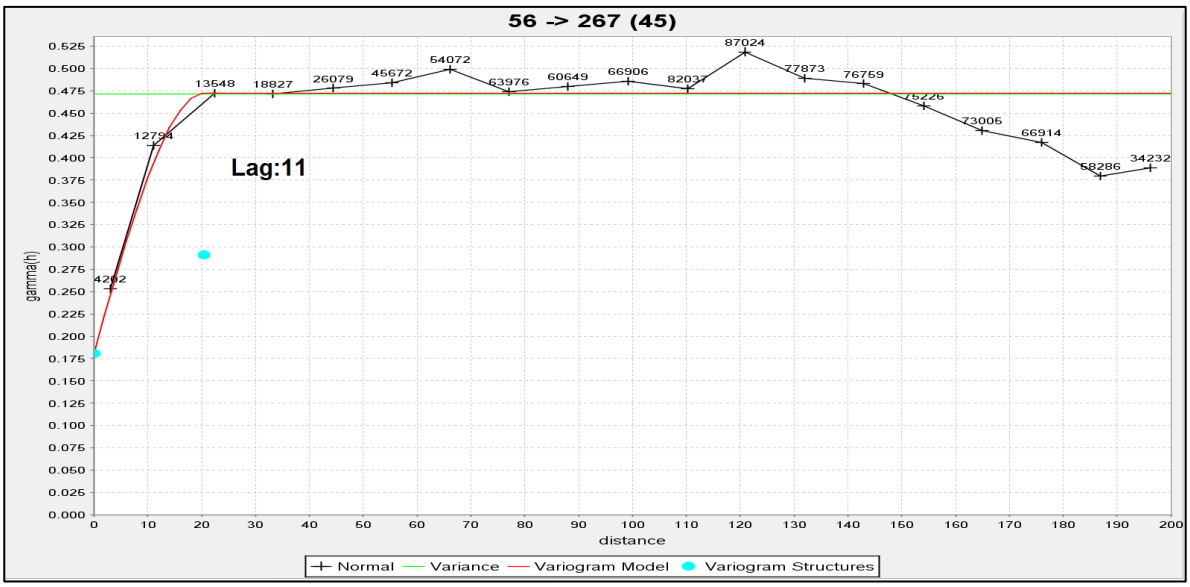

Figure 8-11: Primary direction variograms for gold

8.4.7 Block Model

The dimensions of the block model framework are given in Table 8-13. Standard sub-blocking was used and the block model was not rotated. The block size was chosen as a best fit between the drill spacing and the mining selectivity assuming an open cut mining scenario that also provides a reasonable estimation quality. Qualitative kriging neighbourhood analysis (QKNA) was not used.

Table 8-12: Block model dimensions

	Y	X	Z
Minimum	5485100	675000	550
Maximum	5485600	675600	1150
Block size	10	10	5
Sub-block size	2.5	2.5	1.25
Number of blocks	50	60	120

8.4.8 Ordinary Kriging

For blocks within the mineralised domain, block grades and densities were estimated by Ordinary Kriging (OK). The kriging neighbourhood parameters are given in Table 8-14. Kriging was done in one pass for gold.

Table 8-13: Kriging neighbourhood parameters

Domain	Parameters		Au	Bulk Density
Au0.1ppm	Search directions (plunge ≥ azimuth, negative plunge is down)	Major (U)	56 ≥ 267	-53 ≥ 342
		Semi-major (V)	0 ≥ 177	0 ≥ 72
		Minor (W)	34 ≥ 87	-37 ≥ 162
	Search distance (m)	Major (U)	200	200
		Semi-major (V)	200	158
		Minor (W)	200	158
	Major/Semi-major	U/V	1	1.26
	Major/Minor	U/W	1	1.26
	Bearing	(degrees)	267	342
	Plunge	(degrees)	56	-53
	Dip	(degrees)	0	0
	Minimum number of samples		2	2
	Maximum number of samples		15	15

8.4.9 Validation

The statistics at zero cut-off for the estimated block grades are compared to the composites in Table 8-15. Overall, SRK considers that the mean grades at zero cut-off of the model are acceptably close to the mean grades from the input data.

Table 8-14: Statistics for estimated block grades vs composites at zero cut off

Domain	2 m composites grade (ppm Au)	Block estimate grade (ppm Au)	Variance
Au01ppm	0.53	0.48	-10%

The model was also validated visually in 3D, using Surpac™ and Leapfrog™ software to compare the block estimates against the composites, drill data and wireframes.

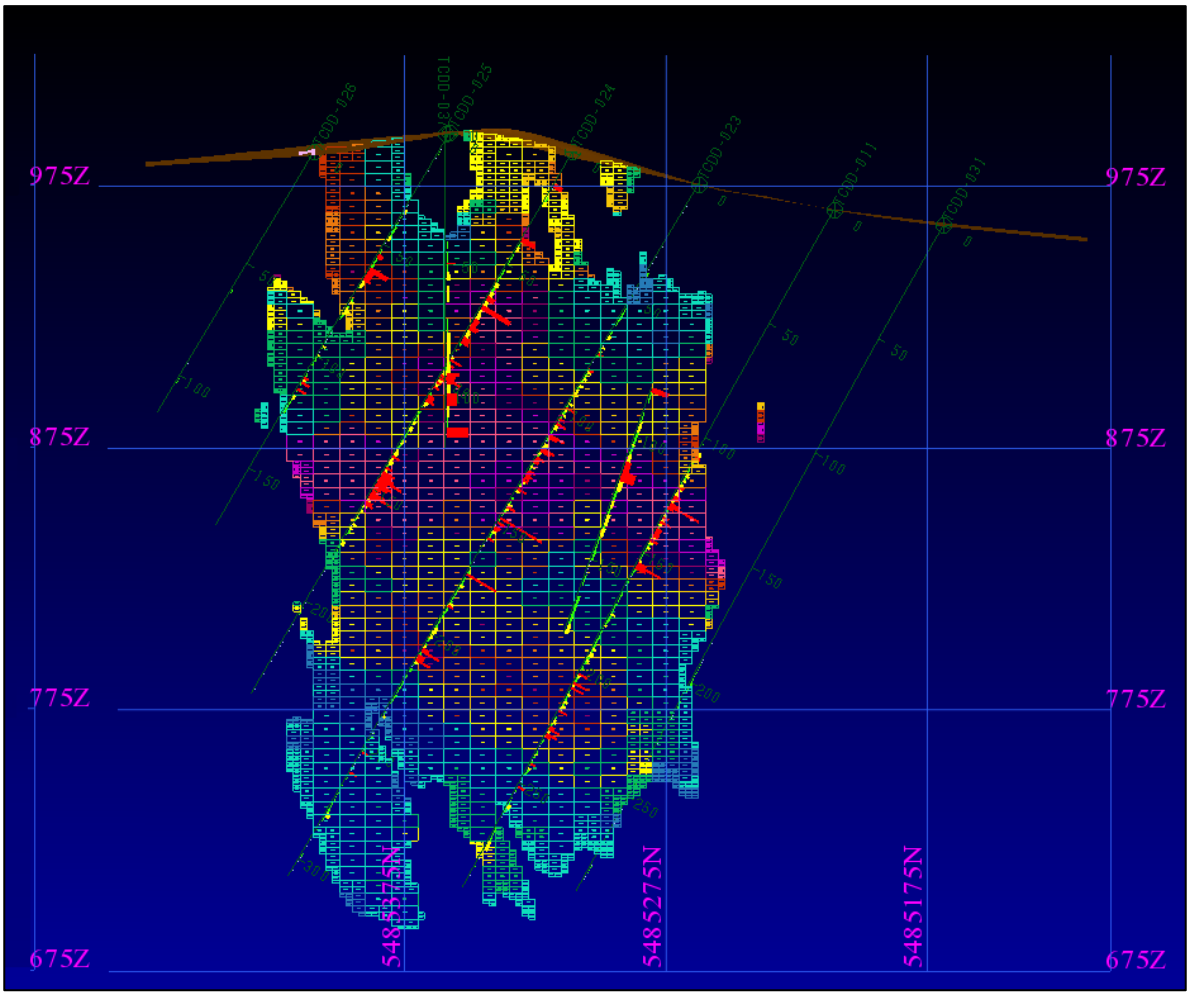

Figure 8-12: Section 5 with sample and block grades

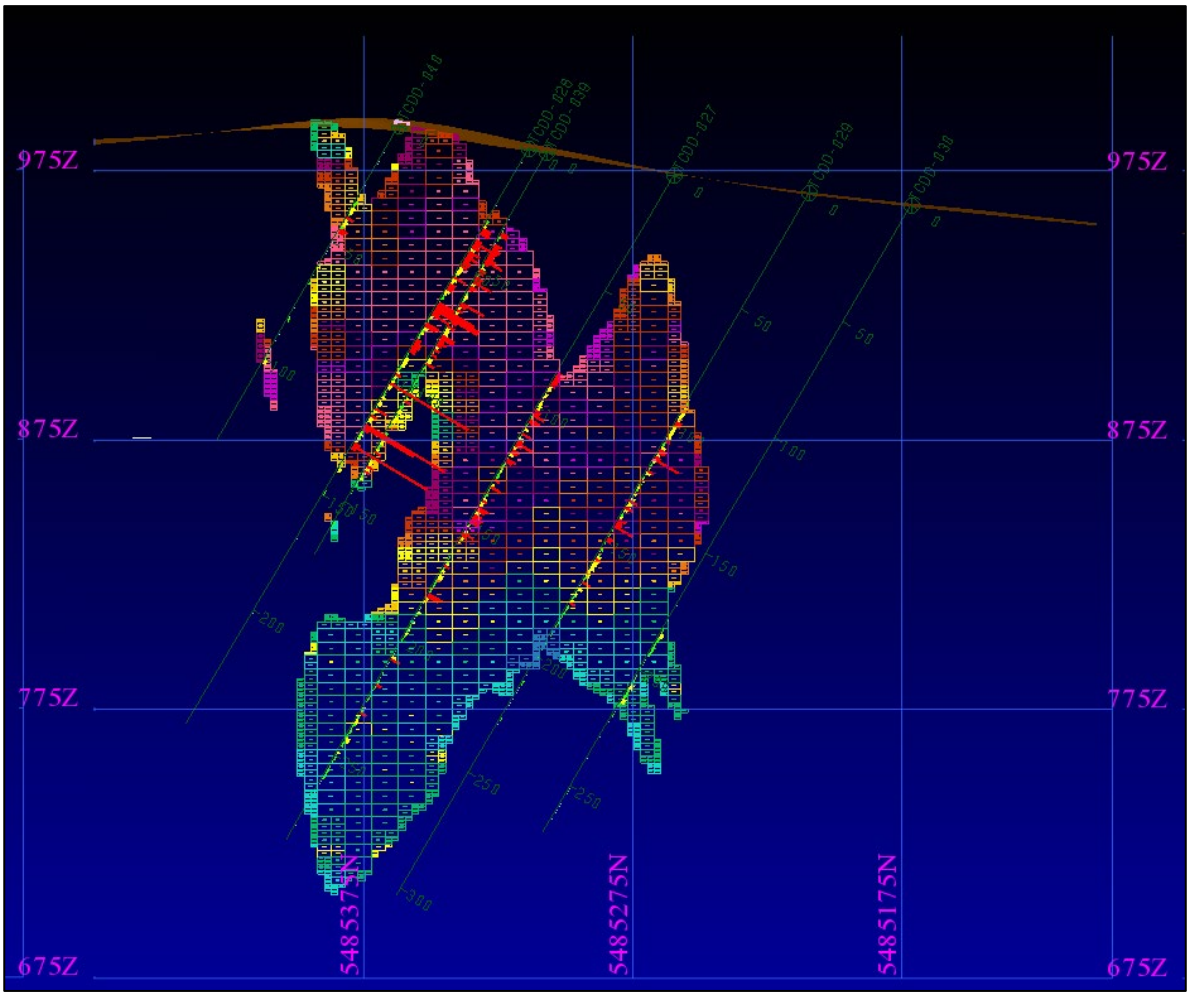

Figure 8-13: Section 6 with sample and block grades

8.4.10 Density Estimate

As discussed in Section 7.9, SRK checked the density data and opines that data within the interval between 1.5 t/m^3 and 3 t/m^3 are reliable, and only density values in this interval were used for modelling. Density was interpolated into the block model using OK. Density values were estimated into 10 × 10 × 5 m parent cells.

8.4.11 Grade-tonnage results

From the block model, the grade-tonnage results were calculated for a series of cut-off grades (Table 8-16). The curves show that deposit tonnage is sensitive to cut-off grade, which is demonstrated by steep decrease of tonnage with increasing grade up to a cut-off grade of 2 g/t.

Table 8-15: Grade-tonnage results

Cut-off grade (g/t Au)	Volume (m^3 `000)	Tonnes (kt)	Average grade (g/t Au)	Contained Metal	
				(koz)	(t)
0.1	12,816.7	32,082.0	0.48	495.11	15.40
0.2	11,203.9	28,888.2	0.52	467.93	15.02
0.3	8,006.7	21,547.0	0.61	409.42	13.14
0.4	5,623.1	15,162.9	0.72	329.80	10.92
0.5	4,192.6	11,332.6	0.81	295.13	9.18

Cut-off grade (g/t Au)	Volume (m^3 `000)	Tonnes (kt)	Average grade (g/t Au)	Contained Metal	
				(koz)	(t)
0.6	3,164.3	8,564.3	0.9	247.82	7.71
0.7	2,434.4	6,594.9	0.98	207.79	6.46
0.8	1,742.2	4,725.9	1.07	162.58	5.06
0.9	1,245.3	3,378.6	1.16	126.01	3.92
1	871.7	2,364.4	1.26	95.78	2.98
1.1	534.1	1,454.5	1.39	65.00	2.02
1.2	374.1	1,017.5	1.5	49.07	1.53
1.3	251.0	682.0	1.63	35.74	1.11
1.4	183.8	498.1	1.73	27.70	0.86
1.5	142.7	387.5	1.82	22.68	0.71
1.6	102.1	277.6	1.93	17.23	0.54
1.7	71.0	193.3	2.05	12.74	0.40
1.8	51.8	141.3	2.17	9.86	0.31
1.9	38.9	105.9	2.28	7.77	0.24
2	30.7	83.7	2.37	6.38	0.20

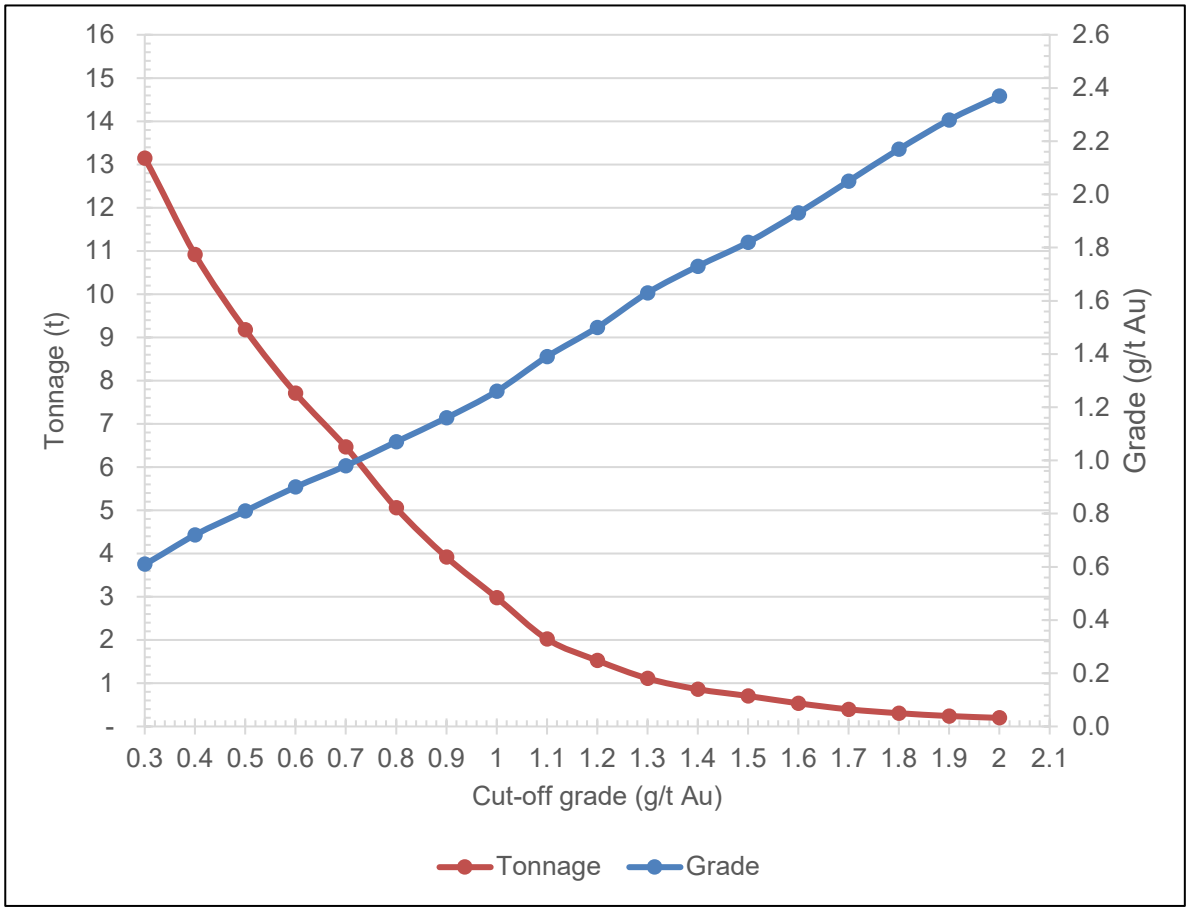

Figure 8-14: Grade vs tonnage curve – gold

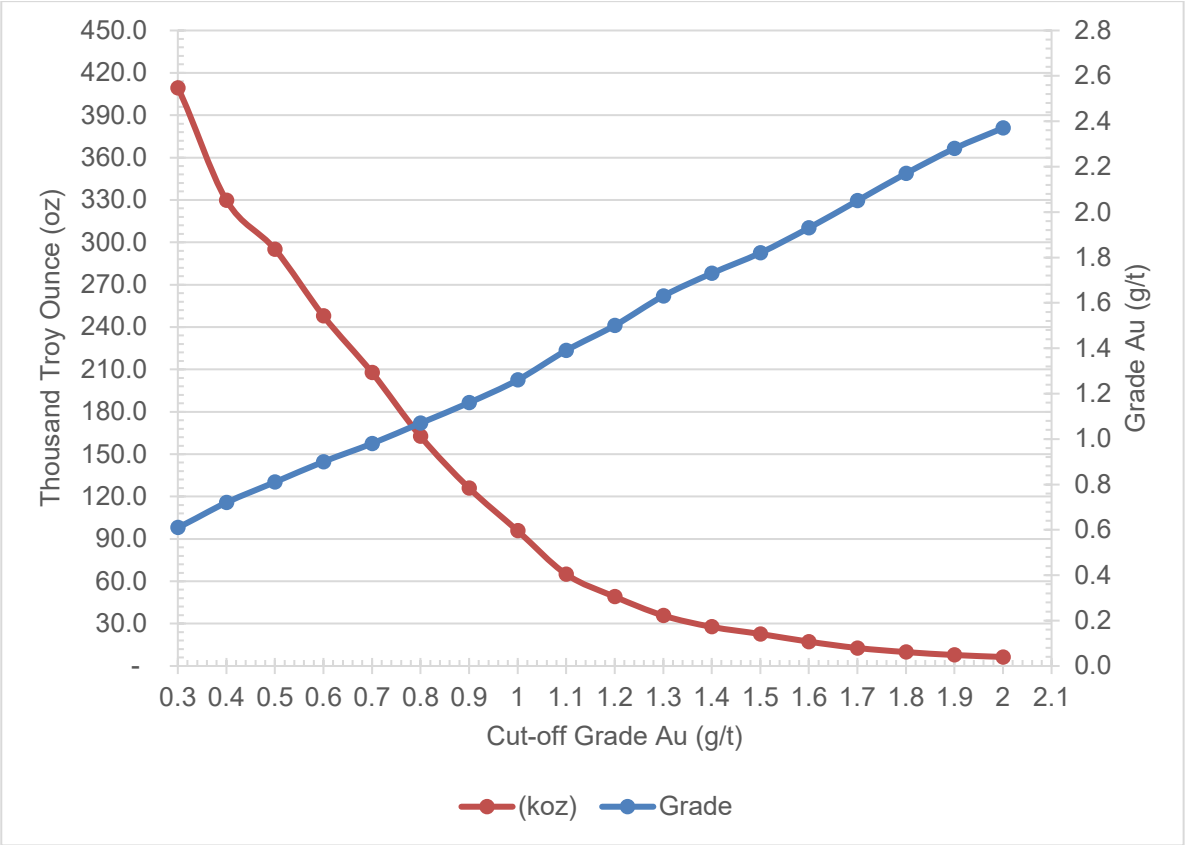

Figure 8-15: Grade vs troy ounces curve – gold

8.4.12 Verification estimate categories

Estimated blocks were classified based on criteria derived from variography. The principal criterion for assigning the Mineral Resource classification was the maximum drill hole spacing compared with the gold variogram range.

Classification was based on the following criteria:

- In the block between 675250E and 675440E, where the closer-spaced drilling exists, the Mineral Resources inside the 0.1 ppm Au domains and above elevation of 750 m above sea level were classified as Indicated.
- In the block outside the 675250E-675440E where drilling is sparser, the Mineral Resources inside the 0.1 ppm Au domains were classified as Inferred.

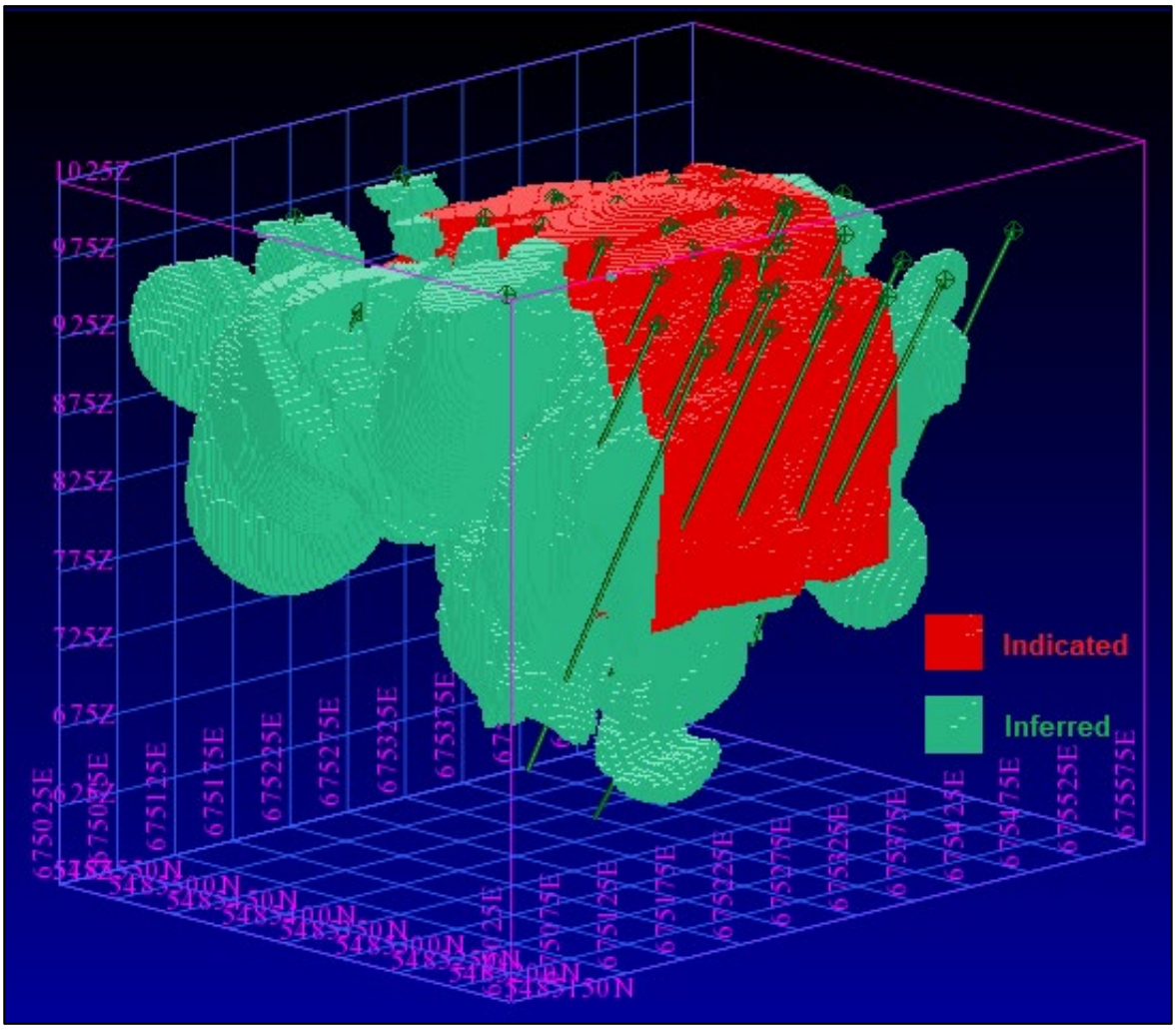

Figure 8-16: Mineral Resource Classification (view from southwest)

8.4.13 Tsagaan Chuluut Project Verification estimate

In order to assess the reasonable prospects of eventual economic extraction, SRK applied following assumptions:

- Mining cost (open pit mining): US$2.5/t
- Processing cost (gravity/flotation): US$13/t
- Gold price: US$38.5/g
- Processing yield: 82%.

While SRK agrees with RPM's conclusion that water supply for processing is key factor of project viability and further hydrogeology and hydrology studies are needed, SRK noted that gold placer mines operating on adjacent licences use water from local streams on both sides of the Tsagaan Chuluut licence (Figure 3-2). SRK made an assumption that water supply can be sourced from nearby properties.

The Mineral Resource estimate for the Tsagaan Chuluut deposit is reported at a cut-off grade of 0.4 ppm Au.

Cut-offs were calculated for the block model using the following formula:

Cut-off = Processing cost (US$/t ore)/(Recovery * gold price (US$/g))

0.4 ppm Au = (US$13/t ore)/(82% * US$38.5/g))

The results of the Tsagaan Chuluut verification estimate are shown in Table 8-17.

Table 8-16: Tsagaan Chuluut verification estimate as at May 2020

Category	Au cut-off grade (g/t)	Volume (km^3)	Tonnes (kt)	Average Grade Au (g/t)	Contained Au	
					(koz)	(t)
Indicated	0.4	4,556.5	12,278.5	0.73	298.83	9.00
Inferred		1,053.5	2,847.3	0.69	65.10	1.96
Total		**5,610.0**	**15,125.8**		**363.93**	**10.96**

A comparison between the 2014 RPM estimate and 2020 SRK estimate is shown in Table 8-18. The difference between the two models can be explained as follows:

- The structural control interpretation of the SRK model (a more steeply dipping fault and hydrothermal breccia control) is different to the RPM model (gently dipping breccia and quartz vein control).
- The cut-off for modelling wireframes is 0.5 ppm Au in the RPM model and 0.1 ppm Au in the SRK model.
- Density used in RPM model is unconstrained and ranges from 0.84 t/m^3 to 92.61 t/m^3, which SRK considered incorrect; SRK applied constraints from1.5 t/m^3 to 3.0 t/m^3.

SRK used a 0.1 ppm Au grade cut-off, which captures all mineralised intervals and prevents false continuation of high-grade intervals. The result is an increased volume and a decreased average grade for the modelled mineralisation in the SRK model.

The tonnage difference is due to a combination of different volume and constraints applied to the density data by SRK. SRK removed density values below 1.5 t/m^3 and above 3.0 t/m^3 from the database on the basis that intrusive rocks of diorite, gabbrodiorite, granodiorite and granite composition are typically within a density range of 2.52–2.98 t/m^3. This leads to decrease of average bulk density from 2.83 t/m^3 (RPM, 2014) to 2.80 t/m^3 (SRK).

In summary, the RPM (2014) model shows, at the same cut-off grade, a lower volume and tonnage, a higher average grade and a lower tonnage of contained gold metal.

Additionally, SRK applied mining and processing assumptions, based on SRK's review of preliminary metallurgical tests and experience from open pit mining in Mongolia, and on this basis, has reported a Mineral Resource above 0.4 ppm Au cut-off grade in comparison with the 0.7 ppm Au cut-off grade used by RPM.

Table 8-17: Comparison between RPM and SRK Mineral Resource estimates

Cut-off grade (g/t Au)	2014 RPM estimate			2020 SRK estimate		
	Average grade (g/t Au)	Contained Metal		Average Grade (g/t Au)	Contained Metal	
		(koz)	(t)		(koz)	(t)
0.40	1.05	224.68	6.68	0.72	329.80	10.92
0.50	1.05	223.78	6.62	0.81	295.13	9.18
0.60	1.07	219.79	6.4	0.90	247.82	7.71
0.70	1.11	208.18	5.84	0.98	207.79	6.46

9 Exploration Upside

SRK opines that the Tsagaan Chuluut Gold Project has significant exploration upside. Based on SRK's assessment of the Project area, several target areas have been highlighted for follow-up investigation. Targeting was based on a combination of geological, geochemical and geophysical vectors and the limited drilling data available and provided by SG.

9.1 Exploration vectors for porphyry-style mineralisation

Several important vectors for porphyry-style mineralisation are summarised below. SRK emphasises that not all vectors could be adequately assessed from the data available.

9.1.1 Geological vectors

- Tectonic setting
- Lithology – quartz diorite porphyry and diorite
- Alteration – prograde (biotite, K-feldspar, magnetite, epidote, actinolite) to retrograde alteration (sericite, clays)
- Fault, veins and breccia styles
- Complex intrusive activity.

9.1.2 Geochemical vectors

- Au ± Cu are moderately mobile proximal to a porphyry source
- Mo, Bi, Te, W, Sn are immobile and good indicators of proximity to a porphyry system and an RIRGS
- Zn ±Pb on the margins of systems.

9.1.3 Geophysical vectors

- Magnetic ing structures
- Gravity lows
- IP –high chargeability associated with phyllic alteration.

9.2 Exploration Potential

RPM (2014) considered the western continuation of the TC1 deposit to be an Exploration Target and estimated a range for grade and tonnage. In addition to this TC1 West target, RPM (2014) reported quartz-sulphide mineralisation of lesser intensities in the Altan Chuluut area, exposed in marmot holes and hand-dug trenches. One DD and 10 RC holes have been drilled at this target and intercepted an interval of 80 m grading at 0.47 g/t Au. A grade and tonnage summary of both Exploration Targets is provided in Table 9-1.

Table 9-1: RPM exploration target areas

TC1 West		
	Low Grade	**High Grade**
Tonnage (Mt)	18.5	8.5
Grade (g/t Au)	0.5	1.5
Au (t)	10	13
Altan Tsagaan Chuluut		
	Low Grade	**High Grade**
Volume of Target Model (Mm^3)	11.5	11.5
Proportion Mineralised	Two Thirds	One Third
Volume of Target Model Mineralised (Mm^3)	7.6	3.8
Density	2.83	2.83
Tonnage of Target Model Mineralised (Mt)	21.7	10.8
Grade (g/t Au)	0.5	2.5
Au (t)	11	27

SRK opines that further work is needed to refine both Exploration Targets identified by RPM.

SRK interpretations of the Project area have highlighted a strong regional northwest-striking control to the mineral potential from the Tsagaan Chuluut Fault (Figure 4-3 and Figure 4-4) and subparallel subordinate faults as well as the related east–west faults and breccia zones. Zones of intersecting northeast-striking structures are additionally considered to be important structural features to the mineral potential. Gold mineralisation is primarily hosted within a diorite intrusion (Table 6-6) as well as hydrothermal breccias (Table 6-5). Quartz and quartz-sulphide veins additionally provide an indication of gold mineralisation and potentially indicate higher-grade zones. Preliminary interpretations of potassic, phyllic and argillic alteration indicate potential target zones. Propylitic alteration is considered as a marker for the more distal parts of the mineralised system. A combination of these vectors/exploration criteria were used for identifying targets for this high-level mineral potential analysis, for follow-up investigation. This is discussed in more detail below.

9.3 Exploration Potential Mapping

In order to identify areas with potential for porphyry-style mineralisation within the Project area and surrounds, the tectonic, alteration, geochemical, chargeability and resistivity data were used as potential vectors/exploration criteria for mineralisation within the area. The relative importance of each of these exploration criteria to the mineralisation potential was then ranked from 1 to 2, with 2 being the highest. Each of these exploration criteria and applied rank (weighting) are summarised in Table 9-2 , with examples presented in Figure 9-1. From these exploration criteria, a map of exploration potential was created by applying the Spatial Analyst toolbox in ArcGIS™. This map was derived as the product of each of the weights of the exploration criteria. This process effectively identifies areas of coincident favourable exploration criteria. Areas with highest mineral potential are identified as areas in the warmer colours in Figure 9-2.

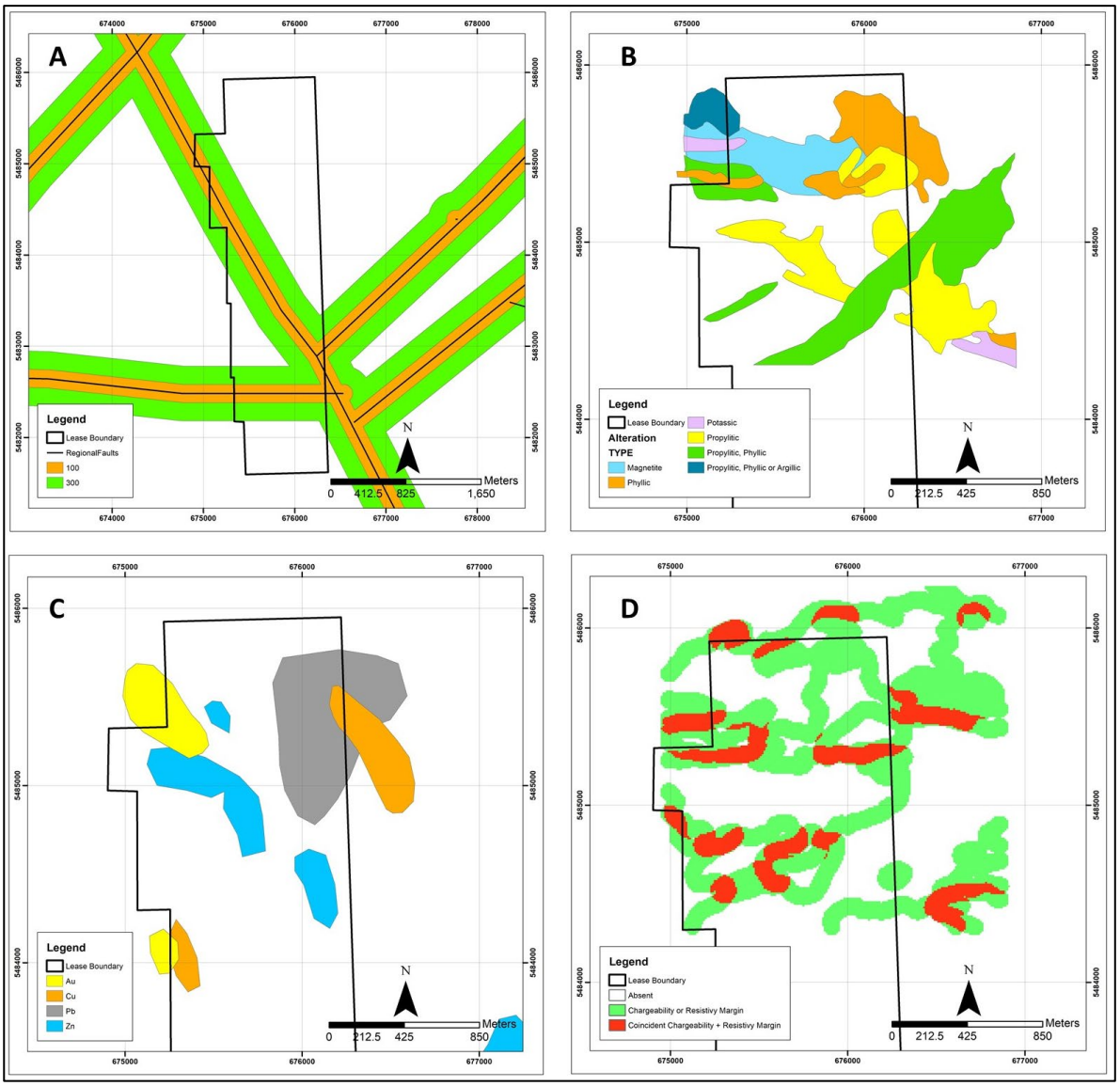

Figure 9-1: Example exploration criteria used in mineral potential mapping: A) proximity to regional faults, B) alteration style, C) surface geochemical signature, D) chargeability and/or resistivity margin

Table 9-2: Exploration criteria and applied weight

Exploration Criteria		Weight
Proximity to local faults	50 m	2
Proximity to regional faults	100 m	2
	300 m	1
Favourable lithological host		1
Induced polarity	Resistivity margin	1
	Chargeability margin	1
	Coincident IP margin	2
Magnetic signature	Demagnetised zone	1
Favourable Alteration	Magnetite	1
	Phyllic	2
	Potassic	1
	Propylitic	1
	Propylitic, phyllic	1
	Propylitic, phyllic or argillic	1
Breccia	Hydrothermal	2
	Intrusive	1
Presence of quartz veining		2
Geochemical signature	Gold	2
	Copper	1
	Lead	1
	Zinc	1

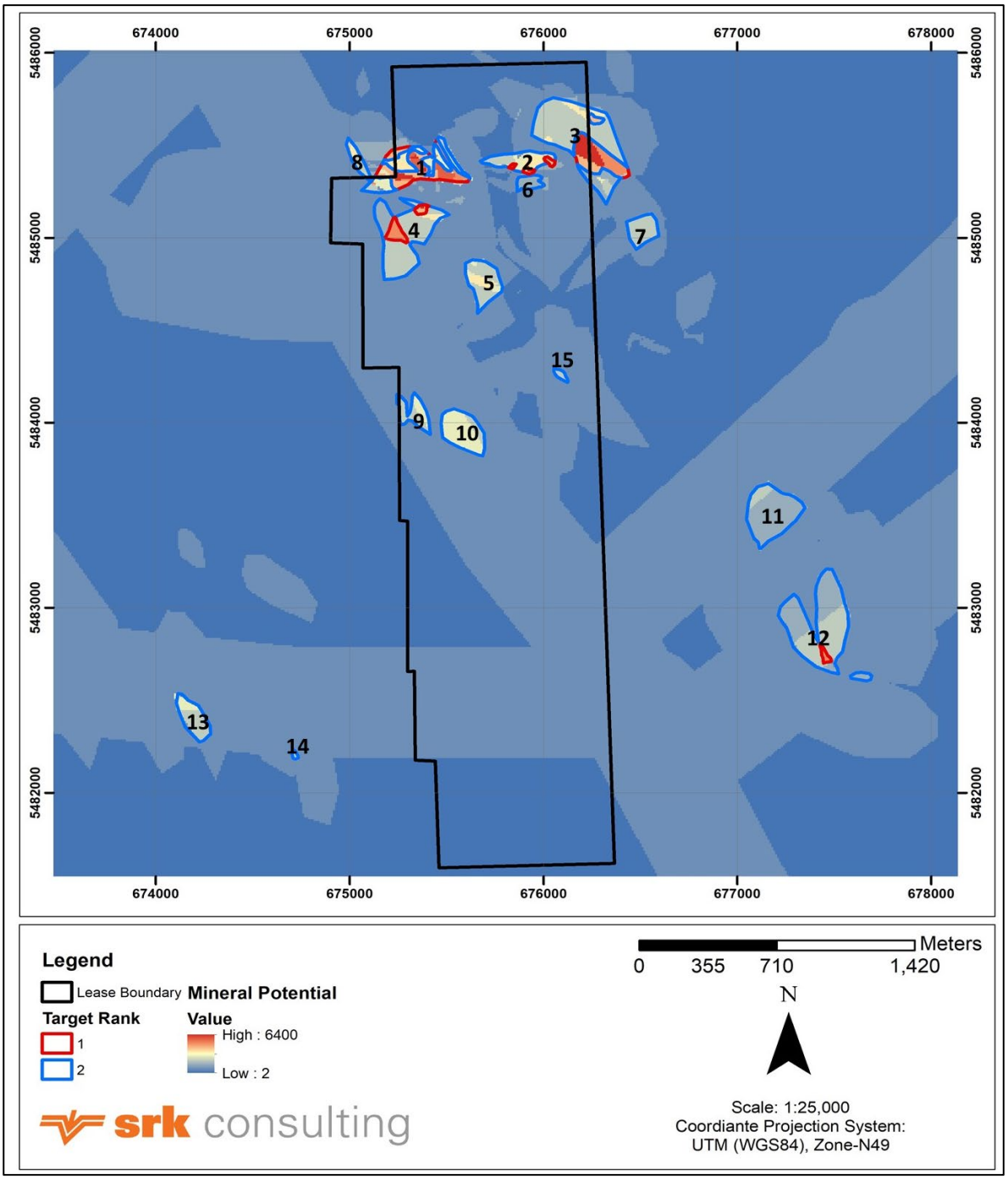

Figure 9-2: Map showing mineral potential at Tsagaan Chuluut

Areas within the north of the licence show the highest mineral favourability, while areas to the south and outside of the lease extents have lower mineral favourability. It should be noted that data coverage is not the same over whole licence and surrounding area, and this is likely to have contributed to a lowering of mineralisation favourability for this review.

Notably, high priority targets 1 and 4 are located on the flanks of TC1 and RPM target TC1 West and are considered direct extension of current Mineral Resource at TC1. High priority targets 2 and 3 are located within Middle–Late Jurassic granodiorite and granite and may represent younger RIRGS mineralisation.

From the mineral potential mapping, a total of 16 target areas considered worthy of follow-up field-based exploration, were identified. Each of these targets has been ranked as a Priority 1 and Priority

2 target, based on the derived mineral favourability within these areas (warmer colours). Each of the coincident exploration criteria observed to occur within each target area is summarised in Table 9-3, indicating the criteria are enclosed within the target area (Y) and defining a partial overlap within that target area (P).

Table 9-3: Exploration Target summary

Target ID	1	2	3	4	5	6	7	8	9	10	11	12	13	14	15
Target rank	1	1	1	1	2	2	2	2	2	2	2	2	2	2	2
Resistivity margin	Y	P	P	P	Y	Y		Y							
Chargeability margin	P	Y	Y	P	P	Y		P							
Demagnetised zone	Y	Y		P											
50 m of local faults	P	Y	P	P	P	Y	P								
Regional faults (100 m)									P	P	P	P	P		
Regional faults (300 m)	P			P				Y			P	P	P	P	
Favourable lithology	Y	P	Y	Y	Y		Y	Y		Y	Y	Y	Y	Y	Y
Favourable alteration	Y	Y	Y		P	Y	Y	Y							
Hydrothermal breccia	P														
Intrusive breccia	P														
Quartz veining	Y	P	P	Y	Y	P	Y		Y	Y					Y
Geochemistry - Gold	P			P				Y	P					Y	
Geochemistry - Copper			P				Y		Y						
Geochemistry - Lead		P	Y		Y										
Geochemistry - Zinc	P			P	Y						Y	P			Y

Targets 1 to 4 are shown to have the highest mineral potential and occurin the northern part of the Project area. Each of these four targets show several overlapping favourable exploration criteria inclusive of proximity to faults, presence of favourable alteration, favourable host lithology, geochemical signatures in soils (e.g. gold, copper, lead or zinc), as well as the presence of quartz veining at surface. Each of these targets occurs at least in part along the margin of a coincident chargeability and resistivity anomaly, which is interpreted to be a favourable indicator for mineralisation.

Targets 5 and 6 show many of these same exploration features, but rank slightly lower based on the derived maps, with fewer overlapping criteria defined.

Targets 9 to 16 lie outside of the extents of the current IP and magnetic datasets and these exploration criteria therefore cannot be applied in these zones. These targets do show favourable geochemistry, lithological host and structural features, highlighting their potential.

Targets tends to cluster in the northern sector of the licence and continue over the licence boundary to the west and east as shown on Figure 9-3 and Figure 9-4.

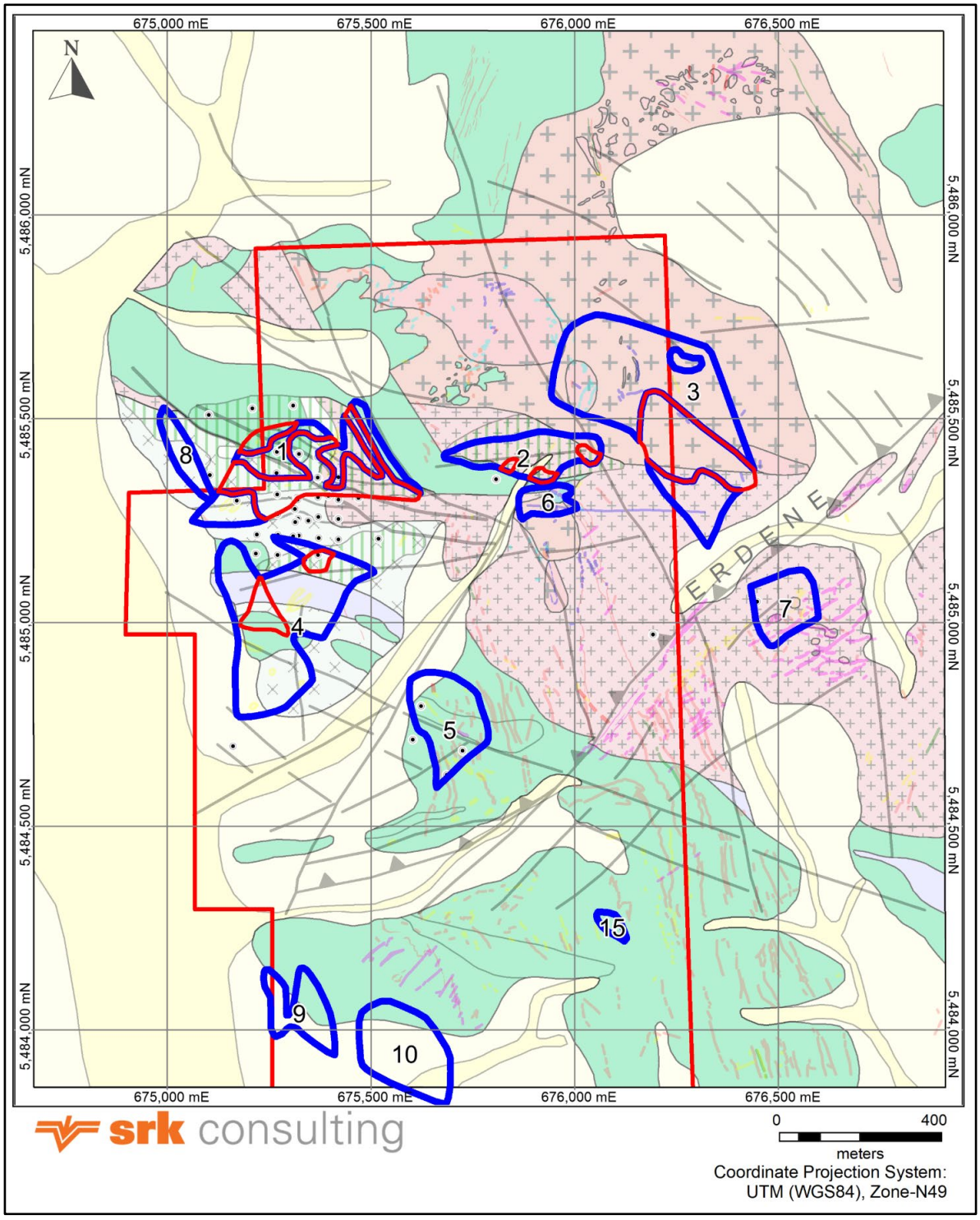

Figure 9-3: Geology map of Project area with exploration targets draped

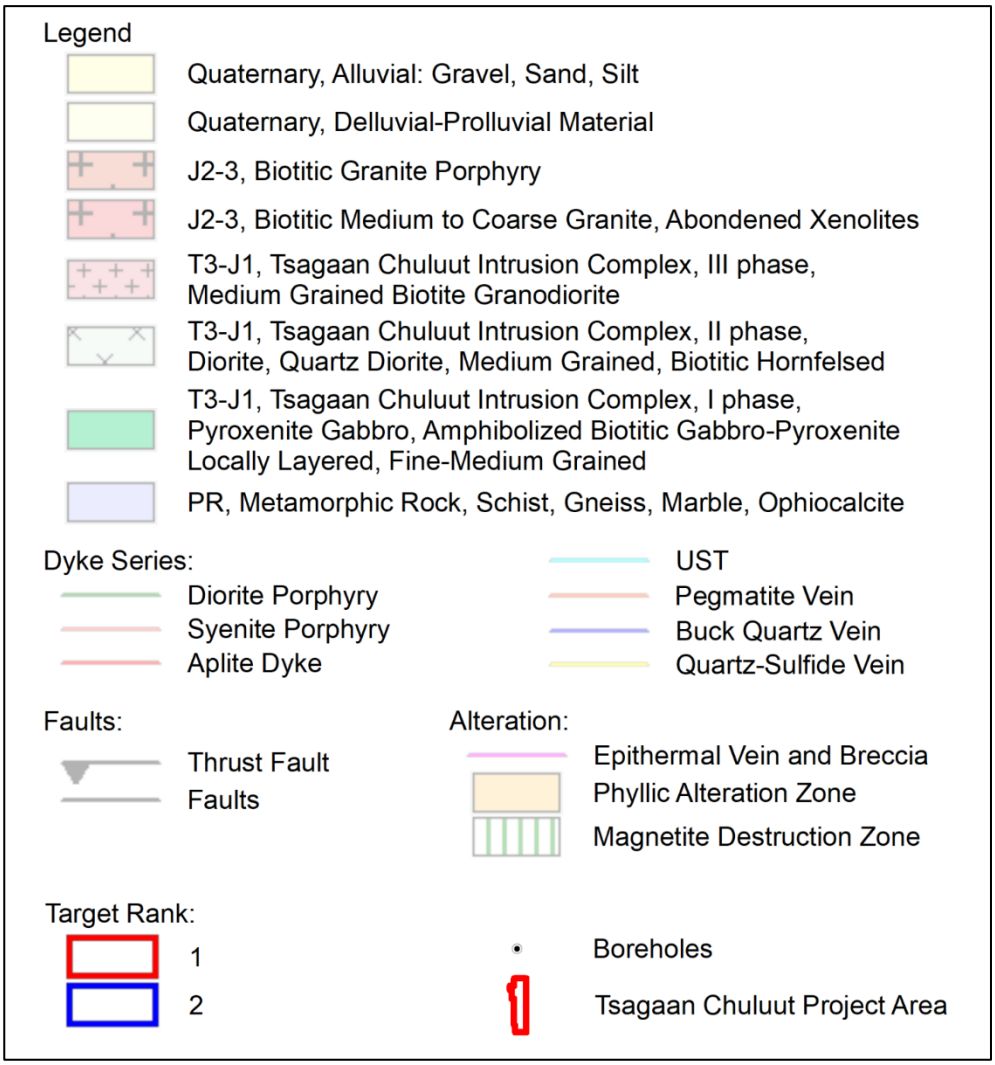

Figure 9-4: Legend to geology map of Project area with exploration targets draped

10 Conclusions and Recommendations

The Tsagaan Chuluut is an advanced exploration project with an identified Indicated and Inferred Mineral Resources. SRK estimated an Indicated Mineral Resource of 12,278 kt grading at 0.72 g/t Au, containing 8.84 t of gold metal (293.8 koz) and an Inferred Mineral Resource of 2,847 kt grading at 0.69 g/t Au, containing 1.96 t of gold metal (65.26 koz). The Total Mineral Resource is 15,125 kt containing 10.81 t of gold metal (358.94 koz). The TC1 deposit remains open along the flanks.

In addition to the Mineral Resource, SRK identified an additional 15 exploration targets which warrant further evaluation.

SRK makes the following recommendations:

TC1 – High-grade test drilling

- Conduct an two phase infill fully cored drilling program aimed at testing potential high-grade structures/ zones, with target drilling depths of 135 m to 250 m from a 6,360 m drill program. Drill holes should be oriented.
- Conduct a structural study of the new drill core and across the broader TC1 surface area.
- Log the additional drill holes by infrared spectrometry in order to identify alteration minerals and better define zones of alteration.
- Conduct additional petrology studies from drill hole samples in the high-grade zones.

Table 10-1: Proposed infill drilling – Phase 1

Borehole ID	X	Y	Z	Designed Depth (m)	Azimuth (°)	Dip (°)
DDH20_001	675443.17	5485310.29	982.14	140	0	60
DDH20_002	675441.93	5485282.07	977.60	190	0	60
DDH20_003	675418.67	5485282.60	978.39	150	0	60
DDH20_004	675421.51	5485326.63	986.42	135	0	60
DDH20_005	675396.83	5485331.60	990.23	155	0	60
DDH20_006	675396.30	5485308.16	984.83	180	0	60
DDH20_007	675395.59	5485285.80	980.35	185	0	60
DDH20_008	675396.30	5485259.52	974.74	225	0	60
DDH20_009	675370.02	5485287.22	982.65	205	0	60
DDH20_010	675368.60	5485336.58	994.73	155	0	60
DDH20_011	675342.68	5485333.03	998.25	180	0	60
DDH20_012	675344.46	5485306.03	989.82	220	0	60
DDH20_013	675345.17	5485282.25	981.81	240	0	60
DDH20_014	675323.14	5485284.02	980.71	240	0	60
DDH20_015	675318.89	5485332.32	995.63	200	0	60
DDH20_016	675293.67	5485339.77	990.41	200	0	60
Total				**3,000**		

Table 10-2: Proposed infill drilling – Phase 2

Borehole ID	X	Y	Z	Designed Depth (m)	Azimuth (°)	Dip (°)
DDH20_017	675444.00	5485257.00	973.65	200	0	60
DDH20_018	675444.00	5485233.00	970.38	200	0	60
DDH20_019	675419.38	5485233.60	970.27	200	0	60
DDH20_020	675395.23	5485236.80	970.57	210	0	60
DDH20_021	675372.15	5485239.64	971.33	250	0	60
DDH20_022	675293.67	5485288.28	979.65	240	0	60
DDH20_023	675294.73	5485311.72	985.92	200	0	60
DDH20_024	675294.73	5485363.92	989.09	185	0	60
DDH20_025	675314.98	5485376.70	989.26	135	0	60
DDH20_026	675266.68	5485389.49	984.69	155	0	60
DDH20_027	675268.46	5485344.74	986.92	210	0	60
DDH20_028	675269.88	5485293.60	977.73	200	0	60
DDH20_029	675241.12	5485293.25	974.83	200	0	60
DDH20_030	675243.25	5485318.11	980.60	230	0	60
DDH20_031	675245.37	5485346.51	984.84	200	0	60
DDH20_032	675246.80	5485369.60	985.01	180	0	60
DDH20_033	675243.96	5485387.71	983.56	165	0	60
Total (m)				**3,360**		

Exploration Targets

- Conduct alteration mapping of the targets.
- Carry out dating of intrusive rocks, whole-rock analyses and inductively coupled plasma-mass spectrometry (ICP-MS) geochemical and rare earth element (REE) analysis to improve understanding of intrusive events, magma composition and classification and understanding of geotectonic affinity.
- Conduct structural geology mapping.
- Based on the alteration and structural mapping, and intrusive rock studies, re-evaluate the current exploration targets and design a scout drilling program.
- Apply for (or acquire as required) additional exploration tenure on the western and eastern flanks of the Project to extend coverage over currently defined exploration targets.

Compiled by

Petr Osvald

Principal Consultant

Peer reviewed by

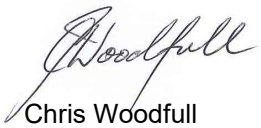

Chris Woodfull

Corporate Consultant

11 References

Badarch, G, Cunningham, D and Windley, B F, 2002. A new terrane subdivision for Mongolia: Implications for the Phanerozoic crustal growth of Central Asia, Journal of Asian Earth Sciences, 21, 87–110.

Bat-Erdene, G, Enkhbayar and Arvinzen, 2006. Report of 2006 geological exploration work conducted at the Tsagaan Chuluut-3 area located in the territory of Bayandun Soum, Dornod Province, report prepared for Troy Mongolia Gold Resources LLC (MRAM Exploration Report).

Batulzi, 2005. Petrology study on Tsagaan Chuluut Project.

Bibikova, E V, Gracheva, T V, Makarov, V A and Vorobjev, V S,1979. Geochronological borders for the southern part of the East Transbaikalia from data of U-Pb method of dating, Geochemistry 2, 204–215 (in Russian).

Bond, W F, Jenkin, G R T and Godfrey, M, 2013. Constraining a mineralisation model of the SG Mining, Tsagaan Chuluut gold deposit, Mongolia – A petrographical and geochemical study.

Bussien, D, Gombojav, N, Winkler, W and von Quadt, A, 2011. The Mongol–Okhotsk Belt in Mongolia — An appraisal of the geodynamic development by the study of sandstone provenance and detrital zircons, Tectonophysics, 510: 132-150.

Corbett, G, 2018. Chapter 4 – Breccia in single page, Short Course Manual.

Ganbaatar, l. et al., 1991. Open file report No. 4489 geological mapping was carried out M-49-95-Б,Г sheet, Dornod, Mongolia into scale 1: 50,000, Ulaanbaatar, Geological Information Center of Mineral Resources Authority of Mongolia.

Gekko Systems, 2013. T0978-Mongolian Metal Mining Holding LLC Python Amenability Testwork.

Hart, C J R and Goldfarb, R J. Distinguishing intrusion-related from orogenic gold systems, Proceedings of Scientific Conference in Minerals, New Zealand [online]. Available from: <http://www.nzpam.govt.nz/cms/pdf-library/minerals/conferences-1/125_papers_48.pdf.

Hart, C J R, 2005. Classifying, Distinguishing and Exploring for Intrusion-Related Gold Systems, The Gangue, 87: 1–18.

Hart, C J R, Baker, T and Burke, M, 2000. New exploration concepts for country-rock hosted, intrusion-related gold systems, Tintina Gold Belt, British Columbia and Yukon Chamber of Mines, Special Volume 2, 145–172.

Hart, C J R, McCoy, D, Goldfarb, R J, Smith, M, Roberts, P, Hulstein, R, Bakke, A A and Bundtzen, T K, 2002. Geology, exploration and discovery in the Tintina gold province, Alaska and Yukon, Society of Economic Geologists, Special Publication, 9, 241–274.

Hepta, 2013. Metallurgical testwork report on Tsagaan Chuluut.

Hutchison, N, 2002. TCH-NE Mongolia, Diamond Drill Program Report, Troy Mongolia Alt Resources, Internal Memorandum.

Kryazhev, S G, Grinenko, V A and Ustinov, V I, 2009. Possible Reasons for the Compositional Evolution of Ore-Forming Fluids at the Berezovskoe Gold Deposit, Central Urals, Geochemistry International, 2011, 49: 95–100.

Mazukabzov, A M, Donskaya, T V, Gladkochub, D P, Paderin, I P, 2010. The Late Palaeozoic geodynamics of the West Transbaikalian segment of the Central Asian fold belt, Russian Geology and Geophysics 51, 482–491.

Micromine, 2012. JORC Compliant Resource Estimation for Tsagaan Chuluut Gold Project – Mongolia.

Minarco Mine Consultants, 2011. Tsagaan Chuluut Gold Project, Mongolia. Stage 1. Geological Review Letter.

Mossakovsky, A A, Ruzhentsev, S V, Samygin, S G, Kheraskova, T N, 1993. The Central-Asian fold belt: geodynamic evolution and formation history, Geotectonics 27, 3–32.

Murao, S, Dorjgotov, D and Tseden, T, 1998. K–Ar dating of granitoids and hydrothermal micas from the northern part of Kherlen Depression, Mongolia, Bulletin Geological Survey of Japan, 49: 249–255.

Parfenov, L M, Berzin, N A, Badarch, G, Belichenko, V G, Bulgatov, A N, Dril, S I, Khanchuk, A I, Kirillova, G L, Kuz'min, M I, Nokleberg, W J, Ogasawara, M, Obolenskiy, A A, Prokopiev A V, Rodionov, S M, Scotese, C R, Timofeev, V F, Tomurtogoo, O and Yan, H, 2010. Tectonic and Metallogenic Model for Northeast Asia, in Metallogenesis and Tectonics of Northeast Asia (ed: W J Nockleberg), U S Geological Survey Professional Paper 1765, 9-1–9-55.

Rudnick, R L and Gao, S, 2014 (revision of Rudnick, R L and Gao, S, 2003). The Composition of the Continental Crust, *Treatise on Geochemistry Vol. 3: 1–64* (Elsevier).

Runge Pincock Minarco Ltd, 2014. TC JORC Report.

SGS, 2013. Flotation and bioleach testwork for gold recovery.

Sillitoe, R, 2000. Gold-rich porphyry deposits: descriptive and genetic model and their role in exploration and discovery, Society Economic Geology Reviews, Vol 13: 315–345.

Xiao, W, Windley, B F, Hao, J, Zhai, M, 2003. Accretion leading to collision and the Permian Solonker suture, Inner Mongolia, China: Termination of the central Asian orogenic belt, Tectonics 22 (6), 1069.

Yantai Xinhai Institute, 2013. Gold ore beneficiation test report.

Zorin, Y A, Zorina, L D, Spiridonov, A M and Rutshtein, I G, 2001. Geodynamic setting of gold deposits in Eastern and Central Trans-Baikal (Chita Region, Russia), Ore Geology Reviews, 17: 215–232.

Appendices

Appendix A: Mining Licence Copy

АШИГТ МАЛТМАЛЫН ГАЗАР

АШИГТ МАЛТМАЛ АШИГЛААЛТЫН ТУСГАЙ

ЗӨВШӨӨРӨЛ

Дугаар 15436А

Ашигт малтмалын тухай Монгол улсын хуулийн 26 дугаар зүйлийг үндэслэн

Дорнод **аймаг /хот/-ийн**

Баяндун **сум /дүүрэг/-ын**

Цагаан чулуут-1 **нэртэй газарт орших**

457.29 **гектар талбай бүхий уурхайн талбайд хуульд заасан нохцол, шаардлагын дагуу ашигт малтмал ашиглахыг зөвшөөрч улсын бүртгэлийн** *9011008070* **тоот гэрчилгээтэй**

... Эс Жи Трэйд ... ХХК **-д**

энэхүү тусгай зөвшөөрлийг *30* **жилийн хугацаагаар олгов.**

Тусгай зөвшөөрөл хавсралттүй бол хүчингүй.

ДАРГА **Д. БАТХУЯГ**

2010 оны 01 сарын 25 өдөр

Улаанбаатар хот

15436А

АШИГТ МАЛТМАЛ АШИГЛАХ . . . . . ТООТ

ТУСГАЙ ЗӨВШӨӨРЛИЙН 1 ДҮГЭЭР ХАВСРАЛТ

(тусгай зөвшөөрөл үл бол хүчингүй)

Тусгай зөвшөөрлөөр талбайн хэмжээ болон тусгай зөвшөөрлийн үзэмшилд орсон өөрчлөлт

д/д	Тусгай зөвшөөролд орох өөрчлөлтийн үндэслэл	Өргөдлийн бүртгэлийн дугаар	Хасагдах талбайн хэмжээ (га-аар)	Үлдсэн талбайн хэмжээ (га-аар)
1.	**Анх олгосон**	**24570А**		**457.29** **2010-01-25**

ТУСГАЙ ЗӨВШӨӨРЛИЙН ГЭРЧИЛГЭЭНИЙ 1 ДҮГЭЭР ХАВСРАЛТ

MV-015436

Тусгай зөвшөөрлийн гэрчилгээгүй бол хүчингүй.

Хөдөлгөөний код	Хөдөлгөөний тайлбар	Гарын үсэг, огноо, тамга
000-CI	• Бүртгэв: Ашигт малтмалын газрын даргын 2010 оны 127 тоот тушаалын дагуу ашигт малтмалын тусгай зөвшөөрлийн талбайн солбицлыг WGS-84 тогтолцоонд албан ёсоор хөрвүүлж талбайн хэмжээг дахин тооцсон.	2010-04-01
003-TF	• Бүртгэв: Тусгай зөвшөөрлийг 9011238018 тоот улсын бүртгэлийн дугаартай Эс Жи майнинг эрдэс ХХК-д шилжүүлэх • ГУУКХ-ийн даргын 2010.05.27-ний 608 тоот шийдвэр	2010-05-27
004-FE	• Бүртгэв: Тусгай зөвшөөрлийн 2 дахь/дэх жилийн төлбөрийг төлөв. Хугацаа 2011.01.25 – 2012.01.25 хүртэл	2011-01-25
005-PL	• Бүртгэв: Тусгай зөвшөөрлийг 9016001003 тоот улсын бүртгэлийн дугаартай Чингисхаан банк ХХК-д барьцаалах • ГУУКХ-ийн даргын 2011.05.05-ний 427 тоот шийдвэр	2011-05-06
006-PE	• Бүртгэв: 9016001003 тоот улсын бүртгэлийн дугаартай Чингисхаан банк Банк-ийн барьцаанаас чөлөөлөх • ГУУКХ-ийн даргын 2011.11.02-ний тоот шийдвэр	2011-11-02
007-FE	• Бүртгэв: Тусгай зөвшөөрлийн 3 дахь/дэх жилийн төлбөрийг төлөв. Хугацаа 2012.01.25 – 2013.01.25 хүртэл	2012-01-19
008-FE	• Бүртгэв: Тусгай зөвшөөрлийн 4 дахь/дэх жилийн төлбөрийг төлөв. Хугацаа 2013.01.25 – 2014.01.25 хүртэл	2012-12-26

ТУСГАЙ ЗӨВШӨӨРЛИЙН ГЭРЧИЛГЭЭНИЙ 1 ДҮГЭЭР ХАВСРАЛТ

MV-015436

Тусгай зөвшөөрлийн гэрчилгээгүй бол хүчингүй.

Дэс дугаар	Тусгай зөвшөөрөлд орох өөрчлөлтийн үндэслэл	Огноо, гарын үсэг, тэмдэг
009-FE	• Бүртгэв: Тусгай зөвшөөрлийн 5 дахь/дэх жилийн төлбөрийг төлөв. Хугацаа 2014.01.25 – 2015.01.25 хүртэл	2013-12-24 01 АМГ КАДАСТРЫН ХЭЛТЭС ХТХ0058
010-FE	• Бүртгэв: Тусгай зөвшөөрлийн 6 дахь/дэх жилийн төлбөрийг төлөв. Хугацаа 2015.01.25 – 2016.01.25 хүртэл	2015-01-12 01 АМГ КАДАСТРЫН ХЭЛТЭС ХТХ0058
011-TF	• Бүртгэв: Тусгай зөвшөөрлийг 9011465066 тоот улсын бүртгэлийн дугаартай Эс Жи Голд Майнинг ХХК-д шилжүүлэх • Кадастрын хэлтсийн даргын 2015.06.12-ны 473 тоот шийдвэр	2015-06-12 КАДАСТРЫН ХЭЛТЭС ХТХ0058
012-FE	• Бүртгэв: Тусгай зөвшөөрлийн 7 дахь/дэх жилийн төлбөрийг төлөв. Хугацаа 2016.01.25 – 2017.01.25 хүртэл	2015-12-16 01 АМГ КАДАСТРЫН ХЭЛТЭС ХТХ0058
013-FE	Бүртгэв: Тусгай зөвшөөрлийн 8 дахь/дэх жилийн төлбөрийг төлөв. Хугацаа 2017.01.25 – 2018.01.25 хүртэл	2017-01-30 1 АМГТГ КАДАСТРЫН ХЭЛТЭС УХА0595
014-FE	• Бүртгэв: Тусгай зөвшөөрлийн 9 дахь/дэх жилийн төлбөрийг төлөв. Хугацаа 2018.01.25 – 2019.01.25 хүртэл	2018-01-24 1 АМГТГ КАДАСТРЫН ХЭЛТЭС УХА0595
015-FE	• Бүртгэв: Тусгай зөвшөөрлийн 10 дахь/дэх жилийн төлбөрийг төлөв. Хугацаа 2019.01.25 – 2020.01.25 хүртэл	2019-01-22 1 АМГТГ КАДАСТРЫН ХЭЛТЭС УХА0595

ТУСГАЙ ЗӨВШӨӨРЛИЙН ГЭРЧИЛГЭЭНИЙ 2 ДУГААР ХАВСРАЛТ

MV-015436

Тусгай зөвшөөрлийн гэрчилгээгүй бол хүчингүй.

Хөдөлгөөний код	Хөдөлгөөний тайлбар	Хүчин төгөлдөр талбайн хэмжээ /га/	Хасагдах талбайн хэмжээ /га/	Тусгай зөвшөөрлийн талбайн солбицлууд, гарын үсэг, огноо, тамга
000-CI	• Ашигт малтмалын газрын даргын 2010 оны 127 тоот тушаалын дагуу ашигт малтмалын тусгай зөвшөөрлийн талбайн солбицлыг WGS-84 тогтолцоонд албан ёсоор хөрвүүлж талбайн хэмжээг дахин тооцсон.	456.68 Га	0 Га	1 113° 26' 2.1" 49° 27' 41.95" 2 113° 25' 17.11" 49° 27' 41.95" 3 113° 25' 17.49" 49° 28' 0.59" 4 113° 25' 12.03" 49° 28' 0.7" 5 113° 25' 12.81" 49° 28' 16.54" 6 113° 25' 10.83" 49° 28' 16.58" 7 113° 25' 12.17" 49° 28' 42.77" 8 113° 25' 10.15" 49° 28' 42.81" 9 113° 25' 11.46" 49° 29' 9.54" 10 113° 25' 2.03" 49° 29' 9.72" 11 113° 25' 3.1" 49° 29' 31.52" 12 113° 24' 54.66" 49° 29' 31.7" 13 113° 24' 55.62" 49° 29' 42.95" 14 113° 25' 12.11" 49° 29' 42.95" 15 113° 25' 12.01" 49° 30' 2.01" 16 113° 26' 1.96" 49° 30' 2.01" 2010-04-01 Э. Заяабат
003-TF	• Тусгай зөвшөөрлийг 9011238018 тоот улсын бүртгэлийн дугаартай Эс Жи майнинг эрдэс ХХК-д шилжүүлэх Шийдвэрийн огноо: 2010.05.27	456.68 Га	0 Га	1 113° 26' 2.1" 49° 27' 41.95" 2 113° 25' 17.11" 49° 27' 41.95" 3 113° 25' 17.49" 49° 28' 0.59" 4 113° 25' 12.03" 49° 28' 0.7" 5 113° 25' 12.81" 49° 28' 16.54" 6 113° 25' 10.83" 49° 28' 16.58" 7 113° 25' 12.17" 49° 28' 42.77" 8 113° 25' 10.15" 49° 28' 42.81" 9 113° 25' 11.46" 49° 29' 9.54" 10 113° 25' 2.03" 49° 29' 9.72" 11 113° 25' 3.1" 49° 29' 31.52" 12 113° 24' 54.66" 49° 29' 31.7" 13 113° 24' 55.62" 49° 29' 42.95" 14 113° 25' 12.11" 49° 29' 42.95" 15 113° 25' 12.01" 49° 30' 2.01" 16 113° 26' 1.96" 49° 30' 2.01" 2010-05-27
011-TF	• Тусгай зөвшөөрлийг 9011465066 тоот улсын бүртгэлийн дугаартай Эс Жи Гоулд Майнинг ХХК-д шилжүүлэх Шийдвэрийн огноо: 2015.06.12	456.68 Га	0 Га	1 113° 26' 2.1" 49° 27' 41.95" 2 113° 25' 17.11" 49° 27' 41.95" 3 113° 25' 17.49" 49° 28' 0.59" 4 113° 25' 12.03" 49° 28' 0.7" 5 113° 25' 12.81" 49° 28' 16.54" 6 113° 25' 10.83" 49° 28' 16.58" 7 113° 25' 12.17" 49° 28' 42.77" 8 113° 25' 10.15" 49° 28' 42.81" 9 113° 25' 11.46" 49° 29' 9.54" 10 113° 25' 2.03" 49° 29' 9.72" 11 113° 25' 3.1" 49° 29' 31.52" 12 113° 24' 54.66" 49° 29' 31.7" 13 113° 24' 55.62" 49° 29' 42.95" 14 113° 25' 12.11" 49° 29' 42.95" 15 113° 25' 12.01" 49° 30' 2.01" 16 113° 26' 1.96" 49° 30' 2.01" 2015-06-12 Д.Мягмарсүрэн

15436А

АШИГТ МАЛТМАЛ АШИГЛАХ . . . . . ТООТ

ТУСГАЙ ЗӨВШӨӨРЛИЙН 2 ДУГААР ХАВСРАЛТ

(тусгай зөвшөөрөлгүй бол хүчингүй)

Тусгай зөвшөөрлөөр олгогдсон талбайн буланчийн цэгүүдийн солбилцлын өөрчлөлтүүд

д/д	Солбицлууд өөрчлөгдөх үндэслэл	Хүчин төгөлдөр солбицлууд											
1.	Талбайн солбицлууд												
	No	град	мин	сек	град	мин	сек	No	град	мин	сек	град	мин	сек
	1	113	25	10	49	30	0	9	113	25	10.05	49	28	40.82
	2	113	25	59.95	49	30	0	10	113	25	8.03	49	28	40.86
	3	113	26	0	49	27	40	11	113	25	9.35	49	29	7.58
	4	113	25	15	49	27	40	12	113	24	59.92	49	29	7.77
	5	113	25	15.39	49	27	58.63	13	113	25	0.99	49	29	29.57
	6	113	25	9.93	49	27	58.74	14	113	24	52.55	49	29	29.75
	7	113	25	10.71	49	28	14.59	15	113	24	53.51	49	29	41
	8	113	25	8.73	49	28	14.63	16	113	25	10	49	29	41

2010-01-25 *Э.Заяабат*

SRK Report Client Distribution Record

Project Number: SMN079

Report Title: Independent Review of Tsagaan Chuluut Gold Project, Mongolia

Date Issued: 16 July 2020

Name/Title	Company
Sodnompil. B, CEO	SG Gold Mining

Rev No.	Date	Revised By	Revision Details
0	22/06/2020	Petr Osvald	Draft report
1	16/07/2020	Petr Osvald	Final report

This Report is protected by copyright vested in SRK Consulting MGL (Australasia) LLC. It may not be reproduced or transmitted in any form or by any means whatsoever to any person without the written permission of the copyright holder, SRK.